2 vol

MASS TRANSFER IN GAS-SOLID-LIQUID DISPERSIONS.

by

JOHN ARTHUR COGGINS B.A.Sc. (TOR)

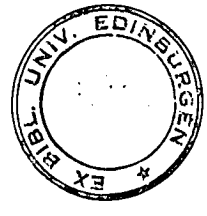

Thesis presented for the Degree of Doctor of Philosophy of the University of Edinburgh in the Faculty of Science.

September 1965.

SUMMARY

The investigation of mass transfer in gas-liquid-solid dispersions involves measuring gas-liquid interfacial areas in an opaque medium, for which the normal physical methods, such as light transmission, are unsuitable. A chemical method was suggested and used by Westerterp (130) in which the rate of oxidation, by air or oxygen, of a sodium sulphite solution can be used to calculate the interfacial area, provided the value of the overall liquid phase mass transfer coefficient, k'_L, is known. Experiments here showed a wide discrepancy between the value of k'_L quoted by Westerterp and those calculated for three types of gas-liquid contactor with known interfacial areas - a stirred cell, an aerated agitated tank and a bubble column. It was found that a value of k'_L could be predicted within acceptable limits of accuracy for the three phase dispersion to be studied. This was $k'_L = 4.5 \pm 0.75 \times 10^{-2}$ $\frac{cm}{sec}$ (for 0.4 to 0.8M sulphite at 36°C containing at least 10^{-3} M cupric ions) which is sixteen times lower than that quoted by Westerterp, but agrees with the value calculated by Charnock (132) in a two phase bubble column.

Experiments were performed to measure interfacial areas, bubble frequencies and gas phase residence time distributions/

distributions in aerated liquid fluidized beds of sand and glass ballotini in a six inch diameter pyrex column. From their results the interrelation of the process variables, gas rate, liquid rate, bed porosity and particle size, and their effect on the gas bubble formation, rate of coalescence and interfacial area was studied, and interpreted with the help of observations in a small two-dimensional column in which individual bubbles could be seen.

A model proposed for the flow of gas through the three-phase dispersion in which it is considered to consist of three portions: one which passes through the dispersion rapidly as large bubbles and, as far as mass transfer is concerned, effectively by-passes it, an ionic bubble portion whose residence time is very long and a portion consisting of bubbles with a distribution of sizes and residence times similar to that in a perfectly mixed system; was confirmed.

The relative sizes of these portions and consequently the interfacial area, depended only on the gas rate and bed porosity being a function of the degree of agitation engendered by their combination, it being higher, the higher the gas rate and bed porosity. The frequency of large bubbles, f_B, formed at the gas distributor was found to depend only on the superficial gas velocity Vs cm/sec, as given by the equation: $f_B = Vs^{0.32} sec^{-1}$, but/

but their size varied inversely with bed porosity. When coalescence of the large bubbles with each other commenced, the rate was independent of gas rate and dependent only on the bed porosity, ϵ, and the results could be correlated by the equation:

$$f_{\beta} = \text{exp.} \left[1.95 - \left(\frac{7.12}{\epsilon} - 4.39\right) \times 10^{3} h\right] \text{ sec}^{-1}$$

where h is the height up the column, cm.

The large bubble coalescence was found to have little or no effect on the specific interfacial area, which remained at the value just above the gas distributor. This value was determined by the size distribution of the gas bubbles formed.

ACKNOWLEDGEMENT

The author wishes to express his gratitude to his supervisor, Professor P.H. Calderbank, for his willing help and encouragement throughout the execution of this work; and to Mr. C. McLeod and the workshop staff of the Department of Chemical Engineering, for their ever ready help and advice in constructing the apparatus and carrying out its many modifications.

Thanks are also due to the British Petroleum Company Limited for the provision of a grant.

TABLE OF CONTENTS

VI/

INTRODUCTION

Considerable industrial interest is developing in three phase fluidized bed reactors for processes where gases and liquids must be contacted in the presence of solid catalyst particles. An example of this is in the catalytic hydro desulphurisation of fuel oil. Under suitable conditions of temperature and pressure liquid fuel oil is made to fluidize a bed of solid catalyst particles and hydrogen is sparged into the bed. Since the reaction between hydrogen and the sulphur present in the oil takes place in the liquid phase the efficiency of gas-liquid contacting, defined as the rate at which gas can be transferred to the liquid, is of primary importance. It is the object of this work to study the behaviour of a gas-liquid-solid fluidized bed and particularly those factors which control the magnitude of the gas/liquid interfacial area.

Water and aqueous solutions of sodium sulphite have been used to fluidize beds of silica sand and glass ballotini in a six inch diameter pyrex glass reactor up to ten feet in height. Air was sparged into the reactor below a gauze used as a solids-bed support. Average interfacial areas for the whole reactor have been calculated from measurements of mass transfer of oxygen from the air to the sulphite solution, where it reacts

to/

to form sodium sulphate. This method of area measurement was first suggested and used by Westerterp (130) for a stirred tank gas/liquid reactor and has been developed here for a three phase dispersion. Other direct ways of measuring interfacial areas, such as the light transmission method of Calderbank (149) and photography, which can give values at specific positions, would have been preferred but could not be used for reasons to be discussed later - the main one being that the presence of particles renders the dispersion effectively opaque.

The main difference between a three phase fluidized bed and a two phase bubble column is that the presence of solid particles promotes coalescence to a considerable and increasing degree as the ratio of bed liquid-to-solid volume, or porosity, is reduced. The gas rate influences the height at which a given amount of coalescence occurs but the rate of coalescence, once initiated, is determined only by the bed porosity. In all other respects this reactor behaves as a normal bubble column, the particles being present only to simulate the catalyst and thus the hydrodynamic conditions, to be found in an industrial reactor of this type; they play no part in the reaction process between oxygen and the sodium sulphite solution.

When/

When developing an experimental program of study it had to be borne in mind that the technique of area measurement used, produces only values for the average specific interfacial area over the total height of the reactor. The effect of coalescence on reducing the interfacial area as one moves up the column can, therefore, only be detected by measuring overall areas for a number of reactors of increasing heights. It can also be appreciated that large changes in area with height are necessary to produce reliably measurable changes in the overall average value. This and other considerations are discussed in detail later.

Another important aspect of a gas-liquid reactor is the residence time distribution of the gas bubbles within it. If part of the gas passes quicly through the reactor in large bubbles then the contact time of this gas is short and the area per unit volume of the gas is low, so that it contributes much less to the overall mass transfer rate than it would do were it to pass slowly in the form of small bubbles. The relative amounts of gas in bubbles of varying sizes were studied here by measuring the residence time distribution function of the gas using a tracer technique.

The thesis is divided into two parts. Part one deals with the choice and development of the oxygen-sodium sulphite technique of measuring average specific interfacial/

interfacial areas. This involved an exhaustive study of the literature on the oxidation of sodium sulphite solutions and the performance of a number of experiments in three types of contacting apparatus, in which the interfacial area was known: a small stirred cell, an aerated stirred tank and a two phase bubble column of the same internal dimensions as the main fluidized bed reactor. Part two deals with the phenomenon of three phase fluidization and with experiments performed to study the behaviour of gas bubbles, the mechanism and rate of coalescence, their interfacial area and residence time distribution.

PART ONE

CHAPTER I

Survey of Techniques for measuring interfacial areas of dispersions.

A. LIGHT TRANSMISSION METHOD

The principle behind this method is that when light is passed through a dispersion of gas bubbles or liquid droplets, a portion of it will be scattered, either by reflection, refraction or diffraction, so that the light which is transmitted is some function of the physical properties of the bubbles or droplets.

Actual Measurements of interfacial areas by this method were first attempted by Clark and Blackman (142) for foams in 1948. On the basis of only qualitative data, they suggested there was a linear relationship between light transmittance and volumetric area. More recently Langlois and co-workers (143,144) published a correlation of light transmission with interfacial area for liquid-liquid and gas-liquid systems. They used a photoelectric probe equipped with a phototube and lamp located behind sealed windows which were 1.0 cm. apart. The light transmission readings were calibrated by high speed photographs of the dispersions, on which droplet-size counts were made to evaluate the interfacial area per unit volume. In the case of gas-liquid dispersions calibration/

calibration was obtained by interpolating between a measurement of a stable glycerol-air emulsion and the values in the liquid-liquid region. They found that a plot of the extinction ratio Io/I, where Io is the initial intensity and I is the transmitted intensity, against interfacial area per unit volume, a, of mixture gave a straight line with an intercept of unity corresponding with the equation

$$\frac{Io}{I} = \beta a + 1 \qquad \ldots\ldots (1)$$

Empirically, β was found to depend on the ratio of the refractive index of the dispersed phase to that of the continuous phase. This equation however applied only to dispersions and emulsions that were completely transparent, without residual cloudiness after settling, and as such was very limited. In addition no provisions were made for variations in the optical path length and each light probe required individual calibration because the reproducibility of results with different probes of the same design was poor.

An attempt to put the light transmission method on a sounder basis was made by Trice and Rodger (145) for 50% emulsions of non-absorbing (water-white) liquid pairs of differing refractive indices. They pointed out that light transmitted through a poly-disperse system of transparent isotropic spherical particles/

particles provides a measure of their interfacial area if it can be shown that the light transmitted is a function of the total projected area. This means that it must be shown that the light transmission is a function of the mean surface volume or Sauter diameter, defined as

$$d_{sv} = \frac{\sum_1^j Nidi^3}{\sum_1^j Nidi^2} \qquad \ldots\ldots (2)$$

where Ni is the number of particles size di in a polydisperse system containing j different sizes of particles. The factors which control light transmission are embodied in the Beer-Lambert extinction relationship:

$$Sndl = dI/I \qquad \ldots\ldots (3)$$

where the scattering cross-section, S, is the ratio of the light energy lost by scattering, to the incident light energy per unit area, and n is the number of particles per unit volume. Integrating over the optical path length, l, between light source and detector as the incident light diminishes from Io to I, yields

$$\ln \frac{Io}{I} = Snl = Ks \frac{d^2\pi}{4} n.l. \qquad \ldots\ldots (4)$$

where

$$Ks = \frac{4S}{d^2\pi} \qquad \ldots\ldots (5)$$

and is called the scattering area coefficient.

Several investigators quoted by Trice and Rodger, obtained experimental data and did calculations based on theory developed by Mie (146) using the simplifying assumption/

assumption that light once scattered from the primary light beam is lost and never reaches the photocell. They were able to show that the scattering area coefficient, Ks, is extremely sensitive to particle size near the wave length of light but that the effect of particle diameter on Ks diminishes with increasing particle size, and that in the case of particles greater than 50μ, such as those used by Trice and Rodger, Ks was essentially constant. This allowed Trice and Rodger to define the drop diameter in terms of sauter mean diameter, d_{sv}, and equation (4) was rewritten in terms of the interfacial area per unit volume of the total mixed phases, A, which is given by

$$A = \frac{6\phi}{d_{sv}} \qquad \ldots\ldots (6)$$

where ϕ is the volume fraction of dispersed phase, N, the number of particles in the dispersion and a scattering factor α, as follows:

$$\ln \frac{Io}{I} = \frac{Ks\pi d^2}{4} \; d_{sv}^2 \; n \; l$$

$$= \frac{Ks\pi d^2}{4} \; d_{sv}^2 \; \frac{N\phi}{N\pi \frac{d_{sv}^3}{6}} \; l$$

$$= \alpha A l \qquad \ldots\ldots (7)$$

In practice they found that $\ln \frac{Io}{I}$ plotted against $\propto Al^{0.8}$ gave results with an overall reproducibility within 5%. They admit in conclusion that their general correlation is valid only for the conditions of their/

their experimental investigation and list the restrictions imposed by the underlying theoretical and practical considerations as follows:-

1. Liquids which are transparent in the incident light spectrum.
2. Dispersions containing 50% by volume of dispersed phase.
3. Systems where the relative refractive index M is between 0.01 and 0.11.
4. Dispersions in which the smallest particle size is greater than 50μ .
5. Dispersions through which the percentage of light transmittance (I/Io x 100) is greater than 0.65% for optical path lengths from 1.0 to 2.0 cms.

Restrictions 2 and 3 are the ones which most hamper the general applicability of their method.

Rose and Lloyd (147) investigated the light transmission method as a means of calculating the specific surface of fine powders by suspending them in a liquid, and developed theory which eliminated all the restrictions enumerated by Trice and Rodger. They placed the light source and photocell at such a large distance apart that they could argue that light which reached the photocell was only that which had passed straight/

straight through the suspension and none of it had done so by multiple scattering (This was one of the assumptions made by Trice and Rodger but their path length of 1.0 to 2.0 cms would throw doubt on its validity in their case) As the powder particles were opaque their projected area, a_p, perpendicular to the light beam blanked off the light and a shadow, assumed to extend behind them the whole optical path length, was cast over the photo cell, reducing the intensity recorded. They derived the relation

$$a_p = \frac{1}{Cl} \ln \frac{Io}{I} \qquad \ldots\ldots (8)$$

where C is the concentration of particles in the suspension.

According to Cauchy (148) in an assembly of irregular particles randomly dispersed, provided there are no concave surfaces, the total interfacial area per unit volume, a, is four times the total projected area per unit volume, a_p, of the dispersion. This fact allowed Rose and Lloyd to calculate the value of, A, directly from the change in intensity of light from

$$a = \frac{4}{Cl} \ln \frac{Io}{I} \qquad \ldots\ldots (9)$$

Calderbank (149) developed his technique for measuring the interfacial area of bubbles in liquids from the method of Rose and Lloyd, the advantage being that their method overcame the difficulty of accounting for multiple/

multiple scattering which is inevitable in highly concentrated dispersions and which makes applying the equation of Mie (146) extremely difficult, as shown by Chu (150). Instead of the beam being cut off, as it was by the opaque powder particles, it is scattered by refraction, reflection and diffraction. If the optical path is long enough, then, as with the suspension of powder particles, only light which has had an uninterrupted passage through the dispersion is measured, and the dispersion will appear to the photocell as a number of round black shadows. Because the light transmitted i n both systems does not depend on the refractive indices of the two phases in the dispersion; on whether the dispersed phase is opaque or not; or the concentration of the dispersed phase, then restrictions 1, 2 and 3 of Trice and Rodger's method are overcome.

However Calderbank states that the Mie theory shows that for particles large compareddto the wave length of the incident light, the scattering cross-section of a particle in the dispersed phase is twice its projected area. For large scattering particles such as the bubbles encountered by Calderbank (0.1 mm diameter) diffracted light is scattered at such a small forward angle that it is practically impossible to avoid its reception by a photocell placed at even vast distances from/

from the light source. Thus for these large scattering particles, Calderbank assumes the two effects compensate for one another and the scattering cross-section of the dispersed phase can be taken to be equal to its projected area, an assumption that would appear to be valid from his experimental results.

The final equation is derived in the same way as that of Rose and Lloyd but as this method is to be used in this work, for measuring areas in an aerated stirred tank and a two phase bubble column, it will be given here in full.

If Ao is the cross-sectional area of the light beam

Ab is the free area at any cross-section of the beam

a_p is the projected area of the bubbles per unit bolume of dispersion and l is the optical path length, then the decrease in free area with distance through the dispersion is given by

$$-\frac{dAb}{dl} = Ab \times a_p \qquad \ldots\ldots (10)$$

and integrating over the total path length gives

$$-\ln Ab = a_p \times l + K$$

when $l = 0$ $Ab = Ao$ $K = -\ln Ao$

$$\therefore \ln \frac{Ao}{Ab} = a_p \times l \qquad \ldots\ldots (11)$$

But if the intensity of the light beam passing through an area Ao is equal to Io and that through the dispersion/

dispersion free area Ab is I, then

$$\frac{Ao}{Ab} = \frac{Io}{I} \qquad \ldots\ldots \quad (12)$$

because the change in the average intensity of light passing through the dispersion is due to the change in the area shadowed. So

$$\ln \frac{Io}{I} = a_p l \qquad \ldots\ldots \quad (13)$$

and from Cauchy (148) $a = 4\, a_p$, so

$$\ln \frac{Io}{I} = \frac{al}{4} \qquad \ldots\ldots \quad (14)$$

A further modification by Calderbank, proposed later (151), was made so that instead of measuring the light intensities Io and I, the times, t_o and t, taken for a given quantity of light, Q, to be received by the photocell after passing through the unaerated liquid and the aerated dispersion, respectively, were recorded by an electric clock linked to a light quantity meter. Then

$$Q = toIo = tI$$

and equation (14) becomes

$$\ln \frac{to}{t} = \frac{al}{4} \qquad \ldots\ldots \quad (15)$$

Equation (14) was tested by suspending a number of polystyrene spheres of known volume-mean particle diameter in water whose density is only slightly less than that of the spheres themselves. They were kept in homogeneous suspension by means of an electrically driven/

driven stirrer. The intensity of the incident and transmitted light was measured over a large range of particle size (0.1 to 1.3 mm diam.), interfacial areas (0 - 3.3 cm^{-1}) and optical path lengths (6 - 50 cms). The results confirmed the validity of equation (14).

B. THE LIGHT REFLECTIVITY METHOD

This method was devised by Calderbank, Evans and Rennie (152) to enable measurements of the interfacial areas to be made in two phase systems involving optically dense dispersions, such as obtain on distillation trays. The light transmission method fails in these cases due to intense multiple scattering. However optically dense dispersions have a high reflectivity and this has been correlated with the interfacial areas of gas/liquid, and liquid-liquid dispersions and beds of close-packed glass beads.

A collimated beam of light was made incident at 45° on the surface of a dispersion which was contained behind a glass window and a photocell was positioned above the window to receive light reflected perpendicularly from it.

The term reflectivity, R, was defined as the ratio of the intensity of that part of the light scattered from the dispersion and incident on the photocell, to the intensity/

intensity of the light similarly scattered from a standard surface - a piece of opal glass - placed in the same position as the window. Values of the interfacial area were obtained by the light transmission method in the case of the liquid-in-liquid and gas-in-liquid dispersions and by calculation in the case of the glass beads. These were then plotted against the corresponding reflectivity as $\frac{1}{a}$ against $\left(\frac{R_\infty}{R} - 1\right)$, where

$$R_\infty = kM \qquad \ldots\ldots (16)$$

and k is a dimensionless constant which was calculated from the data and which it was expected would depend on the standard surface and the geometry of the light probe. M is the Lorentz-Lorentz coefficient $= \frac{m^2 - 1}{m^2 - 2}$, where m is the refractive index ratio of the two phases as before. R_∞ is the value of R corresponding to infinite interfacial area, obtained from a plot of $\frac{1}{a}$ against R for each dispersion. These plots were straight lines with intercepts of R_∞ on the R axis. A further plot of these values of R_∞ against M confirmed the validity of equation (16).

The plot of $\left(\frac{R_\infty}{R} - 1\right)$ against $\frac{1}{a}$ thus produced a straight line, whose equation was

$$\frac{R_\infty}{R} - 1 = \frac{46.5}{a} \qquad \ldots\ldots (17)$$

This correlation was independent of particle size over the diameter range 40 μ to 0.7 cm, values of refractive index/

index ratio M from 0.684 to 1.163 and values of interfacial area from 2 to 67 cm^{-1}. Within the above ranges it was independent of the geometry of the vessel containing the dispersion.

The authors point out as a matter of interest the similarity of their correlation to that of Langlois and Vermeulen, equation (1) rearranged:

$$\frac{I_o}{I} - 1 = \beta a \qquad \ldots\ldots (1a)$$

which was for light transmission in which forward scattered light as well as that transmitted was measured and where β depended on the ratio of the refractive indices.

C. PHOTOGRAPHIC METHODS

Calculating interfacial areas from photographs of dispersions was the only method available until the light transmission work was started, and it was continued and used as a means of calibrating these new devices. Basically it consists of photographing the dispersion using a lens to produce a narrow depth of focus, tracing the droplets or bubbles in the plane of focus and classifying the diameters. If the volume fraction of the dispersed phase, ϕ, is known, then the interfacial area can be calculated from

$$a = \frac{6\phi}{d_{sv}} \qquad \ldots\ldots (18)$$

In/

In a recent paper, Calderbank and Rennie (156) used a statistical method, the so called "Pin-dropping Technique" developed from the original observations by Crofton (153), Chalkley (154) and Rose and Wyllie (155), to evaluate the Sauter mean bubble size, gas holdup and interfacial area of bubble clouds formed by aerating water in sieve plate columns. In principle, a line of length about equal to ten bubble diameters is placed in a random fashion over the photograph and the number of hits and cuts counted. The number of hits, h, is defined as the number of times the ends of the line are totally enclosed by the perimeter of a bubble and the number of cuts, C, by the number of times the line is cut by the surface of a bubble. This operation is repeated a large number of times when, as shown in detail in the paper,

$$d_{sv} = \frac{3\pi h}{C} \qquad Hg = \frac{h}{2n} \qquad a = \frac{2C}{n\pi l} \qquad \ldots\ldots (19)$$

where l is the length of the line, n the number of lines and Hg the volume fraction of gas in the dispersion.

In practice the authors drew a plot of 400 random lines in a $3\frac{1}{2}$ inch square which they placed over a photograph of the dispersion contained behind a transparent window. Results obtained using 400 lines were consistent with those using only 200 lines and this suggested that the bubbles themselves were randomly distributed/

distributed, in which case the grid of lines placed over them could be systematic. This greatly simplifies and speeds up the analysis so to this end they drew a triangular grid on a hexagon circumscribing a 2½ inch diameter circle which contained 462 lines just under 0.18 inches long. This was then mounted with the photograph in a commercial spectrum projector whereby an enlarged image could be analysed.

A comparison between the sauter mean bubble size determined in this way and that deduced by the light reflectivity method was made. Good agreement was obtained at high gas flow rates when froths were produced but the interfacial area was invariably lower than that found using the other method. This was explained as implying that while the bubble sample viewed at the column wall was representative of that obtaining in the bulk of the froth or foam, an unrepresentative and larger volume of liquid was present at the wall and this would increase the value of a calculated from the reflectivity measurements.

D. THE CHEMICAL METHOD

All the previous methods described have relied on physical measurements either at the walls of the containing vessels as in the case of photography and light reflectivity/

reflectivity measurements, or through small local parts of the dispersions as in the case of light transmission probes. The former are subject to the disadvantages of possible unrepresentative conditions existing at the wall and the latter to the likelihood that the dispersion is not homogeneous, necessitating measurements at several positions in the dispersion. This was clearly demonstrated by Calderbank (149) for dispersions in agitated vessels. The additional factor that the probe itself is often large enough to change the natural flow pattern in the vessel is another disadvantage. To overcome all of these disadvantages for the case of gas dispersions in liquids (Westerterp (130) proposed using a chemical method, the principle of which is as follows.

For gas absorption with a moderately fast irreversible 1st order chemical reaction taking place in the liquid boundary layer such as:

$$A + B \rightarrow AB$$

either the film or penetration theory (164, 165, 166) can be used to show (130) that the coefficient for absorption is given as

$$k_L' = (k_C D_A)^{\frac{1}{2}} \quad \ldots\ldots\ldots (20)$$

provided that

$$\phi = (k_C' D_A)^{\frac{1}{2}}/k_L > 2 \quad \ldots\ldots\ldots (21)$$

The coefficient k_L' in equation (20) is defined by

$$N_A = k_L' (C \quad - C \quad) a \quad \ldots\ldots (22)$$

where N_A is expressed in the dimensions $ML^{-3}T^{-1}$. Equation (20) implies that under conditions such that the inequality/

inequality of equation (21) holds, k_L^{II} is independent of the mass transfer coefficient k_L and accordingly of the hydrodynamic conditions. Under such conditions, the whole gas-liquid interface can be considered uniformly effective for absorption. If experiments can be designed where the inequality of equation (21) is satisfied and for which the value of the interfacial area is known, then $(k_c^{I} D_A)^{\frac{1}{2}}$ can be calculated and used in future experiments to measure interfacial areas where these are not known, such as in gas-liquid dispersions, using equation (22). In this equation N_A is the mass transferred of A per unit time and volume, C_{Ai} is the equilibrium concentration of A at the liquid interface, which can be estimated from Henry's Law with the necessary corrections for the presence of electrolyte. The concentration of A in the bulk liquid, C_{AL}, can be assumed to be zero for an irreversible reaction where C_B is large.

In the case of a second order reaction in the liquid film a similar analysis (157) by the film or penetration theory will show that the coefficient for absorption is given as

$$k^{I} = (k_c^{II} C_B D_A)^{\frac{1}{2}} \qquad \ldots\ldots (20a)$$

provided that

$$\phi = (k_c^{II} C_B D_A)^{\frac{1}{2}} / k_L > 5 \qquad \ldots\ldots (21a)$$

so/

so that if the concentration of solute in the liquid phase C_b is large enough to remain substantially constant during the run, and the inequality of equation (21a) holds, then k_L^1 again becomes independent of k_L and hydrodynamic conditions. As before the value of $(k_c'' C_b D_A)^{\frac{1}{2}}$ must be determined from experiments in which the interfacial area is known.

Westerterp used two reactions:- 1) The oxidation of aqueous sodium sulphite in the presence of cobalt and copper ions and 2) the absorption of CO_2 gas by aqueous sodium hydroxide solutions. The reaction between oxygen and sodium sulphite will be dealt with in detail in the following chapter as it was the reaction selected to measure areas in the three phase fluidized bed. Suffice it here to say that its great advantages are that sodium sulphite is obtainable cheaply and the normal laboratory compressed air supply can be used as a source of oxygen. In the case of the absorption of CO_2 in aquous NaOH its main advantage according to Westerterp (and Yoshida (157) who also used it), is that it is insensitive to impurities and the physical properties of the NaOH solution can be altered by adding other liquids without affecting the chemical kinetics appreciably. Its disadvantages, he points out, are 1) the high solubility of CO_2 and the likelihood of resistance/

resistance to mass transfer in the gas phase interfering if it is diluted with an inert gas - this is not supported by Yoshida and Miura who used air with a CO_2 concentration from 1 to 14%: 2) the high absorption rate which makes heat withdrawal a problem, and 3) the obvious difficulties of designing equipment and the inconvenience of handling caustic solutions up to 1 N in concentration.

X-RAY METHOD

Moris (158) in an article describing mass transfer and bubble size studies in solid-gas-liquid systems in a stirred tank, mentioned that an X-ray technique was being developed to measure bubble sizes in opaque slurries, which appears to be a probe similar to that used for light transmission by Calderbank (149) but with the light source replaced by one of X-rays and the photo-cell by a suitable detector. So far nothing has been published.

CHOICE OF MEASURING TECHNIQUES FOR THIS WORK

The project undertaken to study mass transfer in three phase dispersions was only viable if interfacial areas could be measured with a reasonable degree of accuracy. The light transmission method could not be used, as the presence of particles, sand and glass ballotini, would either totally obscure the light beam as in the case of the sand, or, with the ballotini, cause so much of it to be scattered that it would be impossible

to/

to account for that scattered by the particles and that by bubbles. As the particles (and liquid) are moving in very turbulent conditions caused by the passage of large bubbles, their own distribution in the dispersion is far from homogeneous, and quite different from that in the bed before aeration. Thus any attempt to obtain a "blank" reading of light transmission through the solid-liquid bed before aeration would be futile.

The presence of particles also causes gas bubbles to coalesce rapidly, causing considerable down-flow at the walls of the column as a large gas bubble passes. Reflectivity measurements or photographs (which can only be taken at the wall because of the opacity of the dispersion) under these conditions would not be remotely representative of the situation in the bulk of the dispersion. The only suitable method was the chemical one described and used by Westerterp. The reaction selected was the oxidation of aqueous sodium sulphite containing copper, or cobalt, ions as a catalyst, because it was a cheap and very convenient system to use in the laboratory.

It has been shown by Yagi and Inoue (129) and Harris and Roper (138) that the oxidation of sulphite catalysed by cobalt ions is controlled by a second order reaction in the liquid film and in this case the value of k_L^1 depends on the sulphite concentration, and the

concentration/

concentration of cobalt catalyst in so far as this affects the value of the second order reaction rate constant k_c^{11}. In view of these considerations it was decided not to use cobalt as a catalyst.

However, work done elsewhere in this department (130) using a stirred aerated solution of copper catalysed sodium sulphite in a tank, identical to that used by Westerterp, showed a difference by a factor of over twenty between the interfacial area measured directly by a light transmission probe and that calculated from the value of k_L^1 quoted by Westerterp under the same conditions. The quoted value of k_L^1 seemed to be twenty times too high. In view of this large discrepancy it was decided to carry out a thorough investigation of the sulphite oxidation reaction, using the light probe method devised by Calderbank and already described, to measure areas in a stirred tank and a bubble column. This would allow the value of k_L^1 to be calculated under different conditions of agitation, bubble size and solution concentration. This study is reported in detail in chapter III but first of all a literature survey was made to try to discover as much information as possible about the oxidation of sodium sulphite, particularly when using copper as a catalyst. An experimental program was then developed to provide more information [illegible] where there was none already/

already and where conflicting results in the literature demanded it. The overall purpose behind all this was to determine first of all if it is possible to provide experimental conditions such that a value of k_L^1 exists which is independent of the hydrodynamic conditions, and secondly, if there is, what is its value.

CHAPTER II

A. The Oxidation of Aqueous Sodium Sulphite Solutions.

1. LITERATURE SURVEY

The oxidation of a catalysed sodium sulphite solution, has been used recently for the chemical method of measuring interfacial areas in gas-liquid contactors by Westerterp (1963). However for many years it has been used to compare the performance of gas liquid contactors of many types, and predominantly those used for submerged aerobic fermentions. The method here, consists of measuring the rate of oxidation, by air, of an aqueous sodium sulphite solution containing cupric ions as a catalyst. This oxidation rate is obtained by measuring the change in sulphite concentration in the liquid by iodometric titrations at intervals of time, from which the average volumetric mass transfer coefficient $k_L'a$ can be calculated, and these values are compared. In nearly all cases no determination of the value of the interfacial area, a, was attempted and so one could not tell if a quoted improvement in $k_L'a$ was due to a more efficient dispersion of the gas phase increasing a, or an increase in the value of k_L' due to a change in the hydrodynamic conditions or the rate controlling step for the absorption process/

process. The question of what the rate controlling step is - whether there is a mass transfer resistance in the gas film, liquid film or at the interface, or whether it is a chemical reaction - has not yet been answered satisfactorily, although many attempts have been made to do so. The overall reaction is represented by the equation

$$Na_2SO_3 + \tfrac{1}{2}O_2 \longrightarrow Na_2SO_4 \qquad \ldots\ldots (1)$$

and in the case of solutions catalysed by cupric ions it has been suggested by Backstrom (106) that the reaction proceeds as a series of chain reactions initiated by a cupric ion. Work has since been done on the reaction mechanism as such and is reviewed by Bassett and Parker (112). What follows is a chronological survey of work carried out, of, generally, a chemical engineering nature as opposed to that of physical chemistry , to discover more about the absorption process and its rate controlling step.

Miyamoto (101 to 105) working from 1927 to 1932 decided after many experiments that when the liquid is well stirred there is no stationary liquid film adjacent to the interface and that the maximum rate of oxidation of the sulphite is that equivalent to the rate of solution of oxygen in water free of oxygen. It does not depend on the sulphite concentration except that if this is too high, the rate of oxidation decreases. He also states/

states that the rate is proportional to the gas-liquid interfacial area, and the partial pressure of oxygen in the gas, and that it increases with temperature. Shultz and Gaden (120) calculated an activation energy of 12.5 k. cals/mole from Miyamoto's data, which would indicate a chemical reaction control.

Fuller and Crist (107) used a stirred 100 ml quartz reaction vessel containing solutions of very pure sodium sulphite, from 0.01 to 0.05M in concentration, and pure oxygen as the gas. The temperature was controlled at 25°C. Experiments were carried out with no catalyst, with cupric ions from 10^{-9} to 10^{-4} M, and with mannitol in concentrations from 10^{-7} to 3×10^{-2} M. They found the reaction of uncatalysed sulphite solution saturated with oxygen at one atmosphere to be strictly first order with respect to sulphite ion concentration; but with cupric ions present in excess of 10^{-9} M, the rate was independent of the sulphite concentration. Mannitol was found to act as an inhibitor and its effect was uniform over the 10^{5}-fold change in concentration used. They also showed the rate to be independent of pH between 8.8 and 8.2, but that it decreased in a complicated manner between 5.9 and 3.2. An interesting point they made was that the rate increased four fold during a run using cupric ions as a catalyst. They suggested it was due to the alkalinity of the sulphite solution when made up

(pH/

(pH of 8.7) causing the cupric ion to be removed by combining with the hydroxl ion: this then returned as the solution became less alkaline as the oxidation of basic $SO_3^=$ ions to the neutral $SO_4^=$ proceeded. Chain et al. (113) noticed a similar increase in rate after 1 to 1½ hours in a sparged fermentor using 0.25 M sulphite with 10^{-4} M cupric ions. They offered no explanation.

Cooper, Fernstrom and Miller (108) first developed the use of the sulphite oxidation reaction as a means to study the design variables pertinent to agitated gas-liquid contactors. They took up the point of the reaction rate being independent of sulphite concentration when catalysed by cupric ions discovered by Fuller and Crist and tested it over a much wider range (0.015M to 0.5M) of sulphite concentration using a cupric ion concentration of 10^{-3}M. This they found was high enough to avoid the increase in reaction rate as the solution became less alkaline, observed by Fuller and Crist. They used a series of five geometrically similar cylindrical tanks from 6 to 96 inches in diameter. The four smaller ones were made of pyrex and the largest of steel. Four vertical baffles extending from top to bottom of the tanks were placed at equal intervals about the circumference in every case. Varied disk and flat-paddle agitators were used to disperse the air which entered through a single orifice in the centre of the tank bases, under/

under the impellers. The actual rate of oxidation was measured by analysing samples from the tanks for their sulphite content iodometrically - this method was used by all workers and is described in detail in Appendix III.

Wise (111) compared oxygen absorption rates by the sulphite and polarographic methods in a tall cylindrical vessel aerated through a jet at the base, and found the sulphite method gave higher results. From the film theory of gas absorption he arrives at a relation between the two rates, which results in an enhancement of the polarographic rate of $/1 + \frac{kd^2}{2D_A(C_e-C_L)}/$ in the case of sulphite absorption, where d is the liquid film thickness, k the zero order rate constant of the reaction between sulphite ion and oxygen, D_A the diffusion coefficient of oxygen in the liquid film and Ce and C_L, the concentration of dissolved oxygen at the interface and in the bulk liquid respectively. From this analysis it would appear that if the film thickness is decreased, by say increased agitation, the enhancement factor would decrease and so would the absorption rate. The effect of the rate decreasing with increased agitation has been noticed by Schultz and Gaden (120) and Carpanni and Roxburgh (124) in a stirred tank with a horizontal gas-liquid interface.

Bassett and Parker (112), in a paper on the oxidation of sulphurous acid, report an intensive study of the presence/

presence of dissolved metal salts on the oxidation of sulphurous acid by free oxygen. They also include a review of previous work on the catalytic acceleration and retardation of the oxidation of sodium sulphite solutions and in the case of cupric ions, give a series of suggested reactions. In these the cupric ion is supposed to form a complex with the $SO_3^=$ ion, $\left[Cu(SO_3)_2\right]^{\equiv}$ which reacts with oxygen to form another complex $\left[O_2 \rightarrow Cu(SO_3)_2\right]^{\equiv}$ which in turn breaks down to $SO_4^=$, $SO_3^=$, and Cu^{++} ions, leaving the Cu^{++} free to begin the process again. From this paper it would appear that such metal ions as Co^{++}, Fe^{+++}, Ni^{++}, Mu^{++} would also catalyse the reaction.

Maxon and Johnson (114) using the method (and a similar apparatus) of Cooper et al found the oxygen uptake rate varied as the 0.4 power of the air rate and that the effective aeration could be varied from 10 to 700 millimoles of oxygen per litre per hour by varying the gas rate and stirrer speed from 100 to 10^4 mls/min and 500 to 1680 r.p.m. respectively. They also found that increasing the operating liquid volume, in effect making the liquid deeper in the same tank, decreased the uptake. By changing the volume from 1300 mls to 2100 mls the rate decreased by 50%. As they too found the rate of oxidation to be independent of sulphite concentration they conclude the absorption must be gas-film controlled.

Finn/

Finn (116) in a review of agitation-aeration refers to the sulphite reaction and states that copper or cobalt salts can be used as catalysts, which is to be expected from Bassett and Parkers' paper. In considering the individual mass transfer resistances he dismisses the idea of Maxon and Johnson's that the gas film is controlling, on the results obtained by Bartholomew et al. (109), who found that $k'_L a$ increased as the temperature was raised from 27°C. to 32°C. and the activation energy for the overall process was 4200 cals/mole, a value characteristic of a diffusional process through water. If diffusion through a gas film were controlling, $k'_L a$ would vary as the square root of the absolute temperature and this was not observed. In addition he states that for a slightly soluble gas like oxygen, the concentration driving force across the gas film is so much greater than that across the liquid film, that the latter is almost certain to offer more resistance. Also, since the diffusion coefficient of oxygen through water is less than through air by a factor of about 10,000, air films would have to be enormously thicker than liquid films in order to become controlling.

Schultz and Gaden (120) set out to investigate the question of where the controlling resistance to mass transfer was: in the gas film, the liquid film, or at the interface. They used a cylindrical plastic tank

12/

12 inches in diameter and 16 inches high. Approximately 7.5 litres of 0.075M sodium sulphite, about 10^{-4}M in cupric ions, were charged for each run. The pH was adjusted to 6.8 with concentrated sulphuric acid and the whole maintained at 30°C, by a copper heating coil. Air, previously filtered, heated to 30°C and saturated with water was passed over the sulphite solution surface: no sub-surface sparging was used. Both the liquid and gas could be stirred independently and in addition a large pitchless three bladed stirrer, made from flat sheet, was placed about one inch below the liquid surface, on the liquid stirrer shaft. This device was to obtain regular, circular flow at the liquid surface. Vertical baffles were also installed but were terminated below the surface to prevent any breaking of the gas-liquid interface. With this set up, liquid and gas stirring velocities and hence the corresponding film resistances could be varied independently and in a known manner. Furthermore because the surface was unbroken, the interfacial area could be determined and the mass transfer coefficients calculated.

Runs at air stirrer speeds from zero to 550 r.p.m. were made in triplicate but no effect on the absorption coefficient $k_L'a$ was detected. In the case of liquid stirring the absorption coefficient remained fairly constant over the range of lower stirring rates, 0 to 90 r.p.m./

90 r.p.m. but thereafter it decreased until it had dropped by 25% at a stirring rate of 240 r.p.m. This they explain by suggesting that as the mechanism of the reaction is thought to be a chain one, there must be some induction period in the reaction rate while the concentration of intermediates is built up. If the rate of formation of these intermediates is dependent upon the dissolved oxygen concentration - because of the reoxidation of cuprous to cupric ions, for example - the overall rate of reaction will depend on the 'time-average' oxygen concentration level in the liquid phase. With increasing stirring rates, the residence time of an element of fluid in the surface zone, or film, decreases and it follows that the average oxygen level in the liquid there will also fall, causing the drop in reaction rate. The apparent independence of the rate on stirrer speed at lower range of r.p.m.'s is explained by assuming that the residence times in this range are much greater than the reaction induction period. This seems a reasonable explanation, and agrees with the fact that Westerterp, whose work is discussed in a later section, found he could not get reproducible results with copper catalysed sulphite using a liquid jet, where contact times were very short. He considered them to be shorter than an induction period for an auto-catalytic reaction in the liquid film.

Pirt, Callow and Gillett (123) compared sulphite oxidation/

oxidation rates using copper and cobalt ions as catalysts. Using cobalt was mentioned by Finn and used by Downing (118) but no one had as yet made any comparison between the two.

Pirt and co-workers used a small fermentor of the type described by Elsworth et al. (121) charging it with a solution 0.25M in sulphite and 5×10^{-4}M in copper or cobalt sulphate. They found that at low gas rates the cobalt catalysed solution gave an absorption rate about twice that of the copper one and that this factor became as high as five at the highest gas rate. In the presence of Cu^{++} the reaction of sulphite ions was found to be zero with respect to the sulphite concentration, but with Co^{++} the reaction rate decreased with time. The reaction rate with Cu^{++} ions was found to be independent of the Cu^{++} ion concentration over the range 10^{-4} to 10^{-3}M. They did not investigate the effect of Co^{++} concentration.

Solomons and Perkin (125) compared oxidation rates using the polarographic and sulphite methods, as did Wise and found the same discrepancy, that is the sulphite method gave higher absorption rates. However they also say that whilst the polarographic method is dependent on temperature and hence is liquid-film controlled, the sulphite method over a range of 20°C is virtually independent of temperature, corresponding to a gas-film controlled/

controlled reaction. This they feel explains the difference between the two methods, rather than the idea of a finite reaction in a stagnant liquid film suggested by Wise. They used a series of baffled and unbaffled stirred tanks with both single hole and sintered glass spargers, and decided there would be no stagnant liquid films.

Carpani and Roxburgh (124) used a thermostatted pyrex cylinder, 21 cms in diameter, with a flat-bladed impeller, 17.8 cms in diameter, and no baffles; a set-up similar to that used by Schultz and Gaden, with the absorption taking place at the liquid surface, allowing the interfacial area to be measured. Values of overall mass transfer coefficient k'_L were calculated for transfer of oxygen from air to water, 0.5M sodium chloride and 0.05M Sodium sulphite that was 10^{-3}M in $CuSO_4$ and whose pH was adjusted to 8.0 before oxidation (c.f. Schultz and Gaden who used pH of 6.8). In the case of water and sodium chloride the value of k'_L increased with increasing stirrer r.p.m. as expected, but for the sulphite solution k'_L decreased. This agreed with the findings of Schultz and Gaden qualitatively but their values of k'_L were nearly twice as large. They point out that a decrease in the value of k'_L can only be caused by a decrease in the rate controlling step in the complex oxidation of sulphite and this may well be a reduced concentration of a catalyst intermediate/

intermediate as suggested. The values of k'_L in these experiments for a still solution were 15 times higher for sulphite than for water, but dropped to half the value of k'_L for water at the highest stirring rate.

A further series of runs at temperatures varying from 18°C to 34°C showed that the activation energy for k'_L was 1.2 k cals/mole for water and 10.3 k cals/mole for the sulphite solution. This contradicts Solomons and Perkin who used a sparged fermentor, and found no effect of temperature. It does indicate that for water a diffusional process is controlling and for catalysed sulphite it is a chemical one, at least in the case of an unsparged contactor.

Phillips and Johnson (126) derived an expression for the rate of absorption of oxygen assuming that 1) the reaction film is completely contained within the stagnant liquid film; 2) the sulphite concentration remains constant; 3) the oxygen concentration at the interface is constant; 4) the reaction follows the equation

$$-\frac{d[O]}{dt} = k[S]^y[O]^n \qquad \ldots\ldots\ldots(2)$$

The expression is

$$No = \left[\frac{2kDo}{(n+1)}\right]^{\frac{1}{2}} [S]^{y/2} [O]_0^{\frac{(n+1)}{2}} \qquad \ldots\ldots\ldots(3)$$

where D_o is the diffusion coefficient for gas that reacts with solute; k is the reaction rate constant; n the reaction order with respect to the dissolved gas; No the rate/

rate of transfer of gas per unit area at interface; $[O]_0$ the concentration at interface of dissolved gas; [S] the concentration in the liquid phase of the solute which reacts with the dissolved gas; and y the reaction order with respect to the above solute.

They then studied the effect of oxygen partial pressure on the oxygen absorption rate in a variety of pieces of contacting equipment. The first was a 4-litre glass jar with an enclosed gas space above it and a glass stirrer. The contact area was the horizontal liquid surface, and the solution was 1M in sulphite and 10^{-5}M in copper ions. Stirring the liquid and the gas phases to a moderate degree was found to have no effect on the absorption rate, indicating neither ideal gas film nor ideal liquid film control, and that all the oxygen must have been consumed in the liquid film. The actual transfer rate was proportional to the 1.5 power of the oxygen partial pressure, indicating that the transfer was limited by a process other than simple diffusion. From equation (3) then, $\frac{n+1}{2} = 1.5$ and so $n = 2.$, that is the oxygen consuming reaction is second order with respect to oxygen. Now if the major resistance to oxygen transfer were in the gas phase or at the interface, the absorption rate would be independent of the nature of the oxygen consuming chemical reaction, but this is clearly not so from the difference in rate for different catalysts and

for/

for oxygen absorption by pyrogallol and KOH solution. Since then, the absorption rate is not independent of the chemical reaction, the major resistance must be in the liquid phase.

Their next step was to repeat the first experiments but with much higher agitation of the liquid phase, to try and significantly reduce the thickness of the stagnant liquid film. The reaction vessel used was a fully baffled unsparged fermentor with an agitator below the liquid surface. It was operated in a closed system as before. Experiments were made with the same strength copper catalysed sulphite but the results were not reproducible and the oxygen transfer rate increased with time (see Fuller and Crist (107) and Chain et al. (113)). It appeared to them that the erratic behaviour was caused by random metal catalysis from the stainless steel components of the reacting vessel, baffles etc. This same effect of stainless steel was noticed in experiments carried out in this work and described in Chapter III. They overcame this problem by adding Versene (ethylenodinitrilotetraacetic acid) which restored the reproducibility, probably by complexing the metal ions, present as impurities. At low agitation speeds the transfer rate again varied as the 1.5 power of oxygen partial pressure while at high agitation speeds the rate was proportional to the oxygen partial pressure to the first/

first power. This then indicated that only a negligible amount of reaction occurred in the film.

A bubble column was studied next. Bubbles from a single orifice rose 33 cms through copper catalysed sulphite and they found the transfer rate varied as the first power of the oxygen partial pressure; again indicating that most of the reaction took place in the bulk liquid. The transfer rates observed in these experiments agreed fairly well with those observed by Hammerton and Garner (169) for bubbles of the same size in aqueous oxygen-free solutions. Therefore they concluded that oxygen transfer in the sulphite case is probably limited by the same process as for oxygen transfer to water.

More experiments carried out using both cobalt and copper catalysed sulphite solutions in a sparged agitated fermentor gave the same transfer rate for both catalysts, which was surprising in view of the much greater rates with cobalt measured by Pirt et al. The rates in both cases were directly proportional to the oxygen partial pressure, indicating that in these cases too, nearly all of the reaction takes place in the bulk liquid.

The final experiments performed were to study the effect of sulphite concentration on the oxygen absorption rate and this was found to be independent of sulphite concentration in the sparged fermentor down to approximately 0.008M, whereas in the unsparged vessel it was dependent/

dependent on sulphite concentration up to 0.2M. This indicated to them qualitatively the relative independence in an agitated sparged fermentor of the oxygen absorption rate on chemical variables. In the fermentor, the absorption rate varied as the first power of the sulphite concentration below 0.002M, indicating the reaction is first order with respect to sulphite. This was also observed by Fuller and Crist. In the unsparged vessel, however, it was apparent that below 0.015M sulphite concentration, the rate varied as the first power of the oxygen partial pressure. This would be expected if sulphite diffusion as well as oxygen diffusion limited the absorption rate. Above 0.015M sulphite the oxygen absorption rate seemed to approach a constant value, indicating that a factor other than sulphite concentration was limiting the velocity of the chemical reaction.

Yoshida, Ikeda, Imakawa and Miura (128) compared the rates of absorption of oxygen in pure water, sulphate, and sulphite solutions catalyzed by cupric ions, in bubbling gas-liquid contactors of the same type as those used by Cooper et al. They were made of stainless steel however which in view of the experience of Phillips and Johnson/

Johnson and the author of this thesis, can introduce random catalytic effects. They suggest that where oxygen is bubbled through water the rate of absorption is dependent only upon diffusion because of the relatively high turbulence in the liquid phase; however when it is bubbled through catalysed sulphite solution under mechanical agitation the absorption per unit interfacial area is still dependent only upon diffusion but the rate per unit volume is increased because of the greater interfacial area available due to the formation of very small ionic bubbles which have a long residence time in the vessel.

Experiments were also carried out in a bead column and an unsparged stirred tank with a horizontal interface, where in each case the interfacial area was known. In the bead column the values of k'_L calculated for pure water and catalysed sulphite were identical. In the stirred tank they were identical above about 170 r.p.m. but below this the k'_L for the sulphite decreased more slowly than that for pure water and the sulphate solution. This is in disagreement with Phillips and Johnson who found that at similar moderate stirring speeds, the actual r.p.m. had no effect on the value of k'_L for catalysed sulphite solutions.

Yagi and Inoue (129) used the polarographic method in a series of experiments to measure the concentrations of/

of oxygen in sulphite solutions and were able to measure the rate of reaction between dissolved oxygen and the sulphite ion in the liquid phase. This was done by bubbling oxygen through a solution of uncatalysed sulphite controlled at 20°C, to raise the oxygen concentration, and then measuring and recording simultaneously the change in diffusion current due to the dissolved oxygen for a period of several minutes. They had previously obtained a plot of diffusion current against oxygen concentration for 0.25M sulphite at 20°C, which was linear, and they used this as a calibration. By this means they were able to establish that the reaction between oxygen and sulphite in the liquid phase was first order with respect to the oxygen concentration and moreover that the rate constant for this reaction changed linearly with the concentration of sulphite present. From this relation it appeared that the reaction rate was proportional to the sulphite and oxygen concentrations in the liquid. By the same procedure they studied the effect of adding cobaltous ions as a catalyst and found that it was so pronounced that the rate could be obtained only at very low catalyst concentrations owing to the restriction of recorder speed. It appeared that the reaction was first order in catalyst concentration at these low values of from 0 to 6×10^{-7}M $CoSO_4$.

Having satisfied themselves as to what reactions

were/

were taking place in the liquid phase, they then investigated the absorption of oxygen into a cobalt catalysed solution of sodium sulphite at 20°C. By varying the sulphite and catalyst concentrations they obtained a series of curves of absorption rate against catalyst concentration for several sulphite concentrations the results of which they were able to correlate very well with Von Krevelen and Hoftijzer's (163) solution for gas absorption accompanied by a second order reaction in the liquid film. This second order behaviour of cobalt catalysed sulphite was confirmed by Harris and Roper (138).

However from the trend of Yagi and Inones results for the absorption rate against cobalt catalyst concentration it appears that the effect of catalyst concentration would be negligible at values above 10^{-4}M, in which case the value of k''_c would be constant and only the values of sulphite concentration would be required to set the value of k'_L from equation (20a) in Chapter I. As the oxidation in any reactor proceeds the sulphite concentration will fall and so consequently will the value of k'_L which could explain why Pirt et al., and Roxburgh (134) found a decrease in absorption rate with time for cobalt catalysed sulphite. Another explanation is offered by Roxburgh, involving a change in solution pH, which is discussed later.

Roxburgh (134) studied the effect of four metal ions as/

as catalysts, copper, cobalt, iron and nickel, on the absorption rate in four types of contacting equipment:- 1) An unbaffled stir jar as used previously (124) 2) Shake flasks of the Erlenmyer type agitated in a standard rotary shaker with a 1 inch throw 3) Two sparged baffled fermentors of 3 and 15 litres capacity and 4) a horizontal rotating fermentor made of 3 feet of 3 inch diameter pyrex. The only case in which the same absorption rate was recorded with different catalysts, was with copper and iron in the sparged fermentor. However, this was made of stainless steel which makes any results from it untrustworthy, and may well explain the similarity of the two rates as a case of catalysis by Fe^{+++} ions from the steel, masking the effect of the copper ions. Satisfactory oxidation rates using all four catalysts were obtained only in the stir jar. In the shake flasks the rate of oxygen absorption using iron as a catalyst was very high, higher than with cobalt, but it dropped off rapidly as the run proceeded and was not reproducible. In sparged fermentors on the other hand, iron was a satisfactory catalyst but nickel was not. With nickel the chemical rate apparently became the rate controlling step as sulphite oxidation rates levelled off at about 40 millimoles of oxygen per litre per hour as agitation increased. Neither nickel nor iron could be used/

used satisfactorily in the horizontal rotating fermentor as rates varied substantially between runs and on occasion during a run. Roxburgh does not give any explanations for his failures mentioned above, and in the published paper only quotes results, and presents graphs of data, from copper and cobalt runs.

In the stir jar and horizontal fermentor where the interfacial area could be measured, values of k'_L with cobalt varied from 6 to 60 times higher than those with copper, and in each apparatus the ratio of the two increased with increasing agitation. Values of k'_L for both catalysts increased with increasing agitation in the horizontal fermentor, but in the stir jar the cobalt k'_L increased whilst the copper one decreased (cf. Schultz and Gadon, Wise, Carpani & Roxburgh).

In the sparged fermentors the cobalt catalysed solutions gave higher absorption rates than the copper ones; the ratio of the two decreased slightly as the agitation increased, but was always greater than three. These results disagree with Phillips and Johnson's, but agree in principle with Pirt et al's and Westerterp's.

The effect of pH on k'_L for all four catalysts was measured in the stir jar and it was found that the value of k'_L passed through a maximum for each one, but at a different value for each. For copper it was 8.0, cobalt 9.2, iron 7.5 and nickel 9.5. In the case of cobalt/

cobalt the value of k_L' dropped by 60% as the pH changed from 9.2 to 7.5. This he suggests, may explain why some workers have found a drop in absorption rate with time with cobalt catalysed solutions, the pH, if unbuffered, falls during runs as the basic $SO_3^=$ ion is oxidized to the neutral $SO_4^=$ ion (see Fuller and Crist)

2. CONCLUSIONS

From the foregoing it is abundantly plain that the oxidation of sodium sulphite solutions, in the presence of metal ions as catalysts, is a very complicated process. The two principle metal ions that have been used are copper and cobalt and they would seem to give rise to two different types of absorption; absorption of oxygen accompanied by a first order chemical reaction in the case of copper and with a second order reaction in the case of cobalt. The difficulty in drawing conclusions about the process is that although a wealth of information has been obtained it is drawn from many differing types of gas-liquid contactors and when from the same type often under different conditions of agitation, sulphite concentration, catalyst type and concentration, temperature and pH. Authors propose mechanisms and suggest rate controlling steps from the data of their own investigations, at times appearing to ignore, completely, contradictory evidence/

evidence produced by others. However certain aspects of the process have been fairly well established and corroborated by more than one worker and these are summarised below.

(a) The reaction is very sensitive to traces of catalyst - metal ions such as copper, cobalt, iron, nickel and manganese accelerate it and organic compounds such as ethyl alcohol, glycertol and mannitol retard it. Stainless steel has been found to produce random catalysis and irreproducibility of results when used as a material of construction (126,128,138, this work).

(b) In the case of the two main catalysts studied, cobalt and copper ions, the oxygen absorption rate is independent of their concentration above 10^{-3} Molar, and is anything from the same to 60 times faster with cobalt than with copper (123,126,129,134, 138, 139).

(c) When catalysed by copper ions the absorption rate is independent of sulphite concentrations above a certain value of molarity according to different authors, the lowest quoted being 0.008 Molar for a sparged fermentor and the highest being 0.2 Molar for an unsparged vessel with a horizontal interface. (107,108,114,123,126,) and is directly proportional to the oxygen partial pressure in the gas/

gas phase (101,105,107,108,126)

(d) When catalysed by cobalt ions the absorption rate is accompanied by a second order reaction which depends on the sulphite concentration and the oxygen partial pressure in the gas phase, and the catalyst concentration below about 10^{-4} Molar (126,138,139)

(e) The main resistance to the absorption process is in the liquid phase although its exact nature is not known and appears to differ in the cases of sparged fermentors, where there are bubbles of gas, and stirred vessels with horizontal liquid surfaces (101 to 105,108,116,120,126)

(f) The absorption rate into copper catalysed sulphite in a stirred vessel with a horizontal liquid interface decreases with increasing stirring speed. The rate increases with stirrer speed if the solution is catalysed by cobalt. (111,120,124, 126,128,134).

There remain other points such as the actual reaction mechanism in the case of the cobalt and copper catalysed solutions (106,112,107,108,120), the effect of temperature (101 to 105, 109,124) and solution pH (107,120,124,134,139,141) on the absorption rate and rate controlling step under different experimental conditions, that are often isolated and conflicting pieces/

pieces of evidence and are by no means substantiated at this stage.

B. Westerterp's Work

Westerterp's work (130) is considered separately as it is the first to suggest and use the oxidation of sodium sulphite solutions as a means of measuring gas/liquid interfacial areas. The principle is described in Chapter I and the method stands or falls on whether the value of k'_L can be shown to be $\sqrt{k_c D_A}$ in the experiments designed to evaluate $\sqrt{k_c D_A}$. Below is a summary of Westerterp's work and it is followed by a critical discussion in the light of work done in this department and elsewhere.

1 SUMMARY.

In order to be able to calculate a value of k'_L the interfacial area of the gas-liquid contactor must be known. Westerterp was satisfied that the absorption of oxygen in copper catalysed sulphite was accompanied by a fast first order chemical reaction, and set out to measure rates of absorption in a liquid jet apparatus, where the interfacial area can be measured, to obtain the value of k'_L. He assumed that in this type of apparatus the inequality of equation (21) in Chapter I would/

would be satisfied, that is $\phi = \frac{\sqrt{k'_c D_A}}{k_L} > 2$

and so the value of k'_L would indeed be $\sqrt{k'_c D_A}$. However with the copper catalysed solution he observed a strongly varying and non-constant absorption, which was equal to or higher than the physical absorption rate of oxygen into pure water. In view of this then he could not be sure that ϕ was greater than 2, or obtain reliable results. He assumed that this performance indicated that the reaction, under the influence of copper ions, required a finite induction period, before commencing, to allow the build up of complex intermediates in the chain mechanism, as described by Schultz and Gaden. This induction time must have been of the same order of magnitude or longer than the contact time in the liquid jet. He then tried a cobalt catalysed solution in the jet and found no such difficulties with 0.8M sulphite that was 10^{-3}M in cobalt sulphate at 30°C. He thus measured absorption rates at various contact times and found the value of $\frac{k'_L}{He}$ was independent of contact time, where He is the Henry's Law distribution coefficient, and is combined with k'_L because all other quantities in the equation used to calculate k'_L are measurable. He depends on the temperature and sulphite concentration and was not measured by him, but estimated from literature values. The value he obtained for $\frac{k'_L}{He}$ or $\frac{\sqrt{k'_c D_A}}{He}_{Co^{++}}$ according/

according to him was $(1.44 \pm 0.13) \times 10^{-4}$ m/sec.

In order to obtain the value of $\left(\sqrt{\frac{k'_c D_A}{He}}\right)_{Cu^{++}}$ which he could not do directly, he argued that in an agitated gas-liquid contactor, where samples are taken with intervals of three to ten minutes, the few seconds that the reaction requires before starting, after contact with dissolved oxygen, would not be noticeable, and so the value could be obtained in a series of comparative experiments. One must assume in such a case that the substitution of 10^{-3}M Copper ions for 10^{-3}M Cobalt ions does not affect the gas-liquid dispersion interfacial area and that the ratio of specific absorption rates $k'_L a$ with both catalysts will be proportional to the square root of the ratio of their respective reaction velocity constants. After a series of experiments under identical conditions of sulphite concentration, and catalyst concentrations of 10^{-3}M Cobalt and from 0.5 to 4×10^{-3}M copper ions, the ratio of absorption rates was found to be 1.97 ± 0.16 over a wide range of agitation levels. Hence he said that

$$\frac{\left(\sqrt{k'_c D_A/He}\right)_{Co^{++}}}{\left(\sqrt{k'_c D_A/He}\right)_{Cu^{++}}} = 1.97 \pm 0.16$$

and so obtained $\sqrt{k'_c D_A/He}_{Cu^{++}} = (7.3 \pm 0.9) \times 10^{-3}$ cm/sec. The value he ascribed to He for his experiments was 69 so $k'_L = \sqrt{k'_c D_A} = 0.5$ cm/sec. for copper catalysed sulphite.

His next step was to find out whether the rate controlling/

controlling step was a chemical reaction or a mass transfer process by measuring the specific oxygen absorption rate at different temperatures. He rejected the agitated gas-liquid contactor because in this apparatus the combined effect of the influence of the liquid properties and possibly reaction rate on both k_L' and a would be measured. Instead he used a vertical 1 cm diameter glass tube containing copper catalysed sulphite up through which pure oxygen was bubbled. The bubbles soon joined to form bullet shaped slug bubbles from 2 to 8 cms long. For a given gas flow rate the number of these bullet bubbles formed and therefore the interfacial area was constant and independent of temperature. An Arrhenius plot of log $k_L'a$ against $1/T^{\circ}K$ was drawn and the apparent activation energy found to be 8250 cals/g.mole. This was high enough to conclude that the absorption rate must have been governed by a chemical reaction in the liquid film. As a was constant this was in effect the activation energy of k_L' which if it is equal to $\sqrt{k_c' D_A}$, then the activation energy for $k_c' D_A$ is 16,500 cals/g.mole. That for D_A can be calculated as 4200 cals/g.mole. so that for the first order rate constant k_c' must be 12,300 cals/g.mole.

From all the foregoing he concludes that for a 0.8M Sulphite solution more than 5×10^{-4}M in cupric ions the absorption is indeed controlled by a chemical reaction/

reaction in the liquid film and $k'_L = \sqrt{k'_c D_A}$, and numerically equal to 0.5 cm/sec, which is independent of hydrodynamic conditions as long as $k'_L / k_L > 2$.

2. CRITICISM.

When the interfacial area in a sparged gas-liquid contactor containing 0.8M Sulphite 10^{-3}M in copper sulphate was measured using the light-transmission probe developed by Caldertank (149), the value of k'_L calculated from this area and the oxygen absorption rate was found to be about sixteen times less than the value of $\sqrt{k'_c D_A}$ obtained by Westerterp. Two questions then arose:
1) Are the conditions such that $k'_L = \sqrt{k'_c D_A}$ satisfied or 2) Is the quoted value of $\sqrt{k'_c D_A}$ in error? Question one cannot be answered unless we know the answer to question two. Taking up the point of the value of $\sqrt{k'_c D_A}$, we must bear in mind it was obtained by comparing the rates of absorption of cobalt and copper catalysed solutions in an agitated gas-liquid contactor and using the ratio of the rates to convert a value of k'_L for cobalt catalysed sulphite in a liquid jet to that for copper catalysed solutions. In fairness to Westerterp, at the time he carried out his experiments there was no evidence to suggest that the reaction accompanying absorption of oxygen in cobalt catalysed sulphite was in any way different from that accompanying absorption into copper/

copper catalysed sulphite, except that the absolute rate was higher. However Yagi and Inone (128) and Harris and Roper (138) have since demonstrated convincingly that it is in fact accompanied by a second order reaction, not a first order one as with copper catalysed sulphite. Provided then, that the value of $\emptyset$ was > 5 (see Chapter I, equation (21a)) in Westerterps liquid jet experiments, which he estimated was so, then his value of k'_L would have been $\sqrt{k''_c D_A C_B}$, not $\sqrt{k'_c D_A}$. If it could be shown that in the agitated gas-liquid contactor he used, that the values of k'_L for cobalt and copper catalysed solutions were equal to $\sqrt{k''_c D_A C_B}$ and $\sqrt{k'_c D_A}$ respectively and thus independent of the agitation, then the ratio of absorption rates would be the same as the ratio of k'_L's all other things being equal. But results from this work, to be described in the next chapter, and from that in the literature, indicate that the absorption rate into copper catalysed sulphite in agitated sparged fermentors is of the same order as the physical absorption of oxygen into water at 30°C so for this case $\emptyset \approx 1$ and $k'_L \neq \sqrt{k'_c D_A}$. This then invalidates the method of comparative rates used by Westerterp to evaluate $\sqrt{k'_c D_A}$. In addition, as k'_L for cobalt catalyst in the stirred sparged contactor was only twice that for copper, then in this case too, $\emptyset$ was probably less than 5 and so $k'_L \neq \sqrt{k''_c D_B D_A}$. As a result one would assume that the chemical/

chemical reaction rate is not the controlling step in an agitated gas liquid contactor with subsurface aeration, with either cobalt or copper ions as catalysts.

Westerterp's observations with the bullet shaped bubbles in the glass tube showed that the controlling step in that situation was a chemical one as evidenced by the high activation energy. Unfortunately he did not evaluate the interfacial area of the bubbles so a value of k'_L cannot be calculated. As it was chemically controlled, then presumably $k'_L = \sqrt{k'_c D_A}$ and it would have been interesting to know the numerical value for comparison.

In the next chapter experiments are described which attempt to measure values of k'_L in apparatus of the sparged fermentor and horizontal surface type as well as a bubble column; and to study how they are affected by change in temperature in each case, as this gives a good indication as to what process is controlling, a physical or chemical one.

CHAPTER III

Experimental Work

GENERAL CONSIDERATIONS

A survey of the literature on oxygen absorption by catalysed sodium sulphite yields a wealth of information, of which much is well authenticated. However there still remain areas of speculation such as the actual reaction mechanism, the effect of temperature, and the rate controlling step under different experimental conditions. In planning this experimental program the first and foremost object was to try to find a value of the overall mass transfer coefficient k'_L that could be used to calculate interfacial areas in three phase dispersions, the study of which is the main purpose of this thesis. Westerterp proposed that for copper catalysed sulphite in a sparged fermentor, the absorption rate was chemically controlled and that $k'_L = \sqrt{k'_c D_A}$, which is independent of hydrodynamic conditions and dependent only on temperature. As shown in the previous chapter, this proposal is extremely doubtful. In view of this it was necessary, first of all, to carry out experiments in similar equipment to that used by Westerterp and with the advantage of knowing the interfacial area from light transmission/

transmission measurements, actually calculate k_L' over a range of experimental conditions. The second object was complimentary to the first and was to try and discover something about the rate controlling process itself. A point that became clear from the survey was the difference in behaviour of the absorption rate into copper and cobalt catalysed solutions in a stirred vessel with the liquid surface as the interface. As agitation was increased the absorption rate increased for cobalt but decreased for copper catalysed solutions - why was there this opposite effect in the two cases? Schultz and Gaden suggested, in the case of decreased absorption rate into copper catalysed solutions, that it was due to the increased agitation reducing the time-average concentration level in the liquid film of a reaction intermediate. But unless there is a difference in mechanism or rate controlling step for the two catalysts, they should both be similarly affected. Beyond establishing that the rate controlling step is in the liquid phase no one has yet discovered its nature.

The simplest way of telling whether a rate controlling process is chemical or physical is to measure rates over a range of temperatures, and to calculate the activation energy from an Arrhenius plot of the data. Chemical processes are associated with an activation energy over 10 k cals/g.mole and physical ones around 4 to 5 k cals/g.mole.

The/

The types of gas-liquid contactors used by most workers have been stirred vessels with the liquid surface acting as the interface, aerated agitated vessels (fermentors) and unagitated bubble columns. By an experimental study of the effect of temperature on the absorption rate of oxygen in these three types of equipment it was hoped to:

1) determine what, if any, were the differences between cobalt and copper catalysed sulphite in a stirred vessel and

2) make the decision which catalyst would be most suitable for calculating, from the mass transfer data, interfacial areas in a gas-solid-liquid bubble dispersion.

The experimental program was therefore divided into three sections. The first using a stirred cell of the erlenmyer type (500 ml) where the interface was the liquid surface: the second, a sparged agitated and fully baffled tank, similar to that used by Westerterp; and the third, a bubble column 6" in diameter and 2'6" high.

A. The Stirred Cell

1. Description

Refer to figure (1). A 500 mls erlenmyer flask acted as the reaction vessel. It had a glass covered magnet as a stirrer which was driven remotely by the magnetic/

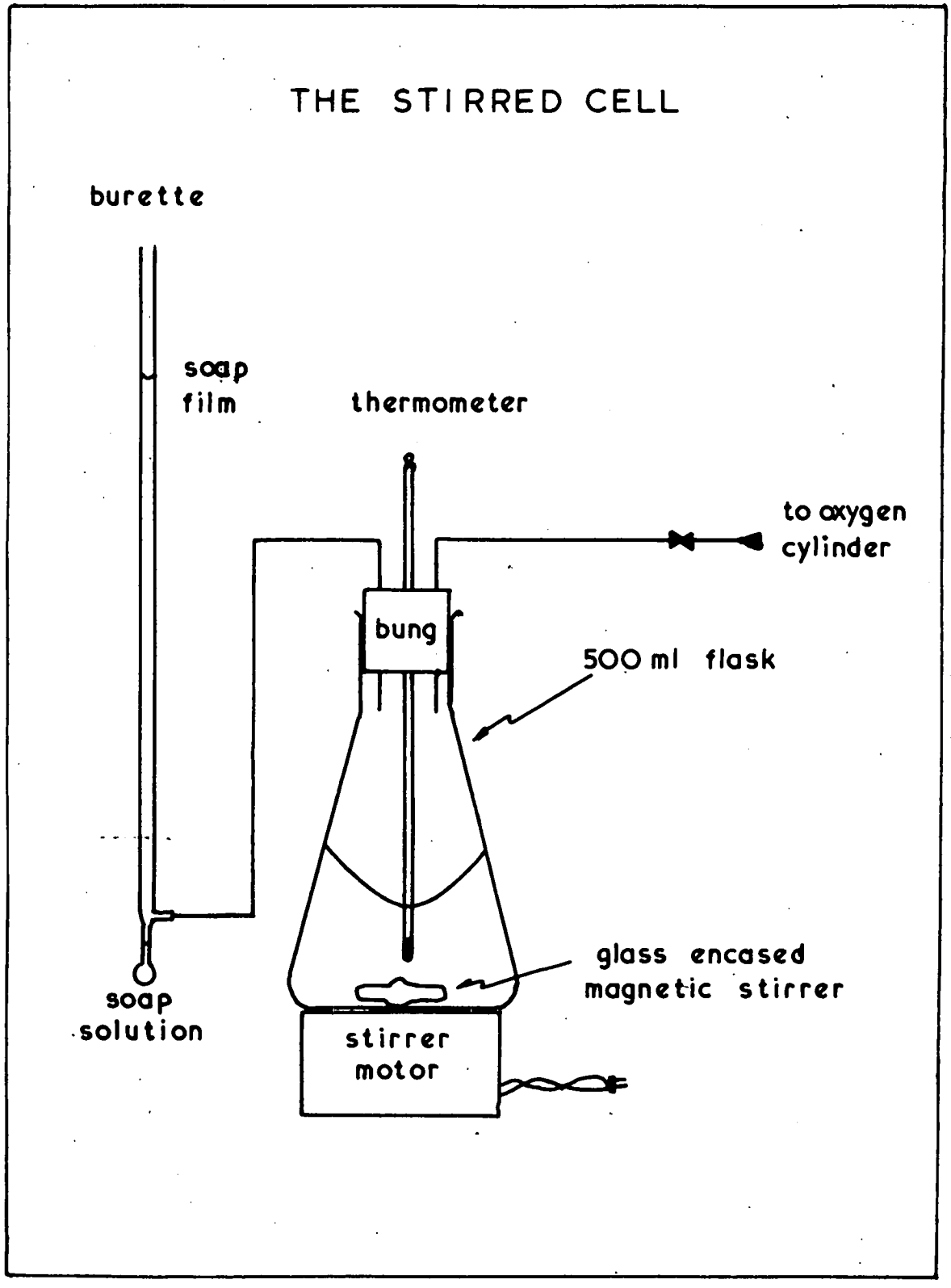
THE STIRRED CELL
burette
soap film
thermometer
to oxygen cylinder
bung
500 ml flask
glass encased magnetic stirrer
soap solution
stirrer motor

FIGURE 1

magnetic stirrer motor, placed under the base of the flask. A stopper in the neck of the flask carried a thermometer which extended into the liquid, a tube connected to an oxygen cylinder and another to a soap film gas flow meter.

2. Operation and Experimental Work.

The flask was charged with catalysed sulphite solution heated to the desired temperature, and the stirring motor switched on. Oxygen from the cylinder was passed through the cell and out through the soap film meter. After thoroughly purging the gas space above the liquid, the oxygen supply line was closed. The temperature was then read and the position of the soap film recorded. After a given length of time, thirty seconds to five minutes, the temperature was again read and the soap film position recorded. There was no temperature control of the apparatus but the length of each experiment was adjusted so that a fall in temperature was never more than half a degree centigrade. A series of measurements at several temperatures could be done with one solution when using copper as a catalyst once it was established that the absorption rate was independent of sulphite concentration over the range used 0.9M to 0.4M. It simply involved charging the flask with a solution at about 50°C (which was the highest/

highest used because of the faster cooling at higher temperatures) and cooling the flask to obtain a drop in temperature for each subsequent run. In the case of cobalt catalysed solutions a fresh charge was made for each run. Catalyst concentrations were 10^{-3}M in all cases.

Cooling Correction. Above room temperature the liquid in the flask cooled at a rate depending on the temperature difference and at 40°C this was 0.8°C per minute. This would cause the oxygen in the gas space to cool too and this would result in a positive error in the absorption rate measured, of the order of 6% at the highest temperature used. From the rate of cooling of the liquid recorded during and in-between absorption runs, and assuming all the gas was at the temperature of the liquid a correction factor versus temperature was calculated, and is shown in figure (47). The value of the correction factor expressed in cm^3/sec must be subtracted from the measured absorption rate at a particular temperature.

3. Treatment of Experimental Data

The experimental results were a series of oxygen absorption rates expressed in cm^3/sec obtained from the soap film meter. The overall mass transfer coefficient, k_L' was calculated using the equation:

$$N_{sc} = k_L' A.C.^{*} f \qquad \ldots\ldots (1)$$

where/

where N_{sc} is the absorption rate (gms oxygen/sec), A is the interfacial area (cm^2), C^* is the solubility of oxygen in pure water (gm/cm^3) and f is the salt factor to correct for the effect of the presence of sulphite salt on the oxygen solubility.

The solubility of oxygen in sodium sulphite solutions was assumed to be the same as in sodium sulphate solutions and this is given in Siedell (160) at 25°C. It was further assumed that the effect of temperature on this solubility is the same as its effect on the solubility of oxygen in pure water. The data of Siedell can then be used to plot a graph of the correction factor, referred to as the salt factor, against sulphite concentration, which can be applied to the pure water solubility at any temperature to convert it to the solubility in sodium sulphite at any strength from zero to 0.9 molar. This salt factor varies from 1.0 at zero sulphite concentration to 0.40 at 0.9M. Figures, (48) and (50), in Appendix II, are plots of oxygen solubility in pure water and [redacted] and the salt factor dependence on sulphite concentration respectively. The area of the liquid surface in the stirred cell was calculated from the equation

$$A = \pi r\sqrt{r^2 + d^2} \qquad \ldots\ldots \quad (2)$$

where r is the radius of the top edge of the vortex and d the depth, both measured in cms. For each experiment the/

the same volume of liquid was added and the stirrer motor had only one speed of rotation - thus the value of A was constant.

An Arrhenius plot of k'_L against $I/T^{\circ}K$ was made to evaluate the activation energy of k'_L. The slope of the straight lines obtained is $\frac{Ea}{R}$, where Ea is the activation energy in $\frac{cals}{g.\ mole}$ and R is the gas constant whose value is 1.987 cals./g.mole $^{\circ}K$.

4. Results

(a) Copper catalysed sulphite

Values of k'_L were calculated over a range of temperatures from 46.5° to 15.2°C for solutions from 0.4M, 0.8M and 0.9M. in sulphite and 10^{-3}M in copper sulphate. The effect of possible contaminants to be met with in the three phase fluidized bed column was tested by placing small quantities of sand, brass filings, copper wire and stainless steel gauze in the flask. The results are tabulated in Table 1 and plotted in figure (2). It will be seen that the points for all the results are in a definite band and 94% of them lie within $\pm$ 15% of the best line. Results from runs with stainless steel gauze in the flask were erratic ranging from very high to very low values of k'_L and are not tabulated. The activation energy associated with k'_L calculated from the line was found to be 16,500 cals./ g.mole/

STIRRED CELL RESULTS – COPPER CATALYST

k_L' vs $\frac{1}{T}$

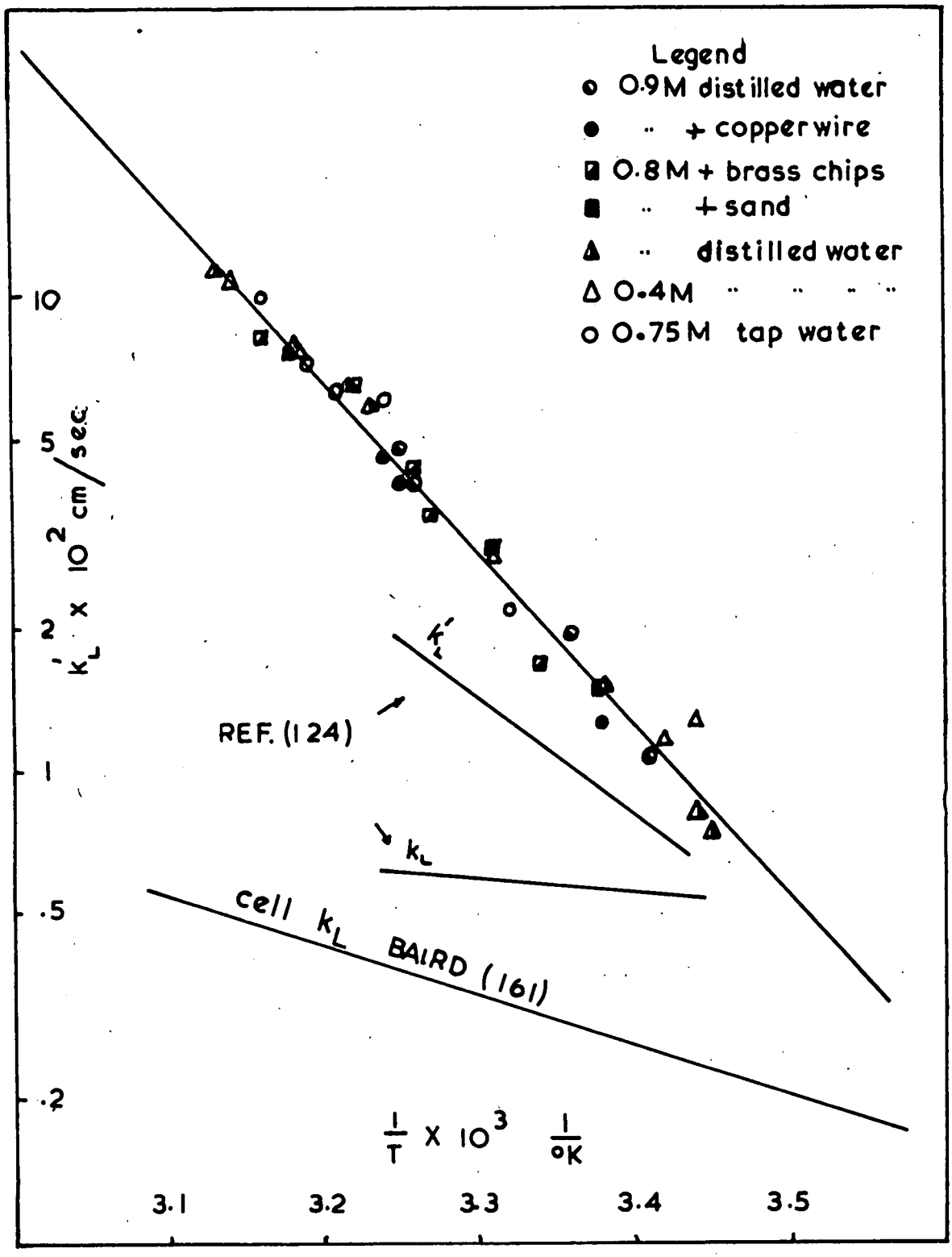

FIGURE 2

g.mole. which shows conclusively that in this case a chemical process is controlling. A plot of the physical mass transfer coefficient, k_L , obtained by Baird (161) using a similar cell and the same stirrer motor and measuring the absorption of CO_2 into water, is also shown on Figure (2). From this it is seen that $k'_L / k_L > 3$ at the lowest temperature used.

(b) Cobalt catalysed sulphite

Values of k'_L were calculated over a similar range of temperatures, from 5.8°C to 55.5°C for solutions 0.04, 0.1, 0.2, 0.4 and 0.8M in sulphite and 10^{-3}M in cobalt sulphate. The results are tabulated in Table 2 and plotted in figure (3). Unlike the results with copper catalysed sulphite, in this case there was a separate line for each sulphite molarity and the activation energies associated with each line increased slightly as the molarity decreased. The values Ea ranged from 4880 $\frac{\text{cals}}{\text{gmole}}$ at 0.8M to 5980 $\frac{\text{cals}}{\text{gmole}}$ at 0.04M sulphite.

5. Discussion

(a) Copper catalysed sulphite

It is clear that the value of k'_L is independent of sulphite concentration over the range studied. This was expected and has merely confirmed what the literature has already/

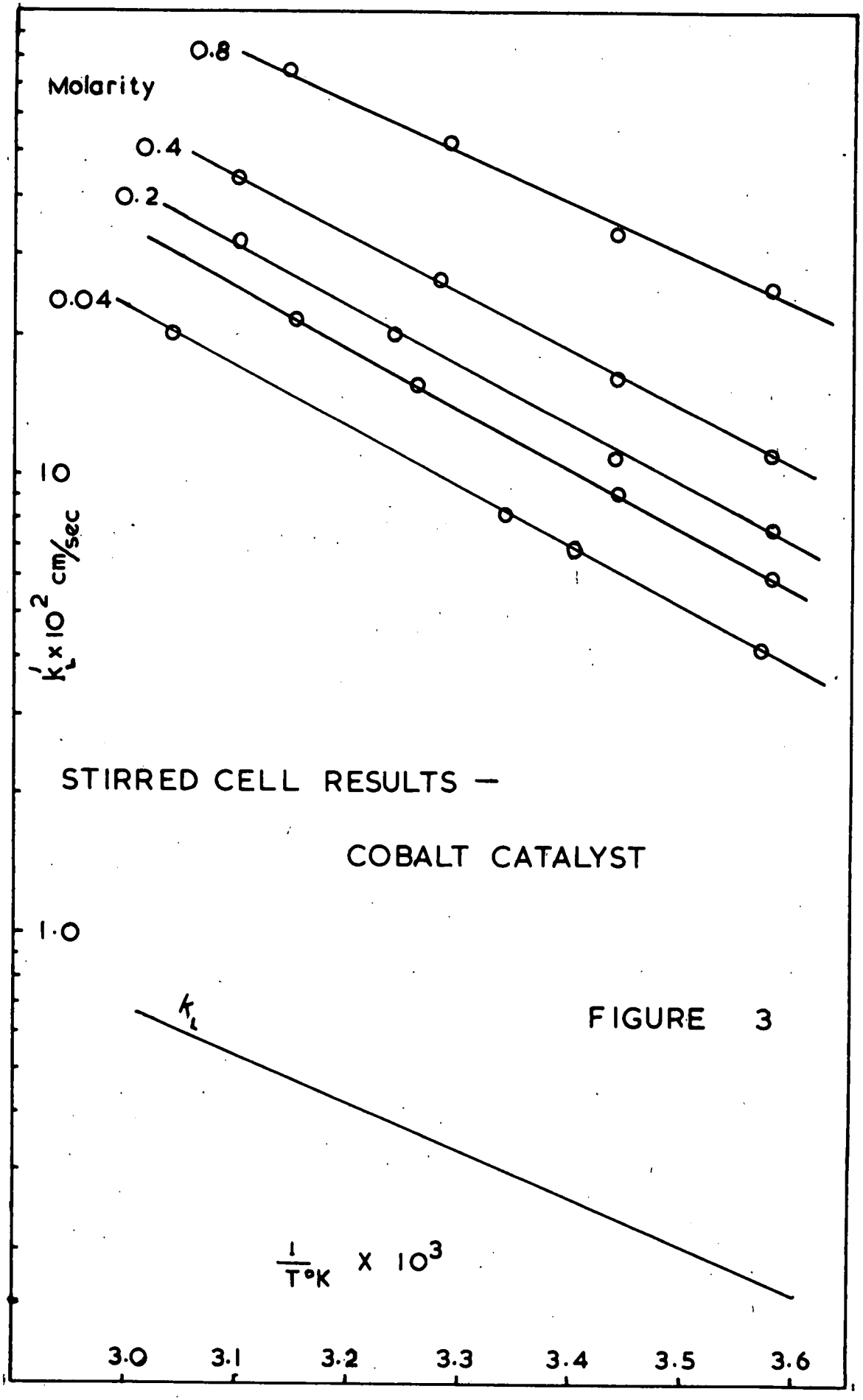
Molarity
0.8
0.4
0.2
0.04
10
$k_L' \times 10^2$ cm/sec
STIRRED CELL RESULTS —
COBALT CATALYST
1·0
k_L
$\frac{1}{T°K} \times 10^3$
3.0
3.1
3.2
3.3
3.4
3.5
3.6

FIGURE 3

already established. The actual value of sulphite molarity at which the absorption rate would begin to be dependant has been quoted as 0.2M by Phillips and Johnson (126) for a similar stirred vessel, whereas for a sparged fermentor it is as low as 0.008 according to these same authors. The activation energy of k_L' obtained was 16,500 cals./g.mole which indicates that the absorption is definitely chemically controlled. This would then support the explanation of the decrease in rate due to increased agitation in a stirred vessel, put forward by Schultz and Gaden (120). It is clear that if the k_L is low enough then in the case of copper catalysed sulphite the absorption rate is independent of k_L. No effect of changes in k_L could be studied here, unfortunately, as the stirrer motor only had one speed of rotation.

As k_L'/k_L is greater than 3 over the whole range of temperatures and as high as 20 at 45°C, then equation (21) in Chapter I is satisfied. This means that $k_L' = \sqrt{k_c' D_A}$, so at 30°C from the line on figure (2) $\sqrt{k_c' D_A} = 2.9 \times 10^{-2}$ cm/sec. If $D_A = 2.7 \times 10^{-5} \frac{cm^2}{sec}$, then $k_c' = 31 \text{ sec}^{-1}$. Other estimates of the value of k_c' at 30°C are as follows:

Schultz and Gaden (120)	15 sec^{-1}
Carparni and Roxburgh (124)	7 sec^{-1}
de Waal (139)	50 sec^{-1}

Carparni/

Carparni and Roxburgh are the only other workers to have used a stirred cell and studied the effect of temperature. Their results are also plotted on figure (2) and have a lower activation energy of 10.6 k.cal/g.mole. They are displaced to the left and lower than the results obtained here. However they do measure the value of k_L' for oxygen into water and this is plotted too. If this is considered to be a measure of the physical k_L, then it is seen that only at the higher temperatures is $k_L'/k_L > 2$ and so in their case, most of the time $k_L' \neq \sqrt{k_c D_A}$. This may explain the lower activation energy and their results must then be considered to be in the transition between physical and chemical control, and nearer to the chemical. This transition between the two controlling processes will be brought out more clearly when the results from the bubble column are discussed later.

(b) Cobalt catalysed sulphite

The values for k_L' obtained using cobalt catalysed solutions showed quite a different trend from those using copper. For any given temperature the value of k_L' depended on the molarity of the solution, and so a series of points was obtained for each sulphite concentration. According to the literature (129,138) oxygen absorption into cobalt catalysed sulphite solutions/

solutions is accompanied by a fast second order reaction in the film. Sherwood and Pigford (162(a)), examining such a situation consider the reaction proceeds so quickly that it is controlled by the rate at which the dissolved gas and solute can diffuse through the film to the reaction zone, and derive the following equation for the overall liquid phase mass transfer coefficient:

$$k'_L = k_L \left(1 + \frac{1}{2}\left(\frac{DB}{DA}\right)^{1/2} \frac{CB}{CA_i}\right) \quad \ldots\ldots (3)$$

from which it can be seen that k'_L is the value of k_L enhanced by a factor which will vary as the first power of the solute concentration in this case the sulphite concentration. The absorption will therefore be physically controlled. From this one would expect to get a series of curves of a low slope on an Arrhenius plot. The actual curves in figure 3 have activation energies from 4880 cals/g.mole to 5980 cals/mole which are higher than the expected value generally found in the case of diffusion controlled processes in liquids namely between 4 to 5000 cals/g.mole. However another discrepancy in the results is that the value of k'_L for any given temperature varies almost as the 0.5 power of the sulphite concentration, except for the interval between 0.4 and 0.8M where it does vary as the first power. In Figure (4) the values of k'_L are plotted against sulphite molarity on log-log paper for three temperatures 20°, 30° and 40°C. It is interesting to note here that

Sherwood/

STIRRED CELL — COBALT CATALYST

k'_L vs SULPHITE MOLARITY

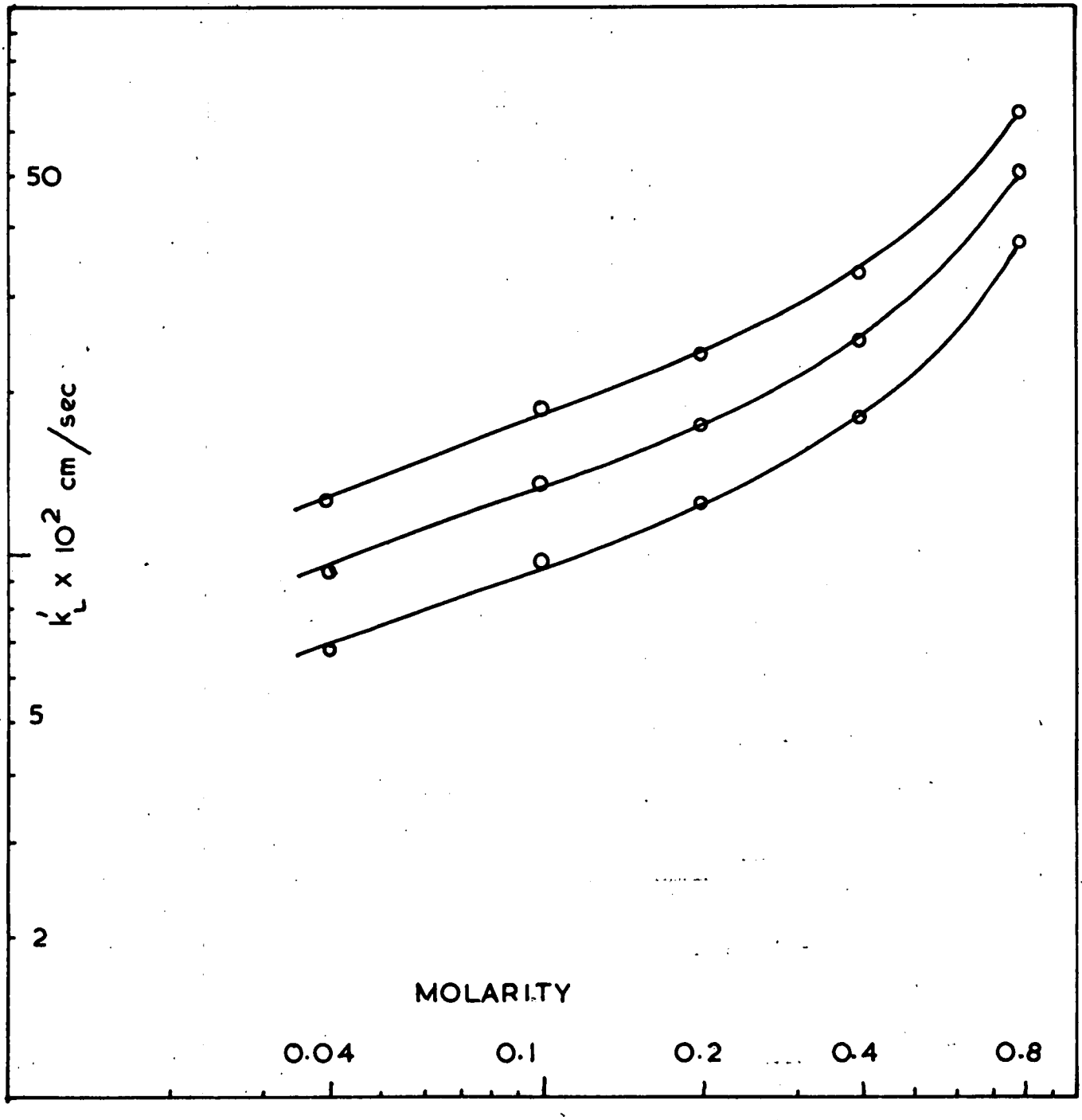

FIGURE 4

Sherwood and Pigford (162 (b))$_2$ after deriving a similar equation to (3) for the case of unsteady-state absorption in the liquid film accompanied by a rapid second order irreversible reaction, they add the statement: "A study of the case leads to the conclusion that k'_L increases in proportion to $\sqrt{\frac{CB}{CA_i}}$, rather than to the first power of this ratio." No explanation is given.

From the magnitude of the activation energies and their change with molarity, as found here, it would appear that the process is in transition between chemical and physical control. As the molarity is increased it approaches physical control and as it decreases it tends more to chemical control. This behaviour can be explained at least qualitatively by considering the approximate solution of the differential equations, obtained in an analysis of absorption accompanied by a second order chemical reaction, by Van Krevelen and Hoftijzer (163). They calculated a series of curves as shown below:

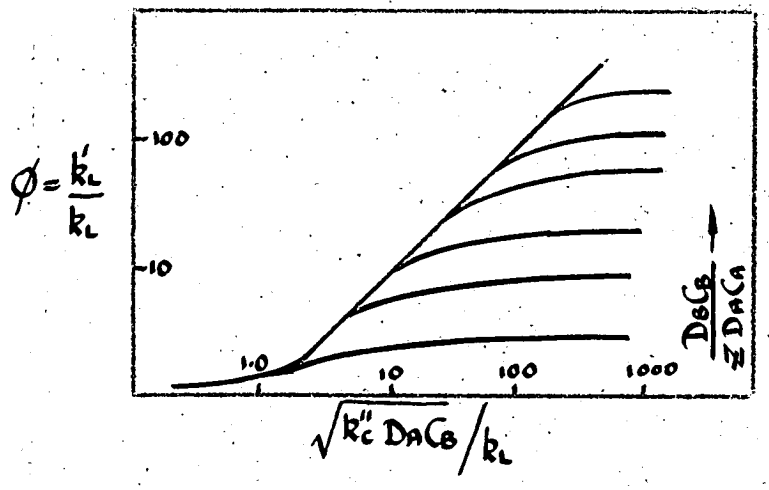

Van Krevelen Plot

Above a value of $\phi = k'_L / k_L > 5$, see equation (21a) Chapter I, we see a straight line at 45° which represents the situation where $k'_L = \sqrt{k''_c D_A C_B}$ and where the reaction is a psuedo first order one. The family of lines for different values of the enhancement $\frac{DBCB}{DACAi}$ spread out to the right and soon become horizontal. For the situation where experimental values of k'_L / k_L lie on the 45° line the activation energy would be that associated with a chemical reaction and where they lie on the horizontal portions would be that associated with a diffusion (physical) process. On the curved sections in between the two limits one would expect intermediate values of activation energy.

If the value of k''_c can be established the stirred cell results can be plotted on a Van Krevelen plot since all other values, k_L, DA, CB and k'_L are known. It was thought valuable therefore, at this point to survey briefly values of k''_c that can be obtained directly or calculated from the results of other workers.

Westerterp (130),

satisfied himself that $\phi = k'_L / k_L > 6$ and so his value of 1.44×10^{-2} cm/sec at 30°C for k'_L was really $\sqrt{\frac{k''_c D_A C_B}{He}}$, not $\sqrt{\frac{k'_c D_A}{He}}$ so we can say:

$$\sqrt{k''_c D_A C_B} = 1.44 \times 10^{-2} \times 69$$

k /

$$k_c'' = (1.44)^2 \times 69^2 \times 10^{-4} / 2.7 \times 10^{-5} \times 0.80 = 45{,}600 \frac{cm^3}{gmole.sec.}$$

Yagi and Inone (129) tabulated date for $\frac{\sqrt{k_c'' D_A C_B}}{ck_L}$ at 20°C and using their assumed value of $k_L = 6 \times 10^{-3}$ cm/sec and $D_A = 2.4 \times 10^{-5}$ cm/sec. values of k_c'' can be calculated. The results are tabulated below.

Calculation of k_c'' from date of Yagi and Inone (129)

$\frac{\sqrt{k_c'' D_A C_B}}{k_L}$	C_B gmole/ℓ	$[Co^{++}]$ gmole/ℓ	k_c'' $\frac{cm^3}{gmole.sec}$
17.8	0.275	7.78×10^{-5}	1730
9.44	0.079		1690
7.60	0.051		1700
6.20	0.034		1690
9.21	0.051	11.67×10^{-5}	2490
7.53	0.034		2500
12.3	0.075	3.89×10^{-5}	825
6.63	0.079		835
4.39	0.034		851
8.74	0.275	1.95×10^{-5}	416
4.69	0.079		417
3.07	0.034		416
5.57	0.275	7.78×10^{-6}	172
2.98	0.079		168
1.97	0.034		171

Extrapolates to 21,000 cm^3/g.mole.sec. at 10^{-3}M Cobalt.

They varied the value of cobalt concentration to change the value of k''_c so they would have a series of points to compare with the Van Krevelen solution, and so an ex trapolation of their value of k''_c must be made to a cobalt concentration of 10^{-3}M as used by Westerterp and in this work. Figure (5) shows this extrapolation and others. In the case of Yagi and Inone's data the value of k''_c varies as the first power of the cobalt concentration, and extrapolates to 21,000 $\frac{cm^3}{g.mole\ sec}$ at 10^{-3}M Cobalt sulphate. This agrees well with Westerterp if one assumes that k''_c doubles every $10^{o}C$, but it also raises doubts about the absorption rate being independent of cobalt concentration above 10^{-4}M.

De Waal (139) recently measured k'_L over a range of cobalt concentrations from 2.5×10^{-5} to 10^{-3}M and at a sulphite concentration of 0.8M. He also found a linear dependence of k'_L with cobalt concentration, and also a marked effect of pH. He actually quotes values of $\sqrt{\frac{kD}{He}}$, where k is the pseudo-first order rate constant and he also assumes that the rate is independent of sulphite concentration at 0.8M. However, to be accurate and for the purposes of comparison his value of $\sqrt{\frac{kD}{He}}$ should be considered to be $\sqrt{k''_c D_A C_B}/He$, i.e. that $k = k''_c C_B$. By extrapolating his experimental lines to 10^{-3}M cobalt values of k''_c can be calculated at this concentration for/

for each pH: See the table below.

Calculation of k''_c from data of de Waal (139)

from extrapolated values of $\sqrt{kD}/He$ to $[Co]^{++} = 10^{-3}M$

$\sqrt{kD}/He$ @ 30°C (cm/sec)	pH	k''_c 30°C $\left(\frac{cm^3 \times 10^{-2}}{g\ mole\ sec}\right)$	20°C
4.65	7.5	47.7	23.9
6.46	8.0	91.8	45.9
8.44	8.5	157.0	78.5
	9.0	206	103

The value of k''_c for against pH can then be extrapolated to pH = 9.0 which is the value of a freshly prepared solution of sulphite used by Westerterp, Yagi and Inone, Harris and Roper and in this stirred cell work. After these two extrapolations procedures the value of k''_c = 20,600 $\frac{cm3}{g.mole\ sec.}$, at 30°C. or 10,300 $\frac{cm3}{g.\ mole\ sec}$ at 20°C. This is just under a half the value obtained from Westerterp and Yagi and Inone. De Waal used a packed column for his experiments but no details were given in his communication. Harris and Roper (138), using a stainless steel sieve plate measured absorption rates into cobalt catalysed sulphite at 20°C and represented their results on a Van Krevelen plot in the same/

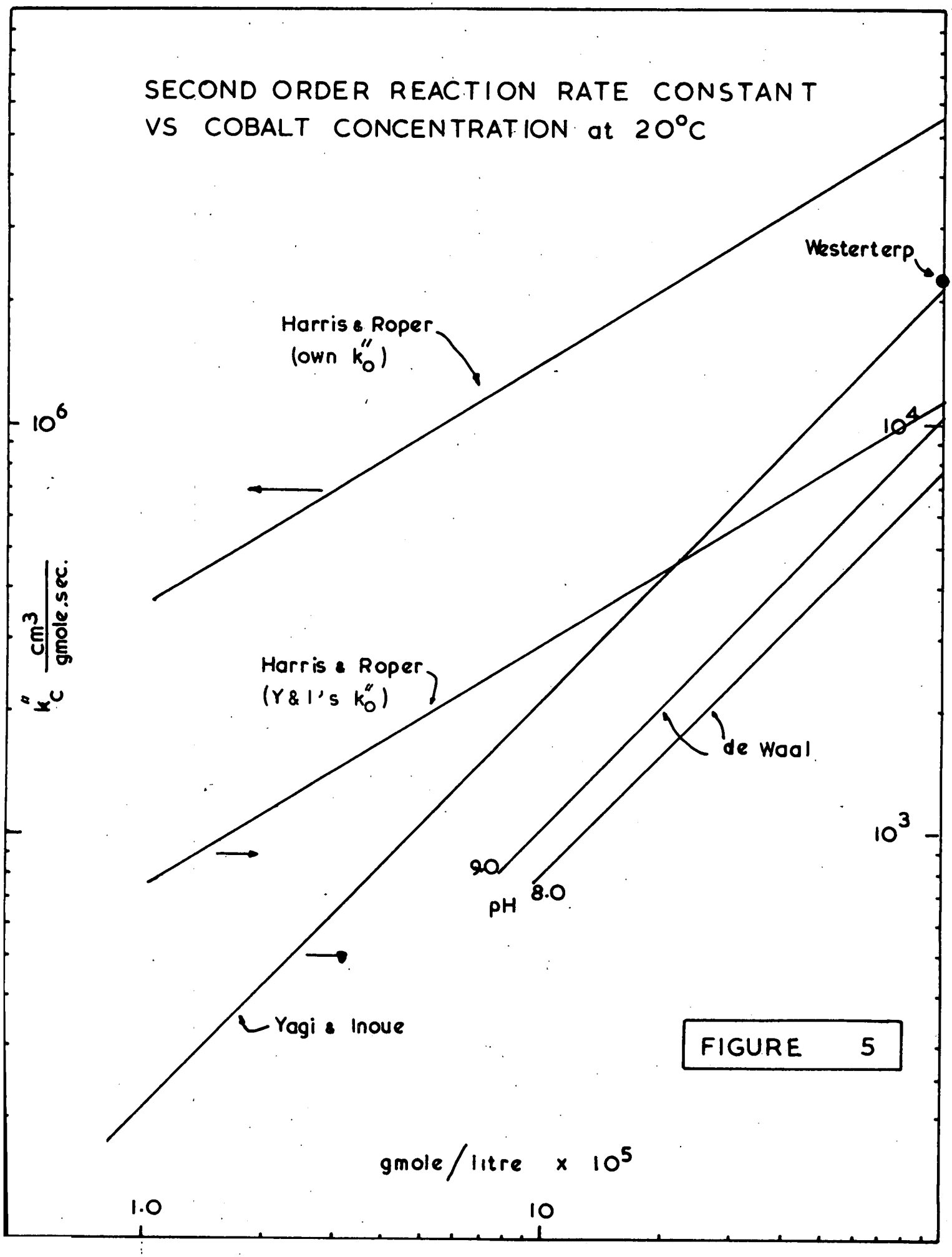
SECOND ORDER REACTION RATE CONSTANT
VS COBALT CONCENTRATION at 20°C
Westerterp
Harris & Roper
(own k_o'')
10^6
10^4
k_c'' $\frac{cm^3}{gmole.sec.}$
Harris & Roper
(Y & I's k_o'')
de Waal
10^3
9.0
pH
8.0
Yagi & Inoue
gmole/litre x 10^5
1.0
10

FIGURE 5

same way as Yagi and Inone. However they used a value of the second order rate constant, k''_o , of uncatalysed sulphite which would make their values of k''_c from their own correlation

$$k''_c = k''_o (1 + 1.53 \times 10^5 [Co]^{++\ 0.59}) \frac{ft^3}{lb\ mole.sec} \quad \ldots\ldots (4)$$

where $[Co]^{++}$ is the cobalt concentration in lb.moles/ft^3, fit their data with Van Krevelen's solution. This value of k''_o had to be 1.1×10^4 ft^3/lb.mole.sec, whereas Yagi and Inone measured it by the polarographic method and found it to be 22.4 ft^3/lb mole.sec. The value of k''_c from equation (4) at $[Co]^{++} = 10^{-3}$Molar, is 5.49×10^6 $\frac{cm^3}{g.mole.sec}$ using $k''_o = 1.1 \times 10^4$ ft^3/lb mole.sec., but using $k''_o = 22.4$ $\frac{ft^3}{lb.\ mole.sec}$ it is 11,200 cm^3/g.mole.sec. This latter value seems more reasonable and does agree with de Waal's extrapolated value. A possible reason, put forward by Harris and Roper, for the large difference between their results and Yagi and Inone's was that their runs were contaminated with a positive catalyst present in the stainless steel plate, and in the light of this author's and other's (126,128,138) work, this seems very likely.

Figure (5) shows values of $k''_{c\ 20^0C}$ plotted against cobalt ion concentration on a log-log plot for all the workers reviewed above, and it will be seen that only Harris/

Harris and Roper's results do not show a linear relationship between k_c'' and cobalt concentration.

Returning to the stirred cell results we must now choose a value for k_c'' at 10^{-3}M cobalt. Actually, whatever value is used will only displace the points on a Van Krevelen plot to the left or right, and the slopes of the lines for each sulphite concentration will, indicate whether they should lie on the 45° line or on one of the horizontal lines, or in-between on the curved portion. To make the necessary calculations a value of k_c'' which was the mean of Yagi and Inone's and Westerterp's value at 20°C was used, i.e. $k_c'' = 21{,}900 \ \frac{cm3}{g.mole.sec.}$, and for the results at 30°C and 40°C it was assumed that k_c'' would double for each 10°C. rise. The calculations are tabulated in Table 3 and represented in Figure 6. It will be seen that, as suggested by the trend in activation energies, the points lie in the transition region between the 45° line and the horizontal ones. It appears that a value of k_c'' roughly three and a half times smaller would make them fit the theory, i.e. $k_{c\ 20°C}'' = 6{,}500 \ \frac{cm3}{g.mole.sec.}$.

6. Conclusions

Because of the nature of the absorption of oxygen into cobalt catalysed sulphite, where the rate depends on/

STIRRED CELL - COBALT CATALYST DATA ON VAN KREVELEN PLOT

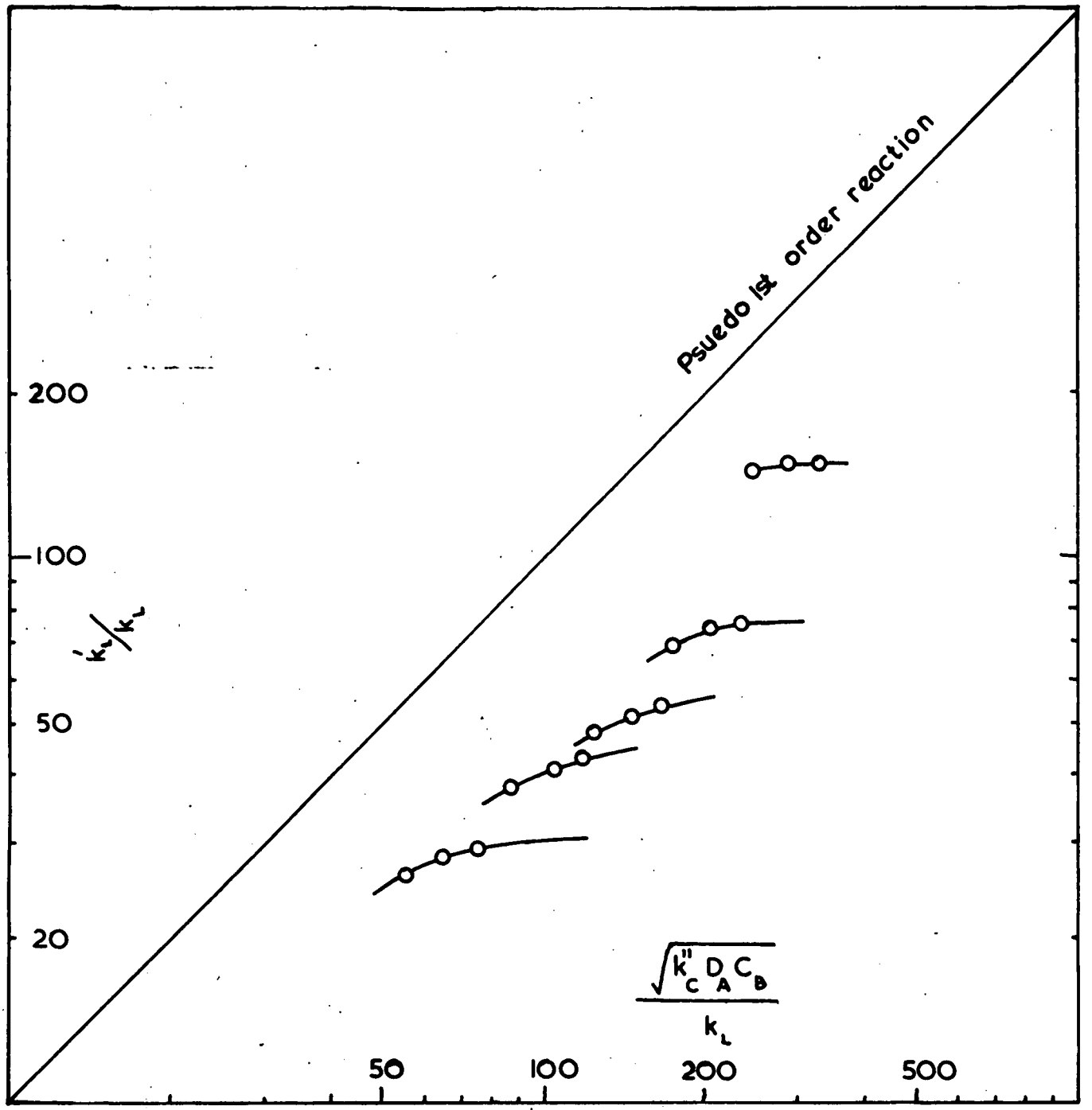

FIGURE 6

on both sulphite and cobalt concentration and the value of k_L ie. the hydrodynamic conditions, it is not suitable for use in the chemical method of measuring interfacial areas, especially when the interfacial area is large and the sulphite concentration drops rapidly. In a situation where the transfer area is small and the liquid volume so large that its concentration remains practically constant, and where the value of k can be estimated, then it could be used. This is not the case in the three phase fluidized bed column. It was therefore decided to discontinue the study of cobalt catalysed sulphite.

In the case using copper as catalyst the stirred cell results showed clearly that where $k_L'/k_L > 2$, the reaction was chemically controlled, and thus the theory put forward for this situation, being absorption accompanied by a first order chemical reaction, seems sound. The results of tests with pieces of brass, copper wire and sand showed that the rate was not affected by their presence but with stainless steel both high and low values were recorded. Using hot tap water to make up the sulphite solution caused no difference in the measured absorption rates. In view of the foregoing it was decided to continue with the study of this system, taking care at all times to exclude any stainless steel or ferrous metal from contact with the solution.

B./

B. The Aerated Stirred Tank

This aerated stirred tank was an exact reproduction in P.V.C. of one that had been used by Romanis (131) in fermentation studies in this department. The oxidation of copper catalysed sulphite solutions that were 0.8M had been used as a means of measuring performance and in the course of this work values of gas holdup and interfacial area as measured by the light transmission probe described by Calderbank (149) had been obtained for a range of stirrer speeds and two air flow rates. These values are shown in Table IV. It was thus convenient to use this piece of apparatus to study the variation in k_L' for a 0.8M copper catalysed sulphite solution. It was the measurement, by Romanis, of k_L' in this tank at 30°C that first showed the discrepancy between it and that predicted by Westerterp, mentioned on page (24). At first it was thought that minute cracks in the araldite coating of the steel tank and the steel stirrer shaft were causing electrolytic deposition of the copper catalyst and thus reducing its catalytic effect. However on reproducing the tank in P.V.C. and electroplating the stirrer shaft heavily with copper to ensure that no copper deposition could take place, the discrepancy was still a sixteen fold difference. In quoting his value of k_L' as $\sqrt{k_C' D_A}$ cm/sec., Westerterp assumed the reaction/

reaction was chemically controlled (see Chapter II) and the results from the following experimental work show that it is physically controlled over the whole range of temperatures used.

1. Description (Refer to figure (7) for a schematic representation)

(a) The Tank

This was 20 inches in height, 15 inches in diameter and fully baffled by four vertical strips the full height of the tank and 1½" wide by ⅛" thick. It was made entirely in ⅛" P.V.C. except for a ¼" P.V.C. base to accommodate tappings for the gas sparger and drain/ line. The whole was sheathed in a 1/16th inch layer of fibre glass to allow it to maintain its rigidity at high temperatures of around 80°C. The impeller, made of brass and mounted on a heavily copper plated steel shaft, was of the turbine type with six square blades. It was 5 inches in diameter, that is one third of the tank diameter which was found to be the most suitable ratio by Calderbank (151) because it gave good gas distribution without undue movement of the free liquid surface. The tank was filled with solution to a depth equal to the diameter, 15 inches, and the impeller set at 7½ inches above the bottom.

A P.V.C. gas sparger having one 1/16" orifice was screwed into the centre of the tank bottom and fed with air/

AERATED STIRRED TANK —
SCHEMATIC DIAGRAM

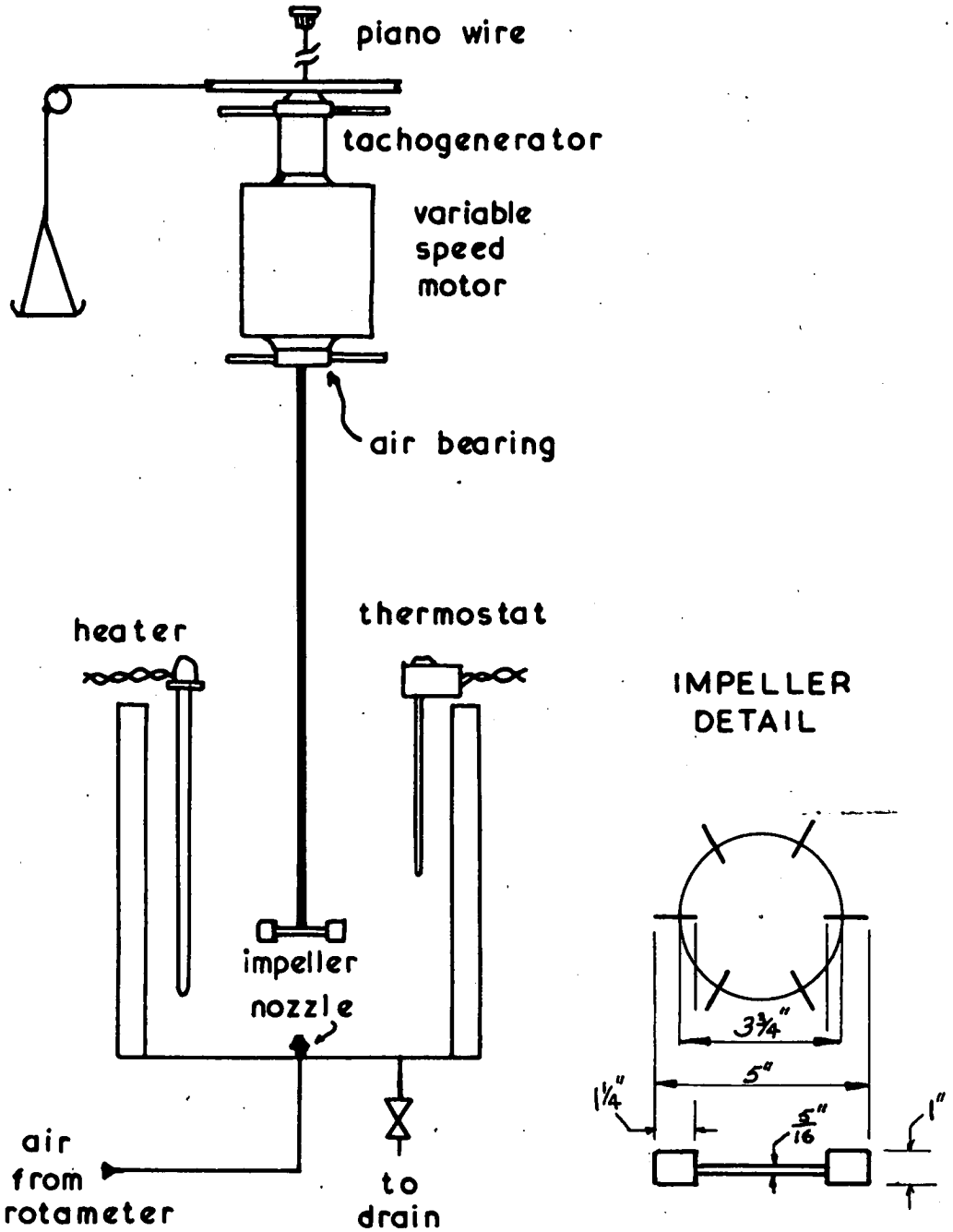

IMPELLER
DETAIL

FIGURE 7

air from a calibrated rotameter. Temperature control was achieved by a quartz sheathed "red-rod" infra-red heater hung in the tank and connected to a Sunvic controller, and a glass water cooler operated manually.

(b) Stirrer Motor and Assembly

The motor was a ½ H.P. Normand Electrical Company D.C. model suspended by a piano wire three feet long, held by a cantilever wall bracket. A Crompton-Parkinson A.C. Tachogenerator was fixed to the top of the motor casing, and was connected electrically to an S. Brod electronic motor controller, which in turn controlled the supply to the motor. A revolution counter was incorporated in the Brod controller and the stirrer r.p.m. could be varied from 0 to 1500 r.p.m. The top of the tachogenerator casing and the bottom of the motor casing were fitted into air bearings which were themselves contained in gimbals rigidly mounted on heavy wall brackets. The dimensions of the air bearings were those recommended by the National Gas Turbine Establishment (171). An air pressure of 30 to 40 lbs/in^2(gauge) was used. A 1 foot diameter pulley was fixed to the tachogenerator casing to enable the torque to be measured by means of a cord, pulley and weighted pan arrangement but this was not used in the work reported here.

2./

2 2. Operation and Experimental Work.

Anhydrous sodium sulphite supplied by British Drug Houses Limited was used to make up the solutions and it was found that it dissolved most readily at a temperature above 60°C. The tank was charged with hot tap water at about 70°C and the stirrer motor switched on. A weighed quantity of sodium sulphite sufficient to make the resulting solution about 0.8M was added slowly. Considerable heat is evolved in the solution and it was for this reason that the tank needed to be sheathed with fibre glass to keep the P.V.C. rigid. Cold water was then passed through the cooler. When the solution had cooled to the required temperature the cooling water was turned off and the red-rod heater switched on, the Sunvic controller having been set previously to control at the desired temperature. After the temperature had remained steady for five minutes the drain cock was opened to allow the solution to run out until it was at a depth of 15 inches. Sufficient of a 1M copper sulphate solution was then added to result in a final concentration of 10^{-3}M. At this point the stirrer r.p.m. was set on the Brod controller to the desired value and the air turned on and adjusted to the required flow rate.

The rise in level of the dispersion surface was measured by an air jet probe attached to a ratchet device with a scale and vernier. The air pressure in the/

the supply line was measured by a water manometer and as the probe came close to the surface this pressure would increase slowly and then jump up as the probe actually touched the liquid surface. At this point the scale was read. The difference in readings before and after aeration gave the increase in height due to the gas bubbles in the dispersion, from which the volumetric fraction of gas in the dispersion, H_g, could be calculated.

Twenty minutes were allowed for the catalyst to be distributed evenly throughout the liquid and steady state conditions to be achieved. 10 ml. samples were then taken at 10 minute intervals for an hour. These were removed by a pipette and transferred to a flask containing a known excess of freshly prepared iodine solution, and after ten minutes were allowed for the reaction to be completed, the excess iodine was titrated with a N/10 Sodium Thiosulphate solution. The analytical procedure is described in detail in Appendix III.

After a few test runs it was found that the sulphite concentration decreased linearly with time, confirming that the oxidation rate was independent of sulphite concentration and so from then samples were taken at twenty minute intervals during the runs which lasted from forty minutes to an hour. Five levels of agitation were achieved by varying the stirrer speed from 200 to 450 r.p.m. and the superficial gas rate from 0.35 to 0.57/

0.57 cm/sec.

One run was performed using pure oxygen as the gas, in place of air, at a higher temperature, 50°C, to see if a gas phase resistance was controlling - there was no significant difference in the value of k'_L from this run and that from the air runs.

3. Treatment of Experimental Data

The results of analysing the samples by titration against a fixed excess of iodine for any one run, was a rate of change in titre volume, r cm^3/min, the following equation was used:

$$N = k'_L \frac{a_{gL}}{(1-Hg)} C^*_{H_2O} f\left(\frac{g.moles}{cm^3 sec.}\right) \quad \ldots\ldots (5)$$

where Hg is the volumetric fraction of the dispersion occupied by the gas and a_{gL} is the interfacial area in $\frac{cm^2}{cm^3 \text{ of dispersion}}$ which has to be divided by (1-Hg) to convert it to an area per unit volume of liquid. As air is used instead of oxygen the value of the solubility is defined by the following equation.

$$C^*_{H_2O} = \frac{p_{O2}}{He\ R\ T} \left(\frac{g.moles}{cm^3}\right) \quad \ldots\ldots (6)$$

uwhere p_{O2} is the partial pressure of oxygen, R the gas constant, T the absolute temperature in °K, and He the Henry's Law distribution coefficient. The rate of change in titre volume, r cm^3/min was converted to a rate of oxygen consumption in g.moles/cm^3 sec. by multiplying it by a constant, C, whose value depended only on the normality of the sodium thiosulphate, the/

the stoichiometry of the basic reaction and the sample volume (see Appendix III). So equation (5) becomes

$$rC = k'_L \frac{a_{GL}}{(1-Hg)} \; Po2/RTHe \; f \; \frac{g.moles}{cm^3 sec.} \quad \ldots\ldots (7)$$

or rearranging for the value of k'_L :

$$k'_L = \frac{rC \; He \; (1 - Hg)}{a_{GL} \; PO_2/RT \; f} \quad \frac{cm}{sec} \quad \ldots\ldots (8)$$

From the data on the solubility of pure oxygen in water quoted in the Handbook of Physics and Chemistry (168), values of He for oxygen from air into water were calculated for different temperatures and plotted in figure (49).

From the measured interfacial area and the gas holdup, the Sauter mean bubble diameter Dm can be calculated from the following equation:

$$D_m = \frac{6Hg}{a_{GL}} \; cm \quad \ldots\ldots (9)$$

4. Results and Discussions

The experimental data and calculated values of k'_L and Dm are tabulated in Table (4) and the values of k'_L are plotted in figure (8). They form a narrow band with a distribution of ±8% around the best line drawn through them, with no definite indication that at the higher agitation level the value of k'_L is any different from that at the lowest. This agrees with the findings of Calderbank and Moo-Young (167) whose results showed that for/

AERATED STIRRED TANK RESULTS

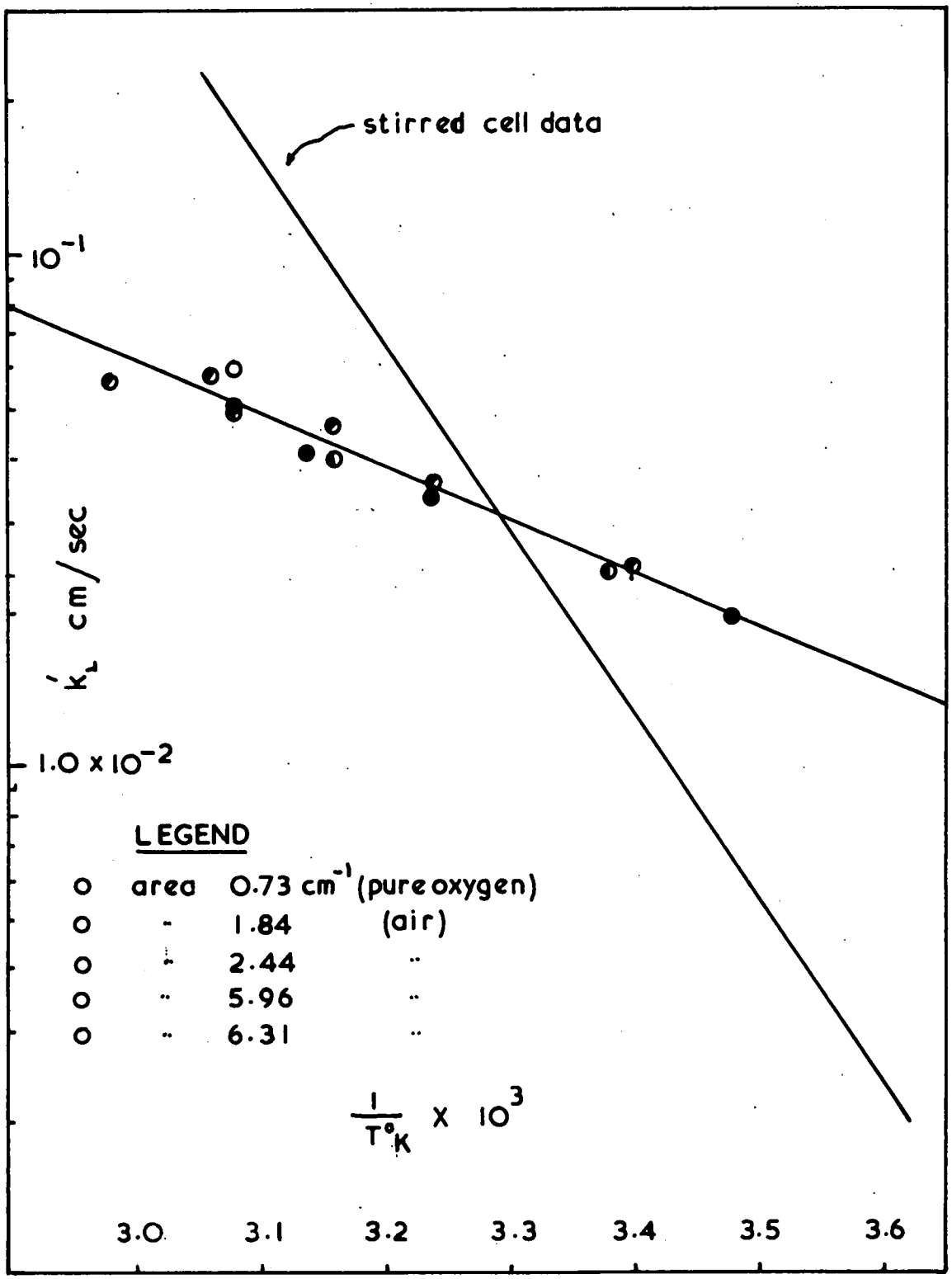

FIGURE 8

for gas bubbles in agitated dispersions and on sieve plates the mass transfer coefficient was a constant value for "small" bubbles with a Dm less than 0.2 cms and a larger but again constant value for "large" bubbles Dm $>$ 0.25 cms. From the holdup and area measurements the value of Dm in these experiments varied from 0.05 cms to 0.19 cms, which are all "small" bubbles, and should have the same k_L .

The activation energy of the best line through the points of figure (8) is 4.8 k.cal/g.mole., which is typical of a diffusion process.

The most surprising thing about these results is that the line has a physical activation energy even beyond the point, i.e. at a higher temperature, where the chemical reaction rate would be expected to control. If the stirred cell data, where the absorption rate was chemically controlled and $k'_L = \sqrt{k'_c D_A}$, is superimposed on figure (8), then it is seen that the stirred cell line crosses the aerated tank line at 30°C. As the chemical rate using copper catalyst is so low, then below 30°C one would expect the physical process to take over control and the value of k'_L fall to k^f_L for the bubble swarm. But at the point above 30°C, when the chemical reaction rate increases it should begin to take control, and when $\sqrt{k'_c D_A}$ is over twice k_L then its control/

control should be complete. This does not happen and leads one to the only conclusion that the chemical reaction rate itself is slowed down, and is much lower than in the stirred cell. Now this is possible if Schultz and Gaden's explanation of the decrease in absorption rate with agitation in stirred cells is accepted.

Their explanation is based on the assumption that the reaction mechanism is a series of steps as suggested by Bassett and Parker, referred to in Chapter II. If the reaction between dissolved oxygen or sulphite and one of the intermediates in the mechanism requires that the concentration of this intermediate is high for it to proceed rapidly, and to completion, and if this intermediate also contains oxygen as suggested by Bassett and Parker, then it is reasonable to assume that the concentration of this intermediate will be higher at the interface than in the bulk of the solution, and so the reaction will proceed rapidly near the interface. If also a finite time is required for this intermediate to build up in concentration, which was suggested by Westerterp for his inability to use copper catalysed sulphite in his liquid jet, then increasing the agitation in the liquid will distribute the intermediate more thinly through the solution as a whole reducing its actual concentration at the interface as well as in the bulk/

bulk liquid. With the reduced concentration of the intermediate in the liquid film the reaction between it and the dissolved oxygen or sulphite will proceed more slowly there, as it will in the bulk liquid. The result would be a change over to diffusion control and the absorption rate would drop to that for the physical absorption of oxygen in water. It can then be appreciated that the amount of agitation could have an increasing effect on the chemical reaction rate depending on how efficient it was at reducing the concentration of the intermediate in the liquid film and so the absorption rate could change from being chemically controlled to physically controlled.

On the basis of this picture it must be assumed that the agitation produced in the aerated tank was sufficiently high at all agitator r.p.m.'s used to keep the absorption rate physically controlled. The drop in absorption rate with increasing agitation in stirred cells with a horizontal liquid surface as the interface has been well established (11,120,124,126,128,134) but in aerated vessels, when no interfacial area measurements have been made, an increase in agitation causing an increase in $k'_L a$ tells nothing about how much the increase caused in $k'_L a$, by an increase in a due to a reduction of the bubble sizes, has or has not been offset by a decrease in k'_L. To discover this one would have to/

to work at 40°C with copper catalysed sulphite in a bubble dispersion with little or no agitation at first, where k_L' should be $(k_C' D_A)^{\frac{1}{2}}$, and where the area of the bubbles could be measured by say a light probe technique; and then slowly increase the agitation and see at what level and at what bubble size range the value of k_L' dropped down to k_L for that bubble size.

C. The Bubble Column

This piece of apparatus was built to see if the absorption rate was again controlled by a physical process over the whole range of temperatures when the dispersion consisted of much larger bubbles, around 0.5 to 1 cm. in diameter. In addition it was felt that these larger bubbles would be more representative of the bubbles expected in the three phase column than would be those in the aerated tank. Calderbank (167) has shown that for "large" bubbles the value of k_L is higher than for "small" bubbles but as long as the agitation is not high enough to cause the decrease in the normal chemical reaction rate, then the changeover to chemical control should take place where $k_L' = (k_C' D)^{\frac{1}{2}} > 2\ k_L$, whatever

the/

the value of k_L . This is what, in fact, was found, with the changeover beginning at about 35°C.

1. Description

Refer to figure (9). The main part of the column was a 5¾" I.D. P.V.C. pipe section 1'6" long with flanges at each end and two diametrically opposed 1" I.D. flanged outlets 1' from the bottom. On top of the column was a 1' section of 6" I.D. Q.V.F. pyrex pipe to allow the surface level to be measured and visual observations of the dispersion made. At the bottom of the column a sieve plate, also made of P.V.C., containing 87 1/32" diameter holes on a triangular grid was held between the 6" to 1" Q.V.F. reducing section and the column. Air from the aerated tank rotameter entered this reducing section through the 1" I.D. side arm and the bottom outlet was used to drain the column. This light source and photocell assembly from the light probe used and described in detail by Calderbank (149) were fitted to the two 1" flanged outlets as shown in figure (9) and the photocell output connected to a light quantity meter linked to an electric clock. Two transparent perspexdpluge were placed in the short lengths of tubing of the two 1" outlets to the photocell and lamp so as to be flush with the inside column wall. This preventeddair bubbles being trapped in the tubesxcausing errors/

LARGE BUBBLE COLUMN - DETAIL

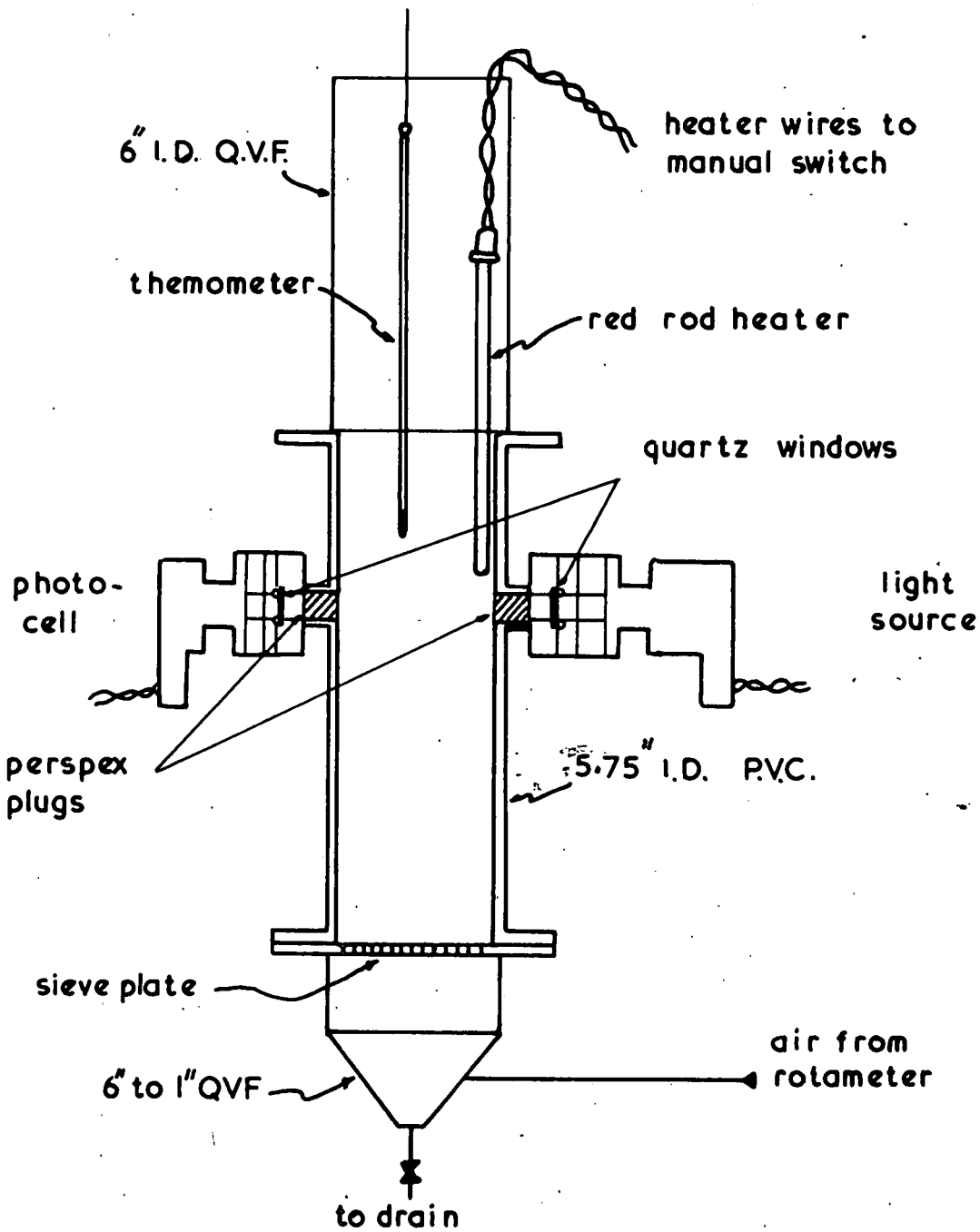

FIGURE 9

errors in the measurement. In between the 1" flanged outlet and the photocell and lamp holder flanges, two brass discs held quartz windows between O-ring seals to contain the liquid, which also allowed the photocell unit to be removed for fitting filters during a run. A thermometer and a quartz sheathed red-rod heating element were suspended in the column.

2. Operation and Experimental Work.

A solution of 0.8M sodium sulphite was made up with hot tap water in the stirred tank and left to cool to the required temperature. The drain line hose clamp was closed and the air supply turned on to give a superficial gas flow rate of around 3 cm/sec. which was of the order of magnitude to be used in the three phase column. About 7½ litres of the sulphite solution were then poured into the bubble column from the top and were supported above the sieve plate by the air passing through it. Sufficient of a IM copper sulphate solution was added to make its overall concentration 10^{-3}M. After waiting fifteen minutes to ensure the copper sulphate solution was completely dispersed and the temperature was steady a 10 ml sample was withdrawn by pipette and analysed iodometrically in the same way as were the aerated tank samples. A run lasted from half-an-hour to one hour, after which a second sample was taken.

The/

The interfacial area measurement was carried out under the same operating conditions as described above. The light source was switched on at least an hour before use to let it achieve a constant light emission. The light housing was cooled by passing a stream of air through it the whole time. The dial of the light quantity meter was set to 10 light units and the starting switch depressed; this operation also actuating the electric clock which automatically switched off when the 10 units had been received by the photocell. This was repeated several times to obtain the average time, t, secs, for this number of light units to pass through the dispersion. The air was then turned off. The solution drained through the sieve plate to fill the space below but there was enough in the whole column for the light transmission windows to be still submerged. A neutral density-filter, factor 60, was then placed over the photocell and after allowing time for all the bubbles to leave the solution, times, to, were again taken for 10 light units to pass through the unaerated solution. The filter was necessary because otherwise the time taken for 10 units to pass through the unaerated solution would be so short that it could not be measured accurately.

The gas holdup was measured by knowing the level of the column during aeration, and from the volume of solution/

solution added calculating what the level would be with no aeration, from the cross-sectional area of the column.

3. Treatment of experimental data.

(a) Oxidation rate: This is calculated from the change in sample titre volume over the time of the run as described earlier for the aerated tank runs.

(b) Area measurements: The value of the interfacial area per unit volume of dispersion a, cm^{-1}, is calculated from the equation:

$$2.303 \log_{10} \frac{tF}{to} = \frac{al}{4} \quad \ldots\ldots (10)$$

where l is the path length through the dispersion (cms) and in this case was the column inside diameter, F is the filter factor of the density filter used, and to and t the times in seconds for the set number of light units to pass through the aerated and unaerated solution respectively.

4. Results and Discussion

These are tabulated in Table 5 and plotted in figure (10) and the best lines from the stirred cell and aerated tank results have been superimposed to show more clearly what is happening. It is seen immediately that in this bubble column there is a changeover from physical to chemical control. The physical part of the line drawn through the experimental points has practically the/

BUBBLE COLUMN RESULTS – COPPER CATALYST

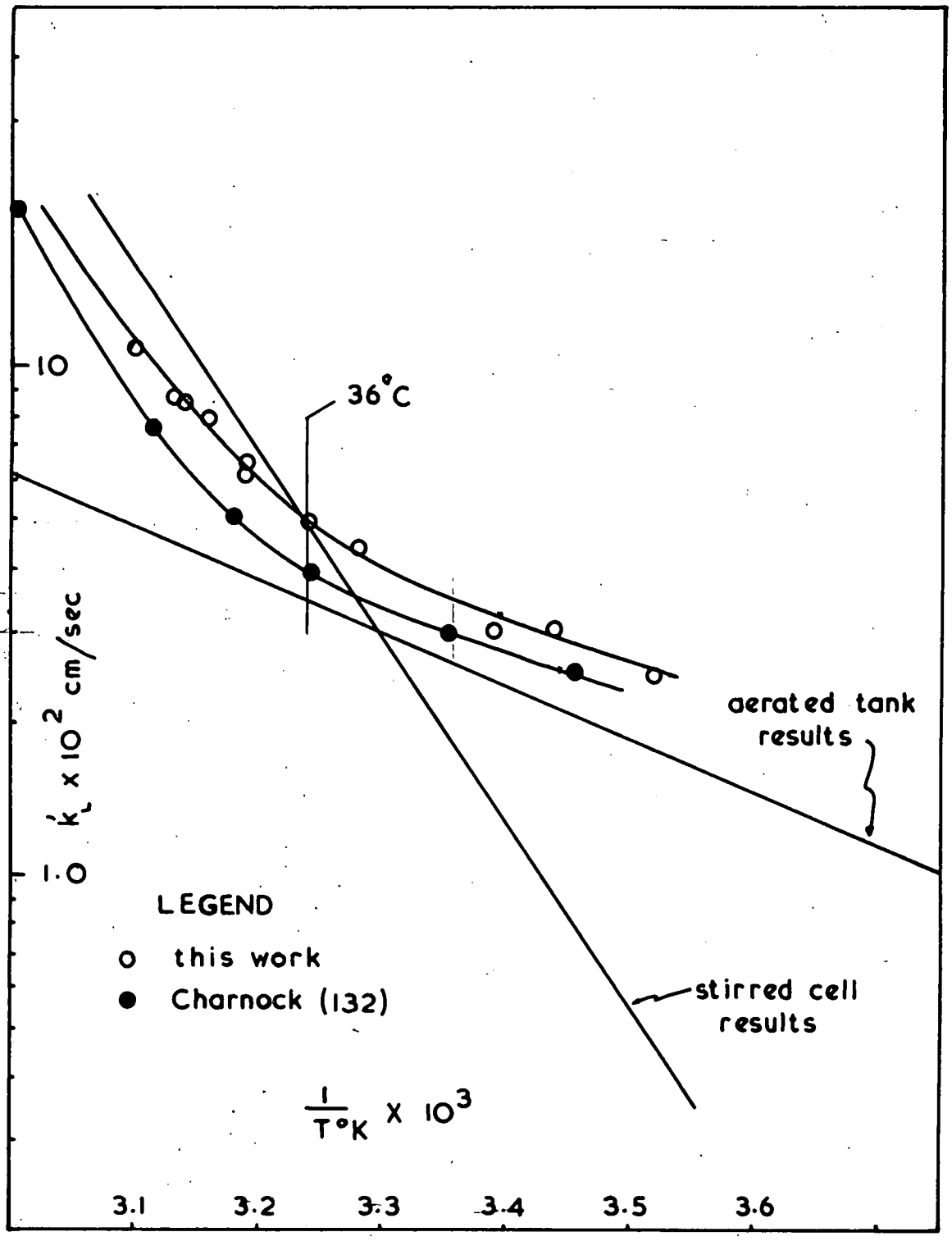

FIGURE 10

the same slope as the aerated tank line but the values of k_L' are about 30% higher which was expected. The chemical part of the line has the same slope as the stirred cell line but here the values of k_L' are about 25% lower. This was not expected since $\sqrt{k_c' D}$ is only dependent on temperature. For comparison the results obtained by Charnock (132) for a taller three inch diameter bubble column at a superficial gas velocity of 0.7 cm/sec are also plotted on figure (10). His results lie in-between the aerated tank and bubble column lines and over the chemically controlled portion are 40% lower than the stirred cell line. Perhaps some systematic experimental error, possibly in the interfacial area measurement, is responsible for the lines not being closer.

However they do show a changeover from physical to chemical control at the same temperature and the slopes of the two portions are the same. Charnock used a crude light and photo cell arrangement to obtain light transmission readings and used Calderbank's equation (equation (10) here) to calculate his interfacial area.

5. Conclusion

The work in this bubble column has shown that it is possible to achieve a changeover from physical to chemical control for the absorption of oxygen in copper catalysed sulphite as suggested earlier and the results of/

of Charnock confirm this. Whether errors in any of the measurements are responsible for the two sets of bubble data falling below the stirred cell line or whether the stirred cell line itself is in error cannot be determined, but one would conclude that there is less opportunity for error in the direct measurements made with the stirred cell than in the indirect sampling of the liquid and titration procedure, as well as the interfacial area measurements, involved in the bubble column work.

D. General Discussion and Conclusions

After the survey of the literature and this study in three different types of gas-liquid contacting apparatus it is clear that Westerterp was wrong to assume first of all that the cobalt and copper catalysed systems were similar in all respects except the speed of reaction, and secondly that the result of the bullet-shaped bubble experiments would apply in an agitated dispersion of bubbles. His basic idea of using a chemical method of measuring interfacial areas in dispersions is sound if the correct experimental conditions can be found. The objects of the experimental work described in this chapter were firstly, to try and discover something of the nature of the rate controlling processes of oxygen absorption into catalysed sodium sulphite/

sulphite under different experimental conditions; and secondly to find the experimental conditions under which the value of the overall liquid phase mass transfer coefficient, k'_L , could be reliably forecast and used to calculate the values of interfacial area in the three phase fluidized bed column, from oxidation rate data obtained therein.

With regard to the first object it has been shown that in the case of copper catalysed sulphite the rate controlling process may be either chemical or physical depending on the value of the physical mass transfer coefficient, k_L , for the system. But in certain circumstances where the conditions would indicate chemical control, such as at high temperatures in a stirred aerated tank, where although $\sqrt{k'_c D} > 2k_L$, it is suggested that the agitation is such that it reduces the local concentration of some intermediate in the chain reaction mechanism to a level that will not allow the chemical reaction to proceed to completion in the liquid film. The absorption then becomes physically controlled by diffusion through the film.

For cobalt catalysed sulphite it may be physically or chemically controlled depending on the sulphite and catalyst concentration as well as k_L as shown by Van Krevelen and Hoftijzer's solution for absorption accompanied /

accompanied by a second order reaction in the liquid film, and confirmed by Yagi and Inone, Harris and Roper and the stirred cell results here.

In both catalyst systems there is a gradual change over from one form of control to the other as evidenced by the curved portions of figures (6) and (10).

In pursuit of the second object, of the cobalt catalysed system was rejected because although it is possible theoretically to predict the value of k'_L using Van Krevelen's plot, if the value of k''_c and k_L can be estimated, it will change as the sulphite concentration changes. In a few trial runs in the three phase column using cobalt catalysed sulphite it was found that over an hour the sulphite concentration dropped by 0.2M. It should be remembered here that in Westerterp's original proposal, he stressed that the advantage of using a chemical method was that the value of k'_L could be made to depend only on the reaction rate constant k_c and the diffusivity of the dissolved gas in the liquid, both of which are independent of hydrodynamic conditions. It has been shown that this is not the case with cobalt catalysed sulphite unless the interfacial area per unit volume is so small that the sulphite or solute concentration remains essentially constant - and this condition applies equally to the other second order reaction/

reaction process, CO_2 - NaOH, suggested by Westerterp and used by Yoshida (157). This condition is seldom acceptable in bubble dispersion work. In the case of a copper catalysed system where one would expect the conditions to be satisfied the level of agitation can still be a factor.

However it was decided, in spite of the last mentioned point, that the copper catalysed system could be used in the three phase column assuming that the hydrodynamic conditions were between those existing in the bubble column and aerated stirred tank. This seemed a reasonable assumption from visual observations in the three phase column, where they appeared closer to the bubble column situation than the aerated tank. Referring again to figure (10), it is seen that the region of least uncertainty about the value of k'_L is where the chemical line from the stirred cell crosses the other lines from the bubble column and aerated tank. At higher and lower temperatures the value of k'_L could lie anywhere in-between the lines; depending on the value of k at lower temperatures and the other agitation effect at higher temperatures. It was decided to work at the temperature at which the chemical line crosses the bubble column line, 36°C, and the value of k'_L chosen was 4.5×10^{-2} cm/sec. This is mid-way between/

between the bubble column line obtained here and that of Charnock's results and is also just above the mean of the aerated tank and bubble column lines. The value of k'_L originally suggested by Westerterp was 5×10^{-1} cm/sec. at 30°C based on his own value of Henry's constant of 69. Assuming the value of k'_c doubles in 10°C, then at 36°C an estimate of Westerterps value is then 6.3×10^{-1} cm/sec which is about 14 times higher than the chosen value of k'_L to be used here.

The maximum possible error is then $\pm$ 17% of the chosen value of k'_L; but in the case of the aerated tank, the actual variation was much less than this, $\pm$ 8%. So although the calculated values of interfacial areas in the three phase column are uncertain to an extent of a possible $\pm$ 17% in true magnitude, their reproducibility should be within $\pm$ 10%. The smooth curves obtained for these areas for series of separate experiments at different heights indicate that this is so.

SULPHITE OXIDATION BIBLIOGRAPHY

101. MIYAMOTO S., Bull.Chem.Soc.Japan, 2, 74,155,192. (1927).

ibid 3, 98,137 (1928).

ibid 4, 132 (1929).

102. MIYAMOTOS., KAYA, S., ibid 5, 229, 125, 321 (1930).

103. MIYAMOTO S., KAYA, S., ibid, 6, 9, (1931).

104. MIYAMOTOS., NAKATA S., ibid, 6, 22, (1931).

105. MIYAMOTO S., ibid, 7, 8 (1932).

106. BACKSTROM H.S., J.Am.Chem.Soc., 49, 1460 (1929).

107. FULLER E.C., CRIST, R.H., ibid, 63, 1644 (1941).

108. COOPER C.M., FERMSTROM G.A., MILLER S.A., Ind.Eng. Chem., 36, 504 (1944).

109. BATHOLOMEW W.H., et al. ibid, 42, 1801 (1950).

110. HIXSON A.W., and GADEN E.L., ibid, 42, 1792 (1950).

111. WISE W.S., J.Soc.Chem.Ind.(London) Supple. 1, 540, (1950).

112. BASSETT H., PARKER, W., J.Chem.Soc., 1540 (1951).

113. CHAIN E.B., et al., Bull.World Health Org., 6, (1952).

114. MAXON W.D., JOHNSON M.J., Ind.Eng.Chem., 45, 2554, (1953)½

115. CHAIN E.B., GUALANDI G., Rend.inst.super sanita, 17, 13 (1954).

116. FINN R.K., Bacteriological Reviews, 18, 254 (1954).

117. NORD Acta Chem.Scand., 9, 430, (1955).

118. DOWNING A.L., Chem. & Ind., 193 (1955).

119. RUSHTON J.H., GALLAGHER J.B., OLDSHUE J.Y., Cehm.Eng.Prog., 52, 319 (1956).

120. SCHULTZ J.S., GADEN EL., Ind.Eng.Chem. 48, 2209 (1956).

121/

121. ELSWORTH R., et al, J.Appld.Chem., 7, 261, 269 (1957).

122. FRIEDMAN A.M., LIGHTFOOT E.N., Ind.Eng.Chem., 49, 1227, (1957).

123. PIRT S.J., CALLOW D.S., GILLETT W.A., Chem.& Ind. 730 (1957).

124. CARPANI R.E., ROXBURGH J.M., Can.J.Chem.Eng., 36, 73, (1958).

125. SOLOMONS G.L., PERKIN M.P., J.Appld.Chem. 8, 251, (1958).

126. PHILLIPS D.H., JOHNSON M.J., Ind.Eng.Chem., 51, 83, (1959).

127. MURPHY D., CLARK D.S., LENTZ D.P., Can.J.Chem.Eng. 37, 157 (1959).

128. YOSHIDA F., IKEDA A., IMAKAWA S., MIURA Y., Ind.Eng. Chem., 52, 453 (1960).

129. YAGI, S., INOUE, H., Chem.Eng.Sci., 17, 411, (1962).

130. WESTERTERP K.R., Ph.D. Thesis Univ. of Delft (1962). later as Chem.Eng.Sci., 18, 157, (1963).

131. KOMANIS G.A., private communication, Dept.Chem. Eng., Univ. of Edinburgh (1962).

132. CHARNOCK ,D.J., Private communication (1962).

133. CLARK D.S., BiotechnolBioengng., 4, 241, (1962).

134. ROSBURGH J.M., Can.J.Chem.Eng., 40, 127, (1962).

136. JAMESON D., Ph.D. Thesis, Cambridge University (1963).

137. SCHROETER L.C., J.Pharm.Sci., 52, 559 (1963).

138. HARRIS I.J., ROPER, G.H., Can.J.Chem.Eng., 42, 34 (1964).

139. DE WAAL, K.J.A., Private communication (1965).

140. YOSHIDA F., AKITA Y., J.Am.Inst.Chem.Engrs., 11, 9 (1965).

141. BRAULICK, W.J., FAIR J.R., LERNER, B.J., J.Am.Inst. Chem.Engrs., 11, 73 (1965).

OTHER REFERENCES

142. CLARK N.O., BLACKMAN M., Trans.Faraday Soc., 44, 1, 7, (1948).

143. LANGLOIS G.E., GULLBERG J.E., VERMEULEN T., Rev. Sci.Instrs., 25, 360 (1954).

144. VERMEULEN T., WILLIAMS G.M., LANGLOIS G.E., Chem.Eng.Progr., 51, 85F (1955).

145. TRICE V.G., RODGER W.A., J.Am.Inst.Chem.Engrs., 2, 205 (1956).

146. MIE G., Ann.Physik (14) 25, 377 (1908).

147. ROSE H.E., LLOYD H.B., J.Soc.Chem.Ind., 65, 52, (1946).

148. CAUCHY A.C.R., Acad.Sci.Paris., 13, 1060 (1841) - quoted in (147).

149. CALDERBANK P.H., Trans.Instn.Chem.Engrs., 36, 443 (1958).

150. CHU C.M., J.Phys.Chem., 59, 841 (1955).

151. CALDERBANK P.H., MOO-YOUNG M.B., Trans.Instn.Chem. Engrs., 37, 173 (1959).

152. CALDERBANK P.H., EVANS F., RENNIE J., Int.Symp. Distillation, London 1960.

153. CROFTON W., Encyclopedia Britiannica (9th Ed.) see "Probability" (London: Encyclopedia Britannica Ltd.).

154. CHALKLEY H.W., CORNFIELD J., PARK H., Science 110 295 (1949).

155. ROSE W.D., WYLLIE M.R.J., Bull.Amer.Ass.Petrol. Geol., 34, 1748 (1950).

156. CALDERBANK P.H., RENNIE J., Trans.Instn.Chem. Engrs. 40, 3, (1962).

157. YOSHIDA F., MIURA Y., Ind.Chem.Eng., 2, 263 (1963).

158. MORRIS R.M., Chem. & Ind., 44, 1836 (1964).

160/

160 SIEDELL A., "Solubilities of Maganic and Metal Organic compounds", 3rd Ed. Vol.II.

161. BAIRD M.H.J., Private communication. (1963)

162. SHERWOOD T.K., PIGFORD R.L., "Absorption and Extraction" (a) p. 323 McGraw-Hill N.Y. (1952) (b) p. 337

163. VAN KREVELEN D.W., HOFTIJZER P.J., Rec.Trav.Chim. 67, 563 (1948).

164. VAN KREVELEN K., HOFTIJZER P.J., Chem.Eng.Sci., 2, 145 (1953).

165. YOSHIDA F., MIURA Y., Am.Inst.Chem.Engrs.J., 9, 331 (1963).

166. HIGBIE R., Trans.Am.Inst.Chem.Engrs., 31, 365 (1935).

167. CALDERBANK P.H., MOO-YOUNG M.B., Chem.Eng.Sci. 16, 39 (1961).

168. Handbook of Physics and Chemistry 43rd Ed., Chemical Rubber Publishing Co., Cleveland Ohio (1962).

169. HAMMERTON D., GARNER F.H., Chem.Eng.Sci. 3, 1 (1954).

171. as quoted in (151) above.

PART TWO

CHAPTER IV

Three Phase Fluidization

A. INTRODUCTION

The term three phase fluidization in the context of this thesis refers to a system where solid particles are fluidized by a liquid to produce an expanded bed of practically uniform porosity, into which gas is introduced through nozzles of porous plates to form bubbles. The result is a three phase, gas-solid-liquid, fluidized bed. Work has been done (203, 208) in systems where settled beds of solids in a column of stagnant liquid are brought into suspension, or fluidized, by passing gas up through them, involving a transfer of momentum from the gas phase to the solid phase via the liquid medium. The result is a three phase dispersion but one whose hydrodynamics are essentially different from those existing in the system studied here.

In the introduction to this thesis it is stated that its object is to study the behaviour of gas dispersions in a liquid-solid fluidized bed and particularly those factors which control the magnitude of the gas-liquid interfacial area. In the next chapter the development of the experimental program is described along with the limitations imposed on the scope of this program by the measuring/

measuring techniques used. Below is a survey of previous work on this type of three phase fluidization.

B. SURVEY OF PREVIOUS WORK

Massimilla, Majuri and Signorini (201) fluidized beds of silica sand and glass pellets with water in columns 3 cms. and 9 cms. in diameter. They injected a gaseous mixture of 87% carbondioxide and 13% nitrogen into the bottom of the liquid fluidized bed through nozzles and also through the porous plate that supported the solids bed. They observed that when the gas rate was low the gas bubbles produced at the nozzles or porous plate moved individually through the bed and there was no coalescence; the bubble sizes were in the range 2 to 6 mm in diameter. However on increasing the gas rate and lowering the liquid rate, causing a lower liquid-solid bed porosity, the bubbles which emerged from the bed were much larger but of the same frequency as before. The production of these large bubbles was attributed to coalescence and by increasing the gas rate even further they could produce bubbles large enough to form slugs in the 3 cm diameter column. They also observed that when gas was injected into the fluidized bed of particles the height of the bed dropped, and the greater the gas rate, the greater was the drop. This phenomenon is studied/

studied by Turner (204), Ostergaard (210) and Stewart and Davidson (209) whose work will be discussed later.

Their next step was to measure the efficiency of gas-liquid contacting by analysing samples of liquid for their carbon-dioxide content and expressing this as a percentage of the value that would be obtained if the liquid were in equilibrium with the gas. On this basis they compared the efficiency of contacting under different conditions of gas flow rate, liquid flow rate and bed porosity; and also for the column operated with and without solid particles present. They concluded that the presence of solid particles reduced the gas-liquid interfacial area, and that this reduction was more marked as the gas rate was increased for a given liquid rate, and as the bed porosity was reduced for a given gas rate. In addition they found an effect of particle size; increasing the particle size for a given gas and liquid rate reduced the efficiency of contacting. These results bore out their visual observations. The comparison between the cases of operation with and without particles was made by placing a solid cylinder in the two phase bed of such a size as to produce the same free section available to the gas and liquid as would be available in the three phase bed whose contacting efficiency was to be compared. The/

The amounts of CO_2 absorbed were in all cases lower when solids were present than when they were not. The amount of absorption was also higher when the gas was injected through nozzles into the columns than when it was allowed to pass through the porous plate bed support, and this they explain by the observation that gas gathered below the porous plate before passing through it, which would facilitate the formation of larger bubbles on emergence into the column, and so reduce the initial interfacial area in both the two phase and three phase cases.

Massimilla, Solimando and Squillace (202) followed up this work by a photographic study of air bubbles emerging from water fluidized beds of silica sand, glass beads and iron sand; and by measuring rise velocities of single bubbles through these beds. The column used in the photographic work was 4 feet high with a rectangular cross-section 3.4 inches by 2.4 inches, and air was injected throgh a single nozzle at the bottom of the bed, above the bed support plate. By varying the quantity of solids put in the column , different heights of the fluidized bed could be obtained for the same degree of bed expansion, or porosity, and photographs taken of bubbles emerging at each height allowed them to plot average bubble diameters against bed/

bed height. This technique was necessary since solid-liquid fluidized beds are essentially opaque. They found that after a large number of experiments involving changing the bed expansion from that just above incipient fluidization to 100% of the settled bed height and using the different particles mentioned above, that the change in bubble diameter with height was mainly dependent on bed expansion. As a first approximation they assumed that the average bubble diameter increased proportionately with the distance above the nozzle and therefore wrote the following correlation:

$$\frac{Dmzz - Dmo}{Z} = a\left(\frac{Lo}{\Delta L}\right)^{b} \qquad \ldots\ldots (1)$$

in which Dmzz and Dmo are the average bubble diameters at height Z and immediately above the nozzle respectively; $Lo/\Delta L$ is the reciprocal of the bed expansion, Lo being the settled bed height and ΔL the increase; and a and b, numerical constants with values 2.7×10^{-3} and 1.3 respectively. They point out that this correlation is only valid in the range of values of Z in which the proportionality between Z and Dmzz exists, and also that as it is purely empirical it is unlikely to be valid in systems of different geometry to their own. There was a large scatter of points around this correlation.

Bubble rise velocities were measured by timing the interval between the release of a bubble and its emergence/

emergence from the bed. The bubble volume was measured before injection by isolating it in an inspection tube. For these experiments a 3.5 inch diameter perspex column 5'2" high was used and the bed height always set to 4.5 feet. Their results showed that the rise velocity increased steadily with bubble diameter and approximated the analogous curves that may be found for viscous liquids. This is quite different for bubble velocities in water, where a plateau is reached where the rise velocity is fairly constant over a range of bubble sizes from 0.12 to 0.78 in inches (215).

A theory of bubble coalescence was also advanced based on the fact that a distribution of bubble velocities is necessary for coalescence since one bubble can only catch another bubble if its rise velocity is higher than that bubble. Using their experimental bubble size and rise velocity data the theory predicted the number of bubble passes that would result in collisions, compared to the total number of bubble passes, expressed as the fraction C. Under certain conditions C was found to be greater than unity. This discrepancy was explained by their bubble velocities determined for single bubbles being applied to velocities of bubble swarms. The difference between the two has been recently studied by Marrucci/

Marrucci (211).

Turner (204) in the discussion of his general paper on Fluidization refers to experiments in which sand particles (44 to 60 mesh) were fluidized by water into which air or nitrogen was then injected. He reports that upon injection of the gas, the fluidized bed contracted. This contraction, already noticed by Massimilla (201), was most marked at the higher values of bed porosity and was brought about by a very small gas flow rate. On the passage of gas at the superficial linear velocity of 0.2 cm/sec, a bed of original porosity 0.74 fell to a porosity of 0.69 and a bed of o.59 to 0.57. As the gas rate was increased further the bed continued to contract but to a much lesser degree until at a gas rate of0.8 cm/sec no further contraction occurred. His range of gas rates extended only to 1.2 cm/sec. Neither Turner nor Massimilla offer an explanation of this phenomenon.

Stewart and Davidson (209) sought an explanation. They carried out similar experiments to those of Turner but used a bed of the two dimensional type whose cross-section was 2.5 inches by 0.25 inches, which allowed them to take photographs, with suitable lighting, showing individual bubbles within the bed and the particles. The particles used were glass ballotini and lead and iron shot. Their results were similar to Turner's

Turner's except that the bed contraction was less marked and in the case of ballotini above a superficial gas velocity of about 0.4 cm/sec the bed actually began to expand, slightly, again. From the analysis of their photographs they show convincingly that in the case of dense particles such as lead shot, which when fluidized by water contain visible water bubbles, the presence of small air bubbles stabilises these water bubbles to a much larger size. In the case of light particles such as glass ballotini for which the indigenous bubbles in a water fluidized bed are very small or non-existent, the injected air bubbles form air-water bubbles which they describe as an air bubble followed by a water wake containing few or no particles. In both cases the presence of air bubbles has produced either water bubbles or wakes which contain none or only a few particles and which move through the bed with the velocity of the associated air bubble. This in effect reduces the residence time of the water and the bed contracts accordingly.

Ostergaard (210) also carried out experiments similar to Turner using glass ballotini fluidized by water into which air was injected and obtained practically identical results for the degree of bed contraction. He used a 7.6 cm diameter column and took photographs of bubbles emerging from the bed, which showed them to be/

be followed by a spout of particles. He thus assumed that inside the bed these bubbles had a wake consisting of particles of a similar porosity to that of the bed as a whole. This was in direct contradiction to the evidence of Stewart and Davidson's photographs and similar results reported in chapter IX of this thesis. A semi-empirical theory is also presented to predict the overall bed porosity in a three phase fluidized bed upon aeration, which involves assuming (a) that the porosity of the wake phase is identical to that of the liquid fluidized phase and moves with the velocity of the associated gas bubble and (b) that the volume of the wake phase in the bed increases with increasing gas rate and also with increasing liquid rate.

The theory agrees quantitatively very well with his own results and those of Turner, but only qualitatively with those of Stewart and Davidson. This latter discrepancy he suggests is due to the differences in bed geometry, which is quite possibly the cause of lower contractions than Turner's being recorded. The particle movement is restricted in a two dimensional bed to flowing only around the sides of a rising bubble, the front and back of the bubble being flat against the column faces.

He explains the contraction in the bed upon aeration/

aeration as being due to the liquid associated with the wake moving through the bed more quickly than the average liquid velocity, causing the remaining liquid to move more slowly than the average, and hence to have a lower porosity. But if this is so then the wake porosity must be higher than that of the remaining liquid and this is inconsistent with his original assumption in developing his theory. Østergaard's work will be referred to again in the discussion of the results of experiments carried out in a two-dimensional bed reported in chapter IX.

Adlington and Thomson (205) discuss the flow properties of gas-liquid-solid fluidized systems and give qualitative relationships between the process variables based on experiments carried out in a 3 inch diameter column using alumina particles and white spirit and in a 10 inch diameter column using sand and water. Air was the gas used in each case. The light transmission method of Calderbank (149) was used to measure the gas-liquid interfacial areas above the fluidized bed in the 10 inch column. Their findings are as follows:

1. The gas-liquid interfacial area.
   (a) fell as height above the column base increased (see 3(a))
   (b) increased with gas rate
   (c)/

(c) was independent of liquid rate over the range investigated

(d) increased slightly with increase of settled bed height

2. Gas holdup

(a) increased with height above the column base

(b) increased markedly with gas rate

(c) was independent of liquid rate

(d) was independent of settled bed height

(e) was depressed by presence of solids at high gas rates especially at low bed porosities.

3. Bubble diameter

(a) increased with height above the column base at five times the rate which could be accounted for by change of hydrostatic head. (i.e. there was marked coalescence)

(b) was independent of gas rate

(c) was independent of liquid rate

(d) was independent of settled bed height.

They also noticed the bed contraction effect upon aeration and found it to be most marked with small particle sizes at high expansions and almost zero gas flow rate. These qualitative findings agree well with Massimilla's and those reported in Chapters VII and VIII of this thesis.

Later/

Later in their paper the authors report briefly on mass transfer work done using oxygen and copper catalysed aqueous sodium sulphite solutions as the gas and liquid phases in a three phase column 3 inches in diameter. The results showed that the interfacial area and gas holdup at any gas rate fall as the bed expansion ratio, i.e. the bed porosity, falls, and that they are both less sensitive to liquid rate and particle size than to bed porosity. This agrees with the results of experiments carried out in chapter VIII.

C. SUMMARY

In the above survey three groups of workers, Turner, Stewart and Davidson and Østergaard studied the phenomenon of bed contraction upon aeration, which was observed when the superficial gas velocities were in the range zero to 2 cms/sec. The agitation caused by the passage of bubbles at higher gas rates than this in a fluidized bed makes it very difficult to determine the actual top of the solid-liquid bed and in fact the system is no longer one in which a small amount of gas rises through a uniformly fluidised bed of solids but one in which the solid and gas phases are highly dispersed in the liquid and a wide distribution of gas residence times exists. As most gas-liquid contactors

of/

of commercial interest would operate in these higher ranges of gas flow rates (141) the results of the work by Massimilla et al and Adlington are of more interest from the point of view of the aims of this study in particular and the development of commercial three phase reactors in general. These latter workers have made qualitative observations on the behaviour of three phase fluidized reactors and Massimilla (202) attempted to make quantitative predictions of the amount of coalescence to be expected for given operating conditions and to correlate bubble sizes with bed expansion. He was not entirely successful. So there remains a lack of information on the relationship between dispersion properties and operating variables. For example, Adlington and Thomson and Massimilla have observed that a decrease in bed porosity increases the amount of gas bubble coalescence but the exact relationship between them has not been studied. Questions such as the following are still unanswered.

1) How is the rate of bubble coalescence related to bed porosity?
2) How does the bed porosity effect the formation and size of gas bubbles at the point of injection into the bed?
3) What are the relative effects of initial bubble formation and subsequent coalescence on the efficiency of/

of gas-liquid contacting?

4) What is the residence time distribution of the gas phase in a three phase system; and how is it related to bed porosity?

The answers are of primary importance to the process designer and the work carried out and reported in the following chapters attempts to provide some of them.

CHAPTER V

Development of the Experimental Program

It is the object of this thesis to study the behaviour of a gas-liquid-solid fluidized bed and particularly those factors which control the magnitude of the gas-liquid interfacial area. In a three phase fluidized bed there are three obvious operating variables which will influence the dispersion properties and they are the liquid flow rate, gas flow rate and the concentration of solid particles present. However the effect each has depends on the particular values of the other two at the time. For example in the work done here one extreme was the situation where, if the solids' concentration was sufficiently low and the liquid flow rate sufficiently high, the gas flow rate could be varied over a wide range and the only effect on the dispersion was an increase in the bubble frequency as the gas rate was increased. At intermediate values of solids concentration and liquid flow rate it was possible to have the situation where at first the bubble frequency would increase with increasing gas rate and then at a particular height up the column the frequency would start to drop as coalescence commenced. The other extreme was that when the liquid rate was sufficiently low and

the/

the solids concentration sufficiently high, the gas bubbles began to coalesce almost immediately, even at the lowest gas rate. The inter-relation of these three main process variables is very complex as the survey of previous work has shown (201, 202, 205), but additional variables are introduced in the nature of the particles themselves, such as their size, shape, density and size range. Increasing the particle size was shown by Massimilla (201), to reduce the contacting efficiency when the three main variables were held constant and Stewart and Davidson (209) showed two distinct types of dispersion when particles of low and high densities, glass ballotini and lead shot, were fluidized. Yet another variable is the column geometry and the existence of wall effects, especially when the bubble size approaches that of the column.

In any one project it is impossible to study all the variables mentioned and so an attempt was made to study those which are of most interest to the process designer. The four questions posed at the end of the previous chapter represent areas of considerable importance from the mass transfer point of view and the experimental program was developed to try to answer them as well as provide more general information about the behaviour of three phase dispersions.

The apparatus used is described in detail in the next/

next chapter. Two solids particles were used, number seven glass ballotini and silica sand: they were of different shapes, the ballotini being approximately spherical and the sand granular; and had different size distributions, the ballotini being all of a similar size and the sand being a wide cut of particles from 30 to 100 mesh. The physical properties, sizes and fluidization curves for these particles are given in Appendix IV.

The program of experiments was divided into four sections:-

1) Bubble Frequency Measurements

Experiments were carried out to study the phenomenon of coalescence in three phase dispersions and how it was related to gas rate, liquid rate and bed porosity. This was done by using two strips of aluminium placed round the column, connected separately to an electronic capacitance gauge. The signal was fed to a pen recorder which recorded changes in the capacitance of the three phase bed in the form of a wavy trace with peaks corresponding to the passage of bubbles. It was possible to count the number of peaks in a given period of time and obtain a bubble frequency at any height at which the strips were placed. The decrease in frequency with height provided a measure of the rate of coalescence.

2)/

2) Interfacial Area Measurements

When planning these experiments it had to be borne in mind that the sulphite area measuring technique produces only values for the average specific interfacial area over the total height of the column. The effect of coalescence on reducing the local interfacial area as one moves up the column can, therefore, only be detected by measuring overall areas for a number of columns of increasing height. It should also be appreciated that large changes in local areas with height are necessary to produce reliably measurable changes in the overall average value. To this end the scope of these experiments had to be reduced and areas were measured in columns of increasing height for different bed porosities, but only at one air rate, which was selected by a study of the frequency measurements results. From these results an air rate was selected for which coalescence was detected within one foot of the bed support gauze. This air rate was 6.75 cm/sec and lower than would have been preferred but was the highest air rate at which the tallest column, 9 feet, could be conveniently operated without excessive foaming and the formation of bubbles approaching the column diameter in size. At the lowest column height used areas were measured at four different porosities for a range of air rates up to that/

that used in the area vs height measurements.

3) Two-dimensional bed work

Here in a bed similar to that used by Stewart and Davidson (209) visual observations of gas bubbles emerging from the injection nozzle were made and some photographs taken. The phenomenon of solids bed contraction was also examined.

4) Gas Residence Time Studies

Experiments were carried out to measure the residence time distributions of the gas bubbles in the column under the same operating conditions as used for the interfacial area measurements. This was done by passing air saturated with mercury vapour through the column for a period of time and then making a step change to pure air. The gas emerging from the top of the column was analysed for its mercury vapour content by its relative absorption of ultra-violet light, as detected by a photo-cell, and the resulting data used to construct F-diagrams.

CHAPTER VI

The Three Phase Fluidization Apparatus - Description

A. GENERAL

Figure (11) shows schematically the flow directions and layout of the apparatus used for the experimental studies of three phase dispersions to be described in Chapters VII and VIII. The column and its ancillary inlet, take-off, cooling and sampling sections were made of 6" I.D. Q.V.F. pyrex pipe sections and fittings. All liquid side piping, fittings and valves were of 1" I.D. rigid P.V.C . except for a length of 1" I.D. flexible P.V.C. tubing connecting the take-off section to the cooling section - this being necessary to accommodate changes in column height. The gas-side piping and fittings from the top of rotameter R2 up to and including the distributor were of ½" I.D. rigid P.V.C. and from the reducing valve V7 to the bottom of rotameter R2½ of ½" I.D. copper. Care was taken to avoid any contact between the liquid and stainless steel or iron and to this end a Korannite float was used in Rotameter R1 and the stainless steel float supports were removed and replaced by copper ones. The rotameter fittings and connections were made of brass. The Stuart-Turner centrifugal/

THREE PHASE FLUIDIZED BED APPARATUS - SCHEMATIC DIAGRAM

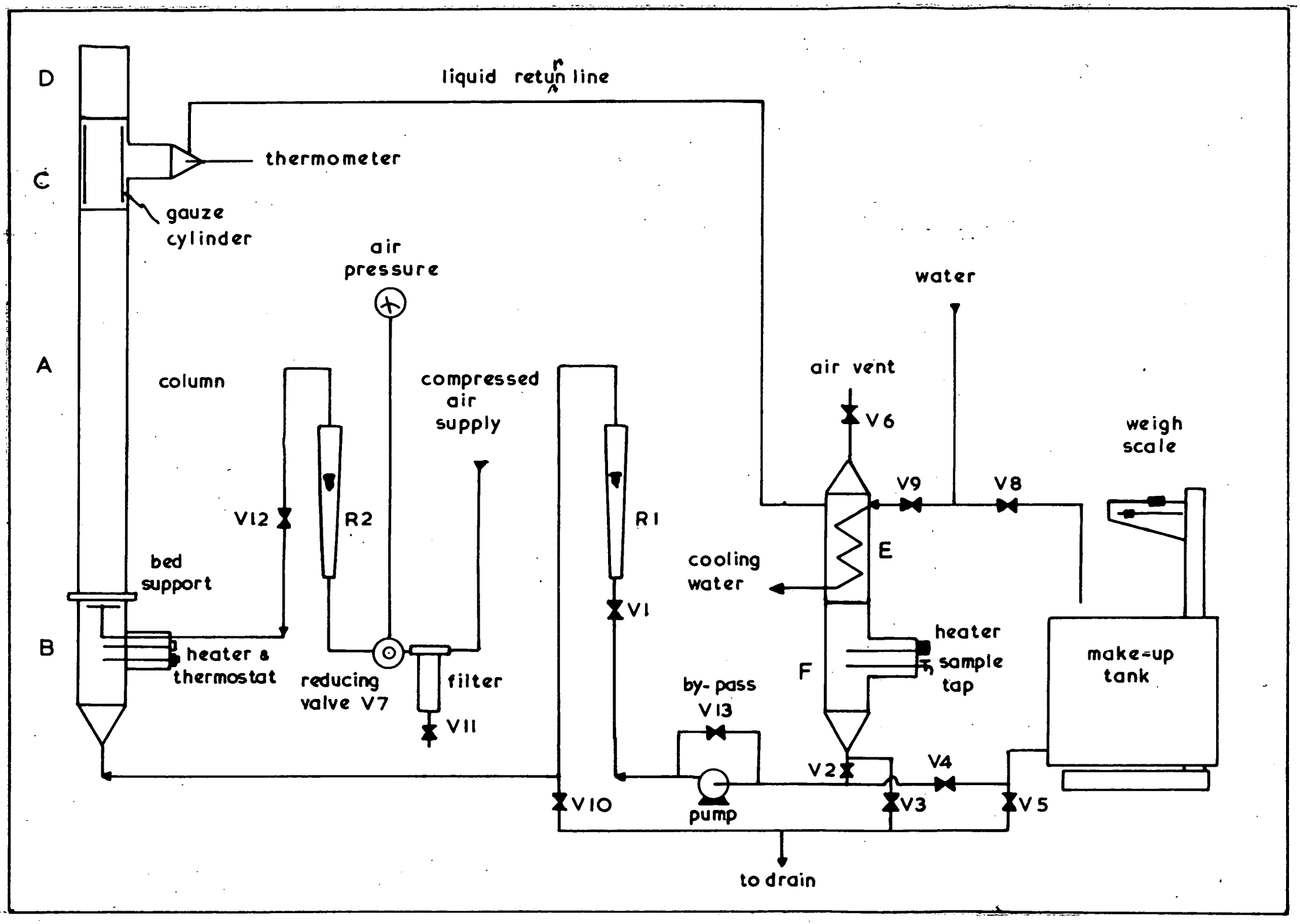

FIGURE 11 -

centrifugal pump was fitted with a brass impeller and served to circulate the liquid and to charge the column from the make-up tank by suitable operation of the valves, to be described later.

B. THE COLUMN

The column itself comprised sections A, B, C and D shown in figure (11). Section A consisted of combinations of, 1', 2', 3', 4' and 5' lengths of Q.V.F. pipe sections so as to give heights from one foot to nine feet in one foot increments. The bottom section had the bed-support gauge flanged assembly, shown in an exploded view in figure 12, attached to it to allow it to be removed from section B whilst still containing the bed material. Section B, a Q.V.F. tee piece, acted as the column inlet section. The liquid, after passing through rotameter R1, entered a 1" to 6" Q.V.F. expansion section attached to the bottom of the tee. A $\frac{1}{8}$" thick P.V.C. flange on the side-arm of the tee carried the gas inlet line which terminated in a cruciform distributor containing $^1/_{32}$" holes in each of the four arms, and which distributed the gas below the bed-support gauze. Figure (13) shows the distributor in detail. The P.V.C. flange also held a $1\frac{1}{8}$ kw immersion heater and a Sunvic thermostat pocket. Section C, another Q.V.F. tee piece, acted as the take-off section. It/

APPARATUS DETAILS

FIG. 12 - BED SUPPORT GAUZE

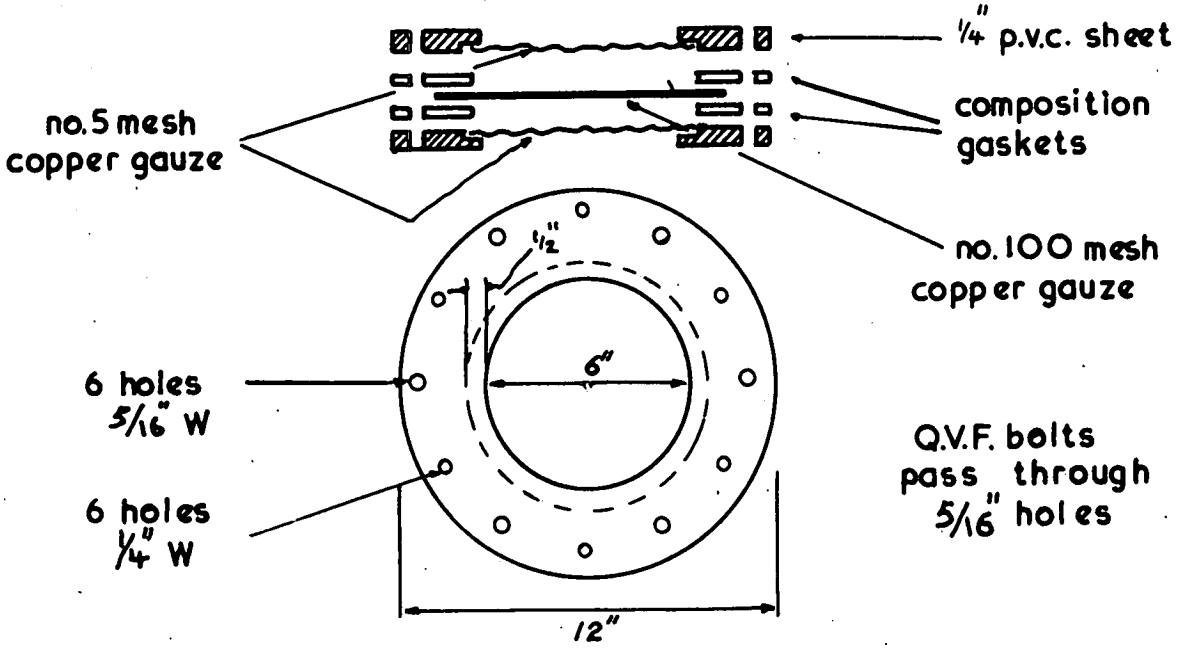

FIG. 13 - GAS DISTRIBUTOR

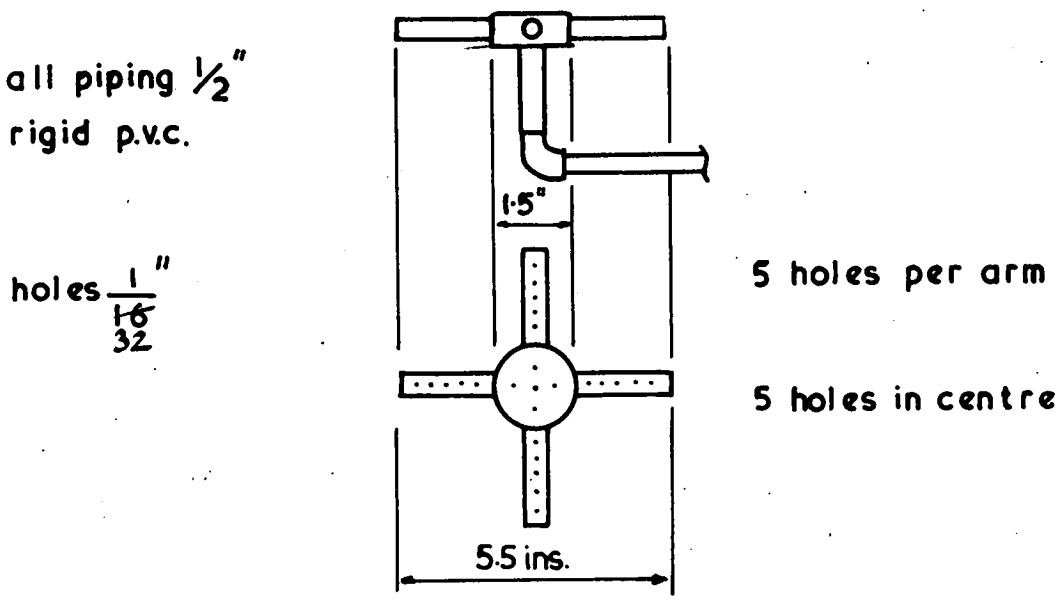

FIGURES 12 & 13

It was provided with a 100 mesh copper gauze cylinder fitting flush with its walls and covering the side-arm outlet, that was held in position by two tightly fitting 6" O.D. perspex collars above and below the side arm. This gauze cylinder prevented the bed material from entering the side arm and also helped to contain the gas bubbles within the column, reducing the amount of gas carried over with the liquid. A 6" to 1" Q.V.F. reducing section was attached to the side arm, with two 1" I.D. outlets, one with a 1" hose connection to the flexible P.V.C. return line and the other with a brass flange holding a standard 'O'-ring sealed thermometer fitting. Section D was a further piece of Q.V.F. pipe of appropriate length to accommodate the increase in dispersion height on aeration. Before aeration the liquid level was set three inches above the top of section C in all experiments.

C. COOLING AND SAMPLING SECTIONS

These two sections, E and F on figure (11), were joined together and were remote from the main column. The cooling section E was a standard Q.V.F. fitting containing a pyrex coil within it provided with two outlets through the side of the fitting to which hose connections were made. Cold water circulated through the/

the coil controlled by valve V9. The liquid return line entered the section through a 1" I.D. inlet and any gas bubbles that had been carried over rose to the top and could be vented to atmosphere through the 1" I.D. outlet there and valve V6. Section F was another Q.V.F. tee piece with a 6" P.V.C. flange on its side arm and a 6" to 1" Q.V.F. reducing section on the bottom outlet. A sample tap, ⅛" B.S.P., was screwed into the flange and a ⅛" P.V.C. tube led from this tap to the centre of the tee to ensure samples were withdrawn from the main stream of the liquid. A 1 kw heater was also mounted on the flange and switched manually to provide booster heating to assist in raising the liquid temperature.

D. MAKE UP TANK

This was a 32 gallon rigid polythene tank mounted on a John White 300 lb. weighing scale. A flexible hose connected the tank outlet to the pump via V4 and to drain via V5. Cold water could be used to fill the tank or wash it out from the supply through valve V8. The provision of the scales allowed the volume of liquid charged to the column and ancillary lines to be calculated from the weight of water in the tank before and after charging.

The/

The operation of this apparatus varies in each of the three series of experiments and will therefore be described in the appropriate chapters. Modifications made during the course of the residence time studies are fully described in chapter X.

CHAPTER VII

Bubble Frequency Measurements

A. INTRODUCTION

Angelino, Charzat and Williams (214) published a paper in which they described a method of detecting bubbles in a gas-liquid and gas-solid fluidized bed, by measuring the change in capacitance at a particular point of the column as a gas bubble passed. Two thin strips of metal were placed around the column wall to act as the two plates of a capacitor, with the column and contents acting as the dielectric material. Since the dielectric constant of the gas was different from that of the solid or liquid, the passage of a gas bubble resulted in a momentary change in the column capacitance, which was detected by a suitable instrument. This method can be applied to the detection of gas bubbles in a liquid-solid fluidized bed provided the difference in dielectric constant of the gas and the liquid-solid bed is suitable. This was found to be so for water fluidized sand and glass ballotini, but not for sodium sulphite solutions as the fluidizing medium. This was due to the fact that the presence of the sodium sulphite reduces the dielectric constant of water which is 78 @ 25°C/

25°C (168) to between 5 and 10 (216) and the sensitivity of the column capacitance to the passage of air bubbles is thus reduced about ten times.

The capacitance measuring apparatus used in this work consisted of two $\frac{1}{8}$" wide strips of aluminium foil attached to the column by means of two rubber bands holding the ends together, but separated, so that there was no electrical contact between them (see Figure 15). A coaxial cable having the central core attached to one strip and the screen to the other was connected via a co-ax plug to a capacitance gauge which was built to the specification given by Attree (213), the circuit diagram of which is shown in figure (14). The main components of the circuit are a triode valve type IT4 with a tuned anode circuit consisting of capacitors C_2, C_3 and C_4 and the choke L_1, and a 4 mega cycle/sec crystal oscillator which is built into the grid circuit of the valve. The tuned anode circuit is so designed that at the resonant frequency of the crystal, the anode impedance is slightly inductive. Under these circumstances a small change in capacitance at the anode causes a large change in the strength of the oscillations, in the anode current and in the voltage drop across the anode load R4. The voltage fluctuations at the bottom of R4 caused by the change in the column capacitance due to the passage of bubbles, were/

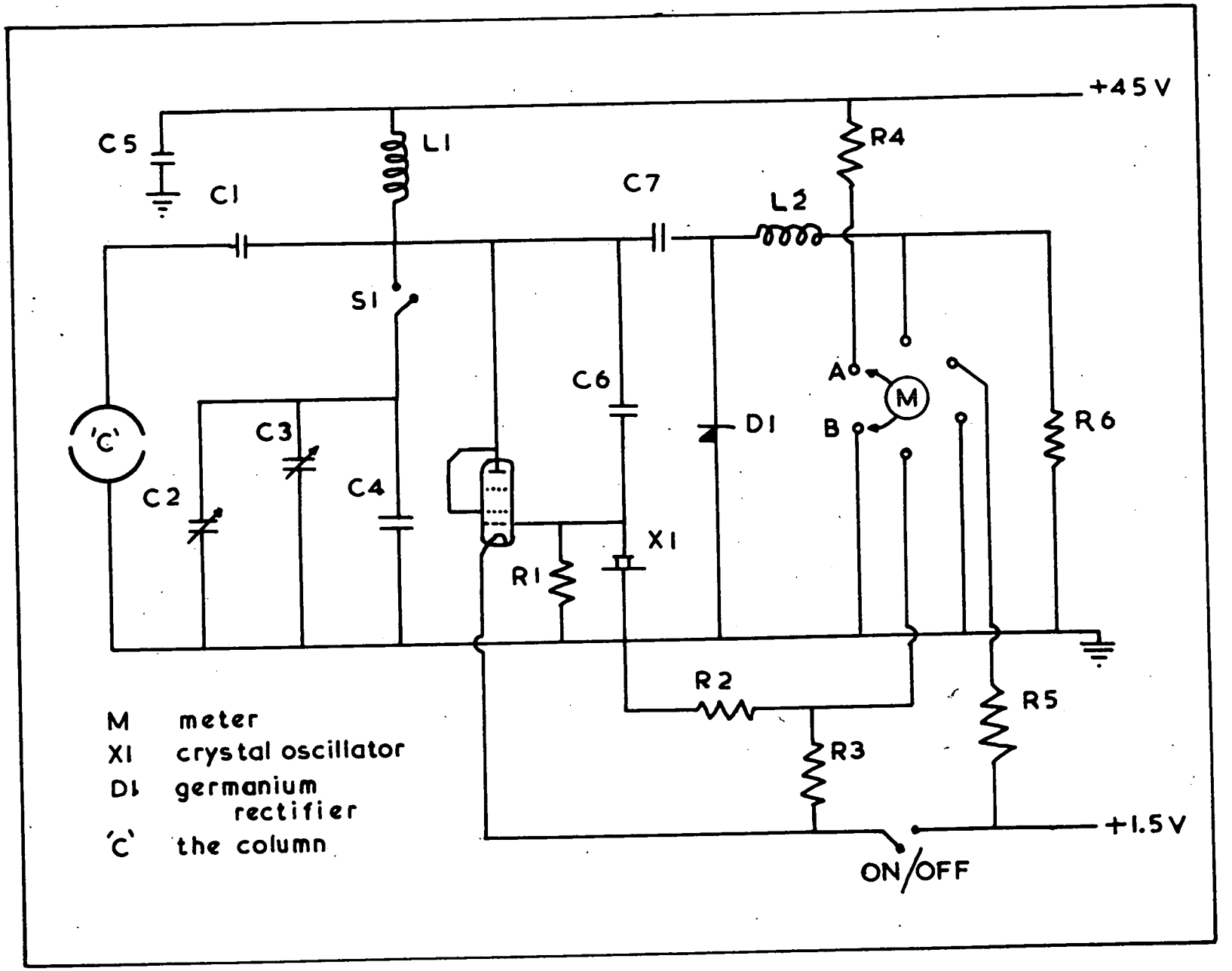

CAPACITANCE GAUGE - circuit diagram

FIGURE 14

were fed to the amplifier of a Southern Instruments Limited pen-recorder and appeared as a wavy trace, with peaks representing large bubbles and 'noise' representing smaller bubbles and fluctuations in the solids concentration. Figure (16) shows two examples of the traces. The detailed operation of this equipment will be given later. Using this method bubble frequencies were measured for fluidized beds of sand and glass ballotini over a range of liquid and gas flow rates and bed porosities, at various heights up the column.

B. EXPERIMENTAL PROCEDURE

1. Column Operation

The apparatus is described in detail in chapter VI and for this series of experiments no modification was necessary. Refer to figure (11). The column section A was built up to a height of eight feet. Valves V12, V10, V2, V3, V4, V5 and V9 were closed and V8 opened to fill the make-up tank with water and switched off when it was full. The pump was then switched on and water was withdrawn from the tank via V4 through V1, and the liquid votameter R1, into the bottom of column section B to fill the column. When the level rose above that of the take-off tee sectionC, water overflowed down the flexible return line to fill up sections E and F. When these were full valve V6 was closed, the pump/

pump switched off and V4 closed. V2 was then opened which completed the liquid side closed circuit between all sections of the column. Sand or Ballotini was then dropped into the column through the top section D, which was three feet in length. The water displaced by the solid particles was drained via valve V3 until the level was three inches above the top of tee-section C. From the fluidization curves for the solid particles, given in Appendix IV, the appropriate settled height of particles was calculated to achieve a bed of the highest porosity to be studied, which would fill the unaerated column to the top of the tee section C. To cover the range of increasing bed porosities it was a simple matter to add more solid particles and reduce the liquid flow rate accordingly. After the correct amount of solids were added the pump and both immersion heaters were switched on to raise the water temperature to 36°C, and when this was reached the booster heater was switched off leaving just the controller heater on. The required liquid flow rate was then set by operating the pump by-pass valve V13 for a coarse adjustment and the rotameter control valve V1, to give the rotameter reading indicated by the calibration curve. The column was then ready for aeration.

Before V12 was opened to admit air to the column, reducing/

reducing valve V7 was set to give an air pressure much greater than the hydrostatic pressure on the liquid side of V12, to prevent water filling up the air lines. When V12 was opened the initial surge of air due to the high supply pressure, coalesced into one large slug which rose to the top of the column. Once the gas flow was established V7 was readjusted to give the rotameter reading for the desired flow rate, indicated by the calibration curve. The air flow rates, expressed throughout as superficial linear velocities based on the empty column cross-sectional area, are those existing half way up the column.

Upon completing measurements at one bed porosity the pump and contrd heater were switched off and the gas flow discontinued by closing valve V12. More solids were then added, the liquid level reset by using V3 and the same procedure for start-up followed as previously described.

To change from one solid material to another the solids already in the column were highly fluidized and syphoned out, using a 1" I.D. hose-pipe, into large buckets where the solids settled out and the water overflowed away to the drain.

2. Operation of the Capacitance Gauge

Refer to figures (14) and (15). The aluminium/

CAPACITANCE MEASUREMENTS -

SCHEMATIC LAYOUT

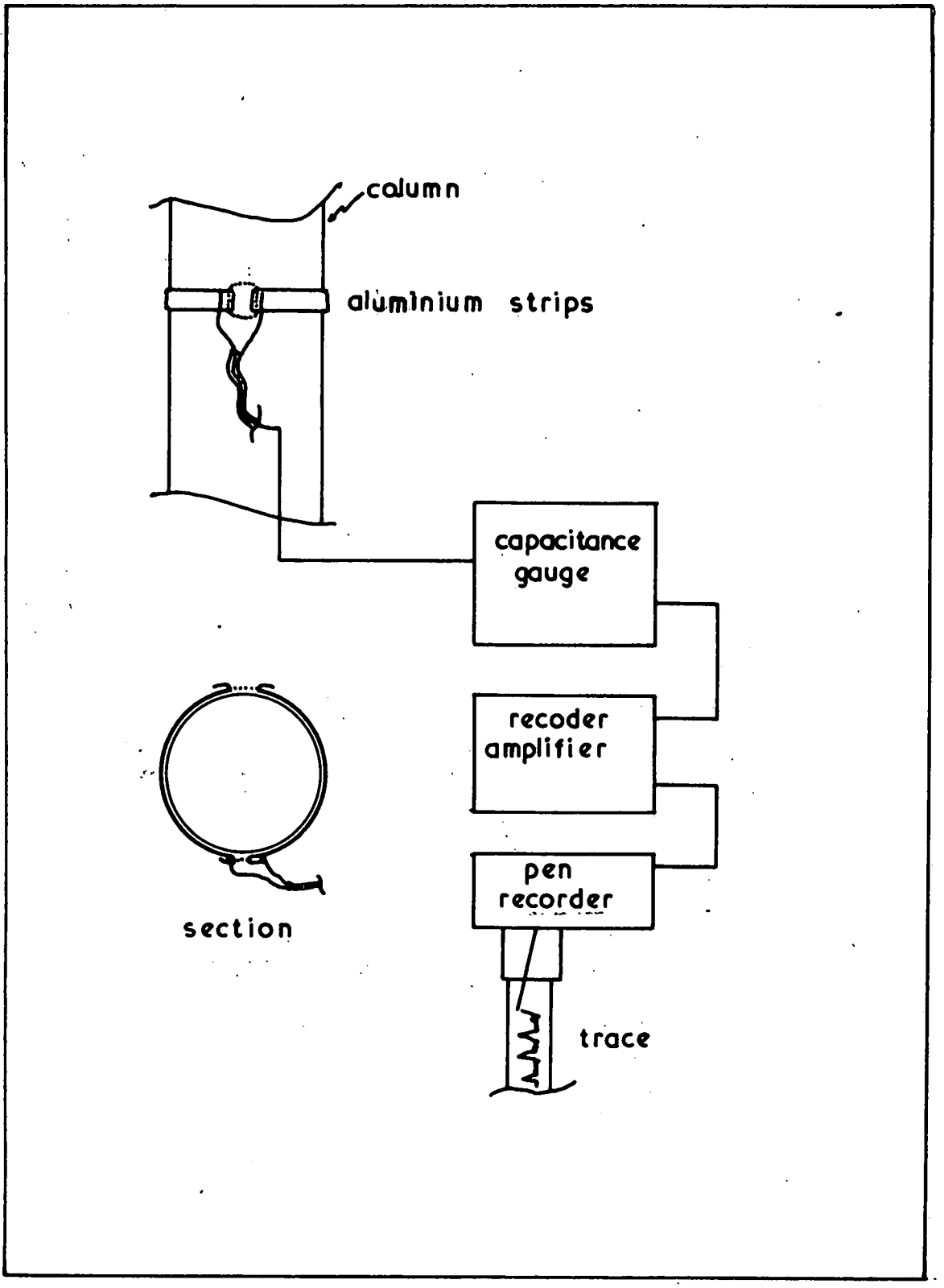

FIGURE 15

aluminium strips were placed around the column as shown in figure (15) at the desired height. Before aeration, when the bed had been expanded to the desired porosity, switch S1 was closed bringing the column capacitance into the anode circuit. The on-off switch was then switched on connecting the 45 v H.T. and 1.5 v L.T. batteries. Next, the variable capacitors C_2 and C_3 were used to tune the anode circuit using the meter, connected as shown, to indicate when the anode current was a maximum. The meter was then disconnected and points A and B connected to the input terminals of the pen-recorder amplifier - a steady trace was produced on the recorder chart. The air supply was turned on and the pen fluctuated back and forth in response to the capacitance changes in the column due to the presence and passage of gas bubbles. When the air flow settled down the chart motor was switched to give a chart speed of 2.5 cms/sec and a wavy trace was produced, similar to those shown in figure (16). About 100 cms of chart were run out for each frequency measurement.

C. TREATMENT OF EXPERIMENTAL DATA AND RESULTS.

The experimental data were a series of strips of pen recorder chart paper with traces on them. The number of large peaks, corresponding to large gas bubbles, were counted for a chart paper length of from

30/

PEN- RECORDER TRACES

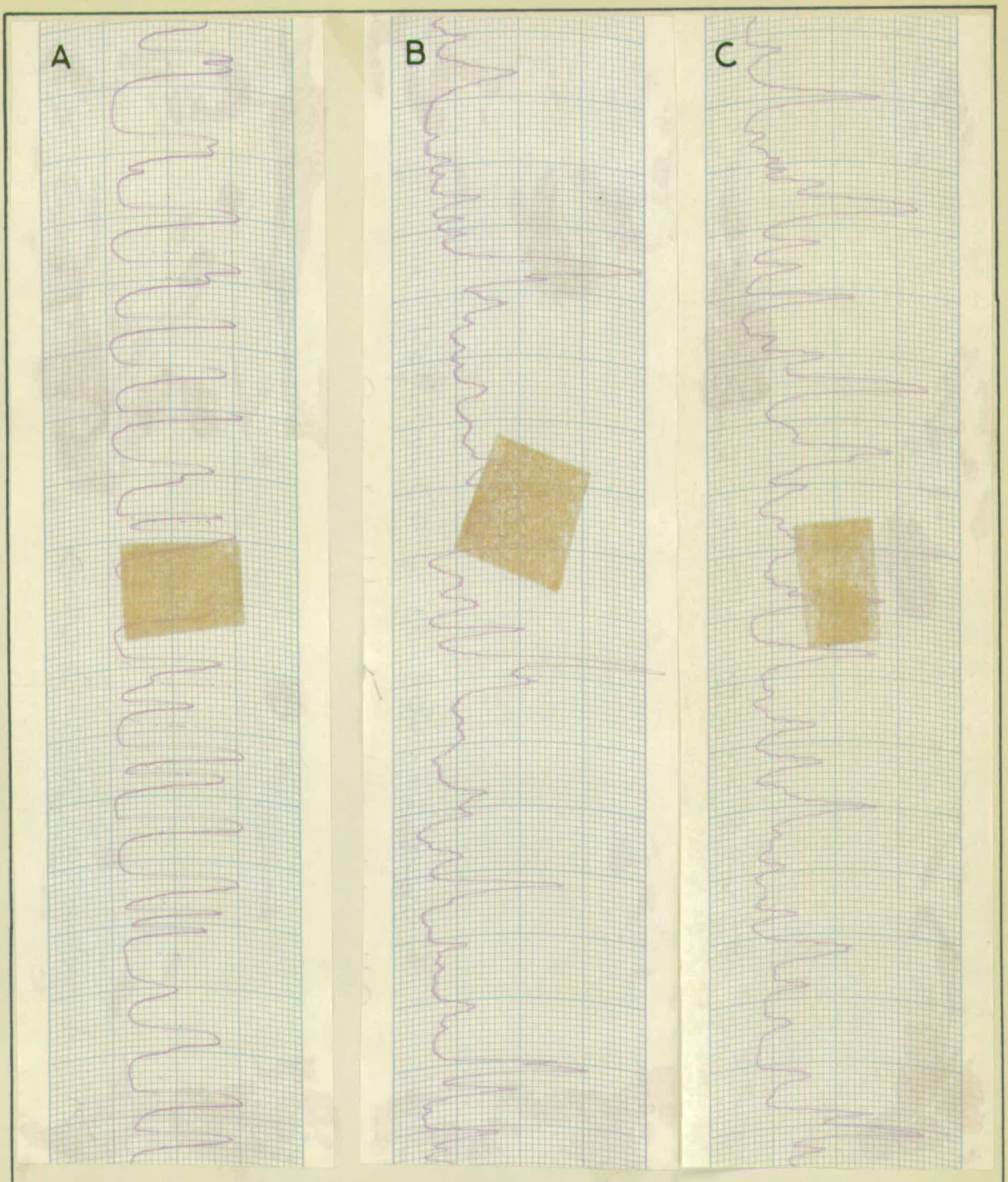

A	B	C
V_s = 6.8 cm/sec	V_s = 5.0cm/sec	V_s = 8.7 cm/sec
h = 75 cm	h = 40cm	h = 90cm
ϵ = 0.51	ϵ = 0.60	ϵ = 0.85

FIGURE 16

30 to 60 cms. The chart speed during the runs was fixed at 2.5 cms/sec. It was thus a simple matter to calculate the corresponding bubble frequencies. These were plotted against the height, in cms, at which they were determined on semi-log graph paper for each bed porosity studied. The results are shown in figures (17) to (19) and figure (20) has the results superimposed on it, together with the correlation developed shown as a family of solid lines.

D. DISCUSSION OF THE RESULTS

The following points of interest can be seen immediately from the results as they are plotted in figures (17) to (20):-

1) The slope of the line drawn through the points for each bed porosity, which gives a measure of coalescence, is different for each bed porosity, increasing as the porosity decreases.
2) The bubble frequencies do not begin to fall until a particular point up the column is reached, and the height of this point depends on the air rate and bed porosity. This point will be referred to as the coalescence point.
3) For a given bed porosity the lower the gas rate the greater the height of the coalescence point and for a given gas rate the lower the porosity/

BUBBLE FREQUENCY(f_B) VS HEIGHT (h)

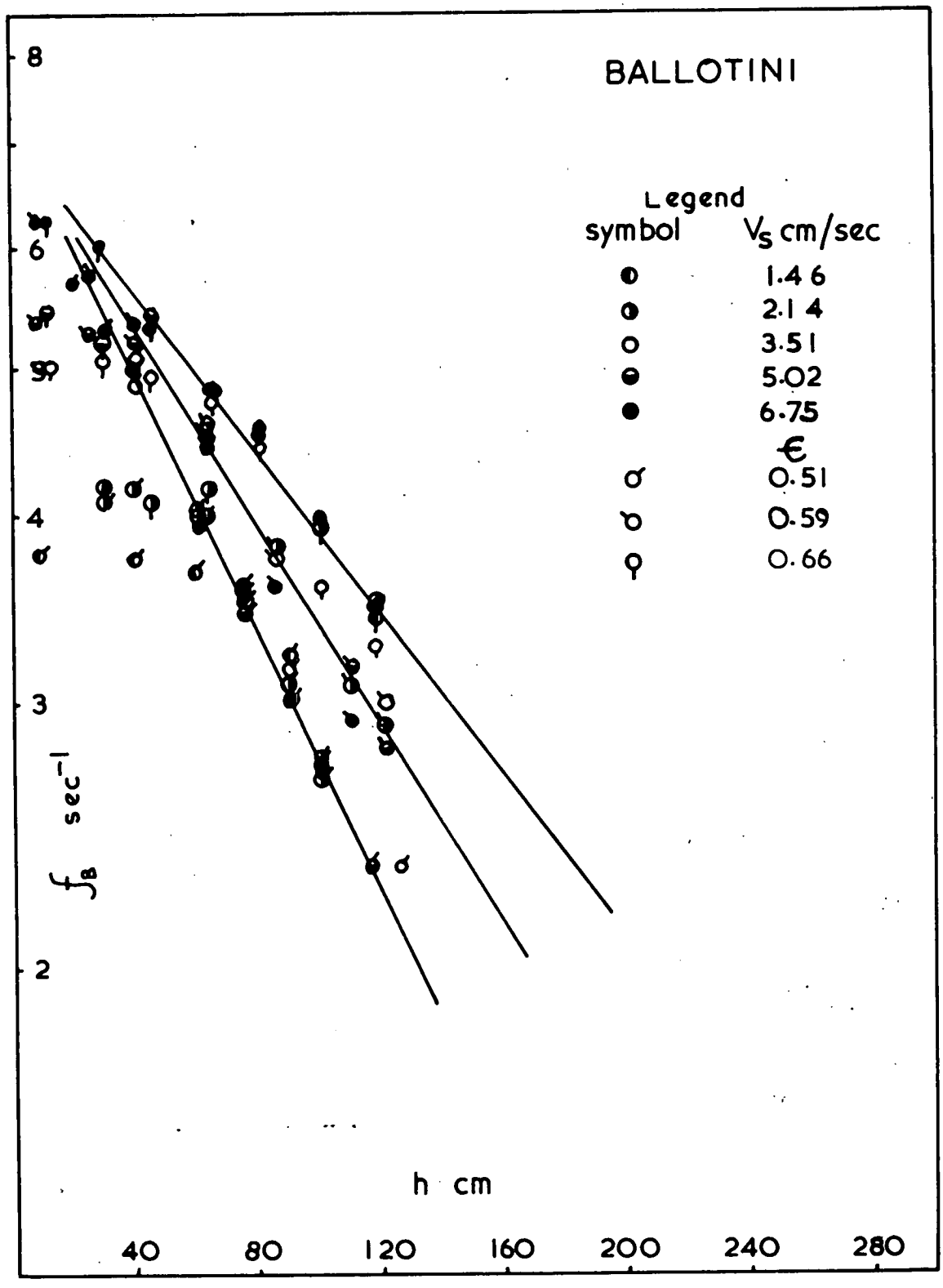

FIGURE 17

BUBBLE FREQUENCY (f_B) VS HEIGHT (h)

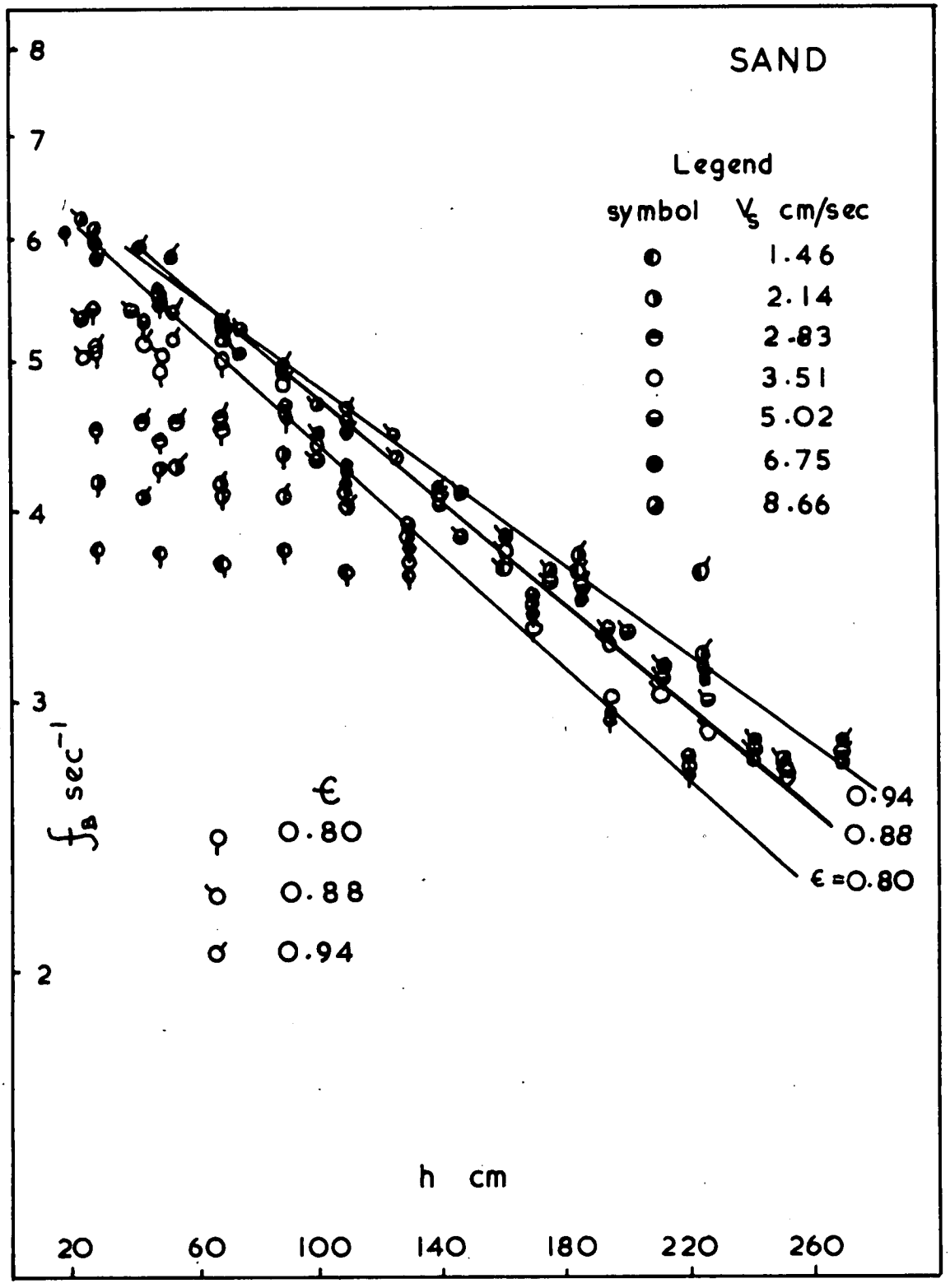

FIGURE 18

BUBBLE FREQUENCY (f_B) VS HEIGHT (h)

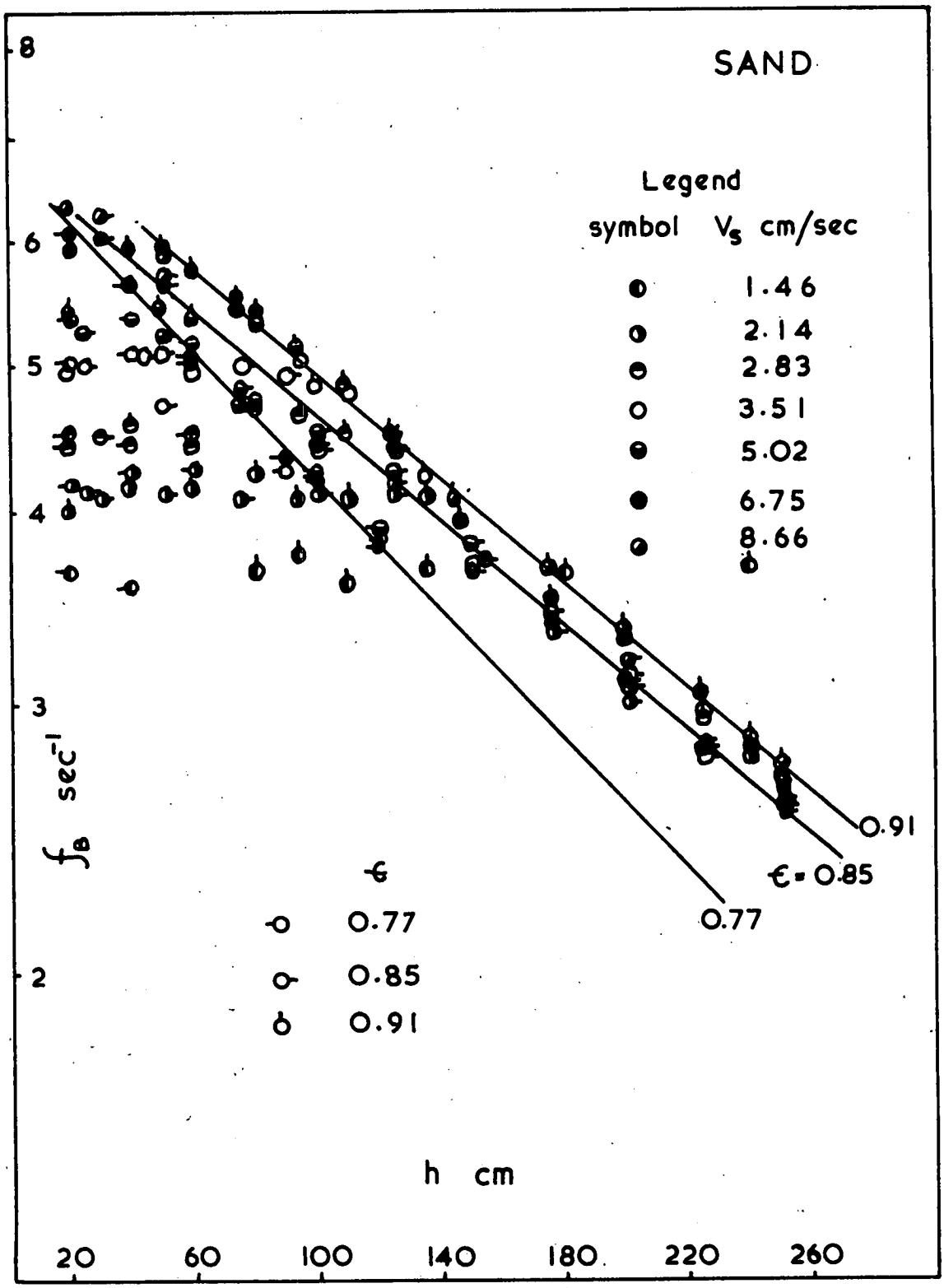

FIGURE 19

BUBBLE FREQUENCY (f_B) VS HEIGHT (h)

Correlation :- $f_B = \exp\left[1.95 - \left[\frac{7.12}{\epsilon} - 4.39\right] \times 10^{-3} h\right]$

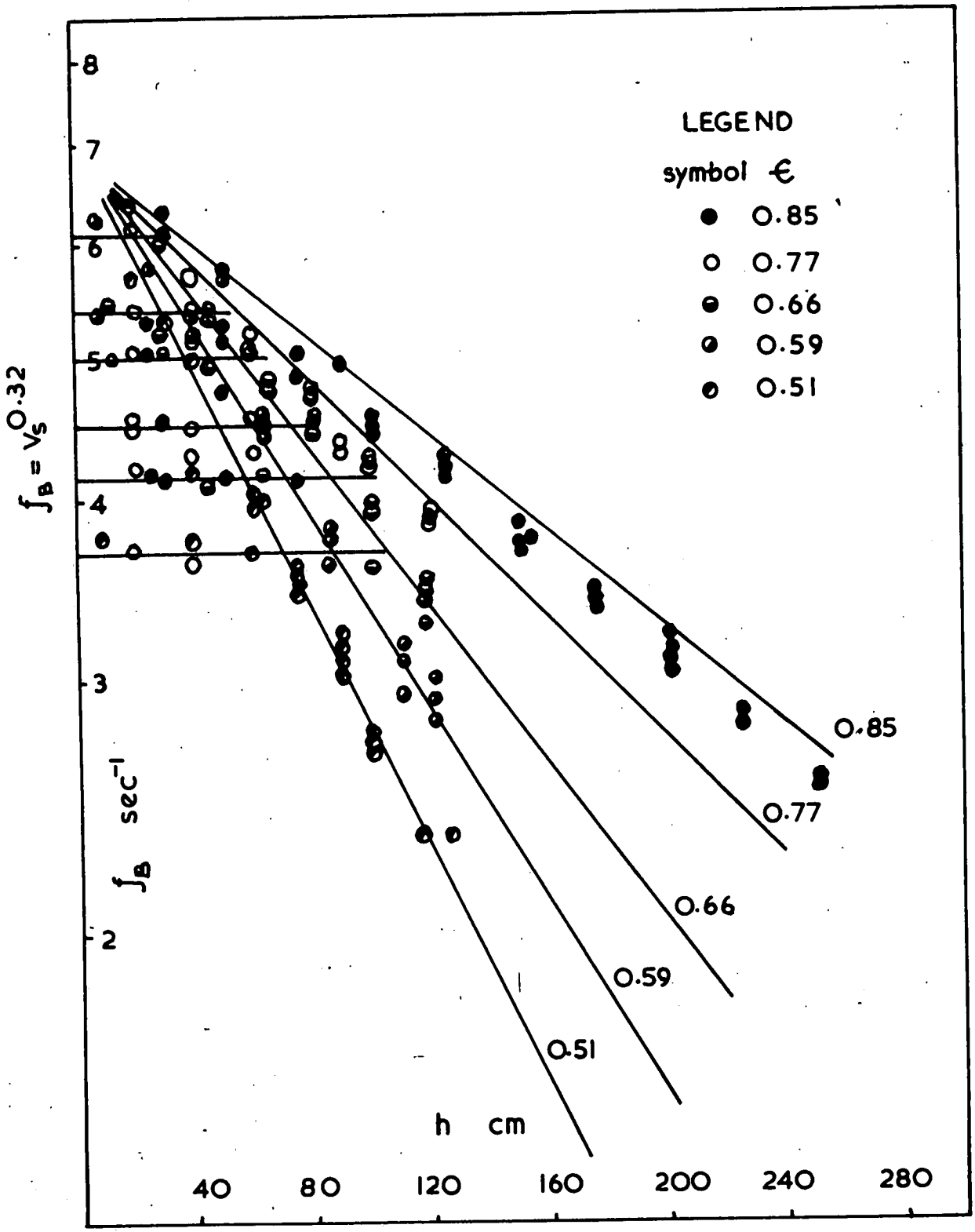

FIGURE 20

porosity the lower the height of the coalescence point.

4) In the region before the coalescence point is reached, the bubble frequency is independent of bed porosity and liquid rate and depends only on the gas flow rate.

5) When the coalescence lines are extrapolated back to zero on the height axis they all cut the frequency axis at approximately the same point, namely at 7 bubbles per second.

The following discussion will be divided into three parts, the first discussing the region in which the bubbles are coalescing with each other, the second the region before this coalescence begins and the third a comparison with other workers' results, namely those of Calderbank et al., (206) and Massimilla (202).

1. The Region of Coalescence

The fact that the sloping coalescence lines all pass through one value of the bubble frequency at zero height means that all the bubble frequency data in this region can be correlated by the equation below:

$$f_g = \exp.\left[1.95 - Qh\right] \quad \ldots\ldots (1)$$

where f_g is the bubble frequency, sec^{-1}, h is the height above the bed support gauze, cm, and Q is the slope of the coalescence lines in figures (17) to (19), cm^{-1}, and depends on the bed porosity.

When/

COALESCENCE RATE Q VS POROSITY €

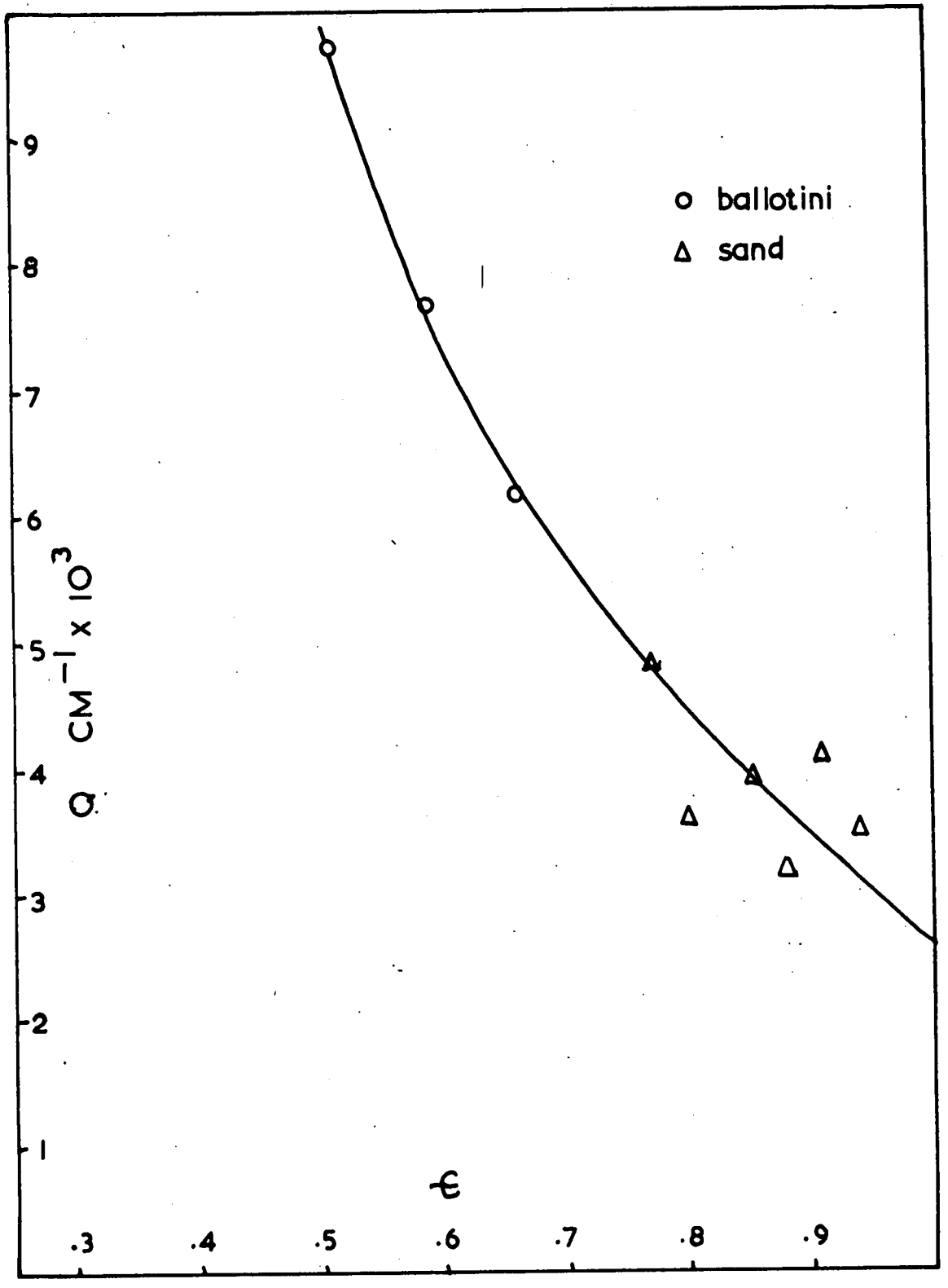

FIGURE 21

When Q is plotted against bed porosity, ϵ, on linear paper, shown in figure (21), the points lie on a smooth curve except at the higher values of ϵ where there is considerable scatter. Values of Q at increasing bed porosities are less reliable because the experimental bubble traces at these values of ϵ showed less differentiation between the high peaks of the large bubbles and the background 'noise' due to swarms of smaller bubbles and ones of an intermediate size. This made counting them and deciding which to consider as large bubbles and which not, much more difficult than it was at lower values of bed porosity, where the traces showed much less evidence of smaller bubbles. In fact at a porosity of 0.51 only large peaks were detected which indicated that most of the gas was formed into large bubbles immediately after passing through the gauze.

As figure (21) shows a smooth curve of Q against porosity this indicates that the rate of coalescence is a unique function of the bed porosity; the nature of the particles forming the bed and the liquid flow rate have no influence on it. The fluidization characteristics of the sand and ballotini were quite different and the liquid rates required to produce beds of the same porosity were different. For example

a/

a water flow rate of 25 litres/min at 36°C would give bed porosities of 0.92 and 0.57 for sand and ballotini respectively. However it must be pointed out that the magnitude of the superficial liquid velocities used varied between 1 and 4 cm/sec which is small compared to the rise velocities expected, for gas bubbles detected by the capacitance probe, and would therefore not be expected to have much influence.

When the values of Q are plotted against the reciprocal of bed porosity a straight line can be drawn through the points, as shown in figure (22). Thus the rate of coalescence, in this column, varies inversely as the first power of the bed porosity, and the equation relating them is:-

$$Q \times 10^{-3} = 7.12/\epsilon - 4.39 \quad cm^{-1} \quad \ldots\ldots (2)$$

which gives an average percentage deviation of 0.75% for porosities below 0.8 , but of 13.6% for porosities above this.

Combining equations (1) and (2) a correlation for all the results in the coalescing region can be given:

$$f_B = \exp\left[1.95 - \left(\frac{7.12}{\epsilon} - 4.39\right) \times 10^{-3} h\right]_{sec^{-1}} \quad \ldots\ldots (3)$$

The family of lines for this correlation is given in figure (20) with the results of [redacted] frequency measurements superimposed.

It/

COALESCE RATE (Q) VS $\frac{1}{\epsilon}$

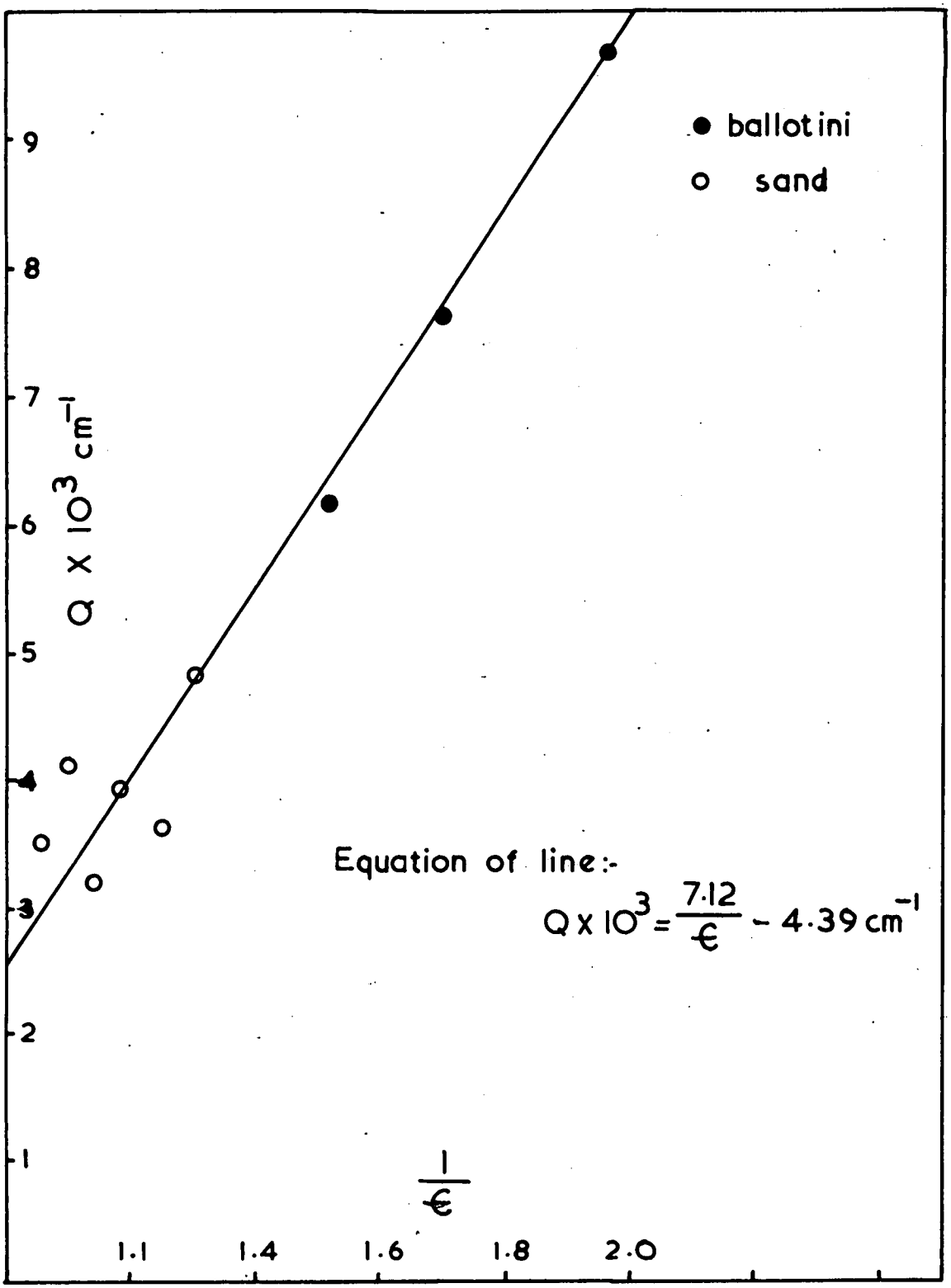

FIGURE 22

It should be noted also that the line in figure (22) intercepts the Q axis at a +ve value, namely 2.6×10^{-3} cm^{-1}, which indicates that at a porosity of 1, or when no particles are present, some coalescence will still occur. This is in agreement with observations of gas bubbles in the column when no particles were present - at the high gas rates used in these experiments bubbles in pure water coalesced, although large bubbles would break up again due to the high turbulence.

2. The Region before Coalescence

Figures (17) to (20) show that the bubble frequency depends on the gas flow rate and not on the bed porosity in this region. At first sight this would indicate that all the bubbles are the same size. Unfortunately the capacitance probe does not give any quantitative information on bubble sizes although for a larger bubble, a larger peak on the trace would be expected. Observations in the two dimensional column, discussed in Chapter IX, showed that the size of the bubble formed immediately above the injection nozzle is related to the bed porosity, being larger as the bed porosity is decreased. With this in mind, one is led to the conclusion that in the column, at any one gas rate the frequency of the bubbles is constant, but their/

their size increases, with decreasing bed porosity. The fact that their size increases with decreasing porosity is also supported by the fact that the lower the bed porosity, the lower the height at which they begin to coalesce; which in turn indicates that they must have been bigger to start with, so needing to grow less before coming close enough to coalesce. But there still remains the anomaly of a constant frequency and increasing size for the same overall gas flow rate. This is reconciled by considering that not all the gas is formed into bubbles of the size of those detected by the capacitance gauge; indeed if this were so, then the bubble sizes corresponding to the frequencies measured would vary from 5 to 8 cms in diameter at the lowest and highest gas rates used, and bubbles of this size would not have escaped notice. From observations of the column during operation it is certain that a large proportion of the gas is present in fairly small bubbles of the order of 4 to 10 mm in diameter. It is these bubbles that allow the growth of the other larger bubbles (by being overtaken and coalescing in the manner described by Calderbank (206) to the size where they are close enough to coalesce with one another. The anomaly is thus solved if the distribution of the gas between large and small bubbles is dependent on bed porosity/

porosity. As mentioned earlier, the pen recorder traces give an indication of the bubbles present besides the large ones by the amount of 'noise', and this 'noise' was greater the higher the porosity (and led to the difficulty of measuring frequencies for porosities higher than 0.8). It can then be assumed that qualitatively there is a wider distribution of bubble sizes at the higher porosities.

This point will be discussed in more detail in examination of the gas bubble residence time distributions in chapter X.

Figure (23) shows a semi-log plot of superficial gas velocity, against height of the coalescence point above the bed support gauze through which the gas enters the column. The points were obtained by reading the value of bed height at which the best horizontal line through the frequency results for each air rate, cut the sloping coalescence lines on figures (17) to (19) for the four values of bed porosity shown. This family of lines marks the boundaries of column operation to avoid the onset of gross coalescence, and shows the sort of practical information necessary for designing bubble column reactors where the occurrence of gross coalescence must be avoided. Figure (24) shows the bubble frequency determined from the best lines/

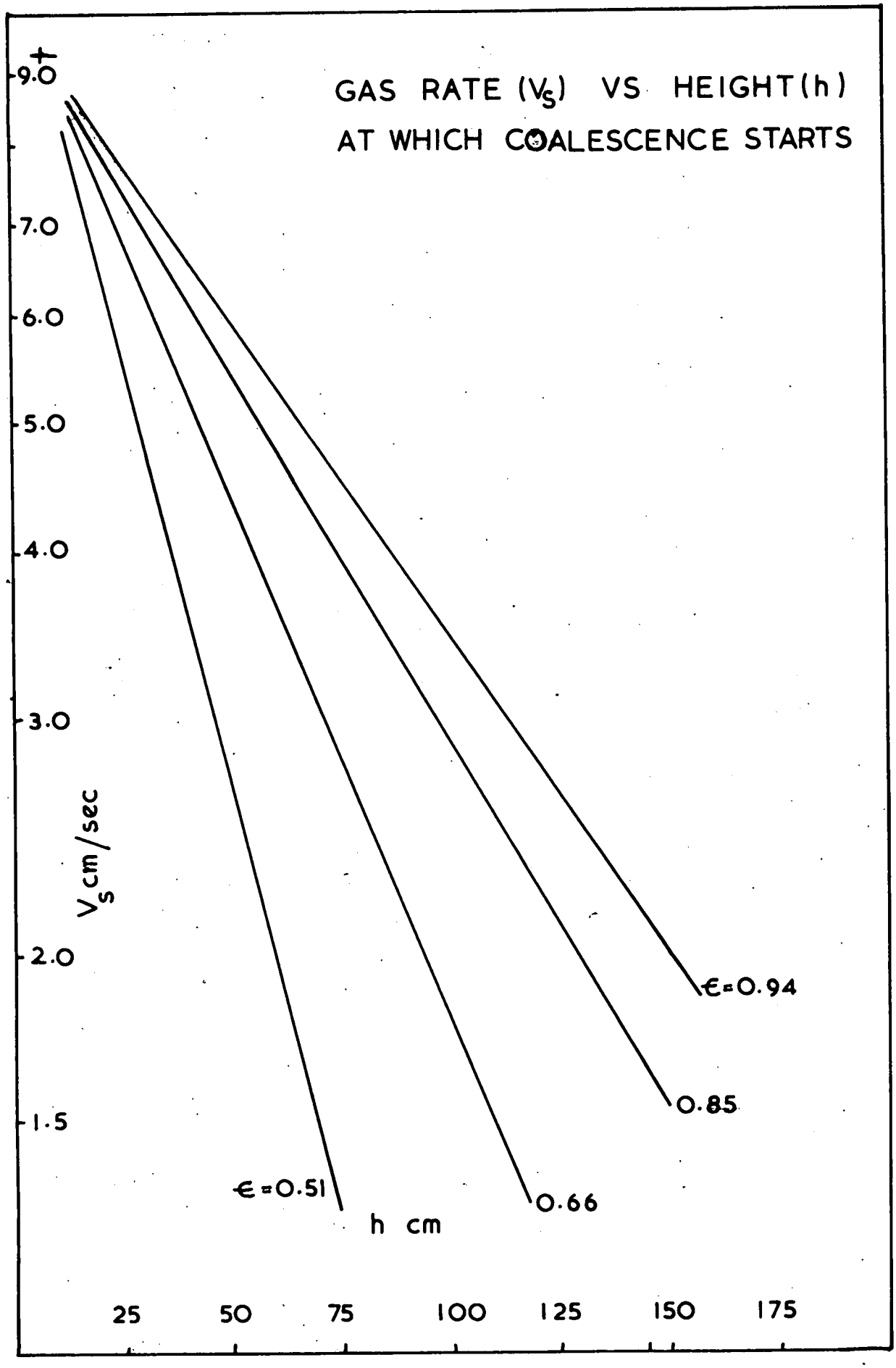
GAS RATE (V_S) VS HEIGHT(h)
AT WHICH COALESCENCE STARTS
9.0
7.0
6.0
5.0
4.0
3.0
2.0
1.5
V_S cm/sec
ϵ=0.94
0.85
0.66
ϵ=0.51
h cm
25
50
75
100
125
150
175

FIGURE 23

BUBBLE FREQUENCY VS SUPERFICIAL GAS VELOCITY

(In the region before coalescence commences)

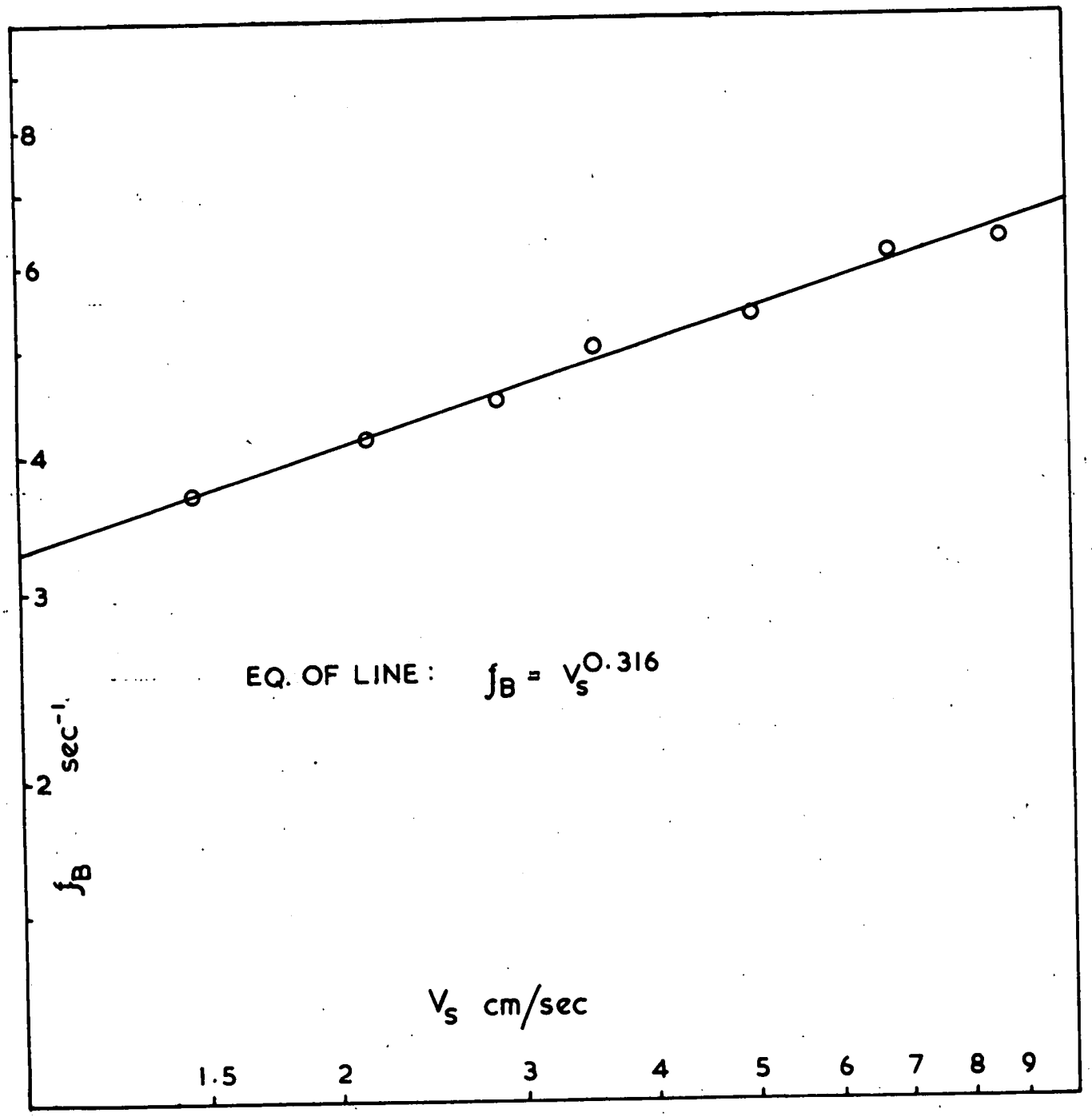

FIGURE 24

lines through the data plotted against the superficial gas velocity. They are related by the equation:

$$f_\beta = Vs^{0.316} \text{ sec}^{-1} \quad \ldots\ldots (4)$$

3. Comparison with results of other workers

The only published work on the coalescence of large bubbles moving through a dispersion of smaller ones in a deep pool is by Calderbank (206) and Massimilla (202).

(a) Calderbank et al's Work (206)

Calderbank using a solution of glycerol and water at a viscosity of about 70 centipoise in a 10 foot high column 4 inches square in cross-section, passed carbon-dioxide gas through a 4" x 4" sieve plate, containing 56 1/64" holes, into the column at superficial gas velocities from 0.5 to 2 cms/sec. He measured the height at which spherical cap bubbles first appeared and their frequency at various heights up the column thereafter. He presented the results on a semi-log plot of bubble frequency in sec^{-1} against α, cms, which is the distance up the column above the height at which spherical cap bubbles first appeared for the corresponding gas flow rate. His sloping line cut the bubble frequency axis at 5.80 bubbles/sec which is lower than in the three phase column, which may be due to the different column geometry. He suggests that the/

the frequency of bubble formation may be determined by the resonant frequency of the dispersion within the column. He correlated his results by the following equation:

$$f_b = \exp\left[1.764 - 4.375\chi \times 10^{-3}\right] \text{ sec}^{-1} \quad \ldots (5)$$

which is of the same form as the correlation for this three phase column. If his value of χ is assumed equivalent to the value of h in equation (3) then the value of porosity ϵ to make the negative parts of the exponential in both correlations the same, i.e. an identical coalescence rate, Q, is 0.81.

This result, coupled with the discovery that in this work, the rate of coalescence is a unique function of the bed porosity, led to the consideration that perhaps the bubble coalescence rate is determined by the viscosity or psuedo-viscosity of the liquid or liquid-solid fluidized bed through which the bubbles are rising. Calderbank, also found that at low gas flow rates neither spherical caps formed nor did coalescence occur until his liquid viscosity exceeded 69 centipoise. (In this work at the low gas rate of 1.46 cm/sec no coalescence could be detected for porosities of 0.88 and 0.94 - see figure (18,)19) He unfortunately did not measure bubble frequencies at liquids of viscosities much greater than 70 centipoise. Massimilla (202) when comparing his single bubble rise velocity data in/

in his liquid-solid fluidized bed with those in viscous liquids, found that if he assumed his bed had a viscosity of 62.5 centipoise, his data could be correlated by the equation of Oseen (217) which he quotes as:-

$$V_b = \frac{-1.33\mu}{r\rho} + \sqrt{\left(\frac{1.33\mu}{r\rho}\right)^2 + 0.593\, gr} \qquad \ldots\ldots (6)$$

$$0.3 < \frac{V_b r \rho}{\mu} \leq 1.$$

where Vb is the bubble rise velocity; r its radius; μ and ρ the viscosity and density of the medium through which the bubble is rising; and g is the gravity constant. He also notes that 62.5 centipoise is of the same order of magnitude as values which have been found by Trawinski (218) for fluidized beds similar to his. However work done recently on measuring the viscosities of fluidized beds of ballotini beads with water, by Anderson and Bryden (219) gave values of between 9.4 and 16 poise for a porosity of 0.49, depending on the rate of shear. They used an annular space between an inner rotating cylinder and fixed outeroone, to contain the bed and varied the shear rate by the speed of rotation of the inner cylinder. As the shear rate was increased the viscosity levelled out at about 9 poise. This value is very high compared to the value of 62.5 centipoise of Trawinski. More work in this field is required before any conclusions can be drawn/

drawn about coalescence rates and dispersion viscosity. An experimental study of spherical cap, or large bubble, coalescence rates in liquids of varying viscosities much greater than 70 centipoise, would provide data that could be compared with the results of this study in a three phase bed. Gas rates of between 2 and 9 cms/sec and a 6" I.D. column should be used to provide a better basis for comparison than Bibby's smaller square column.

(b) Massimilla's Work

A true comparison with Massimilla's work, which was done with a gas-solid-liquid fluidized bed, is difficult because he measured the average diameter of all the bubbles emerging from the bed at different heights, whereas this study measured the frequency of large bubbles only and no estimate of bubble size or rise velocity could be made. In addition the superficial gas velocities used by Massimilla ranged from 0.01 to 0.12 cm/sec. whereas in this work they ranged from 1.5 to 8.7 cm/sec. However the effect of porosity and bed-expansion on the coalescence rate can be qualitatively compared, although the basis of assessing the coalescence rate is different in the two cases. Massimilla measures the change in average bubble diameter with height and this study measures the change in large bubble/

DATA FROM MASSIMILLA'S FIGURE 17

$\left(\frac{L_o}{\Delta L}\right)$ CONVERTED TO POROSITY(ϵ)

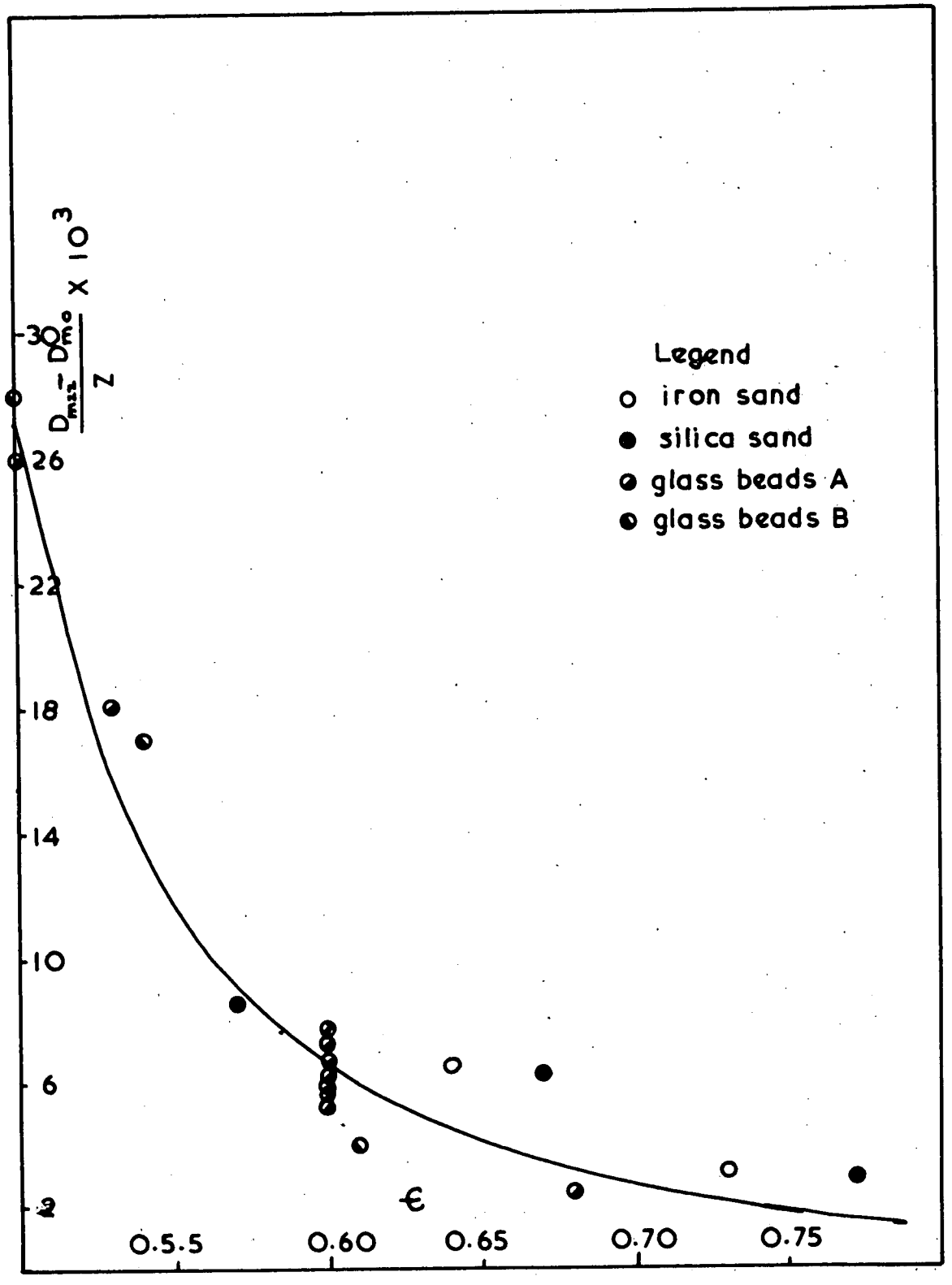

FIGURE 25

DATA FROM MASSIMILLA'S FIGURE 17

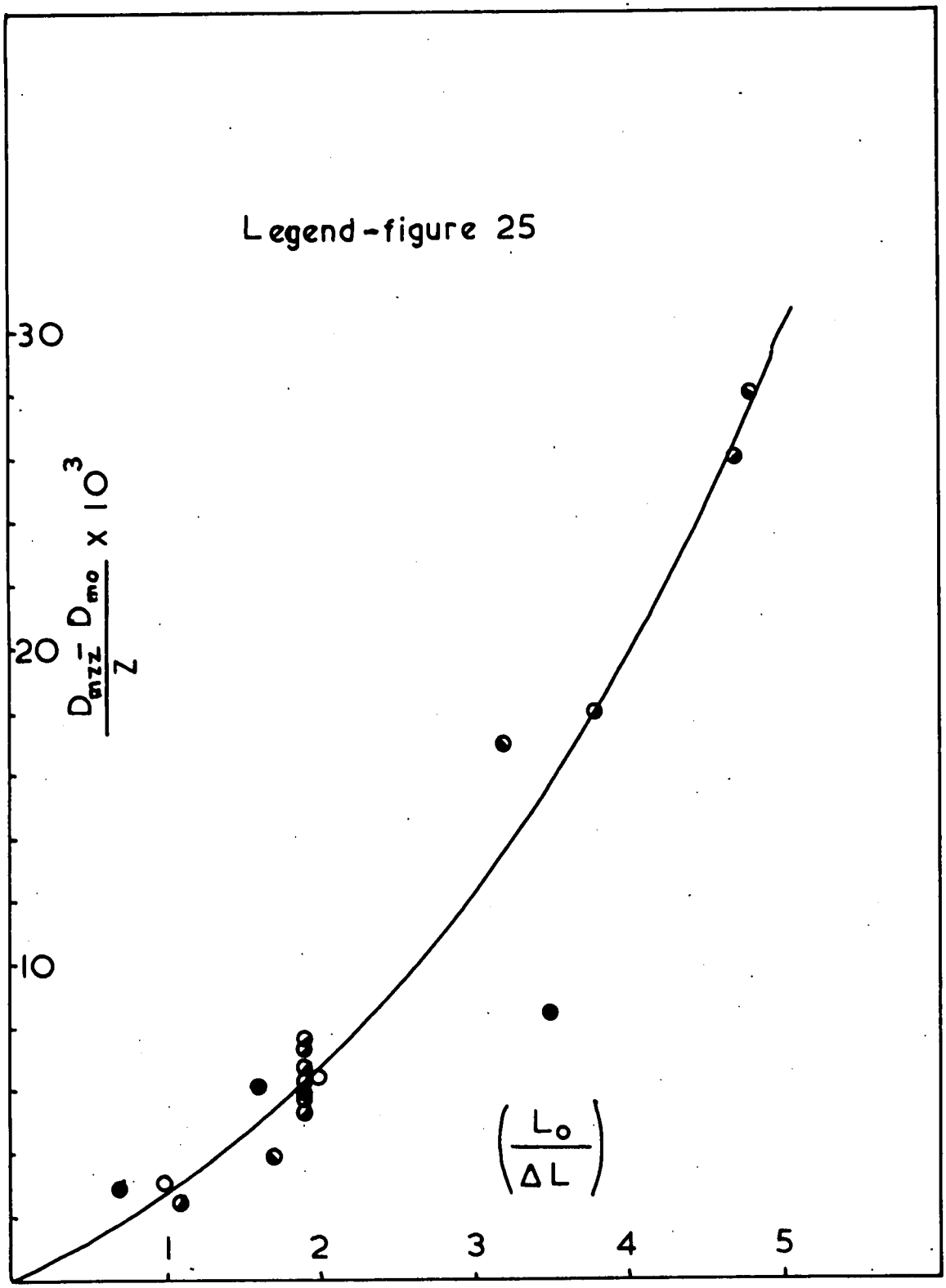

FIGURE 26

bubble frequency with height.

He correlates all his coalescence results by the equation already quoted in Chapter IV:-

$$\frac{Dmzz - Dmo}{Z} = a\left(\frac{Lo}{\Delta L}\right)^b \qquad \ldots\ldots (7)$$

where $(Lo/\Delta L)$ is the reciprocal of the bed expansion. To see if his data correlated with the bed porosity it is necessary to know the values of porosity corresponding to these reciprocals of bed expansion. This data was supplied by Massimilla in a private communication (222). His data given in the log-log plot from which he calculated the values of a and b in his correlation, were extracted and replotted as

$$\frac{Dmzz - Dmo}{Z}$$

against the values of porosity given, on linear paper, in Figure (25). The log-log plot data was also plotted on linear paper, in Figure (26), as it stood, to compare the two sets. There does not seem to be much difference in the scatter of experimental points from the two curves drawn in the figures. No definite conclusion that his rate of coalescence was a unique function of porosity can be drawn, in view of the wide scatter, but it does appear to be so as a general trend.

The values of bed expansion corresponding to the porosities used in this work were used to plot Q against the/

COALESCENCE RATE (Q) VS $\left(\frac{L_o}{\Delta L}\right)$

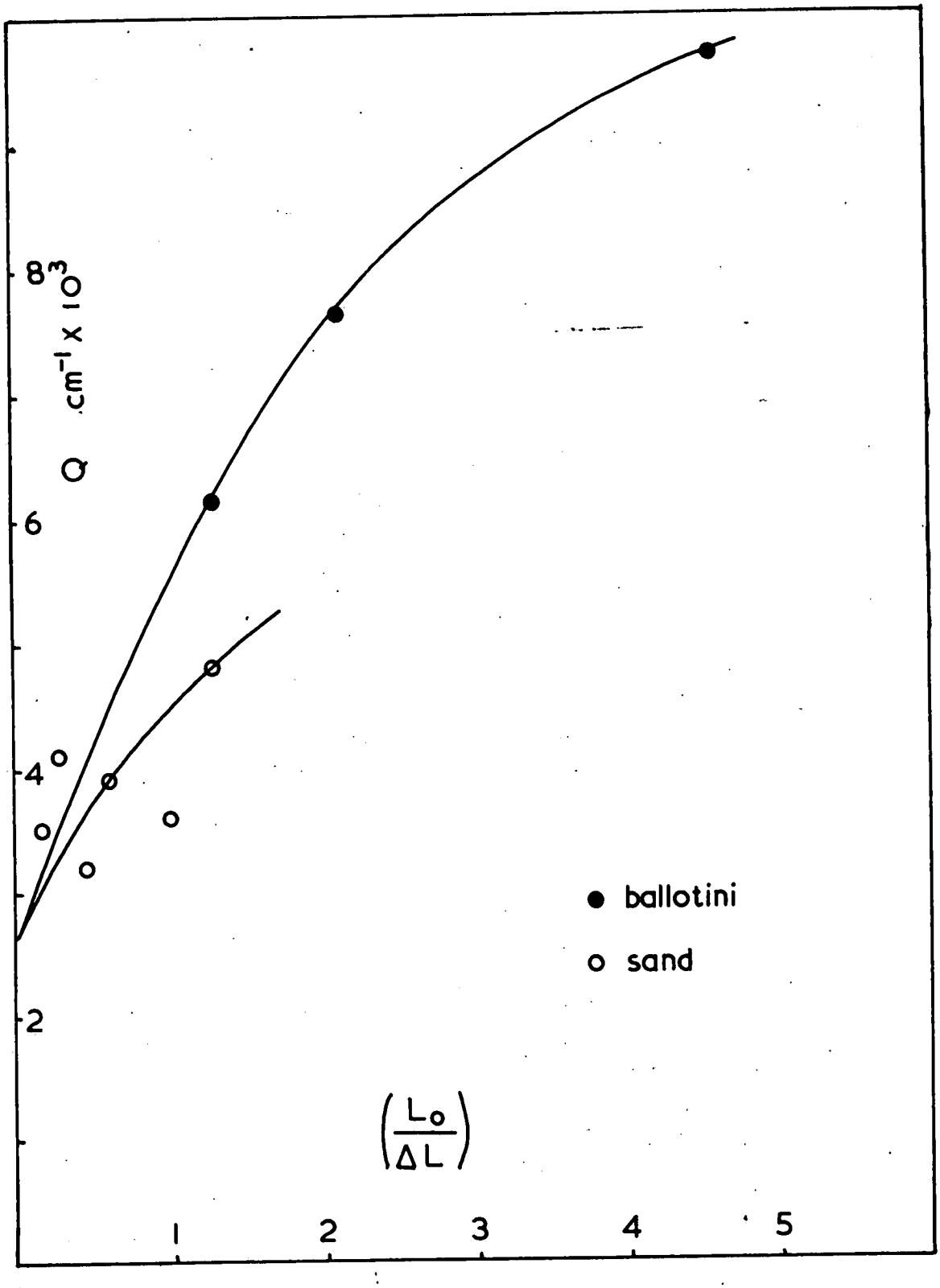

FIGURE 27

the reciprocal of bed expansion on linear paper, shown in figure (27). Here there is a more definite indication that Q is not a unique function of the bed expansion, and two curves can be drawn, one for each material.

It can be noted here that in Figure (24), showing Massimilla's data, the curve passes through the zero on the Dmzz - Dmo/Z axis indicating no coalescence would take place at a porosity of 1. This is quite reasonable since at the low gas flow rates used there would be no coalescence in pure water.

E. CONCLUSIONS

1) The distribution of bubble sizes formed at the bed supporting gauze was related to the bed porosity. At very low porosities most of the bubbles were large with only a few small ones that could be observed, and at the highest porosities there appeared to be a wide range of sizes.

2) In the region before the bubbles began to coalesce, the frequency of generation of large bubbles was independent of the bed porosity: and related to the superficial gas velocity, Vs cm/sec, by the equation

$$f_g = Vs^{0.32} \text{ sec}^{-1}$$

3)/

3) The rate of coalescence of large bubbles, as indicated by the change in bubble frequency with height was:
   (a) a unique function of the bed porosity and independent of particle size, and
   (b) inversely proportional to the bed porosity to the first power.

4) All the bubble frequency results in the region where the large bubbles have begun to coalesce were correlated by the equation:

$$f_B = \exp\left[1.95 - \left(\frac{7.12}{\epsilon} - 4.39\right) \times 10^3 h\right] \text{ soc}^{-1}$$

where h is the height above the bed support gauze, cm.

5) The rate of coalescence agrees well with the rate of coalescence of gas bubbles measured by Calderbank et al (206) in a liquid of viscosity greater than 70 centipoise.

6) Figure (28) shows a pictorial representation of the above conclusions.

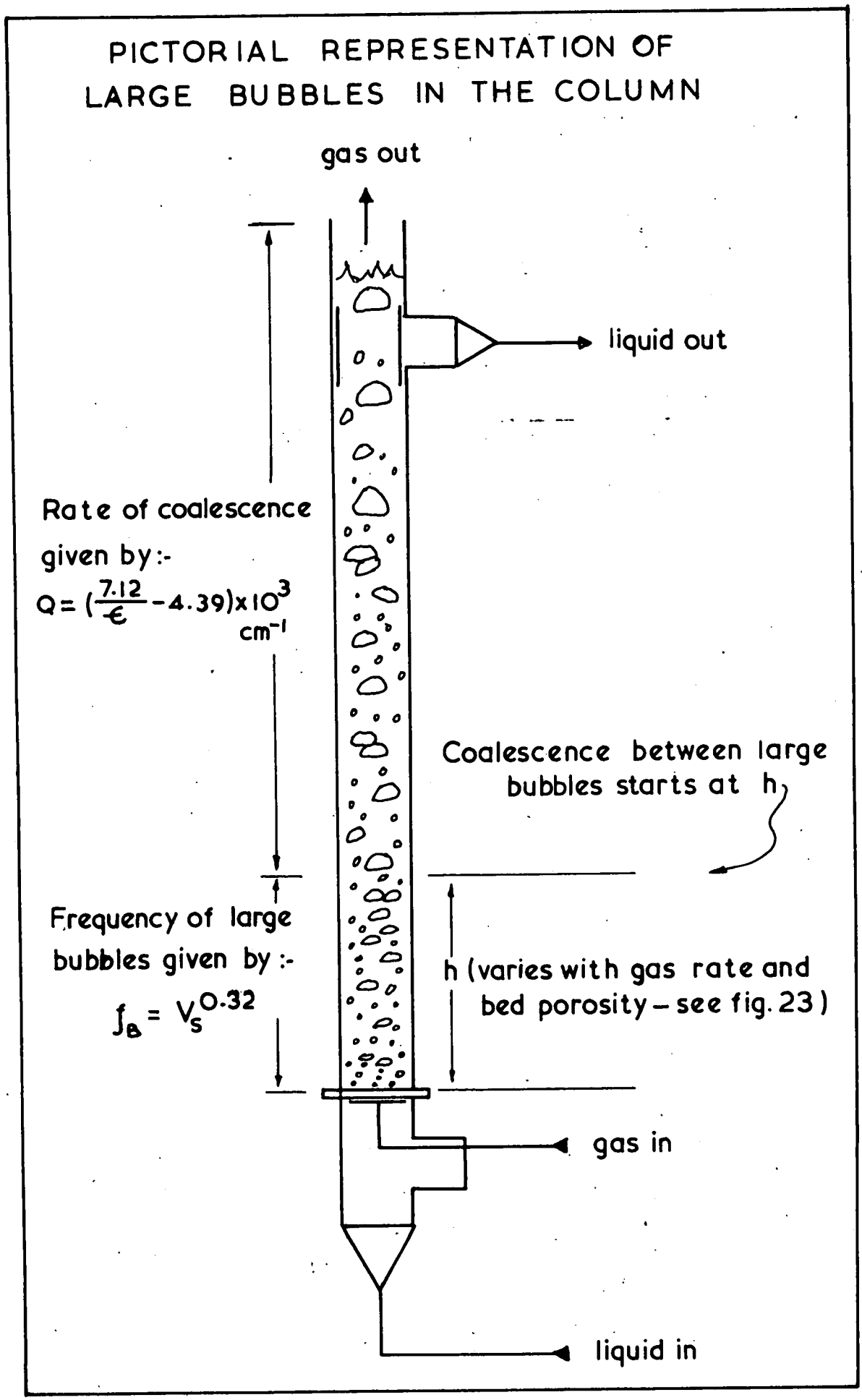
PICTORIAL REPRESENTATION OF
LARGE BUBBLES IN THE COLUMN
gas out
liquid out
Rate of coalescence
given by :-
$Q = (\frac{7.12}{\epsilon} - 4.39) \times 10^3$ cm^{-1}
Coalescence between large
bubbles starts at h
Frequency of large
bubbles given by :-
$f_B = V_s^{0.32}$
h (varies with gas rate and
bed porosity – see fig. 23)
gas in
liquid in

FIGURE 28

CHAPTER VIII

Interfacial Area Measurement

A. INTRODUCTION

In choosing the operating conditions for the column when using the sulphite method of measuring gas-liquid interfacial areas, the considerations discussed in chapter V were borne in mind. The scope of the experiments designed to measure the variation of gas liquid interfacial area with height was thus limited to those conditions which would ensure large changes in local areas with height so that they would be reliably reflected in the change of average areas for the overall column heights used. To this end figure (23) was consulted, so that an air rate could be selected at which it was certain that coalescence began very near to the bottom of the column. Another limitation is imposed by the tendency of the dispersion to foam excessively at the top of the highest column used, 8'9", and for the bubbles to approach the size of the column diameter. A compromise was made by selecting an air rate of 6.75 cm/sec., halfway up the 8'9" column, and average interfacial areas were measured for columns increasing in height in one foot steps from 1'9" to 8'9" at bed porosities of 0.85 and 0.72 using sand, and 0.55 using/

using ballotini.

Gas holdup measurements were made during the mass transfer runs described above but their accuracy cannot be better than ± 10% because of the difficulty of measuring the level of the aerated dispersions which fluctuated up and down as the gas bubbles emerged; this was particularly difficult in the high columns because of the larger gas bubbles and the presence of foam. Holdup measurements were also taken for water fluidized dispersions at each column height used in the mass transfer runs. In these cases there was no foam and the difficulty of measuring the aerated dispersion levels was much reduced.

At the lowest column height of 53.3 cms (1'9") interfacial area and holdup measurements were made for a range of air rates up to and including that used in the runs described above, and at four different bed porosities.

B. EXPERIMENTAL PROCEDURE

1. Column Operation

(a) Charging the column and measurement of total liquid volume.

The column charging procedure was the same as that described in the previous chapter with the following modifications.

1)/

1) Before the valve V4, connecting the make up tank to the pump, was opened, all liquid in the column and lines was drained out through valves V3 and V10, and the weight of water in the tank recorded.

2) When the water level was set to be 3 inches above the top of tee-section C, the excess water was drained back into the make-up tank via V4 instead of to drain via V3. The tank weight was then read and the difference between the two weights, before and after charging, used to calculate the total liquid volume in the column and lines.

(b) Preparation of the sodium sulphite solution

Hot tap water at about 70°C was poured into the make-up tank, whose valves V4 and V5 were closed, to an appropriate volume depending on the height of column being used. Sufficient anhydrous sodium sulphite was added to give a sulphite concentration of about 0.7 Molar, and the solution stirred. When all the sulphite had dissolved a sample was withdrawn and analysed to determine the actual sulphite concentration which was used to calculate the oxygen solubility. The details of the analysis procedure are given in Appendix III.

(c) Charging the column and its operation during the mass transfer runs.

While the sulphite solution in the make-up tank

was/

was still hot it was pumped into the column following the same procedure as already described. As the solids were already in the column this was a quick operation. The sulphite was then circulated around the closed circuit and the cooling water to Section E turned on at valve v9. When the temperature fell to within a few degrees of 36°C, the water was turned off at V9 and the temperature control heater switched on. The liquid flow rate was adjusted to the desired level by rotameter control valve V1. Sufficient of a solution of 1 Molar cupric sulphate, calculated from the total liquid volume in the column, to give a final concentration of approximately 2×10^{-3} Molar, was added through the top of section D. This formed a green precipitate when first contacting the sulphite solution but it quickly redissolved as it was circulated around the apparatus. The air was then turned on, observing the precautions described before, and adjusted to the desired flow rate by V7. The column was then left for thirty minutes to ensure that the copper sulphate solution was evenly distributed throughout the liquid.

At the end of this period, any air that had been carried over to section E through the liquid return line, was vented to atmosphere by valve V6. The air and liquid rates were readjusted if necessary, and the aerated dispersion level in section D was read from a transparent/

transparent calibrated sellotape scale fixed to the glass, and recorded. The temperature indicated by the thermometer was checked to see if it was at 36 ± 0.5°C, and if so, then the run was commenced by taking the first sample and recording the time. During the run checks were kept on the dispersion level and any gas carried over the return line was vented to the atmosphere. If the gas carried over was not vented, then it would displace its volume of liquid from section E which would appear as an increase in the aerated dispersion volume.

(d) Emptying and washing the column

After the last sample was taken the following procedure was carried out. The remaining sulphite solution in the make-up tank was drained off by valve V5 and V8 opened to wash out and then fill the tank with cold water. Without turning the air off or the pump, valve V4 was opened and V2 closed. The dispersion level then began to rise as the water was pumped into the column. By opening valve V3 the sulphite solution was drained from sections E and F and replaced by water that had entered the column from the tank and overflowed down the return line. By leaving the water supply valve, V8, to the tank open, the tank was maintained full of water. In this way, a steady supply of wash water was passed once through the column displacing the sulphite/

sulphite solution. The agitation caused by the aeration helped the solids washing process which was continued for one half to one hour.

2. Sampling

A sample was withdrawn from the sample tap located in the flange of column section F, to completely fill and overflow a 25 ml stoppered flask until it was certain that the stagnant liquid in the line leading from the tap to the centre of the column section was purged, and a true sample of the circulating liquid was obtained. The liquid was fed into the bottom of the flask by a thin glass tube so that after overflowing for some seconds, only the liquid that overflowed was exposed to the air. The tube was then quickly removed and the stopper replaced. The spilt liquid was returned to the column through the top of section D.

After preliminary runs, where samples were taken every ten minutes for an hour, or longer, had shown there to be no deviation from linearity of the sulphite concentration with time, samples were taken at twenty or thirty minute intervals during runs which lasted from one hour to one hour and a half. The samples were analysed by withdrawing 10 mls from the stoppered flask by pipette and adding them to a freshly prepared excess of iodine solution of known strength, ensuring that the tip/

tip of the pipette was submerged, to avoid any oxidation of the sample by the air. This solution was left for ten minutes for the reaction to proceed to completion and then the excess iodine was titrated with N/10 sodium thiosulphite. The value of this titre was recorded, and its change with time gave a measure of the oxygen consumption rate.

3. The values of gas flow rates for simulation of the tall column

As has been mentioned in Chapter VII on the bubble frequency measurements, the value of the superficial gas velocity quoted was in all cases the value existing half-way up the column. For experiments where the column height is unchanged this is a convenient choice of value for comparison. When a series of columns of increasing height are used to simulate sections of a column which has a height equal to the tallest one of the series, then the gas flow rate must be changed for each column in the series. Consider a tall column containing a dense liquid. When gas is sparged in at the bottom it is under a pressure due to the height of the liquid and so it expands as it rises up the column. If a column of one-foot is to simulate the bottom foot of the tall column, then a lower mass flow rate of gas must be used. If the same mass flow rate is used then, under the lower pressure/

pressure due to only one foot of liquid, the volumetric flow rate of the gas would be that of the top, and not the bottom, one foot of the tall column. Therefore to effect the correct volumetric gas flow rate for a true simulation of the sections of the tall column, the volumetric gas flow rate referred to standard conditions used in the small columns, must be reduced by the amount that the pressure is reduced.

As the change in area due to bubble coalescence is being studied, the contribution of the area increase due to the expansion of the gas would have to be calculated, which would be difficult because of the change in shape of the bubbles, and allowed for if a physical method of area measurement were being used. However a mass transfer method is used here, and it has the advantage that the rate of mass transfer depends on the area and the gas pressure. When the pressure becomes less the area of the bubble becomes greater. As the area varies with the gas volume to the two thirds power, then these two effects do not cancel out exactly, but a difference proportional to the pressure to the one third remains. At the pressures used in the column in this work, this would result in a difference of from zero to 3.7% in the calculated areas, which would result in their being this much higher than if the increase in area due to expansion were not present. But this increase, is offset by the depletion/

depletion of the gas flow rate by the amount of oxygen consumed in the chemical reaction which also varied from a minute proportion to about 1.7% under the same conditions. So the net increase is of the order of two per cent at the worst which in view of the other inherent experimental errors involved in measurements such as the total liquid volume, gas hddup, dispersion volume, and so forth, was neglected.

C. Treatment of the experimental data and results.

The experimental data for each run were the following:

1) Overall column height, H (cm)
2) Solid-liquid bed porosity (ϵ) and density, ρ_{sl}, (gm/cm^2)
3) Inlet gas pressure, p, (atms)
4) Gas Flow Rate, V_G(l/min) at 15°C, & 1 atm.
5) Total liquid Volume, V_t, (l)
6) Solid-liquid dispersion volume, V_D, (l)
7) Rate of change in sample titre, r, (mls/min)
8) Sulphite Normality
9) Dispersion levels before and after aeration.

The interfacial area a_{sl} per unit volume of solid-liquid dispersion was calculated because the volume of the aerated dispersion could not be ascertained with sufficient/

sufficient accuracy due to the difficulties described in B above.

The gas holdup, Hg, was calculated by dividing the increase in dispersion height upon aeration by the total aerated dispersion height, and expressing this as a percentage of the aerated dispersion volume. The Sauter mean bubble size is thus calculated from the following equation:

$$D_{bm} = \frac{6\ Hg}{a_{sL}(1 - Hg)} \text{ cm}^{-1} \quad \ldots\ldots (1)$$

The specific interfacial area was calculated from the equation

$$a_{sL} = \frac{4.17r \times 10^{-8}\ He}{k_L\ P_{o2}/RT\ f} \times \frac{Vt}{Vb} \text{ cm}^{-1} \quad \ldots\ldots (2)$$

where P_{o2} is the mean partial pressure of the oxygen in the gas bubbles at the top and bottom of the column. The derivation of this equation, which is similar to equation (7) in Chapter III is given in detail in Appendix I.

Table VI presents the experimental data and calculated results from all the mass transfer experiments. The results are also plotted in figures (29) to (35) as follows:

Figures (29),(30),(31),(34) - Interfacial area results.

Figures (32),(33) - Holdup results.

Figure (35) - Mean bubble diameter results.

D/

D. Discussion of Results

1. Interfacial Area and Gas Holdup measurements at increasing columnmheights.

The results of the interfacial area measurements in the series of small columns of increasing height to simulate the sections of one tall column are shown in figures (29) and (30). The specific interfacial area drops sharply in the first 100 cm of column and then more slowly above this height. As the porosity is decreased the drop is steeper over the whole range of column heights. It was considered easier to understand what these changes in specific interfacial area meant physically by multiplying them by the volume of the solid-liquid dispersion, so obtaining a measure of the total interfacial area, A, in the columns. Figure (30) shows these results, and surprisingly the lines were all straight (the significance of the dotted line for ϵ = 0.55 will be explained in section 2 of this discussion). When the runs at ϵ = 0.55 and ϵ = 0.85, which were done first, gave straight lines it was decided to save time and do only three runs at ϵ = 0.72 to locate the line. These three runs also gave points in a straight line vindicating this decision. To explain why there is no further decrease in area as bubble coalescence proceeds beyond a column height of 50 cms or so, it can be postulated/

SPECIFIC INTERFACIAL AREA (a_{SL})

VS COLUMN HEIGHT (h)

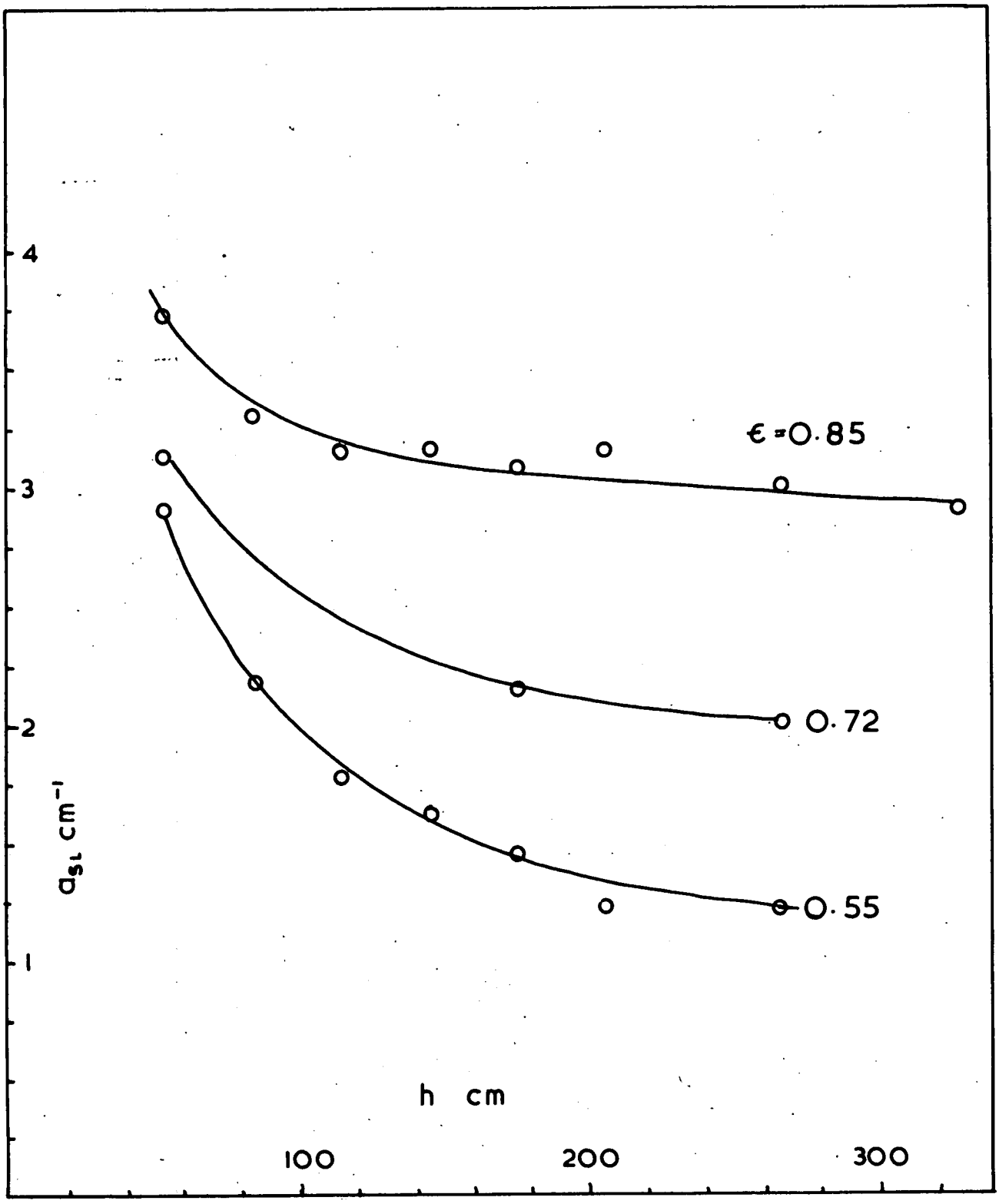

FIGURE 29

TOTAL INTERFACIAL AREA (A) VS COLUMN HEIGHT

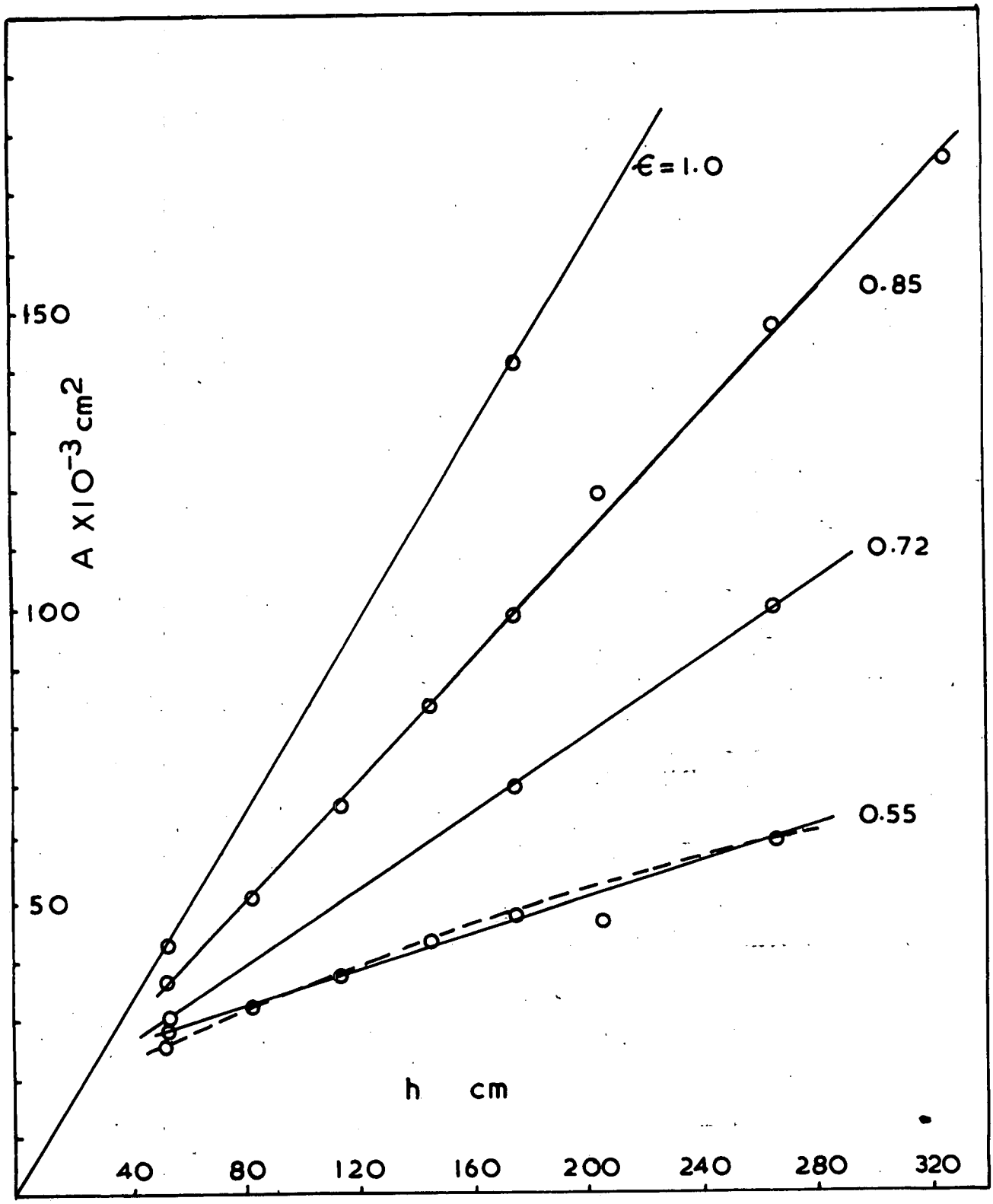

FIGURE 30

SPECIFIC INTERFACIAL AREA (a_{SL})

VS GAS RATE (V_G)

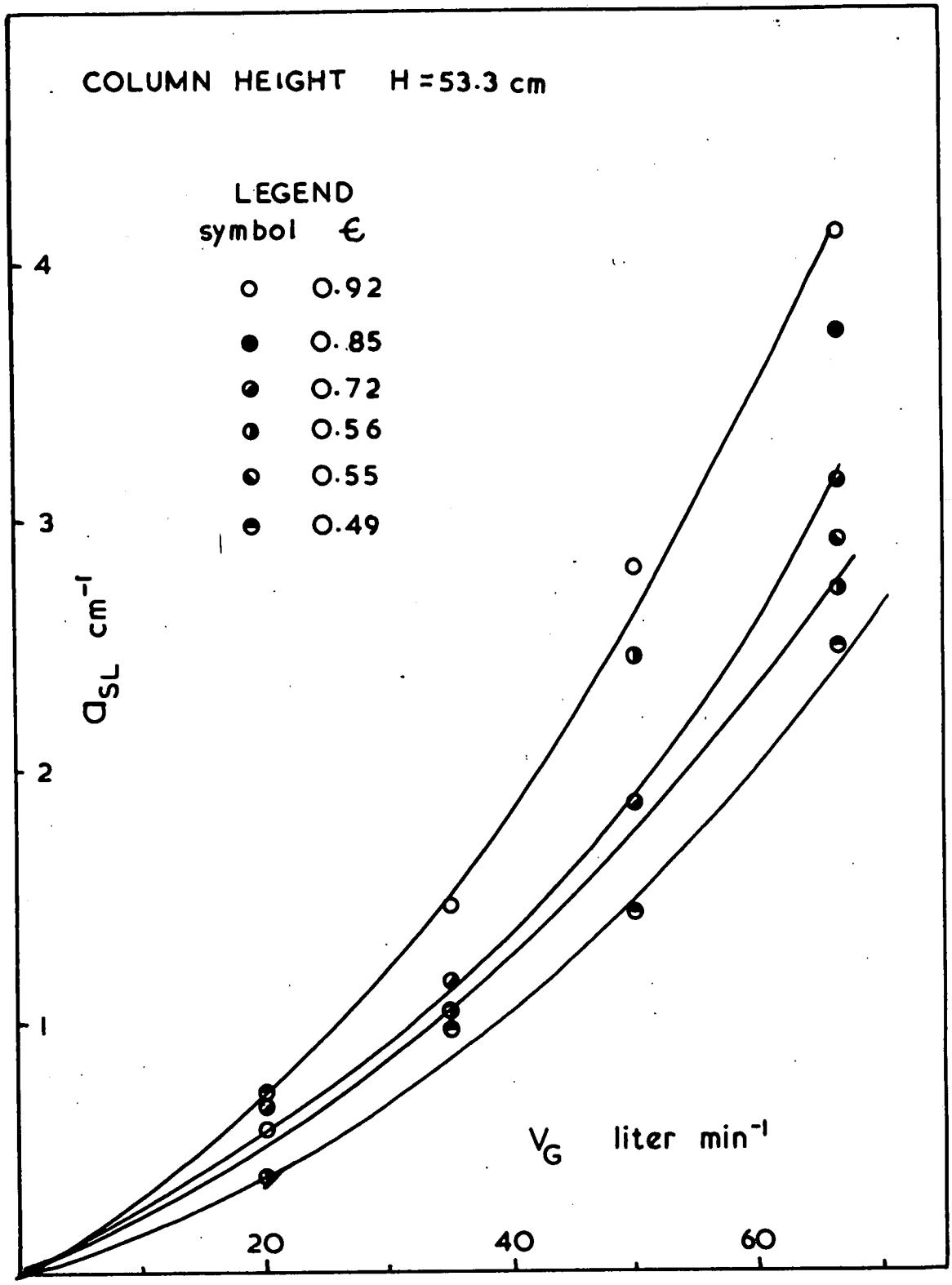

FIGURE 31

GAS HOLDUP (H_g) VS COLUMN HEIGHT (h)

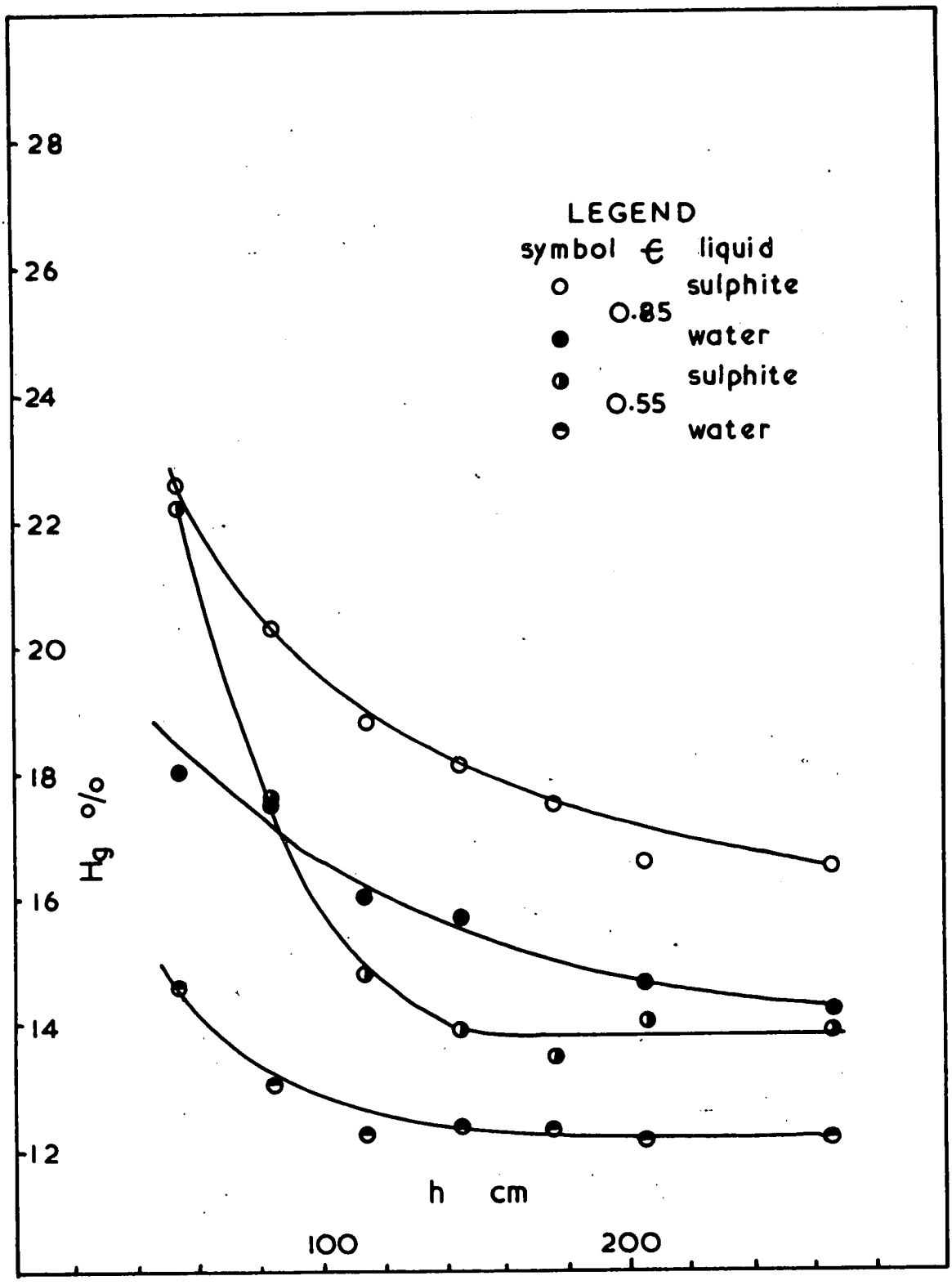

FIGURE 32

GAS HOLDUP (H_g) VS GAS FLOW RATE (V_G)

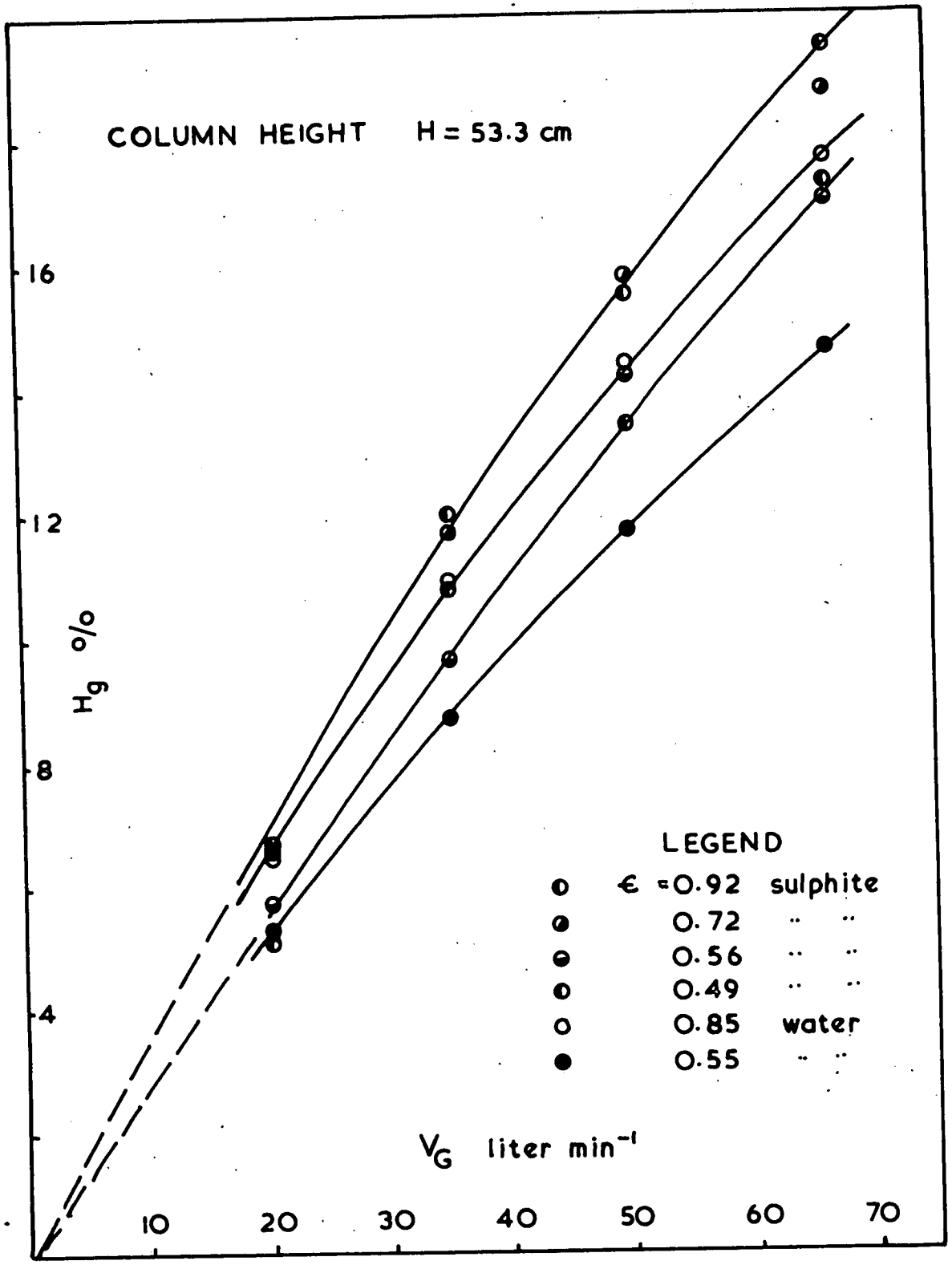

FIGURE 33

postulated that 1) the large bubbles formed by coalescence pass through the dispersion so quickly that they contribute very little to the mass transfer compared to the large number of small bubbles present, and so represent an effective by-pass of this gas, and 2) the reduction in area as a result of their coalescence with each other and smaller bubbles is made up for b y the regeneration of small bubbles by the turbulence set up by the passage of these large bubbles, causing shearing off of some other large bubbles into showers of small ones. This latter process was observed by Braulick et al. (141) in a 6 inch diameter column for air sparged into water and sodium sulphite solutions. As the three phase dispersion is opaque the actual behaviour of the bubbles in it cannot be observed, but "small" bubbles in the range from 3 to 10 mms. were always visible at all heights near the walls of the column. As the porosity was decreased, fewer of them were seen. At all operating conditions the presence of very minute ionic bubbles was observed but this will be discussed later.

The observation that the number of "small" bubbles visible at the walls of the column appears to decrease as the bed porosity decreases, would indicate that more gas is passing through the dispersion in the large bubbles. If the first postulate above, is true, that the gas in these large bubbles effectively by-passes the column/

column, then a smaller interfacial area would be expected, because only the "small" bubbles would contribute to the area measured by the mass transfer method.

This being so then the only way for the area to remain constant as one proceeds up the column, is for the population of these "small" bubbles to remain constant In addition to coalescing with each other the large bubbles will also coalesce with a number of the "small" bubbles that lie in their path by overtaking them and "capturing" them as described by Calderbank (206). Thus in order to maintain the small bubble population, the second postulate, that of the regeneration of small bubbles in the way described above and observed by Braulick (141), must be considered as an explanation of the maintenance of the specific interfacial area at a c constant level. There is thus some measure of interaction between the gas in some of the large bubbles and in the "small" bubbles, but the bulk of the gas in the large b ubbles can be considered to by-pass the column.

Referring again to figure (30) it is seen that the lines of total area against height do not pass through the origin. In this event, the situation just described cannot be true right down to the bottom of the column. There must be a point in this bottom part of the column where there is a changeover from a large specific interfacial area to the lower constant one that is maintained/

maintained thereafter. This must occur during the formation of the large bubbles. In the turbulent conditions of the dispersion and with the flow of liquid through the bed support gauze at the same time as the gas it is unlikely that the large bubbles are formed as the gas emerges through the gauze. It is more likely that they are formed from a number of small ones, that are formed at the gauze and then detached quickly, coalescing within a short distance of the gauze. If this is so then there would be a relatively high specific interfacial area within a few centimetres of the gauze which would then drop to an extent depending on the size of the large bubbles formed, and at a distance from the gauze possibly depending on the amount of turbulence in the dispersion. The work in Chapter IX using a two-dimensional bed was carried out to observe what actually occurred at the bottom of a three phase dispersion at the point of injection of the gas and the basic mechanism suggested here was verified. A more extensive discussion is presented in that chapter.

The gas holdup measurements taken at the same time as the mass transfer runs, referred to above, are shown in figure (32) and it can be seen that they follow a similar trend to the specific areas, dropping sharply at first, especially so in the case of $\epsilon = 0.55$, and then levelling off. Holdup measurements using water instead/

instead of sulphite, at the same gas flow rate, were made after the columns had been well washed to remove all sulphite salt, and these values are also shown in figure (32). They are roughly parallel to the curves for sulphite, but lower, so that the holdup in sulphite fluidized dispersions at this gas rate is about 17% higher than in water. This is attributed to the formation of the very small ionic bubbles mentioned earlier, and described by Yoshida (140). These bubbles occur in well agitated bubble dispersions in aqueous solutions of electrolytes and do not coalesce with one another due, it is thought, to an ionic potential on their surface which causes them to repel each other. Both Yoshida and Braulick found this difference in gas holdup between water and sodium sulphite solutions, in their two-phase air-water and air-sulphite columns. From their published curves of gas holdup in 6 inch diameter columns, at the gas rates used here they both found the difference in holdup in sulphite and water was about 20% of the holdup in water, although their actual values of gas holdup were higher. Braulick found that below a superficial gas rate of about 3 cm/sec there was little difference in the holdup measured for the two systems, concluding that a certain amount of agitation is required to break up the bubble dispersion into these small ionic bubbles, that are about 1 mm in diameter/

diameter and quite stable when formed. He states that the interfacial area and contact time of these ionic bubble clouds is far disproportionate to the amount of gas contained in them and thus they may be a major mode of mass transfer in electrolyte systems which would be absent from hydrocarbon mixtures and pure liquid systems. This is a disadvantage of the sulphite method for assessing gas-liquid reactor performance.

From the difference in the curves shown in figure (32) it would then appear that approximately 12% of the gas in the column at a height of 266 cms is occupied by ionic bubbles at ϵ = 0.55 and 15% at ϵ = 0.85. These ionic bubbles are a portion of the gas with a stable area contribution that will be practically constant throughout the column and from observations here and by Braulick a portion of the gas which has an extremely long residence time compared with the rest of the gas. This is because they are so small that they are carried with the liquid eddies and have only a very small buoyancy force to help them escape the eddies and rise through the column. As the liquid phase is well mixed, by the large bubbles, it can be assumed that they are distributed evenly throughout the dispersion.

To summarise briefly, it is suggested that the gas flow through the three phase column be thought of as being divided into three portions:

1)/

1) A portion which passes rapidly through the dispersion as large bubbles and as far as the mass transfer process is concerned, the gas comprising them effectively by-passes the column, serving only to produce intense agitation and the generation of "small" bubbles.

2) An ionic bubble portion, which is fairly constant in interfacial area throughout the column and which has an extremely long residence time.

3) An intermediate sized bubble portion, with a range of sizes between the large bubble size and about 4 mm. The magnitude and size distribution of this portion depends on the conditions of bubble formation near the gauze and the agitation in the column as a whole.

The experiments described in the following two chapters were designed to test the validity of this suggested gas flow model. Bubbles could be seen inside the two-dimensional column described in Chapter IX and gas residence time distribution functions were measured in Chapter X.

2. Interfacial Area Measurements in the 50 cm column.

At this the lowest column height used in the previous mass transfer experiments, interfacial areas were measured for a range of air flow rates. It is in this

bottom/

bottom section that the dispersion character is formed and it was hoped to throw some light on this by these experiments. The results of the area, gas-holdup and bubble size measurements are shown in figures (31), (33), (34) and (35).

Figure (31) shows that the specific interfacial area increases rapidly with increasing gas rate in an exponential fashion and is higher at higher porosities for a given gas rate. Figure (33) shows the holdup results, which for the sulphite runs are rather erratic. The values for water runs are less erratic because of the easier determination of the aerated dispersion level. They show that the trend of differences between the values for sulphite and water, becomes noticeable after a gas rate of 20 l/min., which is equivalent to a superficial gas velocity of about 1.8 cm/sec.

It would appear that porosity has quite a large effect on the area even at quite low air rates which does suggest that the bubble formation is strongly influenced by it. The rise in area above that expected from the increase in gas flow rate alone, may be due to a greater amount of the gas being broken down into ionic or "small" bubbles by the increased agitation caused by larger bubbles rising through the dispersion.

If the values of the specific interfacial areas measured at the three heights 53.3, 175 and 266 cms., for/

SPECIFIC INTERFACIAL AREA(a_{SL}) VS POROSITY

Extrapolation to $\epsilon = 1.0$

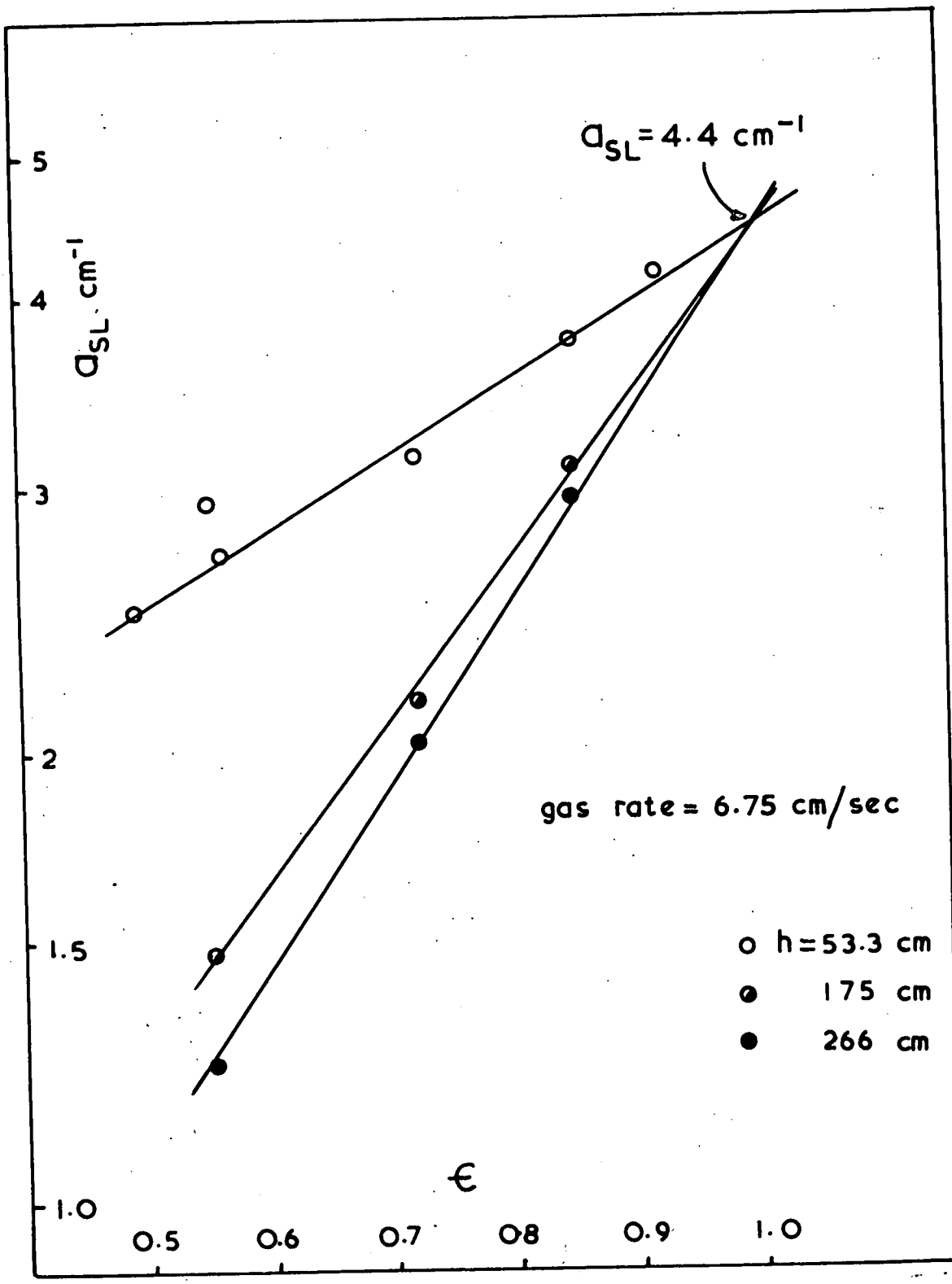

FIGURE 34

for the same gas flow rate, are plotted against the bed porosity then three straight lines are obtained, all of which intersect the $\epsilon = 1.0$ line at 4.4 cm^{-1}. See figure (34). This indicates two things: 1) That the mechanism of coalescence that causes the reduction in interfacial area at the bottom of the column is again a unique function of the bed porosity and independent of particle size and shape and 2) That at the hypothetical value of the porosity of one, the specific interfacial area is the same at all heights in the column, and thus the line drawn on the total area versus height plot of figure (30) will pass through the origin.

It can thus be concluded that if there were no particles in the column then the small bubbles formed at the gauze would not coalesce into large bubbles within a few centimeters, as they do when solids are present, and that their specific interfacial area would be 4.4 cm^{-1} throughout the columns. This is in accordance with experience; although some coalescence of air bubbles in the column filled with water does occur at such a ~~this~~ high a gas flow rate, the high turbulence causes the large bubbles to break up again.

One more point about figure (34) is it shows that the values of the specific area for $\epsilon = 0.55$ at a height of 53.3 cms is inconsistently high and it would seem that a value of 2.65 cm^{-1} would be more reasonable. If

the/

the total area is calculated using this value of the specific interfacial area at 53.3 cms and plotted on figure (30) then the curved line, shown dotted, can be drawn smoothly through all the points for $\epsilon = 0.55$. It would then appear that at this lower porosity in the tall column coalescence of the large bubbles is having a slight effect in reducing the local specific area as one moves up the column. This could be due to the lower level of turbulence and the suggestion that there are fewer "small" and ionic bubbles formed at the bottom of the column, at such a low porosity.

3. Bubble Sizes

Figure (35a) shows the Sauter mean bubble diameter plotted as a function of gas flow rate at four porosities, which were calculated from the interfacial areas and gas holdups measured in the 53.3 cm. column. The reason for their lack of any well defined relation to bed porosity or gas flow rate must be due to the inaccuracy of the holdup measurements, which are plotted on figure (33) and are very erratic. The difficulties of measuring the aerated dispersion level have already been described in the introduction to this chapter, and it was stated that errors of the order of $\pm$ 10% could be expected. This error appears twice in calculating the value of the holdup from the increase in dispersion height/

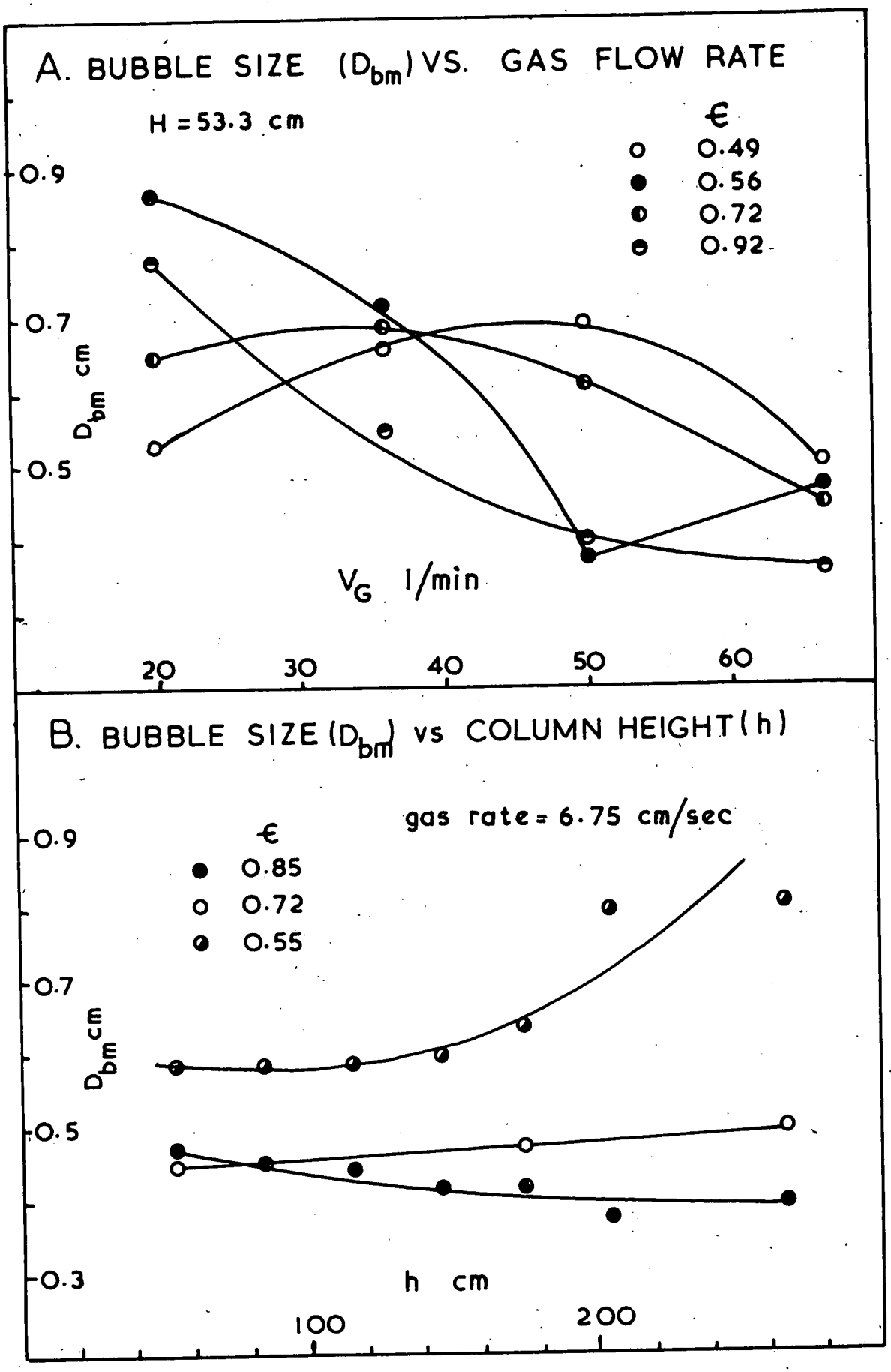
A. BUBBLE SIZE (D_{bm}) VS. GAS FLOW RATE
H = 53.3 cm
€
0.49
0.56
0.72
0.92
0.9
0.7
0.5
D_{bm} cm
V_G l/min
20
30
40
50
60
B. BUBBLE SIZE (D_{bm}) vs COLUMN HEIGHT (h)
gas rate = 6.75 cm/sec
€
0.85
0.72
0.55
0.9
0.7
0.5
0.3
D_{bm} cm
h cm
100
200

FIGURE 35

height divided by the total dispersion height upon aeration. In calculating the mean bubble diameter the value of the holdup is used twice in equation (1). It is not, therefore surprising to find this large scatter of bubble sizes. The only trend that can be distinguished is that bubble diameters are smaller at higher gas rates, which would be expected due to the greater turbulence produced.

Figure (35b) shows the change in mean bubble size with height up the column for the three porosities used in the tall column. Here there is a much more consistent set of results which means that the holdup measurements must have been much more reliable. See figure (32). At the high gas rate used the change in dispersion height upon aeration was greater than in the small column at the low air rates, thus reducing the percentage error for the same reading error, and as the columns were built up higher this change increased still more. This may well account for the obvious improvement in accuracy. The plots of bubble size against height show that only in the case of the ballotine bed, of porosity 0.55, does the mean bubble size increase significantly with height. This would indicate that the specific interfacial area is decreasing with height, so that the curved line (show dotted) on figure (30) is probably a truer representation than the original/

original straight line drawn.

E. CONCLUSIONS

1. Above a height of 50 cm in the tall column, there is no change in specific area with height, except at the low porosity of 0.55 where a slight decrease is measured. The change in total area with height varies from 0.16 cm^2/cm at ϵ = 0.55 to 0.8 cm^2/cm at ϵ = 0.85.
2. The specific interfacial area at any height is a unique function of the bed porosity for the gas flow rate used in the tall column.
3. The measurements in the 53.3 cm column show that the gas flow rate and bed porosity have a large combined effect on the interfacial area due to the amount of agitation they engender. The higher the gas rate anddporosity the greater the agitation and the smaller the bubble size.
4. The gas holdup in sulphite solutions parallels the gas holdup in water for the same operating conditions, but it is higher by an amount which represents the portion of the gas existing as ionic bubbles in the sulphite solution.
5. The gas flowing through the three phase dispersion can be considered to consist of three portions:

a)/

a) Large bubbles with a very short residence time.

b) "Small" bubbles with a distribution of sizes and residence times and

c) Ionic bubbles whose residence time may be much longer than that of either of the other two bubble portions.

CHAPTER IX

The Two-Dimensional Column

A. INTRODUCTION

From the work in the previous chapter it was clear that what happened to the gas when it first entered the column was all important and it was suggested that the observed variations in interfacial area in the bottom of the column were due to a change in the bubble size distribution during formation, as the gas entered the bed through the gauze. In the 6 inch column it was impossible to observe the formation of bubbles above the gauze and it was therefore decided to use a column in which they could be seen. A perspex two-dimensional column was chosen in which gas bubbles could be distinguished within the solid-liquid bed because the number of solid particles in front and behind them was small. Bubbles that would normally have a diameter greater than the space between the front and back faces of the column would appear as cross-sections of such bubbles with only a few particles passing down the column in front and behind. As these bubbles rose through the column most of the liquid and particles flowed around either side of them. By strongly illuminating the column from behind with diffused light

even/

even quite small bubbles could be seen.

B. DESCRIPTION OF THE COLUMN

The column was made of two $\frac{1}{4}$" thick perspex sheets, 6' x 5", with two 6' x $\frac{1}{2}$" and one 4" x $\frac{1}{2}$" square perspex strips acting as spacers at the sides and bottom, so that the internal cross-section was 4" x $\frac{1}{2}$". It was held together by 2 B.A. screws and nuts, and the joints were made water tight with Bostik sealing compound. A short length of 1" I.D. perspex pipe was cemented into the front face of the column from which, a hose led the liquid overflow via a constant head tank, which also acted as a solids separator, to drain. The top of the column was open. The liquid distributor was a horizontal flattened $\frac{1}{8}$" copper pipe, with six slits facing downwards, soldered to a $\frac{1}{4}$" B.S.P. brass fitting that was screwed into the $\frac{1}{2}$" perspex side spacer one inch from the bottom of the column. Air was injected through a single nozzle formed from a horizontal 0.44 mm I.D. hypodermic needle bent upwards at the end, brazed to another $\frac{1}{4}$" B.S. P. brass fitting also screwed into the side spacer one inch above the liquid distributor. When a horizontal gas distributor made of $\frac{1}{8}$" copper tubing was used it impeded the circulation of particles and liquid at the bottom of the column, which caused particles to settle/

settle out in areas of stagnant liquid above and below it. The hypodermic tubing overcame this problem because it was too thin to cause any notable flow disturbance. Sand or ballotini were dropped into the column from the top. A transparent calibrated sellotape scale was fixed to the left hand side of the column. Air and water were used as the gas and liquid phases.

C. OBSERVATIONS

Over the range of gas flow rates used, up to a superficial gas velocity of 1.41 cm/sec, the bubbles emerging from the hypodermic tubing nozzle were of a similar small size, about 5 mm, with their frequency increasing as the gas rate increased. Their detachment from the nozzle was encouraged by the upward flow of water from the liquid distributor below. However, within a short distance above the nozzle there was coalescence of regular numbers of these small bubbles into larger ones, which then rose up through the bed causing circulating eddies of liquid and particles. There was a certain amount of circulation in the fluidized bed before aeration due to imperfect liquid distribution, but as this had also been observed in the six inch column, it was decided that a closer comparison would be obtained if this was left as it was.

1. Effect of bed porosity

For/

For a given gas flow rate the number of small bubbles that coalesced to form a large bubble increased as the bed porosity was decreased. It was as if, for a given porosity, there was a size to which an air bubble had to grow before it would begin to rise through the bed and this size was larger the lower the porosity. The fact that the small bubbles rose a few centimeters after detachment from the nozzle was due to the imperfect liquid distribution causing a channel of upward flowing liquid which swept past the nozzle. When this initial channel, or eddy, dissipated as it came against the other eddies set up by the aeration, then the small bubbles' net velocity was reduced and each one was caught up by the succeeding one. When the resulting large bubble bouyancy was sufficient for it to overcome the downward components of the eddies and the resistance to flow caused by the drag of the particles, it would rise in a zig-zag fashion through the bed. The process was then repeated and a succession of large bubbles rose through the bed.

2. Effect of gas flow rate

For a given porosity, increasing the air rate increased the frequency of initial small bubbles and so also the frequency of the large ones formed from them. However the higher the gas rate the greater the variation in the number of small bubbles actually comprising each large bubble, which depended on the eddy/

eddy flow situation in its neighbourhood at the time, and so the variation in the size of the large bubbles increased. It follows that with an increase in the number of bubbles they would be closer together and their variation in size would cause their rise velocities to differ, so leading to coalescence by their overtaking, and being overtaken by, each other in the way described by Calderbank et al. (206).

D. DISCUSSION

Although the method of injecting the gas into this two-dimensional column by a single nozzle is quite different from the gauze distributor used in the 6 inch column, and the superficial gas flow rates used here are much lower, it does help to indicate how the large bubbles detected by the capacitance probe in the large column, were probably formed.

It will be recalled from the results of the bubble frequency measurements that before coalescence of the large bubbles began, their frequency was a function only of the air rate. This behaviour was also observed here and can be explained if one considers the gauze as a source of nozzles producing small bubbles which coalesce to form large bubbles of the appropriate size, a short distance above the gauze. As the air rate is increased more small bubbles are formed and hence more large ones. The/

The liquid flowing through the gauze will ensure that the bubbles are detached when quite small, as they were in the two-dimensional column, so it would appear unlikely that bubbles of the size detected by the capacitance probe near the bottom of the column would actually be formed at the gauze. This small section of bed above the gauze would then have a high specific interfacial area, which would be decreased rapidly as the large bubbles were formed. This section of high interfacial area would also explain why the straight lines in figure (30) do not extrapolate to the origin.

In the two-dimensional column, the air rates were often so low that every small bubble that left the nozzle became part of a large bubble, but in the large column a range of relatively high air flow rates was used. When high gas rates are used causing conditions of high turbulence it is easy to visualise many of the small bubbles being carried up in strong liquid eddies and never becoming part of a large bubble. There is also the probability that the points through which the bubbles emerge from the gauze may change position with the liquid-solid flow pattern above it, taking the line of least resistance. If these positions change, then a range of bubble sizes will be produced, from the large bubble, characteristic of the particular bed porosity, to the smallest ones detached singly from the/

the gauze, depending on how many small bubbles had joined together a little above the gauze, before the position of emergence changed. Hence it can be seen that increasing the gas rate could increase the distribution of bubble sizes. If this is so then the frequency of the large bubbles detected cannot increase with the gas rate to the first power, but a power less than one. In fact the frequency in the 6 inch column increased by the 0.32 power of the superficial air velocity.

The indications of the observations, just discussed, of how the amount of turbulence in the column can affect the distribution of bubble sizes, supports the explanation put forward in Chapter VII, pages 135 to 137 for the apparently anomalous situation of having a constant frequency of bubbles which changed in size without the gas flow rate being changed. This was, briefly, that as the porosity decreased for a given air rate, the large bubbles were increased in size, but this increase was achieved at the expense of the number of 'small' bubbles, a higher number of which were present at higher porosities.

The next chapter deals with the measurement of gas bubble residence time distributions which will give quantitative evidence of the relative amounts of gas in the large, 'small' and ionic bubbles, at different bed porosities.

E./

E. BED CONTRACTION ON AERATION

As a matter of interest, measurements of the contraction of the liquid-solid fluidized bed height upon aeration were made at two ballotini bed expansions. The results are shown in figure (36) with the data for beds of ballotini of mean diameter 0.46 mm and similar bed expansions, obtained by Stewart and Davidson (209). The two sets agree well.

F. PHOTOGRAPHIC WORK

An electronic flash gun was used to provide back illumination of the column, that was diffused by tracing paper. The diffused light shone through the gas bubbles but was obscured by particles. The photographs were taken from the front of the column with a 35 mm Exakta single-lens reflex camera using Kodak Micro-file film type 5453 that was developed for maximum contrast in full strength Kodak D11 developer for 4½ minutes at 64°F. However they were not entirely successful because the bed width of ½" was not narrow enough to prevent layers of particles being present in front and behind all bubbles except the very largest. These particles obscured some of the light making for poor definition and a loss in contrast, so that good prints were not possible. Stewart and Davidson's bed was ⅛" wide and their/

TWO-DIMENSIONAL BED EXPANSION (%)
VS GAS FLOW RATE (ft sec^{-1})

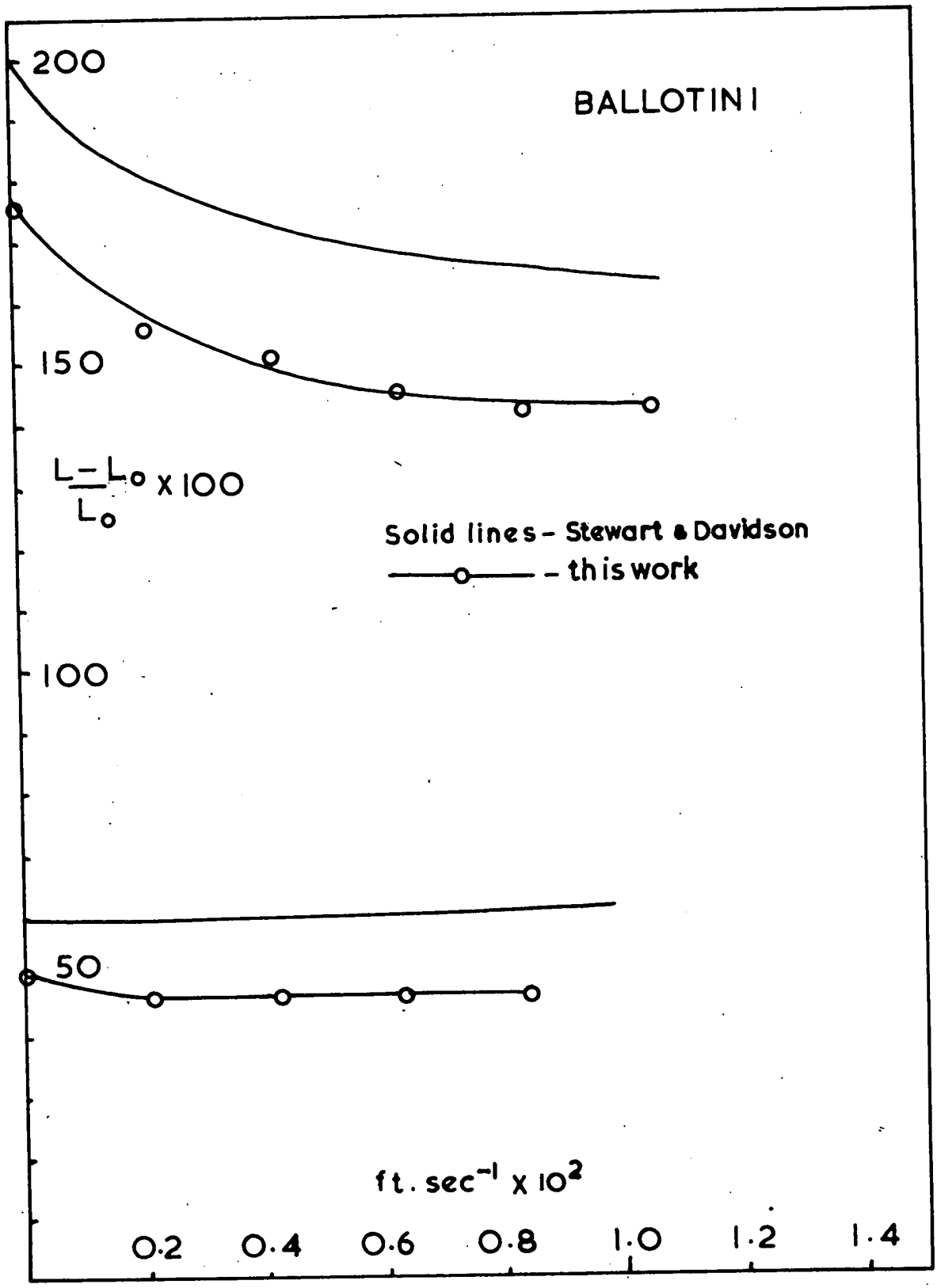

FIGURE 36

their published photographs show good definition of the gas bubbles and water wakes. Figure (37) (a), (b), (c) and (d) shows four of the more successful photographs taken here. They were all taken while gas was passing through the bed at a set flow rate. No single bubble injections were made.

Figure (37) (c) shows a bubble, 1.5 cms in diameter, in a ballotini bed of porosity 0.66 at a gas flow rate of 0.4 cm/sec. Other bubbles can just be distinguished and they appear to be moving in a zig-zag fashion. However, what is clear from this photograph is the wake behind the larger bubble which is practically void of particles (as are those behind the smaller bubbles) and the vortices, that have been shed by it and the other bubbles, containing few particles.

Figure (37) (b) shows a larger bubble, 2.2 cms in diameter at its base and this is of the shape commonly found in gas-solid fluidized beds. The ballotini bed has the same porosity as in (c), 0.66, but the air rate is 1 cm/sec. Again there is a fairly clearly defined wake with few particles in it. The zig-zag path of these two bubbles is shown by their angle and the wakes that have been shed earlier following behind. Stewart and Davidson's figure 3A is almost identical to this photograph in its main features.

Figure (37) (a) shows a bubble which is a perfectly shaped/

TWO DIMENSIONAL BED - PHOTOGRAPHS

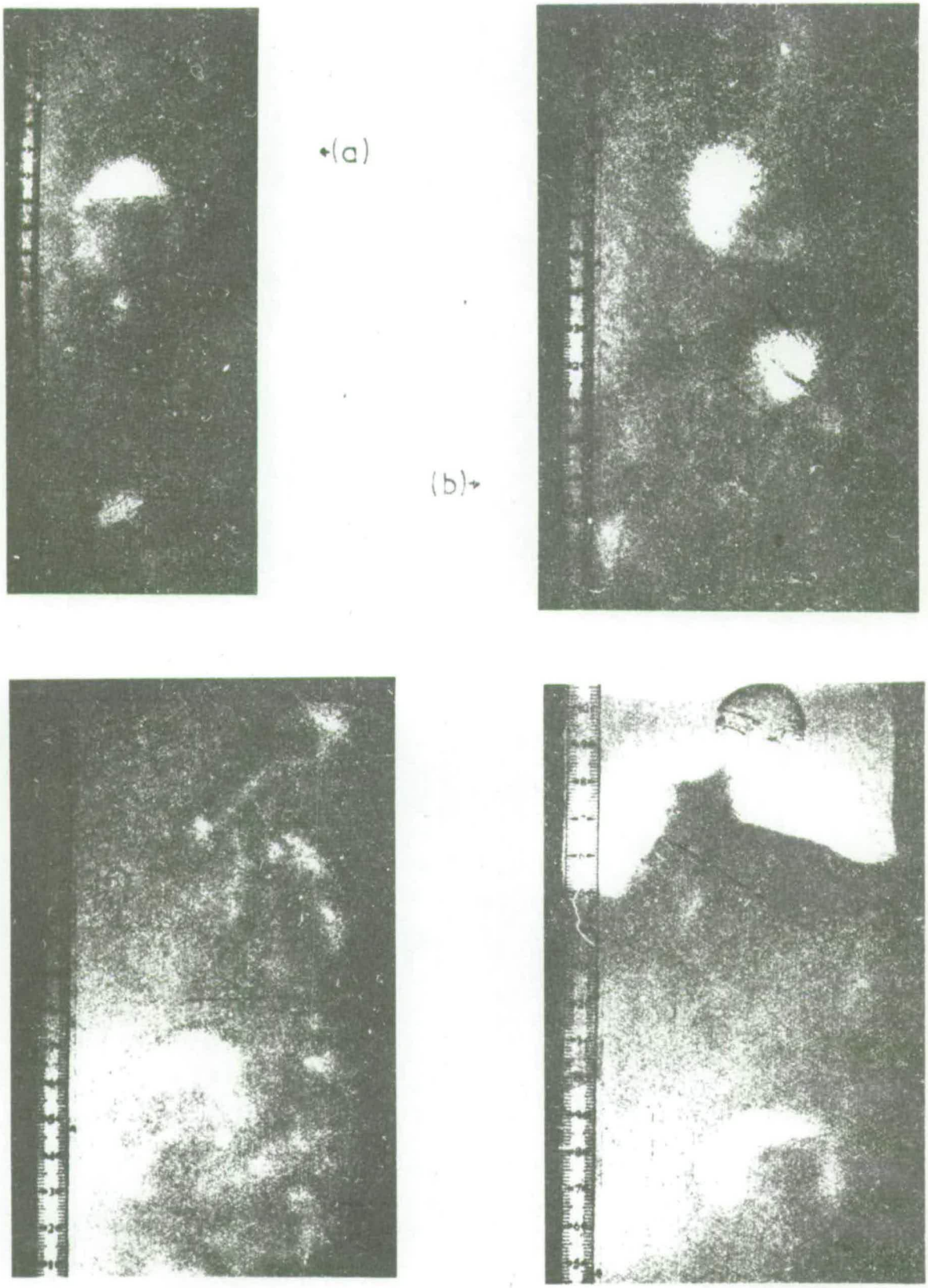

FIGURE 37

shaped spherical cap with a flat base, and behind which there appears to be no particle-free wake. There is evidence that a wake has just been shed by the light streaks snaking down below the bubble, from each edge, ending in two vortices largely free of particles.
A smaller spherical cap bubble, also having just shed its wake, is distinguishable at the bottom of the photograph. The bed porosity here is 0.53 and the air rate 1 cm/sec, as in (b).
Figure (37) (d) shows a bubble just having emerged from the top of the ballotini bed whose porosity is 0.53 and air rate 0.64 cm/sec. It is 2.4 cms at its base. Another bubble in the bed can be seen about to shed the wake from the left hand edge. The bubble that has just emerged has drawn up a spout of particles with it, similar to the spouts shown in the photographs of Østergaard (210) and from which he assumed the wake of such a bubble contained particles of the same porosity as the main bed.

The flat based bubbles in all the photographs taken here do not show areas void of particles immediately behind them as do the smaller round, ellipsoidal and concave-bottomed cap bubbles such as those in Figure (37) (b) and (c). However they do have voids or vortices at their edges which are shed periodically. This creation of voids or vortices, here has the same effect as having/

having a void right behind the bubble since it also reduces the volume of liquid containing particles. These vortices moved upwards with the bubble at a slower rate than the bubble, as described by Stewart and Davidson, and it is the swirling action of these following vortices which draws up the spout seen behind bubbles leaving the bed, in a similar manner to that described by Rowe (220) for gas bubbles rising through a gas-solid fluidized bed. The negatives show bubbles of the shapes in figure (38) (b) and (c) emerging from the beds, also with a spout of particles, so it is not possible to say that the presence of a spout on leaving the bed indicates there is not a water wake, containing fewer particles, associated with the bubbles.

G. CONCLUSIONS

1) When gas enters the three phase dispersion it does so as small bubbles, which are detached from the nozzle or gauze by the upward flow of liquid pas them, and then within a short distance coalesce into large bubbles.
2) The size of the large bubbles formed by coalescence of the small ones is a function of bed porosity, being greater the lower the porosity, and is probably connected with the buoyancy force required to/

to overcome the drag imposed by the bed of particles.

3) The distribution of bubble sizes between that of the appropriate large bubble for the particular bed porosity and the small bubbles entering the bed, is a function of the turbulence in the three phase bed. Large air rates and high bed porosities give rise to the widest range of bubble sizes and low air rates in low porosity beds produce large bubbles almost exclusively.

4) The specific gas-liquid interfacial area is comparatively very high just above the gas distributor in a three phase dispersion, but it drops rapidly as the small bubbles coalesce into large ones.

5) The negatives of the photographs taken bear out 2) above, and show the existence of water wakes and vortices largely free of particles associated with gas bubbles of all shapes in a three phase bed.

6) The contraction of the liquid fluidized bed of ballotini upon aeration agreed quantitatively with the results of Stewart and Davidson (209).

7) Spouts of particles follow behind gas bubbles of all sizes as they leave the solid-liquid bed, but this should not be taken as an indication that they have no particle free wakes or voids associated with them when they are in the bed (see Østergaard (210))

CHAPTER X

Gas Residence Time Distribution Measurements.

A. INTRODUCTION.

It was postulated in Chapter VIII that the gas flowing through the three phase dispersion consists of three portions:

1. Large bubbles with a very short residence time.
2. Small bubbles with a distribution of sizes and residence times, and
3. Ionic bubbles whose residence time is extremely long compared with that of all the other bubbles.

It was therefore decided to measure the residence time distribution of the gas in the three phase column under similar operating conditions to those used for the interfacial area measuring experiments, so that the results could be compared with them and more readily interpreted. This was done by passing air containing mercury vapour through the column for a period of time and then making a step change to pure air. The gas emerging from the top of the dispersion was analysed for its mercury vapour content by its relative absorption/

absorptionoof ultra-violet light, as detected by a photocell, and the resulting data used to construct F-diagrams.

B. MODIFICATIONS TO THE MAIN APPARATUS

1. Mercury Vapo/riser

Refer to the schematic flow sheet of the main apparatus figure (11), Chapter VI and figure (38) here. A 1'6" length of 2" I.D. pyrex glass pipe section with ½" I.D. side-arms at 2" from the top and bottom, was used as the mercury vapo/rising chamber. The bottom of this chamber had a blank ¼" P.V.C. flange and the top a similar flange but one which carried a length of ½" I.D. P.V.C. pipe that protruded 2" from the top and 1'5½" below the flange, so just dipping below the surface of a pool of mercury contained in the bottom of the chamber. The air line from the top of the rota-meter R2 was broken above V12 and a ½" P.V.C. tee fitted. The side-arm of this tee was connected via a flexible ½" P.V.C. hose to the ½" P.V.C. protruding from the top flange of the vapo/riser. The bottom of the tee was rejoined to the valve V12. The line was broken again below V12 and a three-way glass stop-cock inserted. One outlet was rejoined to the bottom of V12, one to the air line to the column, and the other was connected by/

MERCURY VAPOURISER

SCHEMATIC FLOW DIAGRAM

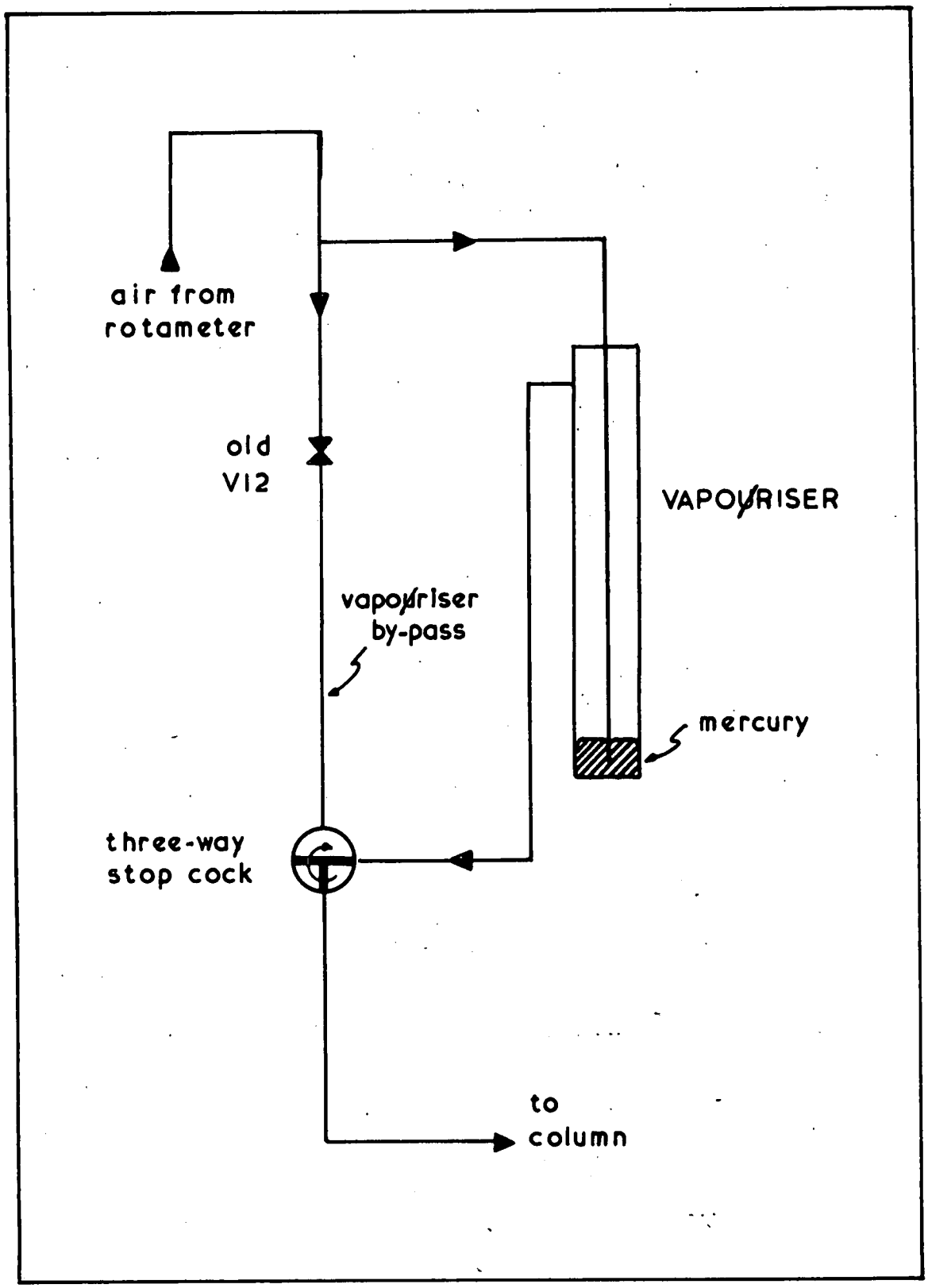

FIGURE 38

by flexible P.V.C. hose to the top ½" I.D. outlet of the vapouriser; the bottom ½" I.D. outlet was blanked off by a small P.V.C. flange.

By turning the glass stop-cock the air from the rotameter could be passed through V12 or the vapouriser, to the column or the column could be closed off. V12 was used to adjust the pressure drop through the line by-passing the vapourizer so that on changing the direction of air flow no change in flow rate to the column would occur.

2. Mercury vapour detector section.

Refer to figure (39). This section consisted of the 1'6" length of 5.75" I.D. P.V.C. pipe with two 1" I.D. side-arms used as the bubble-column in the sodium sulphite oxidation experiments described in section C of Chapter III.

It was placed on the top of the column so that the side arms were one foot above section D. The brass flanges carrying the quartz windows were kept in place as before and two housings made of 1" I.D. rigid P.V.C. pipe ~~see figure (4)~~, containing the photocell and U-V lamp were attached by flanges to the four studs protruding from the brass flanges, as shown in figure (39). The top of the section had the ¼" P.V.C. sieve plate used in the bubble experiments bolted to it. A ¾" diameter hole

was/

MERCURY VAPOUR DETECTOR SECTION

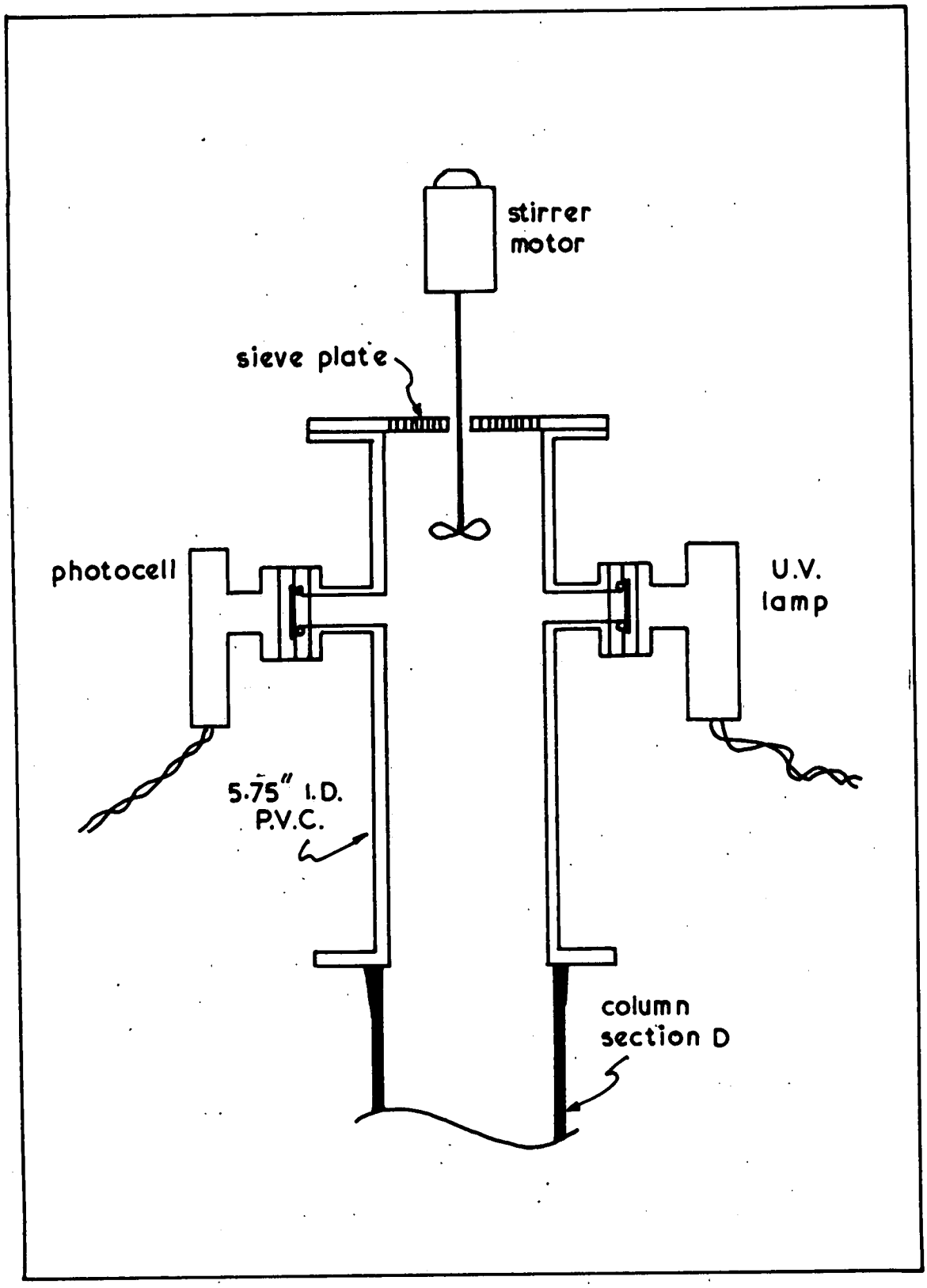

FIGURE 39

was made in the centre of the sieve plate to accommodate the shaft of a stirrer which was driven by a motor above. The stirrer was necessary to ensure that the gas in the detector section was perfectly mixed, a requirement that is explained in the theory to follow in section D of this Chapter. It was found that by enclosing the gas in the detector section with the sieve plate in this way, air from the laboratory was not sucked into the section by the action of the stirrer due to the relatively high velocity of the gas flow passing out the central, $\frac{5}{8}$", and other small holes in the plate.

C. DETECTION AND RECORDING EQUIPMENT

The basic part of the detection equipment was an Engelhard-Hanovia mercury meter which provided a constant voltage supply to the ultra-violet lamp and also amplified the signal voltage from the photocell. This signal was then fed to a Cambridge Instrument Company, recorder which produced a record of the amplified photocell output voltage on an eight inch roll of chart paper. The U-V lamp was a 100 watt mercury vapour type requiring a 500 volt supply.

1. Operation

The column was assembled to a height of 8'9", and filled with the appropriate amount of solid particles, and/

sand or ballotini. It was then charged with sodium sulphite and brought to 36°C in the way described in earlier chapters. The air was turned on, the 3-way cock being set so that it by-passed the mercury vapourizer and set by V7 to the desired flow rate. The aerated dispersion level was then adjusted to be level with the top of column section D by draining from valve V3 or pumping more sulphite into the column from the make-up tank. The pressure drop adjustment valve V12 was set by changing the direction of air flow through it and the vapourizer until both flow paths gave the desired flow rate and operating the 3-way cock quickly, produced no change, and only a minute interruption, in the air flow to the column.

Having allowed the Hanovia meter, U-V lamp, photo-cell and Cambridge recorder at least one hour to warm up, a run could be commenced. The air was passed into the mercury vapouriser where it bubbled through the pool of mercury, becoming partially saturated with mercury vapour which was detected as it passed between the windows in the detector section after leaving the dis-persion. The recorder chart was run at a low speed and after 10 to 15 minutes, when the pen was giving a constant reading, it was increased to 1½ inches per minute. When the pen crossed one of the reference lines on the chart, the 3-way cock was turned simultaneously so that the air flow/

flow by-passed the vapourizer, and it was sealed off. This produced a step change to pure air. As the first bubbles containing pure air reached the detector section the pen began to move across the scale producing a plot which could be used to calculate the change in mercury content of the air with time (see below). It was foumdd that the pen reached a steady reading after about ten to fifteen minutes, but that the greater part of the distance between the initial and final pen positions was covered within about two minutes.

The procedure described above was followed for runs at four different bed porosities of 0.5, 0.6, 0.68 and 0.8. A gas rate giving a superficial linear velocity of 6.75 cm/sec halfway up the column was used in each case.

D. TREATMENT OF THE RESULTS

1. Theory

It was assumed that the photocell gave an output that was directly proportional to the intensity of light falling upon it and that the proportion of the light absorbed by the mercury vapour was in accordance with Lambert's Law expressed as follows:

$$I = I_o e^{-K\,Lp\,C} \qquad \ldots\ldots (1)$$

where Lp, is the path length of the light passing through the gas mixture

K/

K, the absorption coefficient of the light-absorbing phase

C, the concentration of this phase

I_o, the intensity of the ultra-violet light passing into the gas mixture

and I, the intensity of ultra-violet light which has passed through the gas mixture to the cell.

This law can then be rewritten in terms of the cell output voltages, for intensities I and Io as follows:

$$\upsilon = \upsilon_o \, e^{-K \, Lp \, C} \qquad \ldots\ldots (2)$$

In the system used both K and Lp were constant so they can be replaced by K^1. Taking logarithms of both side then gives:

$$C = \frac{1}{K^1} \log_e \frac{\upsilon_o}{\upsilon} \qquad \ldots\ldots (3)$$

or, if χ_o and χ were the deflections on the chart due to voltages υ_o and υ respectively, then:

$$C = \frac{1}{K^1} \log_e \frac{\chi_o}{\chi} \qquad \ldots\ldots (4)$$

For the evaluation of residence time functions the absolute value of C is not necessary, the fraction of the maximum value which C attains being all that is required. The maximum value which C attains is thus taken as unity, and corresponds to the minimum deflection, χ min, of the recorder. K^1 may then be evaluated from the equation/

equation:

$$I = 1/K^{1} \log_e \chi_o/\chi_{min} \quad \ldots\ldots (5)$$

Thus the fraction of the maximum value of C was calculated at any time by substituting the values of χ taken from the recorder chart in equation (4). The value of K' was calculated by substituting the value of the steady chart reading when mercury vapour had been passing through the column before the start of a run as χ_{min}, and the steady value attained after changing over to pure air for 10 to 15 minutes as χ_o, in equation (5).

The step change from mercury vapour and air to pure air is a change from C = 1 to C = 0 and cumulative residence time functions are usually presented in the form given when the tracer concentration changes from 0 to 1. The values of C obtained in the above way were thus subtracted from unity to convert them to the usual form of presentation.

As the detector section must be well above the dispersion level to analyse the gas phase emerging from the column to prevent splashing liquid obscuring the light beam, then the residence time distribution of the gas in this section must also be known so that is can be allowed for in order to calculate the actual residence time in the dispersion. If the gas moved in plug flow through the detector section then the values of C calculated by the above procedure would be the same as

those/

those at the top of the dispersion. However with the detector section open to the air the nature of the violent motion of the dispersion surface would cause a reciprocating piston-like movement of gas in the section and the large gas bubbles emerging would give rise to some superimposed agitation. Obviously under these conditions it could not be assumed that the emerging gas moved in uniform plug flow through this section. The alternative is to assume the emerging gas is perfectly mixed in the detector section. This is just as doubtful as assuming plug flow: but if the section is stirred thoroughly to produce a large degree of back-mixing of the gas in the section then this latter assumption is more reasonable. There is a danger in stirring the open section that air from the surroundings would be sucked into it by the action of the stirrer, diluting the gas emerging from the solution to an unknown degree, and for this reason the sieve plate was bolted to the section as described earlier. Under these circumstances it was assumed that the gas in the detector section was perfectly mixed and this is allowed for in calculating the residence time distribution functions as follows.

Let T be the concentration of the tracer in the step input to the bubble column; S, the concentration of the tracer in the perfectly mixed gas space after time, t; V_M, the volume of the perfectly mixed gas space/

space; V_G the volumetric gas flow rate through the column; and F(t) the fraction of the step input which has reached the top of the dispersion and is about to enter the perfectly mixed gas space, which is the value of F(t) required. Then a mass balance across the perfectly mixed gas space gives:-

$$V_M \frac{ds}{dt} = TV_G F(t) \text{ —— } S V_G \quad \ldots\ldots(6)$$

Dividing through by TV gives:

$$\frac{V_M}{V_G T} \frac{ds}{dt} = F(t) \text{ —— } \frac{S}{T} \quad \ldots\ldots(7)$$

Now $\frac{S}{T}$ is the fraction of the step input in the perfectly mixed gas section after time, t, and is the value obtained from the recorder chart deflections subtracted from unity i.e.

$$\text{let } X = \frac{S}{T} = \left(1 - \frac{1}{K} \log_e \frac{X_o}{X}\right) \quad \ldots\ldots(8)$$

Now T is constant, so differentiating (8) gives:

$$dX = \frac{1}{T} ds \quad \text{or} \quad ds = T dX \quad \ldots\ldots(9)$$

Substituting (9) in (7) it becomes:

$$\frac{V_M}{V_G} \times \frac{dX}{dt} = F(t) \text{ —— } X$$

or rearranging:

$$F(t) = \frac{V_M}{V_G} \frac{dX}{dt} + X \quad \ldots\ldots(10)$$

The/

The ratio $\frac{V_M}{V_G}$ can be obtained from the volume of the detector section occupied by gas, and the volumetric flow rate at the top of the column. The value of $\frac{dX}{dt}$ at any time is obtained by plotting X as a function of time using the values calculated from the recorder chart deflections by equation (8), and taking the gradients of the curve at various values of t.

2. Results

The experimental values of t, and X; and the calculated results of $\frac{V_M}{V_G} \frac{dX}{dt}$, $F(\theta)$ and the reduced time defined as $\theta = \frac{V_G}{V_D} t$, where V_D is the volume of the dispersion; are all tabulated in table 7. The curves of $F(\theta)$ against (θ) are shown in figure (40). In treating the results it was assumed that mercury was effectively insoluble in water: Siedell (160) quotes the data of Stock who gave the solubility as from 2 to 3 x 10^{-8} gm/cm^3 of water at 30°C.

E. DISCUSSION OF RESULTS

The first point of interest in the $F(\theta)$ diagrams shown in figure (40) is the sudden rise in $F(\theta)$ after a few seconds to a level depending on the porosity in the bed. This rise represents the passage of the large bubbles quickly through the dispersion carrying that fraction of the gas flow indicated by the value of $F(\theta)$. This/

GAS PHASE RESIDENCE TIME DISTRIBUTION FUNCTIONS

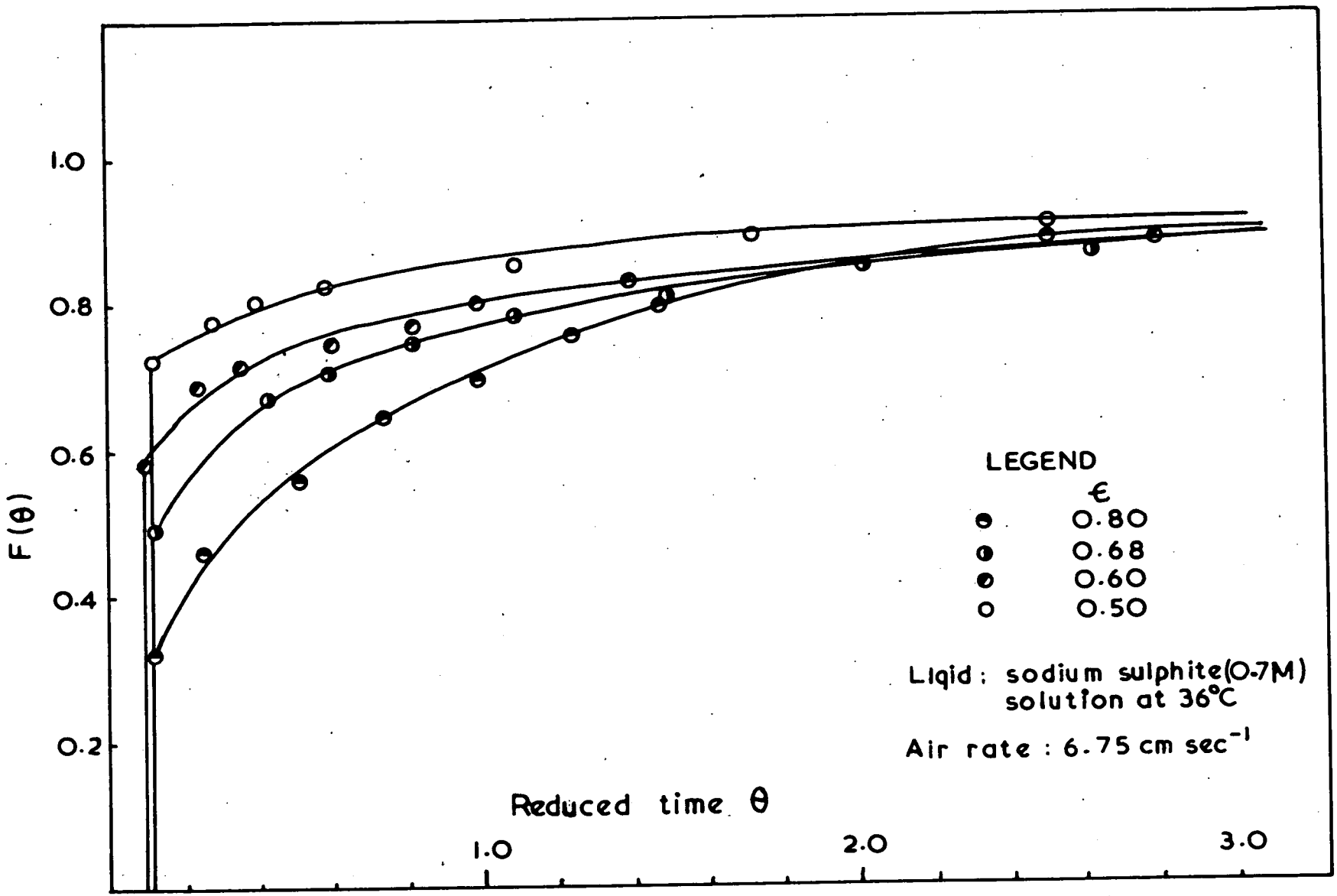

FIGURE 40

This then shows qualitatively and quantitatively how much of the gas is formed into large bubbles for each porosity and that the amount increases as the porosity decreases. By plotting the fraction of the gas remaining, $I - F(\theta)$, against porosity, as shown in figure (41), together with the total interfacial area at the same column height against porosity, it is seen that the two lines are parallel on the semi-log paper, which means the two quantities have the same dependence on porosity as each other. This is what would be expected if the gas in the large bubbles effectively by-passes the column, as postulated in Chapter VIII, and the measured interfacial area is wholly contributed by the remaining gas in the form of "small" and ionic bubbles.

The second point is that the $F(\theta)$ curves level out at a value of $F(\theta)$ of around 0.88 to 0.91. This is also what is expected if it is considered that the ionic bubbles have a residence time that is extremely long compared to all the other bubbles. This fraction, of from 9 to 12% of the gas, agrees with the fraction of gas existing as ionic bubbles indicated by the difference in gas holdup in water and sulphite solution at the same column height and gas rate.

The remaining curved part of the $F(\theta)$ curves is due to the distribution of bubble sizes in the range intermediate between the large bubbles and the ionic bubbles/

THE POROSITY DEPENDENCE OF TOTAL AREA (A) AND THE SMALL AND IONIC BUBBLE FRACTION OF THE GAS FLOW

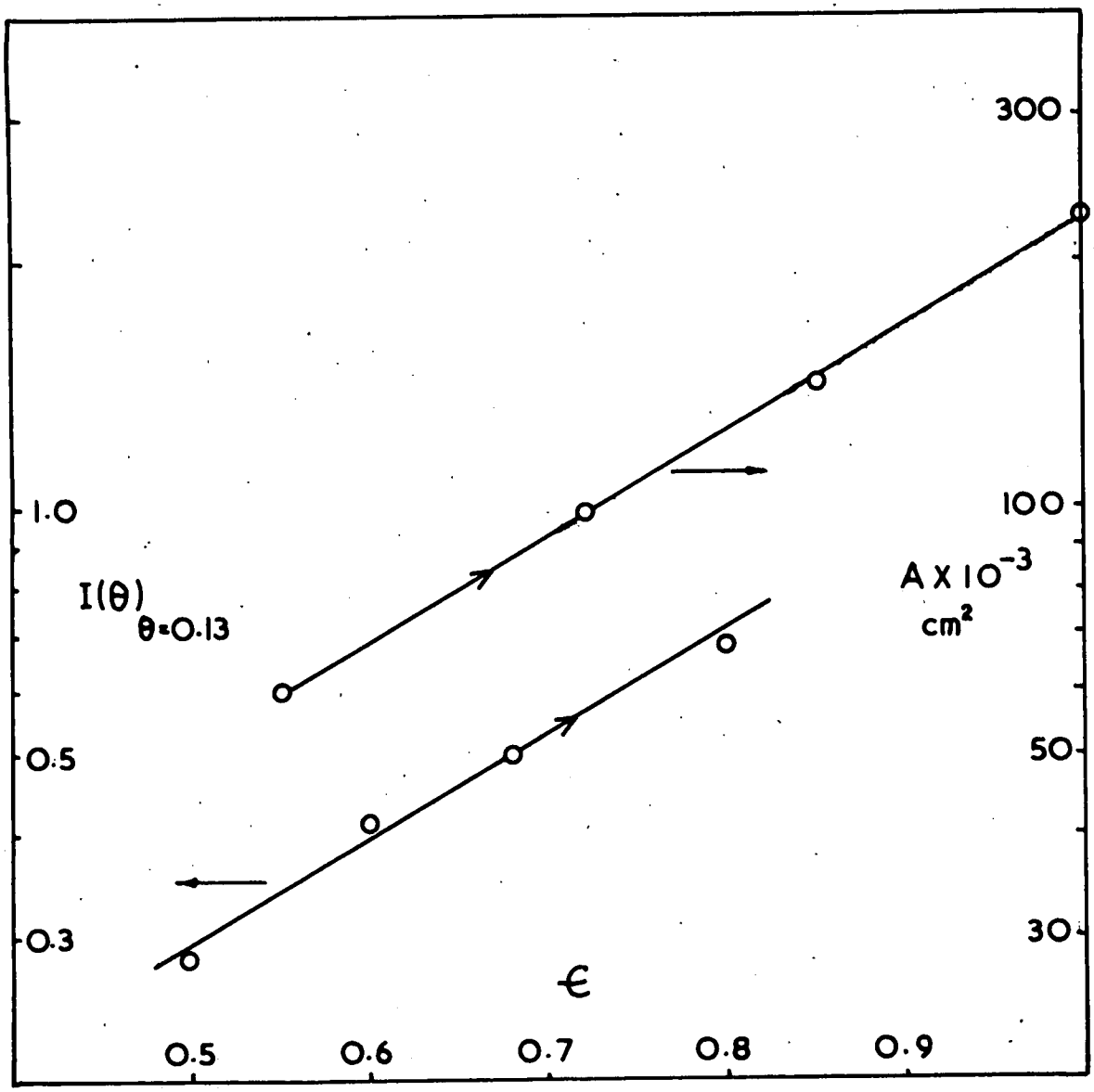

FIGURE 41

bubbles. To account for the complete $F(\theta)$ diagram for each bed porosity, the following model is proposed.

Consider the gas to be divided into three portions:

1) Large bubbles: whose flow rate, expressed as a fraction of the total flow rate, is U_1; that occupy a volume fraction, Vp, of the dispersion; and move in plug flow through the dispersion.
2) Ionic bubbles: that in the time scale considered for these measurements remain within the dispersion; whose fraction of the total gas flow is U_2; and that occupy a volume fraction, Vi.
3) Intermediate sized bubbles: whose fraction of the total flow is U_3; and that occupy a volume fraction V_b.

From the point of view of mixing in the dispersion as a whole, the concept of cross-flow between all these portions of the gas is accepted, on the grounds that the whole dispersion is well agitated by the passage of the large bubbles and some of these large bubbles may be sheared off into showers of "small" ones, and on the other hand some of the small ones may coalesce to reform large bubbles. That this happens to some extent was put forward as an explanation in Chapter VIII, page 155 for the fact that although the interfacial area of the gas is reduced by large bubbles coalescing with themselves and small bubbles, no decrease in local specific interfacial/

GAS FLOW MODEL

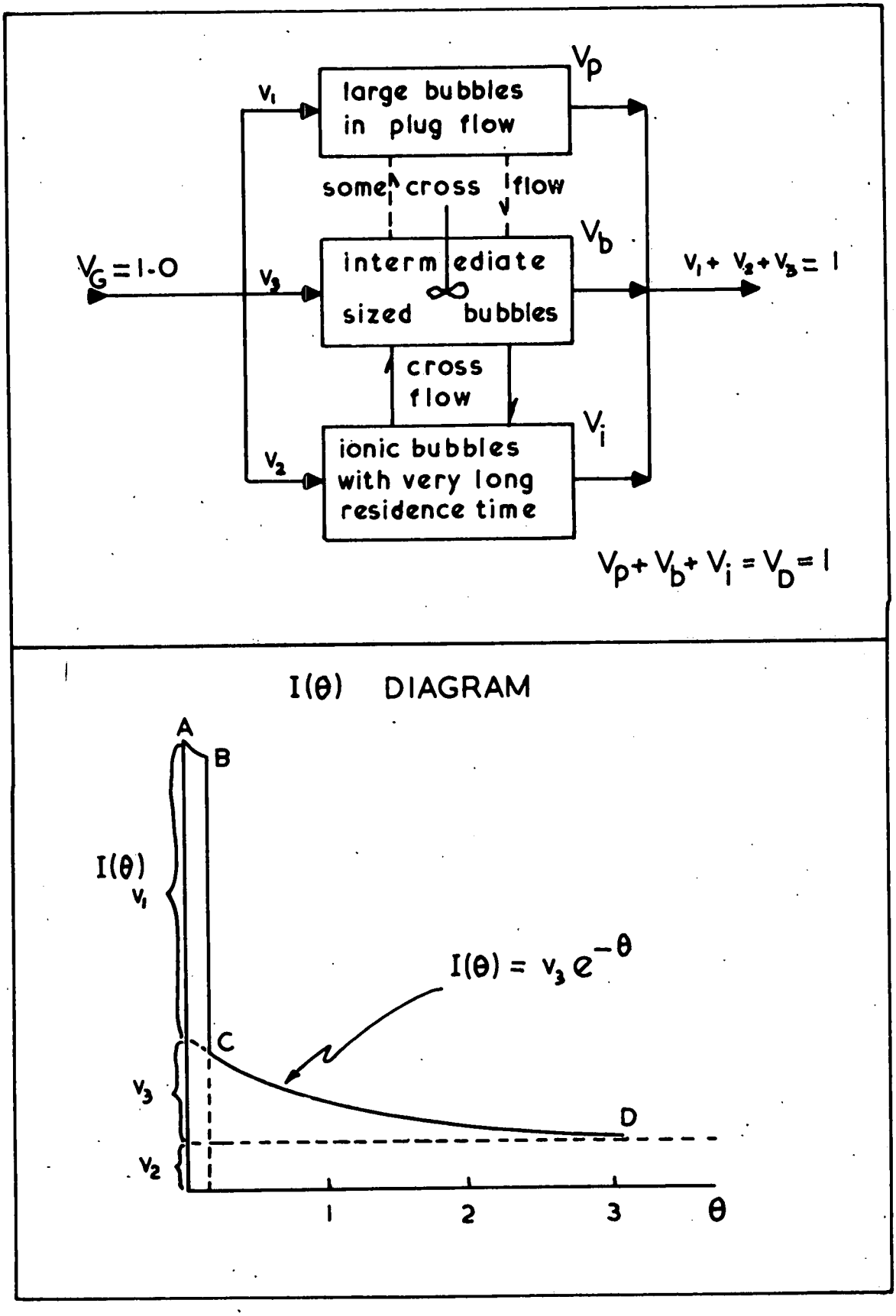

FIGURE 42

interfacial areas occurred as one moved up the column; it must therefore have been kept at a constant level by the regeneration of "small" bubbles.

The model proposed is shown schematically in figure (42) and below is the type of $I(\theta)$ curve expected from it, if the following assumptions are made:

1) That the actual volume of the dispersion occupied by the large bubbles, Vp, is small compared to V_D .

2) That there is complete cross-flow between Vi and V_b (212).

3) That the distribution of residence times of the intermediate sized bubbles is similar to that of a perfectly mixed system.

Portion CD of the $I(\theta)$ curve is represented by $I(\theta) = \tau_3 e^{-\theta}$ for the case of perfect mixing of the portion of gas τ_3. All that is then required to plot the theoretical $F(\theta)$ curve is the values of τ_2 and τ_3 for each experimental condition. This is done as follows: (figure (43) shows an example of the experimental $F(\theta)$ curve)

The value of τ_3 is determined from the difference in $F(\theta)$ where the curve levels out and where the vertical section ends. Values of θ are selected and $I(\theta) = \tau_3 e^{-\theta}$ calculated for each. Then the theoretical value of $F(\theta)$ is obtained by the relation:

F/

EXAMPLE OF AN EXPERIMENTAL F(θ) CURVE

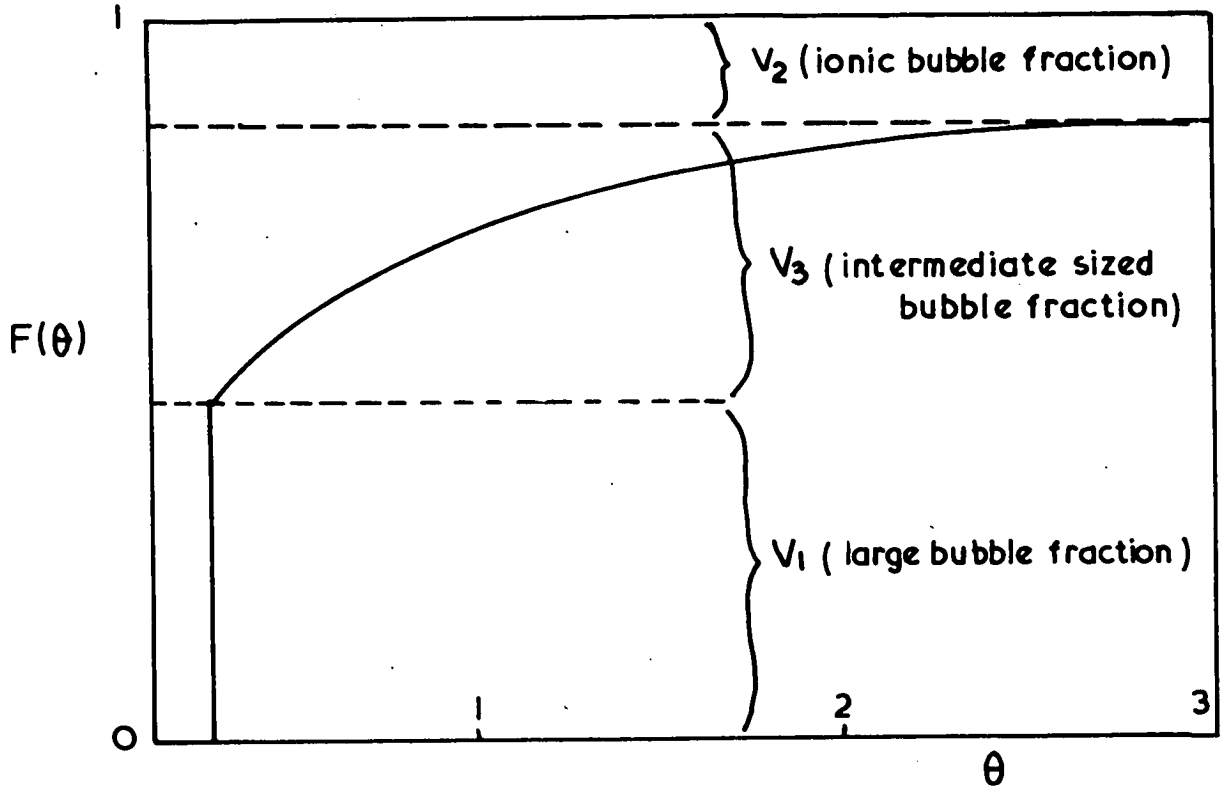

FIGURE 43

$$F(\theta) = (1 - v_2) - v_3 e^{-\theta}$$

since the curve for the intermediate sized bubbles does not attain a value of $F(\theta) = 1$ but $F(\theta) = (1 - v_2)$, due to the presence of the ionic bubbles. In plotting the values of $F(\theta)$ to obtain the theoretical lines shown in figure (44) the following values of v_2, v_3 were used for the appropriate porosities:

ϵ	v_2	v_3
0.80	0.10	0.58
0.68	0.09	0.41
0.60	0.09	0.33
00500	0.08	0.20

Figure (44) shows the calculated $F(\theta)$ curves for the intermediate sized bubbles with the experimental values superimposed. A reasonably close fit is obtained for all porosities and it can thus be concluded that the distribution of residence times of the intermediate sized bubbles is close to that expected from a perfectly mixed system, or in other words the range of residence times is very large. The small curved section which is represented by AB on the $I(\theta)$ curve in figure (42) was not detected for the experimental measurements since the time involved was too short compared to the chart speed, used, and the magnitude of the change in chart reading/

F(θ) CURVES FOR THE MODEL WITH EXPERIMENTAL POINTS SUPERIMPOSED

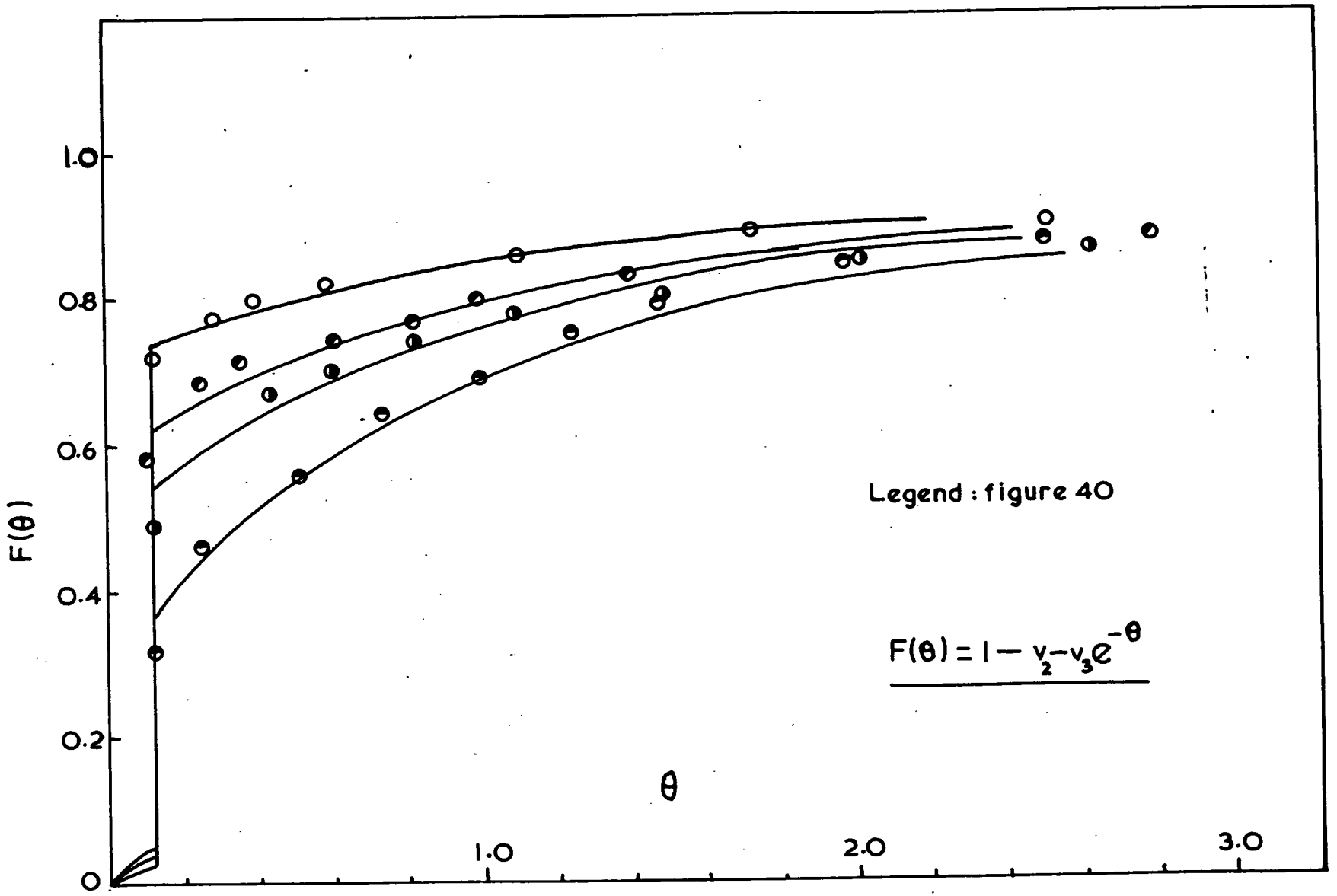

FIGURE 44

reading from $F(\theta) = 0$ to $F(\theta) = 1$.

Other work on residence time distributions of gas bubbles in tall columns was carried out by Bibby (207) and Kölbel (221). Bibby, whose work was a continuation, using the same apparatus and gas-liquid system, of that of Calderbank (206) described earlier in Chapter VII, pages 138 to 140, measured the residence time distribution of carbon dioxide bubbles rising through a solution of glycerol in water under conditions such that coalescence occurred (see Ch. VII), also using mercury vapour as the tracer. He found the small bubbles emerging from the sieve plate that reached the top of the column without being overtaken and captured by large bubbles formed as a result of coalescence, exhibited a range of residence times, but he did not attempt to see how they approached the range expected from a perfectly mixed system. His gas flow rates used were up to a maximum of 2 cm/sec and so there would have been much less agitation in his column than in the three phase dispersion examined here. He did explain the distribution of residence times as the result of the liquid circulation induced in his column by the passage of the larger spherical cap bubbles: some small bubbles were dragged down or held stationary by the circulating eddies near the walls, and others moved quickly through the column by the upflowing stream of liquid in the centre.

Kölbel/

Kölbel used columns from 4 to 19 cms in diameter and from 70 to 200 cms in height. Gas was bubbled into the stagnant column of water through a sintered metal plate and the residence time distribution functio n measured by introducing a step change in the gas from hydrogen to carbon-monoxide. His was not a coalescing system. For the 200 cm column, 9 cms in diameter, he found that by varying the gas rate over a range of superficial linear velocities from 0.5 to 7 cm/sec, the distribution of residence times could be compared to those of a number of perfectly mixed vessels in series. At a gas rate of 0.5 cm/sec the number was 2, rising to a maximum of 15, the closest approach to plug flow, at 3 cm/sec, and then falling back to 7 at 7 cm/sec. Unlike Bibby he did not start with bubbles of a uniform size but quite possibly obtained a range of sizes to begin with, from the sintered plate distributor. However this makes his work more relevant to the three phase column studied here where a range of sizes is formed at the bottom of the column. From the trend of Kölbel's results it would not appear unreasonable that increasing the degree of turbulence in the column, by having coalescence taking place and producing large bubbles, would yield a wider distribution of residence times approaching that of a perfectly mixed vessel.

F/

F. CONCLUSIONS

The measurement of the residence time distribution of the gas bubbles in the fluidized bed has provided a qualitative and quantitative picture of the behaviour of gas in this three phase dispersion. It has also provided evidence to support the model first proposed in Chapter VIII which is enumerated below.

1. The residence time of the ionic bubbles is very long compared to that for the other bubbles.
2. The size of the portion of gas comprising the ionic bubbles agrees well with that calculated from the difference in the gas holdup in water and sodium sulphite under the same experimental conditions (8-15% of the gas flow).
3. The size of the portion of gas comprising the large bubbles is inversely proportional to the bed porosity, and the gas in these bubbles effectively by-passes the column.
4. The actual volume of the dispersion occupied by the large bubbles is small compared to the fraction of the gas flow they represent. At a porosity of 0.8 they occupy about 4% of the dispersion but represent 32% of the gas passing: and at a porosity of 0.55 they occupy about 9% and represent 72%.
5. The distribution of residence times of the intermediate/

intermediate sized bubbles is similar to the

b distribution associated with a perfectly mixed system, at all values of bed porosity.

CHAPTER XI

General Discussion

A. BUBBLE FORMATION AND COALESCENCE

The results of the measurements of bubble frequencies in Chapter VII gave rise to a number of conclusions about the behaviour of the gas inside the three-phase dispersion but the only quantitative data obtained was the frequency of bubbles large enough to cause a distinct peak on the recorder chart. It was firmly established that there were two regions in the column: one in which the large bubbles that were formed near the gauze moved individually up the column; and a second in which the coalescence of these large bubbles with one another occurred. The height up the column of the transition point between these two regions, the coalescence point, depended on the gas flow rate and bed porosity as shown in figure (23). From the decrease in frequency of the large bubbles with height, a measure of their rate of coalescence was obtained, and was found to be inversely proportional to the bed porosity, and independent of particle size. Their rate of coalescence agreed with the rate of coalescence of gas bubbles measured by Calderbank et al (206) in a liquid of viscosity/

viscosity greater than 70 centipoise. Once coalescence had begun in the three phase column, the rate was independent of the gas flow rate, see figures (17) to (19). It was further found that the frequency of large bubble formation at the gauze under conditions such that coalescence of the large bubbles began immediately, at a gas rate of about 9 cm/sec, was 7 bubbles per second. It was thus possible to correlate all the results in the region of coalescence by one equation containing only the value of bed porosity and height above the gauze (see Chapter VII page134). Figure (28) shows a pictorial representation of the bubble situation suggested by results from this series of experiments.

It was shown later, in Chapters VIII and X, that the gas in these large bubbles effectively by-passed the column from the mass transfer point of view. Thus the effect that their coalescence with each other had on the change in measured interfacial area with height was probably small. Unfortunately it is a shortcoming of the frequency measurements that they give no quantitative data about the size of the large bubbles, so it was not possible to estimate how much their growth was due to coalescence with each other in addition to the expansion caused by the change in hydrostatic head, and to coalesce ence with small bubbles that were distributed throughout the column. If a large number of the small bubbles, which contribute the bulk of the effective mass transfer area, were/

were removed in this way then the large bubble coalescence would be a decisive factor in reducing the mass transfer rate. However the interfacial area measurements reported in Chapter VIII showed that after an initial decrease near the gauze, to be discussed later, the specific interfacial area remained constant inspite of the large degree of bubble coalescence. This led to the conclusion that if the large bubbles did coalesce with small ones, which seems likely from the work of Calderbank (206), then this was compensated for by the regeneration of small bubbles as a result of the turbulence set up by the large bubbles, which sheared off some other large bubbles into showers of small ones. On page 156 in Chapter VIII the observations of Bradlick (141) of just such small bubble regneration in a two phase system are recorded. There was evidence, at a bed porosity of 0.55, of a decrease in specific interfacial area with height as shown by the dotted curved line in figure (30) and it was suggested that the degree of turbulence in a bed of such a low porosity may have been too low to permit sufficient regeneration of small bubbles to maintain the specific area. From observations of the three phase column in operation the number of small bubbles visible at the walls of the column decreased with decreasing/

decreasing porosity, which indicated that a larger fraction of the gas was contained in the large bubbles as the porosity was decreased: this explained the anomaly of a constant gas flow rate producing a constant frequency of bubbles of an increasing size as the porosity was reduced. See Chapter VII pages 135 to 137. It seemed that the large bubble size and the distribution of gas between the large bubbles and smaller ones, were important parameters which were dependent on the bed porosity.

A qualitative idea of the effect of bed porosity on large bubble formation and size was obtained by visual observations in the two dimensional bed, reported in detail in Chapter IX. It was clear from the observations that for any bed porosity there was a characteristic large bubble size. The growth of the bubble to this characteristic size was by the coalescence of small bubbles produced at the gas injection nozzle. It was observed that the size of the small bubbles leaving this nozzle was fairly constant under all conditions of air rate and bed porosity and the reason for this appeared to be that the liquid flowing past the nozzle from the liquid distributor, assisted in the detachment of bubbles as soon as they were formed. By considering the gauze in the six inch column as analogous to a series of nozzles this same process of large bubble formation/

formation was envisaged there too. The examination of this analogy is given in Chapter IX pages 171 to 173. No conclusions could be drawn about the coalescence between large bubbles and smaller ones because at the low degree of turbulence in the two-dimensional column at the low gas rates used, very few small bubbles were observed to leave the nozzle without coalescing to form large ones.

The effect of the degree of turbulence in the bed on the distribution of the gas between large and small bubbles was discussed in Chapter IX pages 171 to 173, as a result of the observations of large bubble formation in the two dimensional bed. It was concluded that a greater degree of turbulence, leading to a greater distribution of sizes, is achieved the higher the gas rate and bed porosity.

This conclusion is borne out by the results of the residence time measurements to be discussed later. It also gives an indication as to why there is a finite time required before the large bubbles begin to coalesce with each other, represented by the position of the coalescence point in the column shown in figure (23). Coalescence between large bubbles occurs when the separation distance between them is reduced to a critical value which is a function of their diameters. The separation distance between the large bubbles is reduced by/

by the following three main factors in this column:

1) The gas flow rate - increasing this for a given bed porosity increases the bubble frequency and hence reduces the distance between successive bubbles.

2) The bed porosity - this is a factor in so far as it decides the size of the largest bubble. Thus for a given air rate, larger bubbles will be formed at lower porosities and, since their frequency of formation is constant as mentioned earlier, their separation distance will be smaller.

3) The bed turbulence - the gas rate and bed porosity together influence this and as is explained in Chapter IX page 173 , there can be a range of large bubble sizes, from that characteristic of the bed porosity downwards. This would mean a range of bubble rise velocities which would result in larger bubbles catching up smaller ones. This would accelerate the achievement of the critical separation distance, to a degree depending on the extent of the size distribution.

B. THE SPECIFIC INTERFACIAL AREA NEAR THE GAUZE

In the previous section it was mentioned that after decreasing initially near the bed support gauze, the specific interfacial area remained constant in the remainder/

remainder of the column - except at $\epsilon = 0.55$. It is concluded from the observations discussed in that section on the formation of large bubbles in the two-dimensional bed, that a high specific interfacial area exists near the gauze in the six inch column due to the small bubbles that emerge from it. These bubbles then coalesce, within a short distance, to form the large bubbles and others of intermediate sizes. This causes a rapid drop in specific area to a level which is maintained thereafter. The extent of this drop in area depends on the size distribution of bubbles formed from the small ones and this is a function of the bed turbulence as discussed in Chapter IX page 172. In the six inch column the same air rate was used in measuring interfacial areas at three porosities and the results of the total interfacial areas, A, were plotted against height in figure (30). The main features of these results have already been discussed here and in Chapter VIII pages 154 to 160, but the extrapolation of the lines below a height of 50 cms was not clear at that stage of the investigation. On the basis of the picture that has emerged since, of the coalescence of the small bubbles formed at the gauze, it is suggested that the extrapolation of lines in figure (30) should be as shown in figure (46), which is a diagramatic representation of the bottom section of figure (30) enlarged/

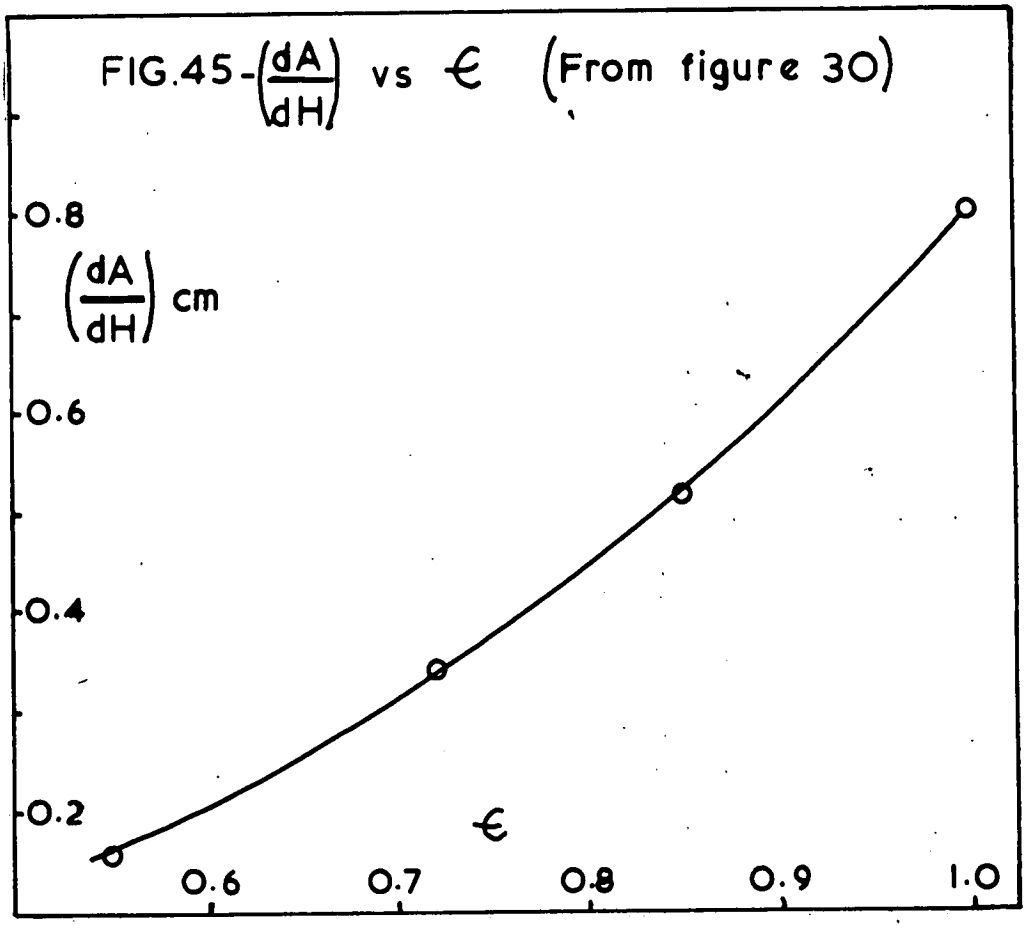

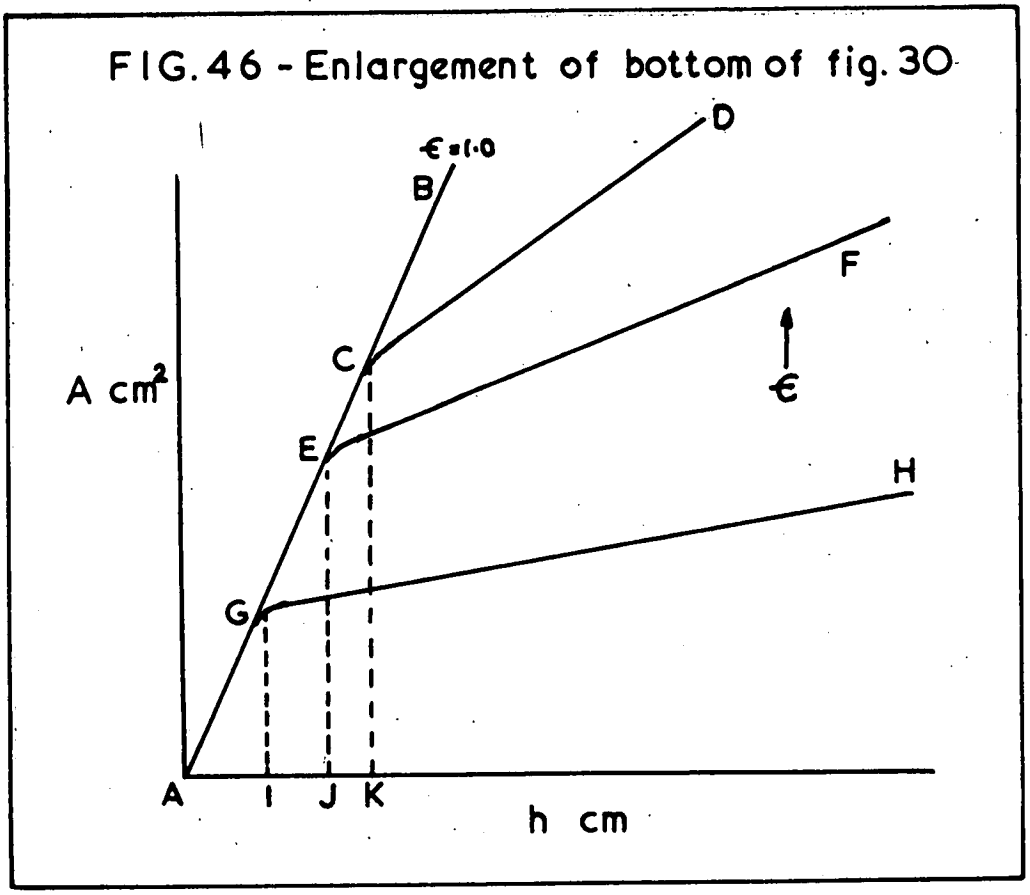

FIGURES 45&46

enlarged. Line AB is the line corresponding to no coalescence of the small bubbles, i.e. line for $\epsilon = 1.0$ on figure (30), and lines CD, EF and GH are the ends of the lines for different porosities. The rapid change in specific area at the point of coalescence of the small bubbles is shown taking place at points G, E and C, and at a greater height above the gauze, points I, J, and K, as the porosity is increased. The dependence of the distance from the gauze that the small bubbles travel before coalescing can be explained by assuming that the strong liquid currents coming through the gauze, which cause the detachment of the small bubbles as they are formed, can travel further before being dissipated, see again Chapter IX page 170, in a bed of higher porosity. The extent of the decrease in specific area is given by the change in slope from that of the line AB. From figure (30) the maximum distance from the gauze that the small bubble coalescence takes place is about 30 cms, at $\epsilon = 0.85$. The fact that this is of the same order as the distance that the large bubbles commence to coalesce with each other for the same air rate, shown in Figure (23) may indicate that the mechanism involved in the commencement of coalescence is similar in both cases. As no plot like figure (30) is available at any other gas flow rate for comparison with figure (23), the possibility of a coincidence cannot/

cannot be ruled out. The actual coalescence of large bubbles has not been visually observed in this work.

C. MODEL OF GAS FLOW THROUGH THE DISPERSION

So far in this general discussion the behaviour of the gas has been examined with respect to the formation, coalescence and size distribution of large and 'small' bubbles and their interfacial areas but no mention has yet been made of the presence of the ionic bubbles. The phenomenon of the existence of these minute bubbles of approximately 1 mm diameter, has been discussed in Chapter VIII and it was shown there that they represented between about 8 and 15% of the total volume of gas present in the dispersion, depending on the bed porosity, at the gas rate used. It was also suggested that their residence time was very long compared to the other bubbles for the reason that their small buoyancy did not allow them to escape from the liquid eddies and rise up through the column. It was also explained that the interfacial area and residence time of these bubbles was disproportional to the amount of gas contained in them and that in view of this they may be a major mode of mass transfer in this column and in electrolyte systems generally. This will be discussed later.

In Chapter VIII a model was proposed to represent the/

the gas flow through the three phase dispersion. It considered the gas to consist of three portions as follows.

1) A portion which passes rapidly through the dispersion as large bubbles and as far as the mass transfer process is concerned, the gas comprising them effectively by-passes the column, serving only to produce intense agitation and the generation of 'small' bubbles and ionic ones.
2) An ionic bubble portion, which is fairly constant in interfacial area throughout the column and which has an extremely long residence time.
3) An intermediate sized bubble portion, referred to as 'small' bubbles, with a range of sizes between the large bubble size and about 4 mm. The magnitude and size distribution depends on the conditions of bubble formation near the gauze and the agitation in the column as a whole.

This summarized the general pattern of the gas behaviour as far as it could be ascertained from the bubble frequency area and gas holdup measurements made in chapters VII and VIII, but no quantitative data as to the relative sizes of each portion could be obtained, except for that of the ionic bubble portion as measured by the difference in gas holdup between water and sulphite used as the liquid in the dispersion. However the/

the measurements of the residence time distribution function of the gas in the tall column under the same operating conditions as used for the area measurements provided this quantitative data.

The model proposed was confirmed in practically every respect by these measurements. The fraction of the gas composing the ionic and small bubble portions together, was related in precisely the same way to the bed porosity see figure (41) as was the total interfacial area calculated in the tall column, indicating that the gas in the large bubble portion did in fact by-pass the column as far as mass transfer was concerned. The percentage of gas with a longer residence time than $\theta = 3$ was of the same order as that calculated for the ionic bubbles from holdup measurements. The fraction of the gas in the large bubbles was inversely proportional to the bed porosity, and the residence time of the bubbles was of the order of 4 to 5 seconds.

Additional information that was gained was of the distribution of residence times of the 'small' bubbles. At all bed porosities the distribution was close to that expected from a perfectly mixed dispersion, which meant that even at the lowest porosity there was a very wide distribution of residence times. So although few small bubbles were observed at the column walls at the low porosity/

porosity of $\epsilon = 0.55$, there must have been a significant quantity of them throughout the dispersion. Another point of interest, is the fact of the short residence of the large bubbles which means that at $\epsilon = 0.85$, they occupy only 4% of the dispersion volume yet contain 32% of the gas and at $\epsilon = 0.55$ they occupy 9% and contain 72%. This point is referred to in the next section.

D. REACTOR DESIGN CONSIDERATIONS

In evaluating the results and conclusions of this study of gas dispersions in a solid-liquid-fluidized bed from the point of view of reactor design, there are one or two factors that must be kept in mind. The sulphite system itself, used to measure the interfacial areas has advantages and disadvantages. The advantage that it has being a mass transfer method, over physical methods such as light transmission, is that it does give the effective interfacial area of the dispersion for mass transfer. For example the area associated with the large bubbles is smaller, and so is the increase in area, with reduced hydrostatic head, caused by the expansion of the bubbles. It's main disadvantage however is that the presence of the small ionic bubbles could provide a major mode of mass transfer that would be absent in pure liquid or liquid hydrocarbon mixtures.

The/

The extent of the contribution of these bubbles to the interfacial areas measured in this work cannot be assessed. The fact that their residence time appears to be extremely long could mean that in the case of a dilute gas mixture like air, they would become effectively exhausted of oxygen for the latter part of their stay in the dispersion and so contribute nothing during that time. This would not be the case if a pure gas, oxygen, was used. A second disadvantage is that the method, by its nature, only obtains integral average values for the interfacial areas: the change in area with column height has to be measured by using a series of small columns of increasing height to simulate one tall one. This imposes the limitations discussed in Chapter V, namely that operating conditions must be used that produce large changes in specific area with height so that changes in the average area with overall height are reliably measurable.

These points having been raised, the effect of the process variables, gas flow rate, liquid flow rate, bed porosity and particle size and shape on the gas-liquid interfacial area and bubble coalescence can be still assessed qualitatively and in some cases, such as the large bubble volume, quantitatively from the work done here.

In/

In trying to ascertain the optimum mode of operation of a three phase reactor in which the gas-liquid interfacial area is an important parameter, the basic opposing factors are a) the requirement of a large amount of agitation to produce small bubbles, which means using high gas rates and b) the prevention of bubble coalescence and gas by-passing, which occur readily at high gas rates. The passage of large bubbles through the dispersion provides very efficient agitation, which might be an important factor depending on the reaction mechanism at the catalyst, and the by-passing could then be considered as an agitation cost, or the gas could be recycled. This latter suggestion would depend on the reaction products, whether they remained in the liquid phase, in which case gas recycling may be simple, or whether they were gaseous in which case a separation would be necessary. Obviously the design of a reactor of this type is not a simple matter of optimising the gas-liquid interfacial area although this is an important aspect. The interfacial area experiments in the short column showed that increasing the gas rate caused an exponential rise in interfacial area but there are limits on the gas rates that can be used in a given column, such as the onset of slug flow caused by rapid rates of coalescence.

The investigation of this work, of the inter-

relation of the process variables such as gas flow rate, liquid flow rate, bed porosity and particle size has been of an exploratory nature and in many ways limited in its scope. However it has shown clearly the factors affecting bubble formation, coalescence and the gas liquid interfacial area, and provided basic qualitative and quantitative data which can be used to point the direction of future research into the special aspects related to a particular three phase fluidized reactor. It has also shown the importance of residence time studies in helping to understand flow systems.

CHAPTER XII

A. General Conclusions

PART I

The chemical method of measuring gas-liquid interfacial areas using the oxidation of a copper catalysed sodium sulphite solution was studied extensively and developed so that under the conditions used for the work in Part II a value of the overall liquid phase mass transfer coefficient could be predicted. This value was, $k_L^1 = 4.5 \pm 0.75 \times 10^{-2} \frac{cm}{sec}$ when using 0.4 to 0.8M sulphite solutions at 36°C containing at least 10^{-3} g.moles/litre of cupric ions. This compares with a value of 0·63 cm/sec, proposed by Westerterp (130) who originally suggested the use of the sulphite oxidation reaction as a means of measuring interfacial areas. See Chapter II section B for an explanation of the discrepancy between these two values.

PART II

An exploratory experimental investigation of the inter-relation of the process variables, gas rate, liquid rate, bed porosity and particle size in a gas-solid-liquid dispersion was carried out. The effect

of/

of these variables on the formation of gas bubbles as they enter the bed, the onset and subsequent rate of bubble coalescence, the efficiency of gas-liquid contacting and the mode of gas flow through the dispersion was studied. The study showed that the two most important process variables are gas rate and solid-liquid bed porosity. The scope of the experiments and thus the information obtained was restricted by the limitations imposed by the experimental techniques used, but the general conclusions, both qualitative and quantitative are listed below.

1. Gas enters the three phase dispersion as small bubbles which are detached immediately from the gas distributor, gauze or nozzle, upon formation and travel a short distance before coalescing into large bubbles and small ones with a distribution of sizes. The distance they travel and the distribution of bubble sizes formed, increases as the degree of turbulence, as observed in the two dimensional bed, above the distributor increases.
2. There is a characteristic size, inversely proportional to the bed porosity, to which the large bubbles must grow before leaving the vicinity of the distributor in a bed with a very low gas rate. This size becomes the maximum size/

size of large bubbles formed under turbulent conditions.

3. The frequency of formation of large bubbles is a function only of gas flow rate and is given by the equation:

$$f_{\beta} = Vs^{0.32} \quad sec^{-1} \qquad \text{where}$$

$$Vs = cm/sec$$

(see figure (24), Chapter VII).

4. The large bubbles commence to coalesce with each other after a certain time, depending on the gas flow rate and bed porosity (see figure (23) chapter VII).

5. The rate of coalescence of large bubbles, as measured by the change in bubble frequency with height, is inversely proportional to the bed porosity and independent of particle size and gas flow rate. All the results from the bubble frequency measurements in the region of large bubble coalescence were correlated by the equation:

$$f_{\beta} = \exp\left[1.95 - \left(\frac{7.12}{\epsilon} - 4.39\right) \times 10^{3}\, h\right] \quad sec^{-1}$$

where h = height (cm). (See figure (20) Chapter vII)

6. The specific interfacial area, measured as the area per unit volume of the unaerated solid-liquid dispersion, is relatively high just above the gas distributor but drops rapidly, as the small bubbles/

bubbles coalesce, to a level which is then maintained throughout the column. The reduction in mass transfer area by the coalescence of large bubbles with small ones distributed throughout the column is thus assumed to be compensated for by the regeneration of small bubbles from larger ones as a result of agitation. See Chapter VIII and the work of Braulick (141).

7. The specific interfacial area increases exponentially with increasing gas flow rate and bed porosity (see figure (31) and (34) Chapter VIII) and the mean bubble size decreases (see figure 35).

8. The gas flowing through the solid-liquid-gas dispersion may be conveniently regarded as consisting of three portions:

a) A portion which passes rapidly (within a reduced time equal to approximately 0.13) through the dispersion as large bubbles and, as far as the mass transfer process is concerned, the gas comprising them effectively by-passes the dispersion, serving only to produce intense agitation and the generation of 'small' and ionic bubbles.) This portion contains, at the flow rate used, from 30 to 70% of the total gas flow at/

at bed porosities of from 0.85 to 0.55 respectively.

b) An ionic bubble portion, 8 to 15% of the total gas flow used here, which is fairly constant in interfacial area throughout the column and which has an extremely long residence time compared to the other bubbles (a reduced time greater than 3.0)

c) A portion consisting of intermediate sized bubbles, with a range of sizes between the large ones in portion a) and about 4 mm in diameter. The size of this portion depends on the other two. At the flow rate used here the distribution of residence times associated with this gas portion was close to that for a perfectly mixed dispersion at all bed porosities.

B. Recommendations for Future Work

1. Since the rate of coalescence of large spherical cap bubbles measured by Calderbank (206) in a liquid of viscosity greater than 70 centipdse was the same as found here for a bed porosity of 0.81, it would be interesting to measure coalescence rates in two phase gas-liquid systems using liquids of much higher viscosities. The relation between coalescence rate and viscosity could then be compared/

compared to that between coalescence rate and bed porosity found in this work.

2. A follow up to the above would be to measure the viscosity of the solid-liquid beds used in this work, begun by Anderson and Bryden (219). The fact that they found a ballotini bed of porosity 0.49 to have a viscosity of approximately 9 poise may explain the great increase in coalescence rate at the lowest porosity used here of 0.51, over that at 0.94.
3. Experiments using water and air but a much wider range of particle size and density to further test the result that rates of coalescence and interfacail areas were unique functions of bed porosity for a given gas rate.
4. With the model developed here for gas flow through a three phase dispersion as a guide, residence time studies in dispersions of gases and solids in liquids such as hydrocarbons, would give quantitative data of the fraction of gas by-passing and that likely to take part in a reaction, when there was no method available for measuring the gas-liquid interfacial area.

APPENDIX I

Equations for calculating the values of k_L' and interfacial areas, a.

A. STIRRED CELL EXPERIMENTS

The experimental data consists of rates of absorption of oxygen expressed as (cm^3/sec) obtained by measuring the movement of the soap film down the burette and the liquid temperature. The effect of the reduction in the gas volume above the liquid in the cell as the liquid cools is shown in figure (47). This reduction in volume, expressed as (cm^3/sec), must be subtracted from the measured absorption rates, as indicated in Chapter III section A (3).

The basic mass transfer equation shown below holds if it is assumed that the concentration of oxygen in the bulk liquid is zero.

$$N_{sc} = k_L' \; a \; c^* \qquad \ldots\ldots (1)$$

where N_{sc} = gm. Oxygen absorbed per second (gm/sec.)

$\hat{k_L}$ = overall liquid phase mass transfer coefficient (cm/sec).

a = interfacial area (cm^3)

C^* = solubility of oxygen in the sodium sulphite solution (gm/cm^3)

The/

STIRRED CELL COOLING CORRECTION
(to be subtracted from the observed absorption rate given by the soap film meter, $cm^3 sec^{-1}$)

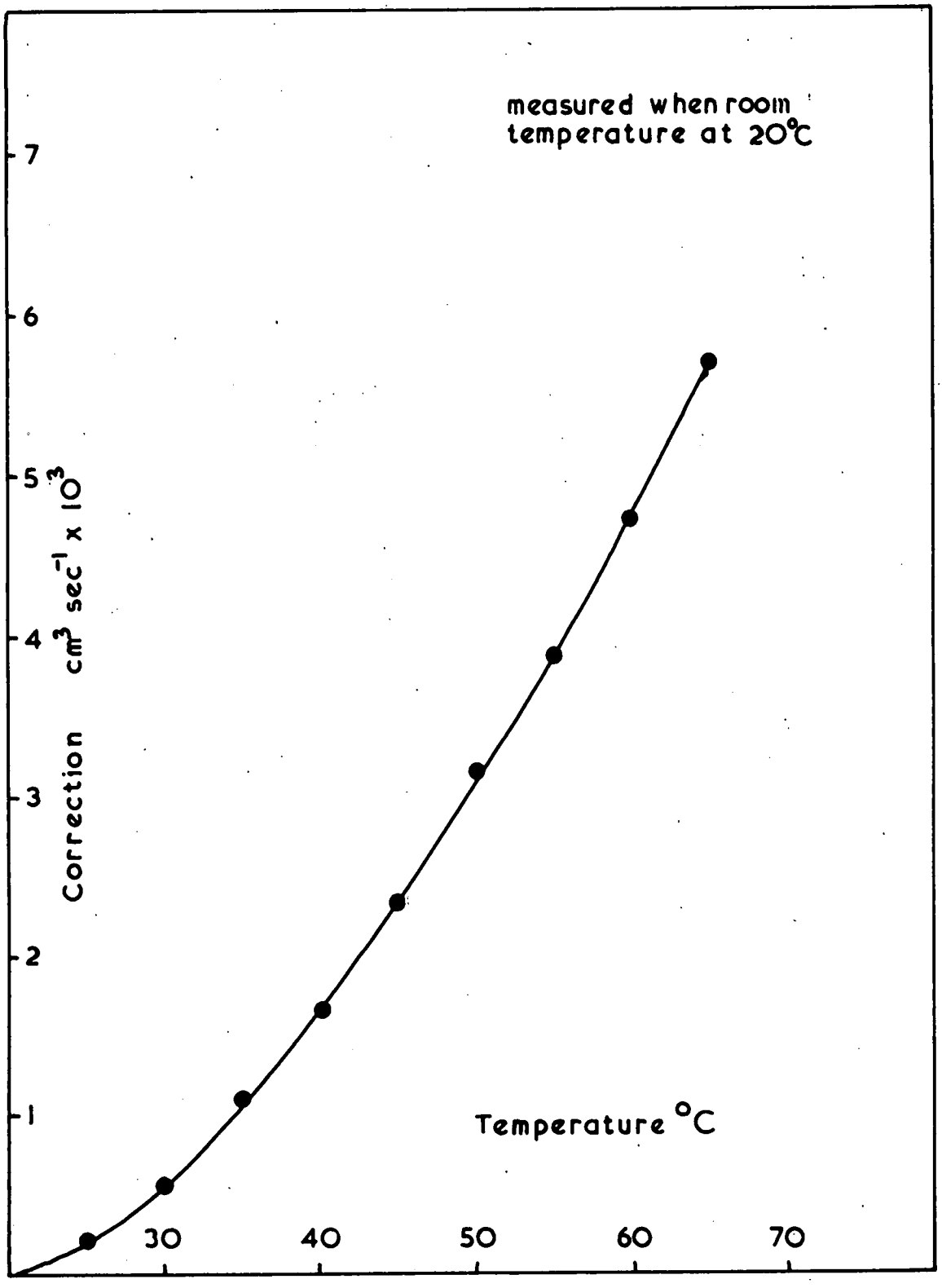

FIGURE 47

The value of Nsc

Let r_a be the corrected observed absorption rate (cm^3/sec). Assume the oxygen in the soap film meter is at room temperature $t(^oC)$.

$$\text{Then } N_{sc} = r_a \frac{cm^3 O_2}{sec} \times \frac{32 gm O_2}{1 \text{ g.mole } O_2} \times \frac{1 \text{ g.mole}}{22400 cm^3} \times \frac{273^oK}{(273 + t)^oK}$$

$$N_{sc} = r_a \times \frac{0.390}{(273 + t)} \frac{\text{gm of oxygen}}{\text{sec.}}$$

The value of a

The interfacial area, a, cm^2 was the area of the vortex created by the stirrer. A constant stirrer speed was used and a constant volume of liquid charged to the cell, so the value of a was constant and calculated from the radius of the top edge of the vortex r and its depth d as follows:

$$a = \pi r \sqrt{r^2 + d^2}$$

$$\text{thus } a = \pi\, 3.45 \sqrt{(3.45)^2 + (1.55)^2} = 41.0 \text{ cm}^2$$

The value of C^*

Figure (48) in Appendix II gives the solubility of oxygen in pure water at any temperature, $C^*_{H_2O}$.

Figure (50) in Appendix II gives the value of the correction/

correction factor, the salt factor, f, to convert the oxygen solubility in pure water to that in a sulphite solution of any normality in the range 0 to 1.6N.

$$\text{Hence } C^* = C^*_{H_2O} \times f$$

The value of k'_L

This is calculated by equation (1) substituting the above derived values for C^*, Nsc and a:

$$k'_L = \frac{r_A \times 0.390}{(273 + t)} \Big/ 41.0 \times C^*_{H_2O} \times f \ \frac{cm}{sec} \quad \ldots\ldots (2)$$

B. THE AERATED TANK AND BUBBLE COLUMN EXPERIMENTS

The experimental data from both these experiments consisted of the following:

1) The rate of change of sample titre expressed as r, $\frac{mls}{min}$, of 0.1N Sodium Thiosulphate.
2) The sulphite liquid temperature in the tank or column T^oK.
3) The interfacial area measured by the light probe expressed as a_a, cm^2/cm^3 of aerated dispersion.
4) The fractional gas holdup Hg in the aerated dispersion.

The same basic equation is used,

$$N = k'_L \ a_a \ C^* \quad \ldots\ldots (3)$$

but where N the oxygen consumption rate expressed as g.moles/

g.moles Oxygen/cm^3, sec, a_ℓ is the interfacial area per unit volume of liquid (cm^{-1}), and C^* is the solubility of oxygen in the sulphite solution expressed as g.moles Oxygen/cm^3.

The Value of N

Let vs be the volume of the sample of sodium sulphite (cm^3). From the equation for the reaction, $SO_3^= + \frac{1}{2}O_2 \longrightarrow SO_4^=$, it can be seen that one half mole of oxygen is consumed for each mole of sulphite ion, therefore the measured molar rate of oxidation of sulphite must be divided by two.

$$N = r \frac{\text{mls}}{\text{min}} \times \frac{0.1 \text{ g.equiv}}{10^3 \text{ cm}^3} \times \frac{1 \text{ g.mole } SO_3^=}{2 \text{ g.equiv}} \times \frac{1}{v_s \text{ mls}} \times \frac{1 \text{ min}}{60 \text{ secs}} \times \frac{1 \text{ g.mole } O_2}{2 \text{ g.mole } SO_3^=}$$

$$N = 4.17r \times 10^{-8} \quad \frac{\text{g.mole } O_2}{\text{sec. cm}^3} \quad \text{when vs = 10 mls.}$$

The value of C^*

If C is expressed in g.moles/cm^3, then it can be defined as follows:

$$PV = nRT \quad \text{(gas law)}$$

$$P = \frac{n}{v} RT = C\,RT$$

$$C = P/RT.$$

If $C^*_{H_2O}$ is the solubility of oxygen in gm.,moles/cm^3 given by the Henry's Law distribution coefficient for oxygen/

oxygen, He, in pure water, then

$$p_{O_2} = He \times C^*_{H_2O} \times RT$$

where p_{O_2} is the partial pressure of oxygen in the inlet air. Then

$$C^*_{H_2O} = p_{O_2}/RT\ He$$

to convert this to the solubility in solutions of sodium sulphite it must be multiplied by the salt factor, f, given by figure (50) in Appendix II.

Thus $C^* = (p_{O_2}/RT\ He) \times f$ $\frac{g.moles\ O_2}{cm^3}$

Values of He against temperature are plotted in figure (49) in Appendix II.

The Value of a_ℓ

The value of interfacial area measured by the light probe is a_d in the units cm^2/cm^3 of aerated dispersion. To convert this to a_ℓ cm^2/cm^3 of liquid, it must be divided by the fraction of liquid in the dispersion, which is (1 - Hg) $a_\ell = ad/(1 - Hg)$ cm^{-1}

The value of k'_L

The value is calculated using equation (3) and substituting the above derived expressions for N, C^* and a_ℓ, hence

k/

$$k_L' = \frac{4.17r \times 10^{-8} \times He\ (1 - Hg)}{p_{O_2}/RT \times ad \times f} \qquad \ldots\ldots (4)$$

C. THE THREE PHASE DISPERSION INTERFACIAL AREA MEASUREMENTS.

The experimental data for the mass transfer rate is the same as for the experiments in the aerated tank and bubble column, with exception that k_L' is assumed to be 4.5×10^{-2} cm/sec and it is a_{SL} expressed as cm^2/cm^3 of solid-liquid fluidized bed, that is to be calculated.

Referring to equation (3):

The value of $N = 4.17r \times 10^{-8}$ g.moles $O_2/sec.cm^3$.

$C^* = (p_{O_2}/RT.He) \times f$ g.moles O_2/cm^3

The value of a_{SL}

The value of a_p calculated from equation (3) will be in units cm^2/cm^3 of liquid. To convert this to the area in cm^2/cm^3 of solid-liquid dispersion it must be multiplied by V_L/V_D, where V_L is the total volume of liquid and V_D is the volume of the liquid-solid dispersion.

$$a_{SL} = a \times \frac{V_L}{V_D}$$

Thus $$a_{SL} = \frac{(4.17r \times 10^{-8})\ He}{p_{O_2}/RT \times k_L \times f} \times \frac{V_L}{V_D} \qquad \ldots\ldots (5)$$

The/

The value of P_{O_2}

In the case of a tall column containing a fluidized bed of solid particles, there would be a sizeable error involved in assuming the partial pressure was 0.21 atm. because of the hydrostatic pressure under which the air enters at the bottom of the column. It was decided to take the mean value of the oxygen partial pressure at the bottom and top of the column, as recommended by Yoshida (14). The value at the bottom was taken as 0.21 times the total pressure due to the column of liquid-solid fluidized bed plus one atmosphere. The partial pressure at the top of the column was calculated from the depletion of oxygen by the reaction. The following shows the calculation procedure.

Data required

Bed height - H (cms)

Bed porosity - ϵ

Density of solid particles - ρ_s (gm/cm^3)

Density of the sodium sulphite - ρ_l (gm/cm^3)

Total liquid volume - V_t (l)

Air flow rate entering the column V_G (l/min) at 15°C 1 atm.

Sulphite oxidation rate - r (mls/min)

Value of P_{O_2} at foot of column

Solid-liquid-bed density $\equiv (\epsilon\rho_l + (1-\epsilon)\rho_s)$ gm/cm^3

Pressure/

Pressure due to bed = $\frac{H \times (\epsilon \rho_f + (1 - \epsilon)\rho_s)}{1033}$ atm.

p_{O_2} at gauze = $0.21 \left(\frac{1 + H(\epsilon \rho_f + (1 - e)\rho_s)}{1033}\right)$ atm.

Value of p_{O_2} at top of column

From Section B above, oxygen consumption N is given by $N = 4.17r \times 10^{-8}$ g.moles/cm^{3}sec.

Converting this to (l/min) at 15° 1 atm:

$$O_2 \text{ depletion} = 4.17\, r \times 10^{-8} \frac{\text{g.mole}}{\text{cm}^3\ \text{sec.}} \times \frac{60 \text{ sec}}{1 \text{ min}} \times Vt \times 10^{-3}\text{cm}^3 \times 22.4 \frac{\text{litres}}{\text{g.mole}} \text{ at } 0^\circ\text{C} \times \frac{288\ ^\circ\text{K}\ (15^\circ\text{C})}{273\ ^\circ\text{K}\ (^\circ\text{C})}$$

O_2 depletion = $5.89r\ Ve \times 10^{-2}$ (l/min) at 15°C 1 atm.

Thus p_{O_2} at top = $\frac{0.21V_G - 5.89r\ Vt \times 10^{-2}}{V_G - 5.89r\ Vt \times 10^{-2}}$ atm

The value of p_{O_2} substituted in equation (5) is the arithmetic mean of p_{O_2} at gauze and p_{O_2} at top. Strictly speaking this arithmetic mean should only be used if the gas moves through the column in plug flow, but it is assumed the error involved is small, because the absolute quantities of oxygen consumed by the reaction were small.

APPENDIX II

Oxygen Solubility Data

Figure 48 - Oxygen solubility in Pure Water ($C^*_{s,o}$)

This is a plot of the weight in grams of oxygen dissolved in one cubic centimeter of water when the total pressure, including the water vapour, is 760 mm. for each temperature, ^oC.

Reference: Handbook of Physics & Chemistry (168).

Figure 49 - Henry's Constant for the system Oxygen-Water.

This is a plot of He versus temperature, ^oC, where He is defined as $He = \frac{p_{O_2}}{RT} \Big/ C^*_{H_2O}$

Reference: Handbook of Physics & Chemistry (168)

Figure 50 - Salt Factor versus Sulphite Normality

It is assumed that the solubility of oxygen in aqueous solutions of sodium sulphite is the same as in solutions of sulphate which are quoted in Siedell (160) at 25^oC. The salt factor is calculated by dividing the solubility in sodium sulphate at each concentration quoted, by the solubility in pure water at 25^oC. The factor varies from 1 at zero sulphite normality to 0.410 at/

OXYGEN SOLUBILITY IN PURE WATER

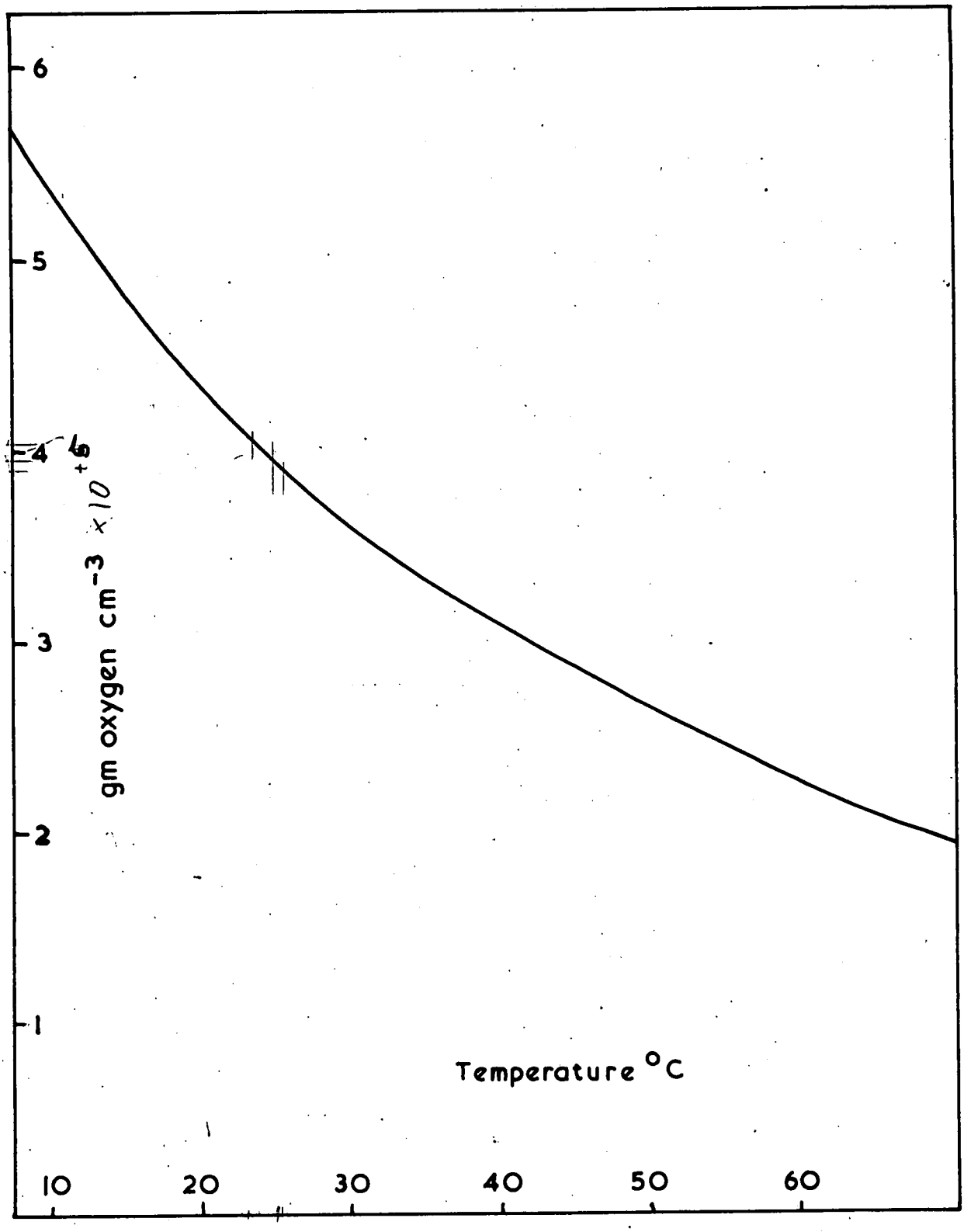

FIGURE 48

HENRYS CONSTANT : for the system O_2 - H_2O

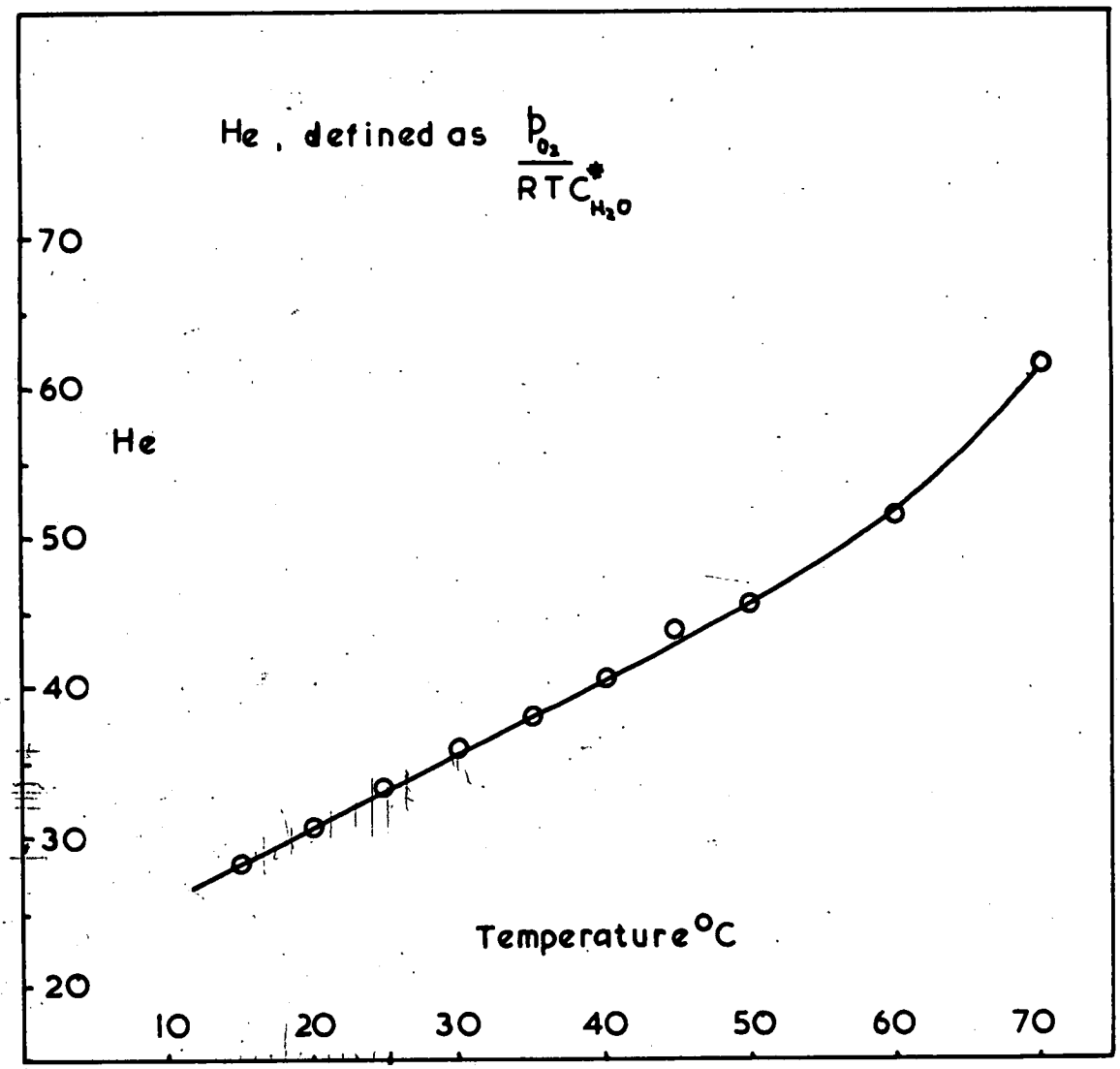

FIGURE 49

SALT FACTOR (f) vs SULPHITE NORMALITY

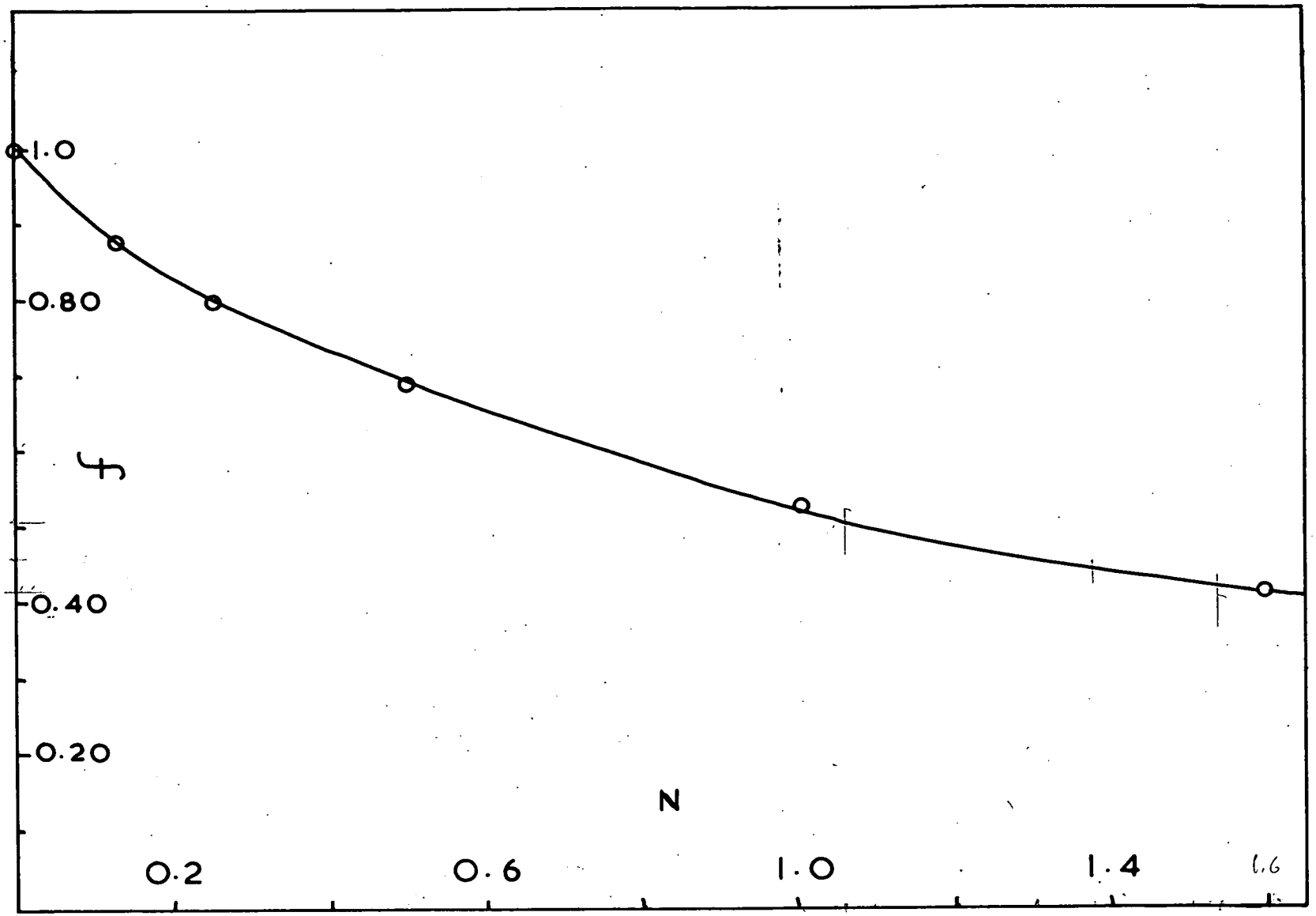

FIGURE 50

at 1.6N sulphite. To obtain the solubility of oxygen in sulphite at any other temperature it is assumed that the factor does not change with temperature. Figure 50 is a plot of the salt factor, f, against sulphite normality.

APPENDIX III

Sulphite Analysis Procedure

The procedure was an iodometric one. A sulphite sample was added to a known solution of iodine and the excess iodine was titrated with a standardized solution (N/10) of sodium thiosulphate. The solution strengths of the reagents used were as follows:

Sodium thiosulphate 25 gms $Na_2S_2O_5$ $5H_2O$ per litre (0.1N)

Potassium iodate 56.5 gms KIO_3 per litre (1.6N)

Potassium iodide 130 gm KI per litre

Sulphuric Acid 4N made by adding 220ml of concentrated acid to 1600 ml of water.

Standardization of the Sodium Thiosulphate solution.

An accurately weighed sample, about 0.1 gm, of potassium iodate was placed in a 250 ml erlenmeyer flask with 25 ml of the potassium iodide solution. After the iodate had dissolved 10 ml of the 4N sulphuric acid were added from a burette. The iodine liberated was titrated against the sodium thiosulphate solution. This procedure was repeated twice and the mean value of thiosulphate normality for each of the three samples was taken.

The normality of the sodium thiosulphate is calculated from the following equation:

Normality/

$$\text{Normality} = \frac{\text{weight of iodate sample (gm)} \times 10^3}{35.57 \times \text{thiosulphate titre (ml)}}$$

Standardization of the Potassium Iodate solution.

Two to three ml. of the potassium iodate solution were added from a burette to an erlenmeyer flask containing 25 ml. of potassium iodide. 10 mls. of sulphuric acid were added to liberate iodine which was titrated against the sodium thiosulphate. Three samples of iodate were taken and the mean value of their normalities calculated. The equation is as follows:

Normality of Iodate:

$$\frac{\text{volume of thiosulphate (ml.) x its normality}}{\text{volume of iodate (ml.)}}$$

Analysis Procedure for the sulphite ion

10 ml. of potassium iodate and 25 ml. of potassium iodide were placed in 250 ml. erlenmeyer flasks in readiness before a run was started. Just before a sample was taken 10 ml. of acid was run into one of the flasks from a burette to liberate the iodine. This proceduredwas followed because the solution would lose iodine if it was liberated and allowed to stand for any length of time. The sample from the apparatus was contained in a stoppered flask as described in Chapter VIII section B2. 10 mls. of this were withdrawn by pipette/

pipette and added to the flask ensuring that the tip was submerged to prevent further oxidation of the sulphite by the air in the flask. This was left for ten minutes to allow the oxidation reaction to proceed to completion and then the excess iodine was titrated against the standardized sodium thiosulphate and the titre recorded.

This procedure was repeated for each sample taken at twentyhto thirty minute intervals and on completion of a run the rate of change in thiosulphate titre, $r \frac{ml}{min}$ was used to calculate the oxygen consumption rate as shown in Appendix I.

To calculate the normality of the sulphite solution before a run to determine the salt factor, f, the same procedure was followed and the equation below used.

$$\text{Sulphite normality} = \frac{10 \times \text{Normality of } KIO_3 - \text{Vol. of thiosulphate} \times \text{its normality}}{10}$$

APPENDIX IV

Solid Bed Material Data

A. PHYSICAL PROPERTIES OF THE SOLID PARTICLES

1. Density: Sand 2.60 $gm.cm^{-3}$

   Ballotini 2.95 $gm.cm^{-3}$

2. Particle Size or Size range:

   Ballotini - No. 7 mean diameter 0.64 mm.

   Sand - Size Analysis (Approximate)

B.S. Mesh			%
30	d	60	21.3
60	d	72	56.0
72	d	100	22.7

3. Chemical Analysis of Sand:

	%
SiO_2	99.8
Al_2O_3	0.15
Fe_2O_3	0.05
CaO	0.04
MgO, Na_2O, K_2O	Trace

as supplied by the Consett Iron Co. Ltd.

B./

B. FLUIDIZATION DATA

1. Settled bed porosities

Sand	0.6
Ballotini	0.4

2. Bed Porosity vs liquid rate

Fig 51 - Sand: Water and Sulphite 36°C

Fig 52 - Ballotini: Water and Sulphite 36°C

SAND FLUIDIZATION - POROSITY vs LIQUID RATE

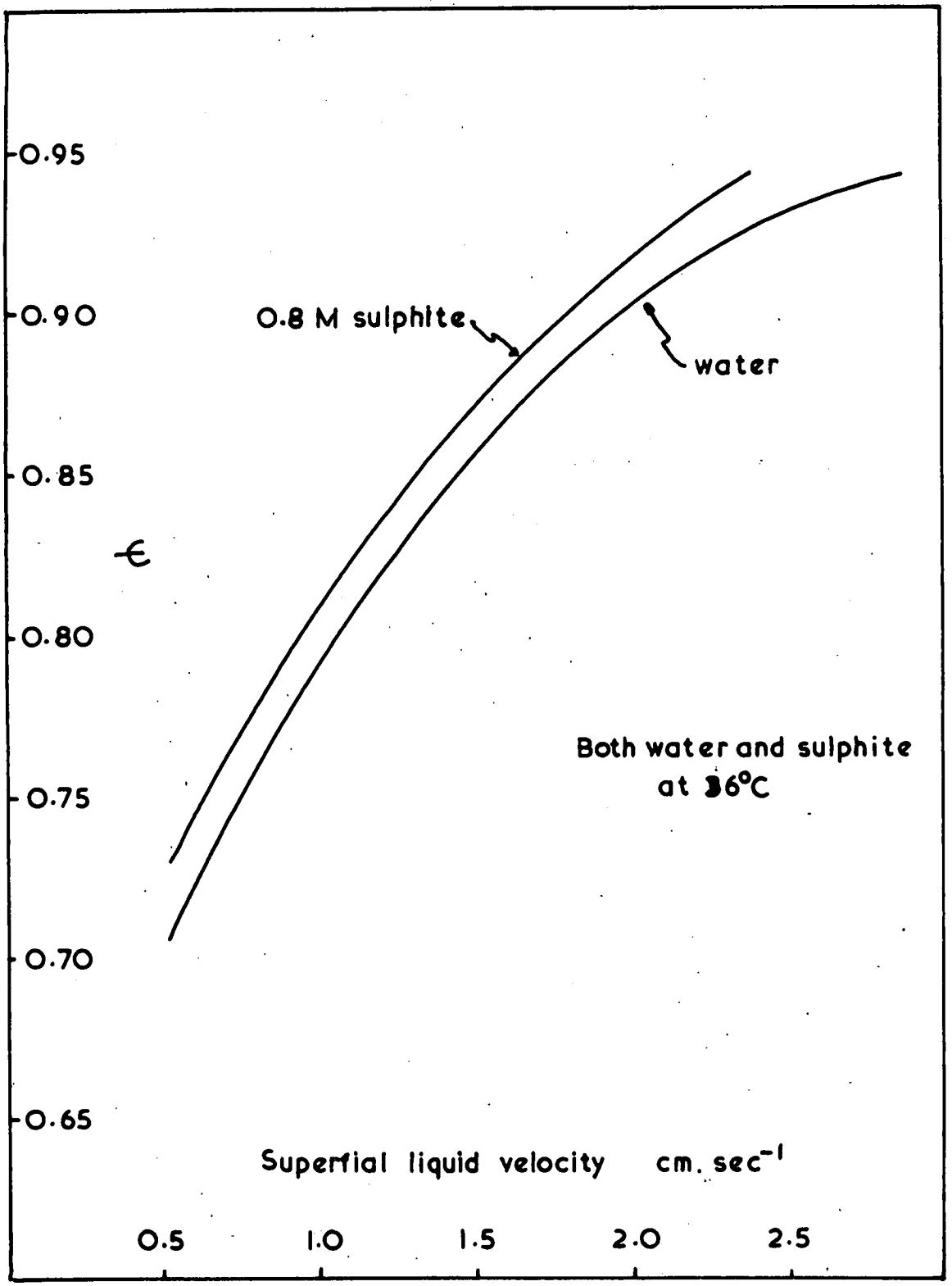

FIGURE 51

BALLOTINI FLUIDIZATION – POROSITY vs LIQUID RATE

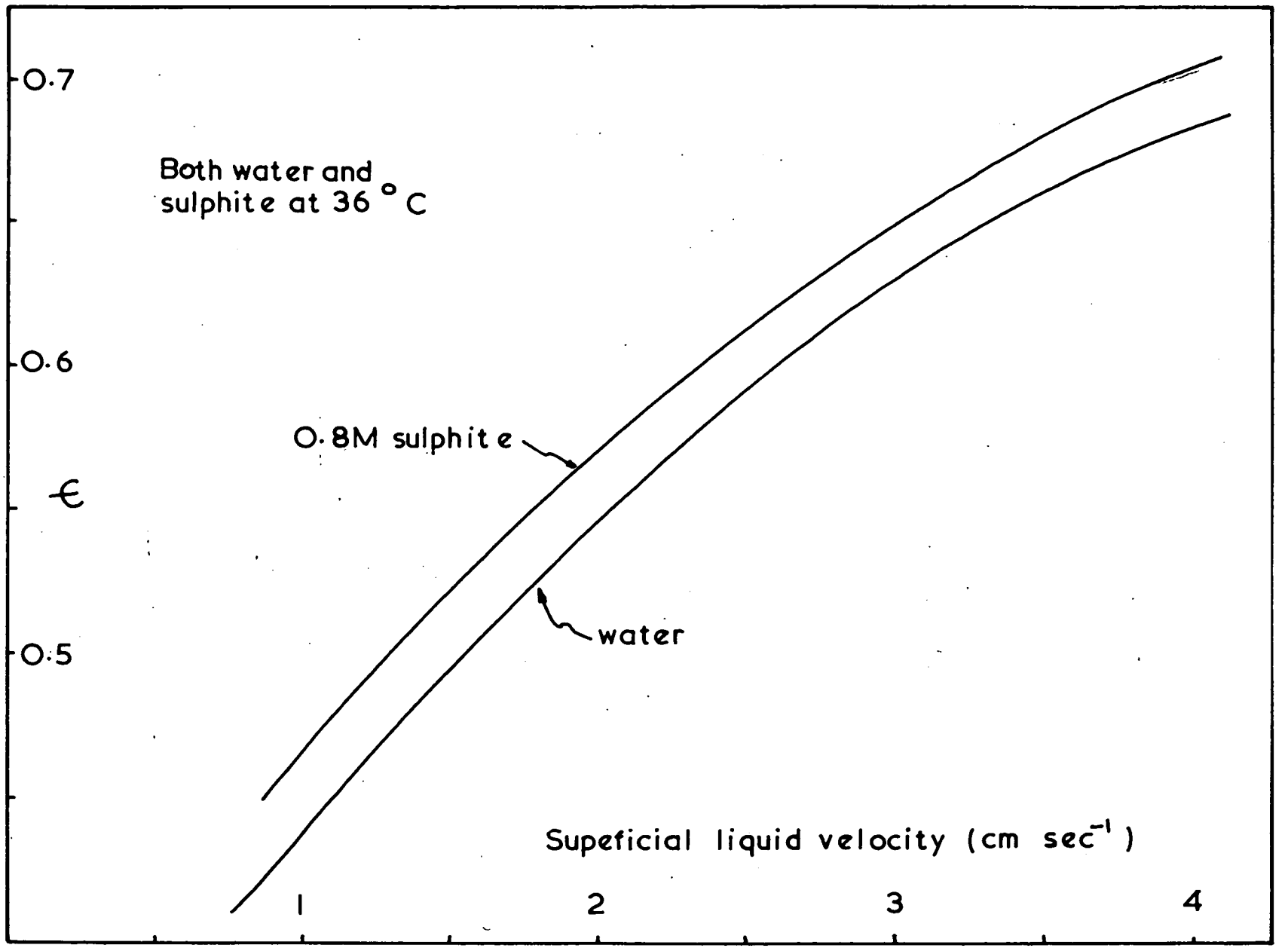

FIGURE 52

APPENDIX V

Tables of Results

I - Stirred Cell Results - Copper catalyst

II - Stirred Cell Results - Cobalt catalyst

III - Stirred Cell Results - Cobalt catalyst
Data for Van Krevelen Plot.

IV - Aerated Tank Results

V - Bubble Column Results

VI - Interfacial Area Measurements

VII - Residence Time Distribution Measurements.

TABLE I

STIRRED CELL RESULTS - COPPER CATALYST

Temperature	Absorption Rate (Corrected)	Oxygen Solubility C*	Sulphite Concentration	Salt Factor	Remarks	$k'_L \times 10^2$
(°C)	(cm/sec)	$\frac{gm O_2}{sec \times 10^{-3}}$	$\frac{gm O_2}{cm^3 \times 10^{-5}}$	(Molar)	(-)		cm/sec
42	.0289	3.85	3.00	0.9	0.40	Distilled	7.822
38.7	.0242	3.22	3.14	"	"		6.25
35.0	0.0195	2.60	3.32	"	"	water	4.78
33.8	0.0167	2.22	3.38	"	"		4.01
24.7	0.00953	1.27	3.95	"	"		1,96
19.5	0.00583	0.776	4.40	"	"		1.07
36.0	0.0186	2.48	3.28	"	"	copper wire	4.62
34.6	0.0167	2.22	3.34	"	"	suspended in	4.05
22.7	0.00635	0.845	4.10	"	"	the solution	1.26
46.5	0.0392	5.22	2.80	0.8	0.41		11.1
44.3	0.0358	4.77	2.88	"	"		9.90
38.3	0.0258	3.44	3.16	"	"		6.50
37.2	0.0238	3.17	3.20	"	"	Silica	5.89
29.0	0.0130	1.73	3.65	"	"	Sand	2.82
28.9	0.0133	1.77	3.66	"	"	in	2.88
22.8	0.00767	1.02	4.10	"	"	Cell	1.48
17.0	0.00423	0.563	4.62	"	"		0.726
18.0	0.00467	0.622	4.52	"	"		0.818
43.5	0.0300	3.99	2.92	0.8	0.41		8.14
41.3	0.0292	3.88	3.02	"	"	Brass	7.65
34.0	0.0186	2.48	3.38	"	"	Filings	4.38
32.9	0.0149	1.98	3.42	"	"	in	3.45
25.6	0.00833	1.11	3.88	"	"	cell	1.69
41.9	0.0439	5.84	3.00	0.4	0.59		7.95
40.5	0.0403	5.37	3.06	"	"	Distilled	7.27
29.4	0.0202	2.68	3.62	"	"	water	3.06
29.3	0.0197	2.62	3.63	"	"		2.99
18.1	0.0105	1.40	4.52	"	"		1.29
19.1	0.00917	1.22	4.42	"	"		1.15
45.4	0.0392	5.22	2.84	0.78	0.415		10.8
43.3	0.0375	4.98	2.94	0.78	0.415	Hot	10.0
35.2	0.0263	3.50	3.30	0.74	0.425	Tap	6.09
28.6	0.0107	1.42	3.67	0.725	0.430	Water	2.19

TABLE II

STIRRED CELL RESULTS - COBALT CATALYST

Temperature	Absorption Rate (Corrected)		O_2 Solubility	Sulphite Concn.	Salt Factor	Activation Energy	k'_L
°C	Cm./sec	gm.O_2/sec x 10^{-3}	gm. x 10^5 / cm^3	g.moles/litre		k.cals./g. mole	cm./sec
5.8	0.178	0.236	5.88				.248
17.6	0.182	0.242	4.56	0.8	0.410	4.88	.325
31.1	0.232	0.309	3.52				.523
45.4	0.267	0.356	2.84				.745
6.0	0.117	0.156	5.86				.110
18.3	0.133	0.177	4.48	0.4	0.590	5.69	.163
32.4	0.163	0.217	3.46				.260
49.9	0.213	0.283	2.66				.440
6.0	0.0985	0.131	5.86				.0750
18.1	0.113	0.150	4.52	0.2	0.730	5.88	.111
35.2	0.163	0.217	3.52				.205
49.3	0.187	0.248	2.68				.310
6.5	0.0889	0.118	5.80				.0600
18.0	0.106	0.141	4.52	0.1	0.830	5.98	.0918
33.3	0.135	0.180	3.40				.156
44.5	0.160	0.212	2.88				.217
6.8	0.0670	0.0890	5.76				00410
21.4	0.0741	0.0984	4.20	0.04	0.920	5.98	.0680
26.4	0.0896	0.119	3.84				.0820
55.5	0.142	0.188	2.44				.204

TABLE III

STIRRED CELL RESULTS - COBALT DATA-VAN KREVELEN PLOT DATA

k_L' (cm/sec)	k_i'/k_L' (-)	Sulphite Molarity (g.moles/litre)	Temp. (°C)	$\sqrt{k_c'' D_A C_B}$ (cm/sec)	$\sqrt{\frac{k_c'' D_A C_B}{k_L'}}$ (-)	$k_L^* \times 10^3$ cm/sec
0.0670	26.2	0.04	20	0.142	55.6	2.55
0.093	28.2		30	0.217	65.8	3.30
0.126	29.3		40	0.324	75.4	4.30
0.097	38.0	0.10	20	0.224	87.8	2.55
0.137	41.5		30	0.343	105	3.30
0.185	43.0		40	0.511	119	4.30
0.122	47.8	0.20	20	0.318	125	2.55
0.171	51.8		30	0.486	147	3.30
0.230	53.5		40	0.725	169	4.30
0.178	69.8		20	0.449	176	2.55
0.246	74.5		30	0.685	208	3.30
0.326	75.8	0.40	40	1.025	238	4.30
0.370	145	0.80	20	0.635	249	2.55
0.490	148		30	0.971	294	3.30
0.630	147		40	1.45	337	4.30

Assumptions k_c'' = 21,900 @ 20°C, 43,800 @ 30°C, 87,600 @ 40°C, D_A = 2.4×10^{-5}, 2.7×10^{-5}, 3.0×10^{-5}

TABLE IV

AERATED TANK RESULTS

Temp.	Oxidn. Rate	Henry's Constant	Sulphite Normality	Salt Factor	Gas Holdup	Area	Air Rate	Stirred Speed		Mass Transfer Coefficient	Sauter Mean Bubble
	r	He	N	f	Hg	a_d	v_s	r.p.m.	Po_2/RT	k_L'	D_{bm}
°C	$\frac{ml}{min}$	-	$\frac{g.equiv}{litre}$	-	%	cm^{-1}	$\frac{cm}{sec}$	min^{-1}	$x10^6$	$\frac{cm}{sec}$ $x10^2$	cm
51.5	0.383	-	1.38	0.435	0.967	0.728	0.35	200	Pure O_2	5.93	0.186
52.9	0.188	47.3	1.38	0.435	0.967	1.84	0.35	300	7.85	5.05	0.108
62.6	0.211	53.5	1.38	0.435	0.971	2.44	0.57	300	7.63	5.64	0.127
53.7	0.253	47.0	1.37	0.438	0.971	2.44	0.57	300	7.83	5.77	0.127
43.6	0.217	42.5	1.45	0.415	0.971	2.44	0.57	300	8.07	4456	0.127
36.3	0.203	38.7	1.29	0.450	0.971	2.44	0.57	300	8.28	3.50	0.127
21.0	0.182	31.0	1.35	0.440	0.971	2.44	0.57	300	8.70	2.46	0.127
14.9	0.397	28.2	1.42	0.430	0.935	5.96	0.35	450	8.89	1.92	0.0512
52.9	0.572	47.3	1.38	0.435	0.911	6.31	0.57	450	7.85	4.87	0.0626
45.4	0.535	43.5	1.40	0.430	0.911	6.31	0.57	450	8.04	4.06	0.0626
43.6	0.550	42.5	1.29	0.445	0.911	6.31	0.57	450	8.07	3.99	0.0626
36.3	0.524	38.7	1.29	0.450	0.911	6.31	0.57	450	8.28	3.27	0.0626
23.1	0.477	32.0	1.27	0.455	0.911	6.31	0.57	450	8.65	2.34	0.0626

TABLE V

BUBBLE COLUMN RESULTS

COPPER CATALYSED SULPHITE

Temp. °C	Oxidn. rate r	He	Sulphite N	Salt Factor f	$Po_2/RTx10^6$	k
				0.455		
49.7	0.353	45.4	1.32	0.455	7.93	10.8
46.5	0.217	43.5	1.47	0.415	8.00	8.72
45.8	0.217	43.0	1.47	0.415	8.02	8.58
43.2	0.222	42.2	1.29	0.450	8.07	7.84
40.8	0.193	41.0	1.26	0.457	8.15	6.50
40.6	0.170	41.0	1.41	0.430	8.15	6.13
36.0	0.153	38.6	1.42	0.430	8.28	4.97
32.0	0.142	36.6	1.45	0.428	8.38	4.47
22.3	0.113	31.8	1.49	0.420	8.68	3.01
18.2	0.125	29.7	1.50	0.420	8.78	3.10
11.0	0.134	26.0	1.38	0.436	9.00	2.60

Area = 1.08 cm^{-1} Holdup = 20.6% @ 24°C.

(cm)	(atm)	760 mm. (l/min)	(cm)	(l)	(l)	(ml/min)	760 mm. (l/min)	(atm)	(N)	(-)	(cm^{-1})	(cm^{-1})	(cm^2)	(%)	(cm)	(-)	(gm/cm^3)
53.3	1.069	67.0	11.3	46.0	9.7	0.0883 0.0785	0.239 0.213	0.215 0.215	1.20 1.40	0.470 0.435	3.81 3.65	3.73	36.2	22.6	0.470		
83.7	1.108	69.5	22.6	50.7	15.3	0.108 0.104	0.322 0.311	0.220 0.220	1.32 1.35	0.445 0.440	3.35 3.26	3.30	50.5	20.4	0.453		
114	1.148	72.0	33.4	55.5	20.9	0.117 0.119	0.382 0.388	0.223 0.223	1.58 1.62	0.410 0.405	3.12 3.20	3.16	66.0	18.8	0.440		
145	1.187	74.5	45.2	60.2	26.4	0.145 0.154	0.514 0.546	0.226 0.226	1.36 1.50	0.437 0.420	2.99 3.35	3.17	83.6	18.1	0.419	Sand ϵ = 0.85	1.34
175	1.226	77.0	56.6	65.0	32.0	0.169	0.647	0.229	1.32	0.445	3.08	3.08	98.5	17.5	0.414		
205	1.266	79.5	67.9	69.7	37.6	0.195 0.197	0.800 0.808	0.233 0.233	1.30 1.35	0.450 0.440	3.16 3.17	3.17	119	16.6	0.374		
266	1.345	84.5	90.5	79.3	48.7	0.210 0.207	0.981 0.970	0.240 0.240	1.41 1.43	0.430 0.430	3.04 2.98	3.01	147	16.5	0.394		
327	1.423	89.0	113	88.7	60.0	0.236 0.246	1.23 1.32	0.248 0.247	1.23 1.35	0.463 0.440	2.78 3.05	2.92	175	16.2	0.397		
53.3	1.100	66.0	23.2	44.3	9.7	0.0677	0.181	0.220	1.36	0.440	2.92		28.3	22.2	0.581		
83.7	1.158	69.5	46.5	47.3	15.3	0.0758	0.211	0.225	1.40	0.435	2.19		32.0	17.6	0.585		
114	1.215	73.0	68.5	50.3	20.9	0.0845	0.250	0.231	1.29	0.450	1.79		37.4	14.8	0.583		
145	1.272	76.5	93.0	53.3	26.4	0.0913	0.287	0.237	1.37	0.438	1.63		43.0	13.9	0.594	Ballotini	
175	1.330	79.8	116.0	56.4	32.0	0.0918	0.305	0.243	1.54	0.415	1.47		47.1	13.5	0.637	ϵ = 0.55	1.95
205	1.388	83.3	140	59.4	37.6	0.0910	0.324	0.249	1.40	0.435	1.24		46.7	14.1	0.793		
266	1.503	90.2	186	65.4	48.7	0.1140	0.438	0.260	1.36	0.440	1.23		60.0	13.9	0.800		
53.3	1.079	66.4	17.8	45.5	9.56	0.0689	0.180	0.217	1.41	0.430	3.13		30.0	18.8	0.443	Sand	
175	1.258	77.4	107	61.8	32.0	0.126	0.460	0.234	1.36	0.440	2.16		69.4	14.5	0.470	ϵ = 0.72	1.53
266	1.395	85.8	171	73.7	48.7	0.150	0.650	0.247	1.36	0.440	2.02		99.2	14.2	0.492		
53.3	1.106	20.0	21.6	44.40	10.1	0.0174	0.0456	0.220	1.36	0.440	0.722		7.30	5.73	0.527		
53.3		35.0		44.35	9.95	0.0233	0.0608	0.220	1.36	0.440	0.982		9.77	9.65	0.653	Ballotini	
53.3		50.0		44.30	10.2	0.0350	0.0913	0.220	1.36	0.440	1.44		14.7	14.2	0.689	ϵ = 0.49	2.06
53.3		66.5		44.25	9.95	0.0591	0.154	0.220	1.36	0.440	2.48		24.6	17.1	0.500		
53.3	1.100	20.0	18.6	44.50	10.6	0.00883	0.0231	0.220	1.54	0.415	0.371		3.93	5.08	0.866		
53.3		35.0		44.50	9.8	0.0233	0.0611	0.220	1.35	0.440	1.02		10.0	10.8	.712	Ballotini	
53.3		50.0		44.50	9.8	0.0568	0.149	0.218	1.36	0.440	2.46		24.1	13.4	.378	ϵ = 0.56	1.93
53.3		66.5		44.50	9.8	0.0627	0.164	0.218	1.36	0.440	2.71		26.6	17.3	.465		
53.3	1.079	20.0	17.8	44.45	9.97	0.0150	0.0393	0.217	1.42	0.430	0.655		6.53	6.65	.647		
53.3		35.0		44.4	9.56	0.0255	0.0666	0.217	1.42	0.430	1.16		11.1	11.7	.685	Sand	1.53
53.3		50.0		44.35	9.56	0.0410	0.107	0.217	1.42	0.430	1.86		17.8	15.8	.605	ϵ = 0.72	
53.3		66.5		44.3	9.56	0.0689	0.180	0.217	1.42	0.430	3.13		30.0	18.8	.443		
53.3	1.064	20.0	5.1	44.45	9.79	0.0118	0.0309	0.216	1.58	0.410	0.553		5.42	6.69	.778		
53.3		35.0		44.4	9.79	0.0312	0.0816	0.216	1.58	0.410	1.47		14.3	12.0	.546	Sand	
53.3		50.0		44.35	9.66	0.0588	0.154	0.216	1.58	0.410	2.80		27.0	15.5	.393	ϵ = 0.92	1.24
53.3		66.5		44.3	9.64	0.0867	0.226	0.216	1.58	0.410	4.12		39.8	19.5	.353		

TABLE VII

RESULTS OF RESIDENCE TIME DISTRIBUTION FUNCTION EXPERIMENTS

Time t (secs)	x	$\frac{dx}{dt}$	$\frac{Vm}{Vg}\frac{dX}{dt}$	F(θ)	θ	Porosity ε
5	0	0.0631	0.322	0.322	0.130	0.80
10	0.323	0.0275	0.140	0.463	0.260	
20	0.498	0.0133	0.0678	0.566	0.520	
29	0.600	0.00933	0.0476	0.648	0.754	
39	0.663	0.00662	0.0338	0.697	1.01	
48	0.730	0.00566	0.0289	0.759	1.25	
57	0.775	0.00488	0.0249	0.800	1.48	
78	0.848	0.00237	0.0121	0.860	2.03	
97	0.878	0.00096	0.00482	0.883	2.52	
5	0	0.100	0.498	0.498	0.130	0.68
10	0.370	0.0451	0.224	0.592	0.260	
16	0.611	0.0128	0.0637	0.675	0.416	
23	0.676	0.00727	0.0362	0.712	0.597	
31	0.727	0.00477	0.0238	0.751	0.806	
42	0.768	0.00315	0.0157	0.784	1.09	
58	0.802	0.00158	0.00787	0.810	1.51	
82	0.842	0.00114	0.00568	0.848	2.13	
101	0.859	0.00114	0.00568	0.865	2.62	
4	0	0.114	0.585	0.585	0.104	0.60
9.5	0.468	0.0430	0.221	0.689	0.247	
14	0.616	0.0196	0.101	0.716	0.364	
24	0.714	0.00649	0.0333	0.747	0.611	
32	0.752	0.00404	0.0208	0.773	0.832	
40	0.786	0.00287	0.0147	0.801	1.04	
54	0.817	0.00249	0.0128	0.830	1.40	
108	0.870	0.000875	0.00448	0.875	2.81	
5	0	0.143	0.722	0.722	0.130	0.50
11	0.627	0.0301	0.152	0.779	0.286	
15	0.729	0.0157	0.0793	0.808	0.403	
22	0.792	0.00727	0.0367	0.829	0.572	
43	0.843	0.00167	0.00843	0.851	1.12	
67	0.887	0.000967	0.00488	0.893	1.74	
97	0.907	0.000262	0.00132	0.908	2.52	

NOMENCLATURE

Symbol		Units
a	Constant in Massimilla's correlation	-
a	Interfacial area	cm^2
a_{GL}	Specific interfacial area per unit vol. of gas-liquid dispersion	cm^{-1}
a_g	" " " " "	cm^{-1}
a_l	" " " " liquid	cm^{-1}
a_{SL}	" " " solid-liquid bed	cm^{-1}
a_p	Projected area of particles or bubbles per unit volume of dispersion	cm^{-1}
A_b	Free cross-sectional area of light beam at any point	cm^2
A_o	Cross sectional area of light beam	cm^2
A	Total interfacial area	cm^2
b	Constant in Massimilla's correlation	-
C C	Concentration of tracer in the gas (Ch. X only)	-
C	Conversion factor to convert r to N (Ch. VIII only)	-
$C^* = \frac{p_{O_2} f}{RT\,He}$	Solubility of oxygen in su, sulphite solution	g mole. cm^{-3}
C^*	Solubility of oxygen (Ch. III only) in pure water	$gm.cm^{-3}$
$C^*_{H_2O} = \frac{p_{O_2}}{RT\,He}$	Solubility of oxygen in pure water	g mole cm^{-3}
C_{A_L}	Concentration of gas in liquid phase	g mole cm^{-3}
C_{A_i}	Concentration of gas at gas-liquid interface	g mole cm^{-3}
C_B	Concentration of solute in liquid phase	g mole cm^{-3}
d	diameter of particle b	cm
D/		

D_A	Diffusivity of gas in liquid phase	$cm^2\ sec^{-1}$
D_B	Diffusivity of solute in liquid phase	$cm^2\ sec^{-1}$
D_{bm}, d_{sv}	Sauter Mean bubble diameter	cm
D_{mzz}	Mean bubble diameter at height Z	cm
Dmo	Mean bubble diameter at nozzle	cm
E_a	Activation Energy	$cals.\ g\ mole^{-1}$
F(t), F(θ)	Residence time distribution function	-
f	Salt factor to convert $C^*_{H_2O}$ to C^*	-
f_B	Large bubble frequency	sec^{-1}
h	height in column above bed supporting gauze	cm
H	overall column height	cm
Hg	gas holdup as percentage of aerated dispersion	-
He	Henry's Constant = $P / C^*_{H_2O} RT$	-
I	Intensity of light passing through a dispersion	any consistent units
I_o	Intensity of light incident to a dispersion	any consistent units
I(θ)	Internal Age Distribution Function	-
K	absorption coefficient of tracer in gas (Ch. X)	cm^{-1}
k'_c	1st order catalysed reaction rate constant	sec^{-1}
k''_c	2nd order catalysed reaction rate constant	$cm^3 gmole^{-1} sec^{-1}$
k_L	liquid phase physical mass transfer coefficient	$cm\ sec^{-1}$
k/		

k_L'	overall liquid phase physical mass transfer coefficient	cm sec^{-1}
k_o''	2nd order uncatalysed reaction rate constant	cm^3 g $mole^{-1}sec^{-1}$
$K = KL_p$		-
l, Lp	optical path length	cm
L_o	settled bed height of particles	cm
ΔL	increase in bed height of particles upon fluidization	cm
$\frac{Lo}{\Delta L}$	the reciprocal of bed expansion	-
M	molarity	g mole litre
n, N	normality of sulphite solution	g equiv. $litre^{-1}$
N, N_A	rate of mass transfer of gas (A)	g mole $sec^{-1}cm^{-3}$
N_{sc}	rate of mass transfer in stirred cell	gm sec^{-1}
P	total gas pressure	atm
p_{O_2}	oxygen partial pressure	atm
Q	rate of large bubble coalescence (Ch. VII only)	sec^{-1}
Q	Quantity of light that passes through the dispersion	L.U.
r	rate of change of sample titre	cm^3min^{-1}
r_a	oxygen absorption rate in stirred cell	cm^3sec^{-1}
R	gas constant	as suitable
S	concentration of tracer in perfectly mixed gas space	gm cm^{-3}
s	rate of surface renewal	sec^{-1}
t	room temperature (Ch. III only)	^oC

t,/

t_1	time (time for Q L.U. to pass through aerated dispersion)	sec
to	time for Q L.U. to pass through unaerated dispersion	sec
T	temperature	^oK
T8	concentration of tracer in step	gm cm^{-3}
υ_1	fraction of volumetric gas flow due to large bubbles	-
υ_2	fraction of volumetric gas flow due to ionic bubbles	-
υ_3	fraction of volumetric gas flow due to intermediate sized bubbles	-
υ_o	Voltage from photocell caused by light intensity Io	volts
υ	Voltage from photocell caused by light intensity I	volts
V_D	volume of solid-liquid dispersion before aeration	litre
V_t	Total volume of liquid in three-phase apparatus	litre
V_M	Volume of perfectly mixed gas space	litre
V_G	Volumetric gas flow rate	litre min^{-1}
V_s, υ_s	superficial gas velocity	cm sec^{-1}
V_p	Volume fraction of dispersion occupied by large bubbles	-
Vi	Volume fraction of dispersion occupied by ionic bubbles	-
V_b	Volume fraction of dispersion occupied by intermediate sized bubbles	-
X = S/T		-
xo	deflection on recorder chart caused by voltage υ_o	cm
x	deflection on recorder chart caused by voltage υ	cm
x/		

x	height above point of formation of spherical-cap bubbles	cm
Z	height above nozzle	cm
ϵ	bed porosity	-
ρ_s	density of solid particles	gm cm^{-3}
ρ_L	density of sodium sulphite solution	gm cm^{-3}
ρ_{SL}	equivalent density of solid-liquid fluidized bed	gm cm^{-3}
θ	reduced time	-
ϕ	enhancement factor	-

REFERENCES

(201) MASSIMILLA L., MAJURI N., SIGNORINI P., La Ricerca Scientifica 29, 1934 (1959)

(202) MASSIMILLA L., A. SOLIMANDO., SQUILLANCE E., Brit. Chem. Engl. 6 232 (1961).

(203) KATO, Y., Chem.Eng.(Japan) 27, 7 (1963).

(204) TURNER, R., "Joint Symposium on Fluidization", Soc.Chem.Ind - Instn. Chem.Engrs., 47, (1964).

(205) ADLINGTON, D., THOMSON, E., 3rd European Symposium on Chemical Reaction Engineering, Amsterdam, 1 (1964): Suppl. Chem. Eng. Sci., 203 (1964)

(206) CALDERBANK, P.H., MOO-YOUNG, M., BIBBY, R., ibid, 91.

(207) BIBBY, R., Ph.D. Thesis, Univ. of Edinburgh (1964)

(208) ROY, N.K., GUHA, D.K., RAO, M.N., Chem.Eng. Sci., 19, 215, (1964).

(209) STEWART, P.S.B., DAVIDSON, J.F., ibid, 19, 319 (1964).

(210) ØSTERGAARD, K., ibid., 20, 165 (1965).

(211) MARRUCCI, G., Ind.Eng.Chem. Fundamentals, 4, 224 (1965).

(212) LEVENSPIEL, O., "Chemical Reaction Engineering", Wiley, N.Y., (1962).

(213) ATTREE, V.H., Electronic Engineering, 24, 284 (1952).

(214) ANGELINO, H., CHARZAT, C., WILLIAMS, R., Chem. Eng.Sci., 19, 289 (1964).

(215) ROSENBERG: David Taylor Model Basin, Navy Department, Washington, D.C., U.S.A., Report 727, quoted in (202) above.

(216) International Critical Tables.

(217) OSEEN - quoted in (202) above.

(218)/

(218) TRAWINSKY, H., Chemie.Ing.Techn., 25, 229 (1953) - quoted in (202).

(219) ANDERSON, J., BRYDEN, J., B.Sc., Research Project, Dept.Chem.Engrg., Univ. of Edinburgh (1965).

(220) ROWE, P.N., Symposium on the interaction between fluids and Particles, London, p. 135 (1962).

(221) KOLBEL, H., LANGEMANN, H., PLATZ., J., Dechema Monograph 41, 225 (1963).

(222) MASSIMILLA, L., Private communication to P.S.B. Stewart, U. of Cambridge.